Engineering Geological Investigations of Two North Canterbury Landslide Complexes.

A thesis
submitted in partial fulfilment
of the requirements for the Degree
of
Master of Science in Engineering Geology
at the
University of Canterbury
by
T. Richard Justice

University of Canterbury
1994

Frontispiece: A cold winters day at the toe of Coringa Landslide Complex.

Abstract

Engineering geological investigations of the Mt. Vulcan and Coringa Landslide Complexes, situated near Motunau Beach, North Canterbury, New Zealand, have been carried out with the intention of determining the nature and causes of the complexes. Descriptions of the landslide complexes and field investigations undertaken for each site are discussed. In particular, the forms of slope movement termed 'earthslides' in this thesis are examined in detail. The term 'earthslide' is defined in this study as a slow moving, lobate or elongate mass of accumulated debris which advances primarily by sliding on discrete bounding shear surfaces. The average grain size distribution of the earthslide mass contains more than 50% sand, silt and clay combined.

Mt. Vulcan Landslide Complex comprises an area of about 85 ha, and is developed within a lower Tertiary marine succession, specifically failing within smectitic silty clays (Ashley Mudstone) and massive glauconitic sands (Waipara Greensand), underlying strong limestone (Amuri Limestone). Rotational slumping occurs at the head of the complex, involving limestone and/or clayey silt/sand blocks, which subsequently develop into translational slide/earthslide movements downslope of the head zone. An age of formation for the complex proved difficult to ascertain, however, the probable minimum and maximum ages of the complex are postulated at about 5000 b.p. and 100 000 b.p. respectively.

Coringa Landslide Complex comprises an area of about 50 ha and is developed within a structurally disturbed sequence of Ashley Mudstone and Waipara Greensand. The silty clay and sandy units, and the blocks of overlying limestone are interpreted to have initially failed by rotational sliding in smectitic silty clays and to have subsequently developed a southwesterly slide motion on a stiff mudstone (Loburn Mudstone), stratigraphically underlying the complex. The landslide is interpreted to have developed at about 100 000 years b.p. in response to uplift on thrust faults which underlie the complex.

Earthslide A and Earthslide 3 occur within the Mt. Vulcan and Coringa Landslide Complexes respectively. Detailed examination was made of both of these features, in terms of surface and boundary morphology, displacement rates and characteristics, the effect of rainfall, and geotechnical properties. In general, it has been found that the earthslides examined in this thesis move primarily by sliding or plug-flow on discrete bounding shears. The surface morphology typically has an undulating appearance which may show transverse tension cracking or bulging, depending on the longitudinal strain rate. Regions under extension typically display tensional cracking, while compressive regions display transverse bulges and/or multiple basal thrust development. Lateral shear zones display typical features

analogous to those developed along strike-slip faults, and lateral bulges formed immediately adjacent to the lateral shear zone are often (but not universally) associated with zones of constricted earthslide movement.

Geotechnical properties determined for the earthslides examined in this study indicate plastic limits of 27-38%, liquid limits of 15-43%, plasticity indices of 14-45%, clay fractions of 14-47% and bulk densities of 1633-2004 kg/m^3. This wide range in values is attributed to both the variable sand fraction encountered in different areas of both earthslides, and the various sources for debris supply. Typical residual friction angles were found to be just over 13°, while effective residual cohesion was found to be close to 0.

Both Earthslide A (part of the Mt. Vulcan Landslide Complex) and Earthslide 3 (part of the Coringa Landslide Complex) are found to move by sliding and/or plug-flow on basal and lateral shear zones, and the average particle size distribution contains more than 50 % sand, silt and clay. Furthermore, Earthslide 3 was found to move at slow (0.5-2.3 m/yr) rates. Because of these characteristics, the previous term widely used in New Zealand for these types of failure (creeping earthflow) has been modified to 'slow earthslide'.

Movement rates and characteristics determined for Earthslide 3 on the Coringa Landslide Complex indicated regions of compressive, extensional and plug-flow within the earthslide. Likewise, regions of steady and unsteady state behaviour were recognised. The accumulation zone of Earthslide 3 was found to be a region of unsteady- state compressive flow, while the majority of the track zone was found to be a region of steady-state plug flow.

A correspondence was noted between earthslide movement rate and precipitation, and a lag time of 2-3 weeks was indicated. The mechanism of momentum transfer of head zone disturbances for the earthslide is found to be a mixture of plastic (advective) and viscous (diffusive) styles.

Remedial options for both Earthslide A (Mt. Vulcan Landslide Complex) and Earthslide 3 (Coringa Landslide Complex) involve either reforestation or drainage and/or stream control of key areas of both earthslides.

Acknowledgments

Thanks to my supervisor, Mr David Bell, for advice and critical review, Prof. John Hutchinson (Erskine Fellow 1993) for advice and guidance in the field, and Dr Chris Phillips (Landcare Research) for clarification of a few points. I am grateful also to the following Geology department technicians: Mrs Michelle Wright, for her skill and patience in surveying; Mr Rob Spiers for his help with locating survey markers; Mrs Catherine Brown for her advice and help with X-ray diffraction analysis and grain size analysis, Mr Kerry Swanson for some photographic work; and, Mr Michael Finnemore for his help with unveiling the intricacies of Autocad.

Thanks also to my colleagues, (and friends): Ginny Cunningham, for advice, aid in setting up monitoring points, and an insistence on regular coffee breaks; Hamish MacLauchlan, for the use of his most excellent Landrover and considerable help in augering holes through 'horrible clay', and; Georg Winkler for advice and discussion on the merits of ring shear vs box shear testing, East Cape North Island clay vs. North Canterbury clay and snowboarding vs. the noble art of skiing.

Thanks to Mr Dick Carmicheal (owner of Coringa farm) and Mr. Ross Little (owner Pacific Downs) for granting access to their land, and for their helpful comments.

I am grateful to my parents, especially Dad for providing critical review of some chapters.

Lastly, a huge thankyou to Karen, for her patience and enthusiasm for colouring in large maps, her humour, warm companionship and for her skill at cooking apricot chicken.

This work is dedicated to

Karen,

with love and thanks.

Table of Contents

List of Figures

Chapter 4

Map Volume

Note that maps included in this volume are noted in the general text by a bolded number

List of Symbols Used

A	Landslide cross sectional area
B	Bearing
CF	Clay Fraction (>2μm)
Ip	Plasticity Index
F_2	Two dimensional factor of safety
F_3	Three dimensional factor of safety
K	Coefficient of lateral earth pressure
L	Length of landslide body
L_e	Length of earthslide body
P_e	Landslide Peclet Number
S	Horizontal distance
T	Rigid body thickness of earthslide
V	Volume
W	Weight
Y	variable defined in equation (4.2)
a	Ratio of rigid body thickness to earthslide thickness
a	Annum (year)
c	Cohesion
c'_r	Effective residual cohesion
d	Depth of water below ground surface
d_h	Height (elevation) difference
g	Gravitational acceleration
k	Coefficient of permeability
m	Height of water table above basal shear surface in terms of z
m	Metre
r_u	Pore pressure ratio = $u/\gamma z$
s	Second
t	Time
u	Pore water pressure
v	Earthslide velocity
w	Natural moisture content
w_L	Water content at liquid limit
wP	Water content at plastic limit
z	Vertical height of displaced mass of earthslide
β	Earthslide inclination
β_u	Angle of ultimate stability
γ	Soil unit weight =ρg
λ	Width of displaced landslide mass.
λ_e	Width of earthslide
μ	micro-
ρ	Bulk soil density
ρ_s	Saturated bulk density
ρ_w	Water density
σ	Shear stress
τ	Shear strength
ϕ	Friction angle
ϕ'_r	Effective residual friction angle
Φ	Particle size parameter
Σ	Summation

Abbreviations

R.L.	Reduced level
m.a.s.l	Metres above sea level

Chapter One: Introduction

1.1. Background

Landsliding is a common geological process (Williams, 1989), and forms an important major natural hazard in New Zealand.

The stratigraphy of New Zealand is dominated by predominantly deformed Mesozoic and Cenozoic rocks. Relief in New Zealand is relatively steep, with 65% of the landmass having slope angles in excess of 15°. These factors, together with extensive deforestation, a cyclonic weather pattern and frequent high intensity rainfall cells, create an environment in which landslide erosion predominates (Blong & Eyles, 1989). Most landslides in New Zealand are less than 100-1000 m^3 in volume, but landslides with failures greater than 100 000 m^3 are not uncommon (Blong & Eyles, 1989). Individual landslides have damaged many houses and other structures, but deaths resulting from landslides are relatively infrequent.

This thesis presents the results of Engineering Geological investigations into the nature of two large, complex landslides in the coastal North Canterbury region. The Mt. Vulcan Landslide Complex[1] is situated on the coast approximately 9 km southwest of Motunau beach (fig. 1.1) and is the larger of the two complexes, covering an area of approximately 85 ha. The Coringa Landslide Complex involves an area of about 50 ha and is situated 3 km inland from Motunau beach. Both landslides are located in generally weak[2] lower Tertiary lithologies.

1.2. Study Objectives

The objectives of this study were to investigate the nature and causes of the Coringa and Mt. Vulcan Landslide Complexes in North Canterbury. Descriptions of the landslide complexes and field investigations undertaken for each site are discussed. In particular, particular portions of both complexes classified in this thesis as 'earthslides' (see section 1.6.3.3) were examined in detail. Objectives here were to (i) describe the surface morphology and characteristics of displacement boundaries; (ii) determine movement rates and failure mechanisms; (iii) determine the geotechnical parameters of

---

[1]previously called "Montserrat Landslide" by Wilson (1963)

[2]Engineering geological descriptions are given in accordance with the method of Bell & Pettinga, (1983); see Appendix B.

material involved in the earthslides and compare this to other earthslides and associated features; and (v) assess the probable future activity of the earthslides.

1.3. Physiography of the Study Area

1.3.1. Location

The study area lies approximately 65 km north-northeast of Christchurch (figure 1.1), and is situated inland and to the southwest of Motunau Beach, a fishing settlement of about 130 houses. The area as shown in figure 1.1 and figure 1 (map volume) covers an extent of some 60 km^2, comprising mostly undulating farmland.

The topographically highest points of the study area are Montserrat (457 m) and Mt Vulcan (411 m), while the main water course is the Motunau River (fig.1.1). The study area has gentle to moderate slopes (15° to 20°) inland; however, the shoreline in the southwestern part of the study area is generally marked by sea cliffs up to 70 m in height.

1.3.2. Climate, Vegetation and Land Use

The study area usually experiences warm, dry summers (December - March) with temperatures in the range 20°C-30°C; at times when dry northwest Fohn winds blow, temperatures can exceed 30°C. In winter months (June - September) the area is generally cold (0°C - 10°C) with easterly and southerly winds prevailing. Frosts are common at this time, often to sea level. The annual temperature range between winter and summer is around 10°. Annual rainfall for the year ranges between 800 and 1200 mm, with maximum precipitation usually in the late winter. The study area usually receives close to 2000 sunshine hours per year.

Vegetation consists of mainly exotic grasses (white clover, rye grass, sward) mixed with scrub consisting of gorse, kanuka and broom. Most trees are introduced *pinus radiata,* either self sown or planted for use as a forestry resource. Native ribbonwood and 'cabbage trees' occur sporadically throughout the study area, while introduced Willow and Poplar trees stand along many stream and river banks. Most flat or gently inclined surfaces are covered in pasture, however many gullies remain scrub-clad.

The study area is typically used for farmland, with sheep and bovine stock units dominant. Limited pine forestry, as mentioned above, occurs throughout the study area. Some cropping occurs on the flat coastal plains.

Figure 1.1 Location of Field Area
Scale 1: 50 000

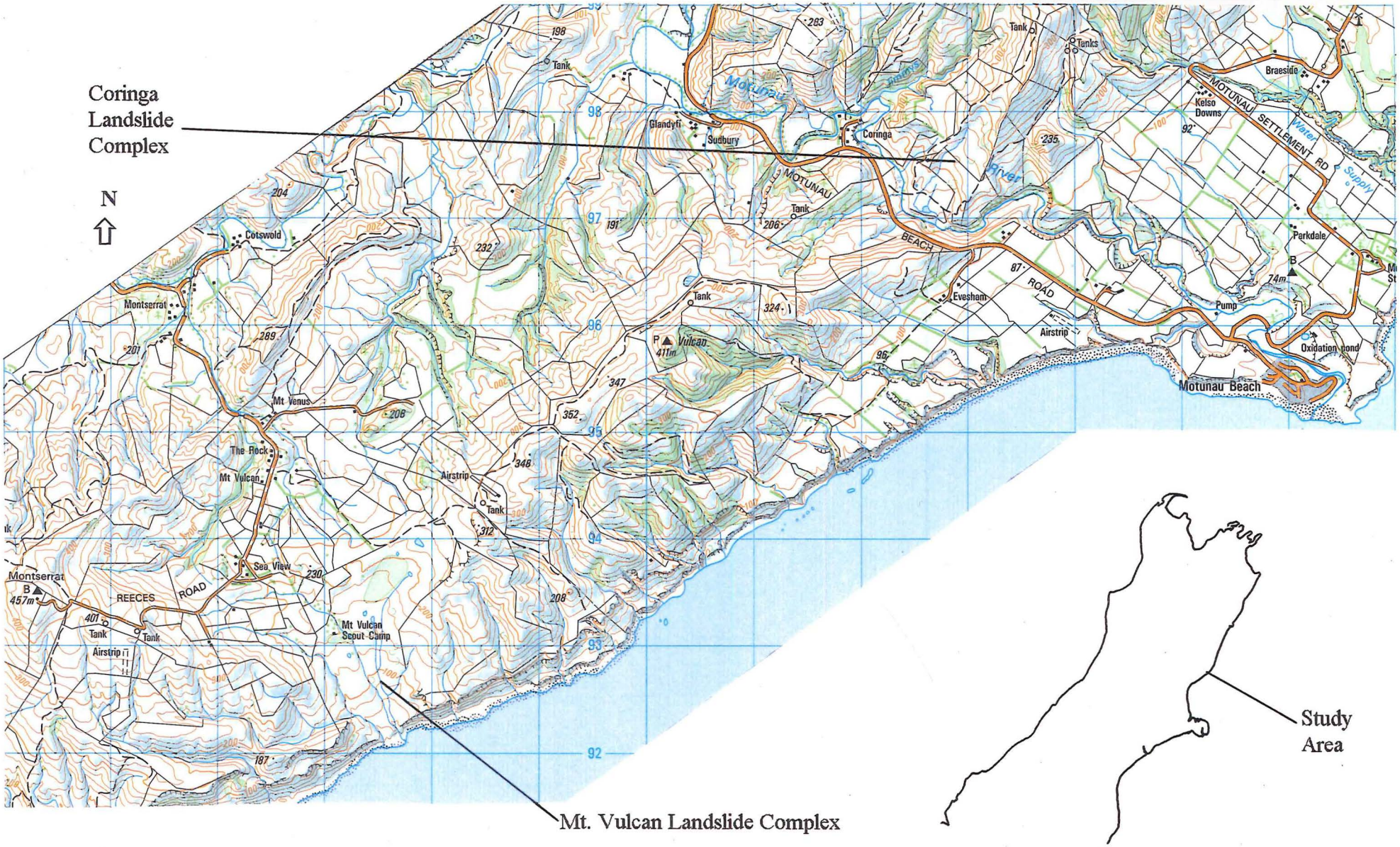
Coringa
Landslide
Complex
N
Mt. Vulcan Landslide Complex
Study
Area
Motunau
River
Coringa
Sudbury
Glandyfi
Tank
Tanks
Braeside
Kelso
Downs
MOTUNAU SETTLEMENT RD
Water
Supply
BEACH
ROAD
Eveshom
Parkdale
Pump
Airstrip
Oxidation pond
Motunau Beach
Cotswold
Montserrat
Mt Venus
The Rock
Mt Vulcan
Vulcan
411m
Sea View
REECES
Mt Vulcan
Scout Camp
457m

1.4. Scope of Thesis

1.4.1. Investigation Methodology

1.4.1.1. Regional Setting

Investigation of the area including the Coringa and Mt. Vulcan Landslide Complexes consisted of engineering geological mapping at a scale of 1: 12 500 (fig **1**). This map was compiled from (i) aerial photographic interpretation, using several aerial photographic runs and series, (ii) field mapping, and; (iii) existing publications (Wilson, 1963; Brown & Field, 1985; Yousif, 1987; Barrell, 1989). Rock and soil descriptions are given according to the procedure of Bell & Pettinga (1983); see Appendix B.

1.4.1.2. Mt Vulcan Landslide

The geology and geomorphology of the landslide complex were mapped in detail at a scale of 1: 2 500 by field mapping and aerial photographic interpretation (fig. **2**).

Long term movement rates were determined for various areas of the complex by the analysis of different stes of aerial photographs (Appendix B).

A geotechnical analysis was performed on material involved in the lower and most active part of the complex (termed 'Earthslide A' in this study). Laboratory tests were performed according to set procedures documented in either NZS 4402, or the appropriate instruction manual (for example, Wykeham Farrance(a); Law, 1987; for ring shear analysis). Tests included, (i) natural moisture content; (ii) Atterberg limits (plastic and liquid limits); (iii) Linear shrinkage; (iv) whole sample and clay fraction X-ray diffraction analysis for determination of mineralogy; (v) pipette analysis for grainsize distribution, and; (vi) ring shear analysis for effective cohesion (c_r') and friction angle (ϕ_r') values. Values of effective residual friction angle were determined for limiting equilibrium conditions on Earthslide A using standard stability analysis (or back analysis) techniques.

1.4.1.3. Coringa Landslide

The study of the Coringa Landslide Complex is a more detailed investigation than that of Mt Vulcan landslide, and re-examines, and expands on, initial work completed by Barrell (1989).

Coringa Landslide was, like Mt Vulcan Landslide, mapped by site walkover at a scale of 1: 2 500, using similar methods (fig. **3**). The particular part of the Coringa Landslide Complex named 'Earthslide 3' (figs **3** and **4**) was surveyed using an infra-red

(E.D.M.) theodolite (see Appendix G) and subsequently mapped in detail at a scale of 1: 1 000.

A surface monitoring network was installed on Earthslide 3, with the intention of observing both horizontal and vertical surface displacements over the period of one year. The positions of points within the monitoring network were surveyed using the E.D.M. theodolite located on a stable control point at the western edge of the landslide complex. Resurveys were conducted approximately bi-monthly.

Limited subsurface investigations were conducted on Earthslide 3 using a simple hand auger. The boreholes were subsequently fitted with Casagrande piezometers to measure ground water pressures. The boreholes also provided information on the depth to the basal shear surface of the landslide.

A geotechnical analysis was performed on the material involved in Earthslide 3. Laboratory tests included: (i) natural moisture content; (ii) Atterberg limits; (iii) linear shrinkage; (iv) whole sample and clay fraction X-ray diffraction analysis; (v) pipette analysis for grainsize distribution; (vi) ring shear analysis for residual cohesion intercept and friction angle values; (vii) repeated reversal direct shear tests for residual cohesion intercept and friction angle values, and; (viii) falling head permeability tests. Values of effective residual friction angle were determined for limiting equilibrium conditions on Earthslide 3 by back analysis techniques.

1.4.2. Thesis Organisation

Chapter 1 provides background information on the study area, including the physiography and geological setting. A review of landslide terminology and a description of the geomorphic features peculiar to these types of landslide failure is given. An introduction is presented on the terminology, morphology and movement patterns of earthslides.

Chapter 2 is concerned with the Mt Vulcan Landslide Complex. The study here is an initial investigation of the landslide complex, and delineates areas of active movement within the complex as a whole. No short term movement data is presented, but long-term rates of movement for various areas of the landslide complex are postulated. In particular, the area of the complex termed 'Earthslide A' is examined in detail. A description of the surface morphology of the earthslide is given and results of a suite of geotechnical analyses performed on the material comprising Earthslide A are presented. Data concerning the stability of the earthslide acquired from back analyses are given.

Chapter 3 is concerned with Coringa Landslide Complex. The area of current movement, termed 'Earthslide 3'[3] is examined in substantial detail. Again, the surface morphology of the slide is examined. Short term (yearly) rates of movement are given, and are compared with (i) rainfall data; and (ii) inferred long-term rates of movement (averaged movement rate over a 10-year, or longer, period). Limited subsurface data for Earthslide 3 is presented and results of a substantial geotechnical analyses of material involved in Earthslide 3 are given. Data obtained from stability analyses are presented.

Chapter 4 provides a synthesis of data supplied in chapters 2 and 3 and compares observations and inferences made as part of this study with literature sources. A detailed account of the morphology and mechanisms of movement of earthslides and a description of the terminology used in this thesis is given.

Chapter 5 provides summaries and conclusions of work presented in the previous four chapters.

1.5. Regional Geology

1.5.1. Geological Setting

The study area lies at the southern end of the Marlborough Shear Zone (fig. 1.2). This zone is a system of transform faults that connect the oblique slip movement of the Alpine fault with the subduction boundary of the Hikurangi margin. Faults of the Marlborough Shear Zone have developed successively southward with time, with the Porters Pass Fault Zone (Nicol & Wise, 1992; IASPEI, 1994) and the Motunau Fault system (Carter & Carter, 1982) or Motunau Fold Belt (Barrell, 1989) being the most recently formed.

1.5.2. Stratigraphy

The stratigraphic sequence of the inland Motunau area comprises Mesozoic basement of very strong, highly deformed and fractured marine sandstones and mudstones (Torlesse Supergroup) which are unconformably overlain by generally weak to moderately weak late Cretaceous to early Cenozoic (Haumurian-Heretungan or later; see Appendix A) marine sedimentary lithologies (the Eyre Group of Brown & Field, 1985). Strong to very strong Amuri Limestone of Whaingaroan age conformably overlies the Eyre Group and is disconformably overlain by predominantly sandy and muddy marine sediments of the Motunau Group. (Otaian-Nukumaruan). A stratigraphic

---

[3]The area of recent activity was termed 'Earthflow 3' by Barrell (1989). However, for reasons explained in chapter 4, this feature is called 'earthslide 3' in this study.

Figure 1.2 Regional Tectonic Setting (modified from Nicol & Wise, 1992)

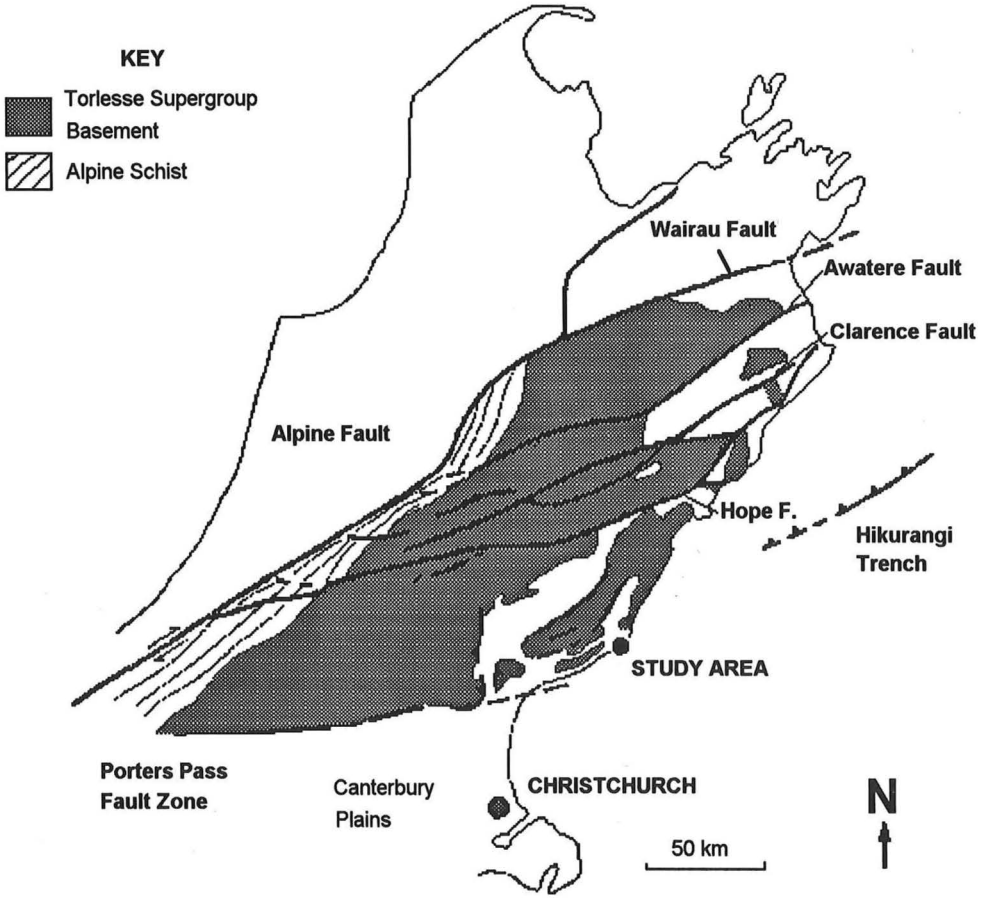

Figure 1.3 Stratigraphy of Study Area (compiled from Brown & Field, 1985; Yousif, 1987 and Barrell, 1989).

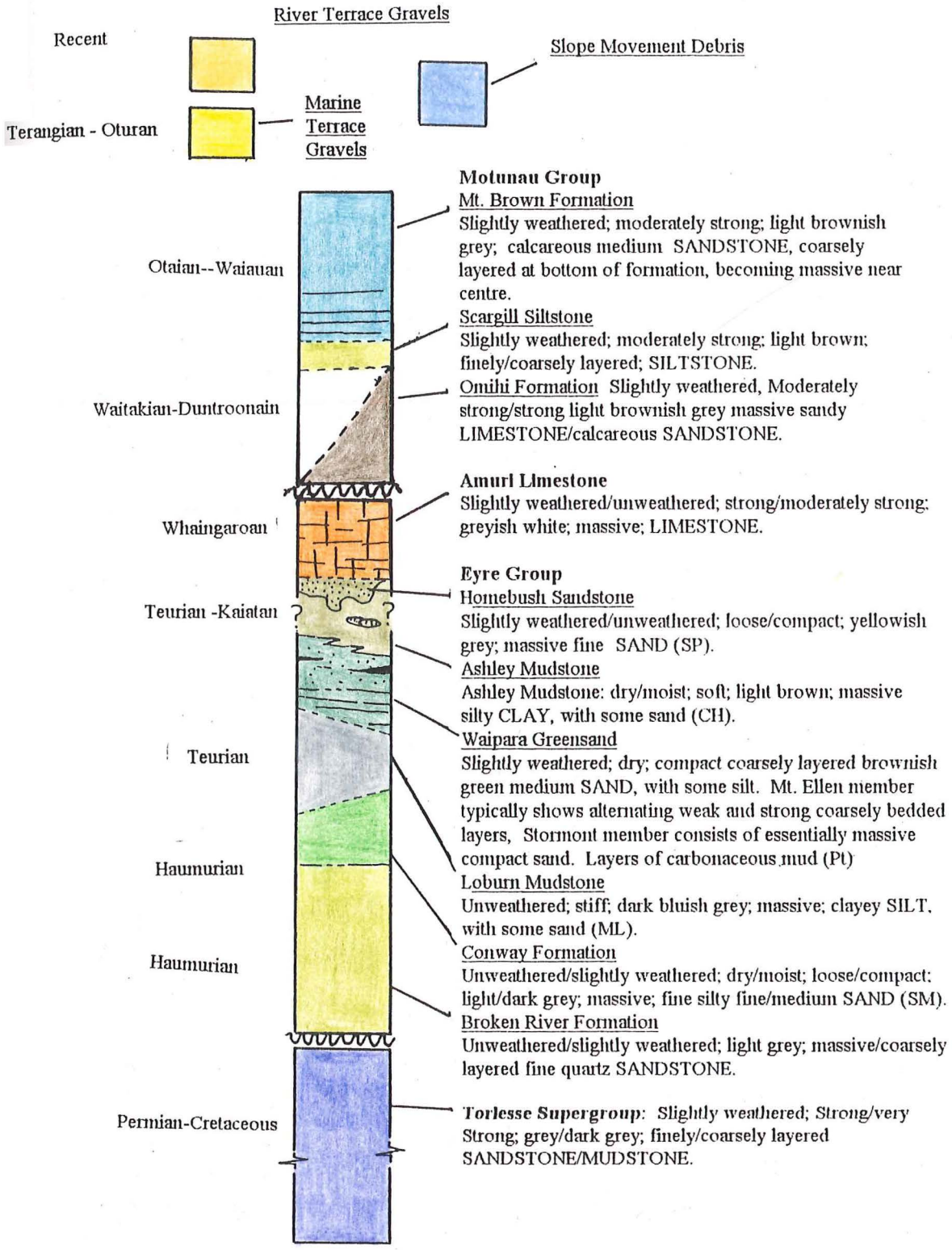

column of the study area is shown in figure 1.3, and full descriptions of units are given in Appendix C. The Eyre Group represents a transgressive marine sequence that was deposited under extensional tectonic condition, as the New Zealand and Australian continents rifted (Brown & Field, 1985). Amuri Limestone sedimentation took place at the culmination of continental extension, when the New Zealand continent was largely submerged and sedimentary basins were starved of terrigenous sediment supply. The Motunau Group was deposited concurrently with the development of the present plate boundary in the Oligocene-early Miocene.

The uppermost member of the Eyre Group is a smectitic clayey silt unit termed 'Ashley Mudstone' which in places displays complex synsedimentary deformation with a quartz sandstone unit termed 'Homebush Sandstone'. From an engineering geological point of view, the mudstone is one of the most important lithologies in the study area, as the unit forms the source material for a number of landslide complexes, including both the complexes presented in this study. Properties of the Ashley Mudstone are discussed in sections 2.6.3, 3.5.4 and 4.4.

To the south and east of the Coringa Landslide Complex are a series of uplifted marine terraces, mapped as Terangian to Oturan in age (NZGS, 1973). Barrell (1989) postulates that this succession of terraces formed on the southeastern limb of the rising Montserrat Anticline (fig. 1) as a result of a number of cycles of glacioeustatic sea level change.

1.5.3. Structure

The study area is located on the south-eastern limb of the Montserrat Anticline (fig. 1), which was named by Yousif (1987) and was formerly called the Cass Anticline by Wilson (1963). Torlesse rocks are exposed in the topographically elevated part of the anticline core located to the northwest of Coringa Landslide Complex. Lower members of the Eyre Group (Broken River Formation, Conway Formation) are exposed in the core of the anticline as it plunges to the southwest, passing inland from the Mt. Vulcan Landslide Complex.

The main structures of the study area are shown in figure 1., and in particular, note the following 2 faults or fault systems:

1. Coringa Fault System (Barrell, 1989); This fault system is conjectured to pass beneath Coringa Landslide Complex and comprises 2 north-south trending, eastwardly dipping thrust faults. The fault system is inferred (Barrell, 1989; this study) to be responsible for the formation of Coringa Landslide Complex. The fault system results in the thickening of Ashley mudstone to the north of Coringa Landslide Complex and displaces Loburn Mudstone over Broken River Formation

(Barrell, 1989). This fault system has not been shown on fig 1, because of the lack of surface expression and the uncertainty of extent of the system outside of the area immediate to Coringa Landslide Complex.

2. Montserrat Fault (Yousif, 1987). This fault lies to the west, and is inferred to underlie the toe of, the Mt Vulcan Landslide Complex, and was thought by Wilson (1963) to be reverse in movement. However, Yousif suggested that this fault may in fact be a regional slump feature. From field work conducted as part of the investigation of the Mt. Vulcan Landslide Complex, I suggest that Wilson's suggestion may be correct, however, geological mapping further along the fault from the Mt. Vulcan Landslide Complex is required to adequately resolve this situation. The Montserrat Fault is inferred to be partly responsible for the development of the Mt. Vulcan Landslide Complex.

1.5.4. General Comments

Barrell's work concluded that the stratigraphy and structure of the area is more complicated than previous workers had suggested, and field work undertaken as part of this study suggests likewise. It must be stressed, however, that the purpose of this study is not to undertake a detailed investigation of the geology of the Motunau/Montserrat area, but rather an engineering geological study of two large landslide complexes in the area. Readers are referred to Wilson (1963); Brown & Field (1985); Yousif (1987); Barrell (1989) and Field and Brown (1989) for more detailed accounts of the geology of the Motunau district.

1.6. Review of Landslide Terminology

1.6.1. Definitions of 'Landslide' and 'Slope Movement'

Sharpe (1938) defined the term 'landslide' as "the perceptible downward and outward sliding or falling of a relatively dry mass of earth, rock or a mixture of the two", whereas Cruden (1991) defined landslide more simply as "A movement of a mass of rock, earth or debris down a slope". However, Hansen (1984) noted that the term 'landslide' itself suggests that it should only be applied to those features moving across a distinct slide surface. This position was also held by Schuster (1978) who defined 'landslide' as "...the group of slope movements wherein shear failure takes place along a specific surface or combination of surfaces".

Schuster (1978) and Varnes (1978) used the term 'slope movement' in the same context as Sharpe (1938) had previously defined for 'landslide'. The term 'slope movement' has been broadly defined by Schuster and Varnes as "the downward and outward movement of slope-forming materials - natural rock, soils, artificial fills or combinations of these materials".

In this thesis, the position of Schuster (1978) and Varnes (1978) will be adopted, that is, the term 'landslide' will be restricted to those slope movements where sliding occurs along one or more specific surfaces. It will be demonstrated in chapters 2 and 3 that the two complexes described in this thesis fall within the given definition of 'landslide', as they are inferred to involve shearing along a specific basal surface (or surface of rupture; WP/WLI, 1990b), but also include components that must be described as 'slope movements', for example, rock falls and rock-block toppling.

1.6.2. Classification of Slope Movements

Sharpe (1938) was one of the earliest attempts to classify slope movements. The main factors used in Sharpe's classification were (i) the type of movement and (ii) the proportion of water, air or ice present. Secondary factors in Sharpe's classification were (iii) speed of movement and (iv) the size of the moving material. However, Sharpe's classification does not include the category of 'complex'.

More recently, Hutchinson (1988) proposed a morphological classification of sub-aerial slope movements, which places slope movements under the headings of rebound, creep, sagging of mountain slopes, landslides, debris movements of flow-like form, topples, falls and complex slope movements. It should be noted however, that some types of slope movement that can be considered to comply with the definition of 'landslide' have not been included in this category by Hutchinson. For example, Hutchinson (1988) defines mudslides (categorised under 'debris movements of flow-like form') as features "....which advance chiefly by sliding on discrete bounding shear surfaces", and therefore can be considered a type of landslide. However, the inclusion of the category 'debris movements of flow-like form' is one of particular significance to this study as it includes some types of landsliding observed on both complexes.

Varnes (1978) proposed one of the most widely used classification systems for slope movements in use today. This classification is based on the type of movement and the type of engineering geological material involved in the slope failure. Varnes' classification is shown in figure 1.4a. Note that an allowance in this scheme is made for complex slope movements, defined as involving two or more of the other 5 categories. The Varnes classification is supplemented by a rate of movement scale, which ranges from 'extremely rapid' ($v \geq 3$ m/s) to 'extremely slow' ($v \leq 0.06$ m/yr) where v is the movement rate of the landslide (fig. 1.4b). When describing a slope movement using Varnes' scheme, it is normal for the rate of movement to be given first, followed by the classification type (for example, "slow rock block slide").

Figure 1.4 (a)

Type of Movement			Type of Material		
			Bedrock	Engineering Soils	
				Predominantly coarse	Predominantly fine
Falls			Rock fall	Debris fall	Earth fall
Topples			Rock topple	Debris topple	Earth topple
Slides	Rotational	Few units	Rock slump	Debris slump	Earth slump
			Rock block slide	Debris block slide	Earth block slide
	Translational	Many units	Rock slide	Debris slide	Earth slide
Lateral Spreads			Rock spread	Debris spread	Earth spread
Flows			Rock flow (deep creep)	Debris flow	Earth flow (soil creep)
Complex	Combination of two or more principle types of movement				

Figure 1.4 (b)

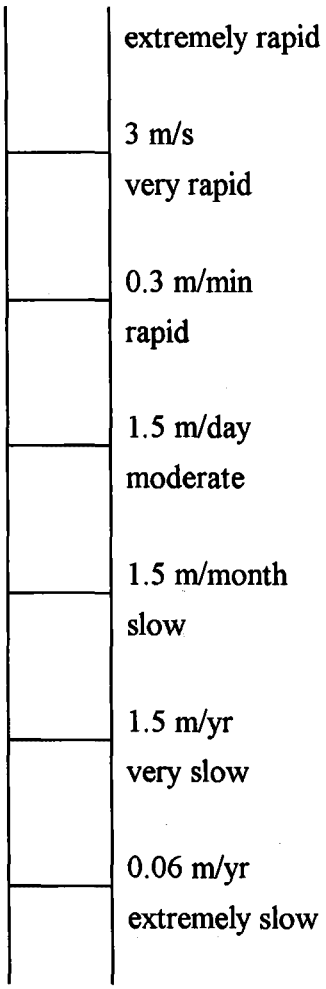

Figure 1.4 (a) Varnes (1978) slope movement classification scheme **(b)** Rate of movement scale (both figures modified from Varnes, 1978).

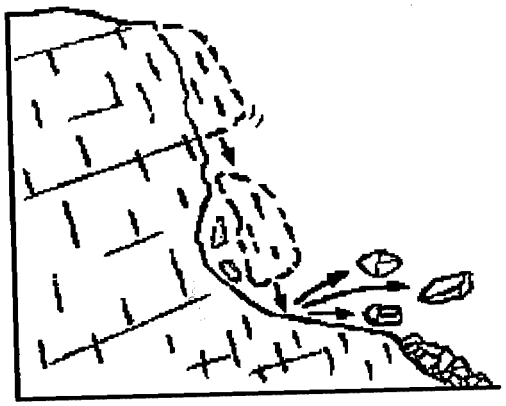

1.5 a. Rock Fall

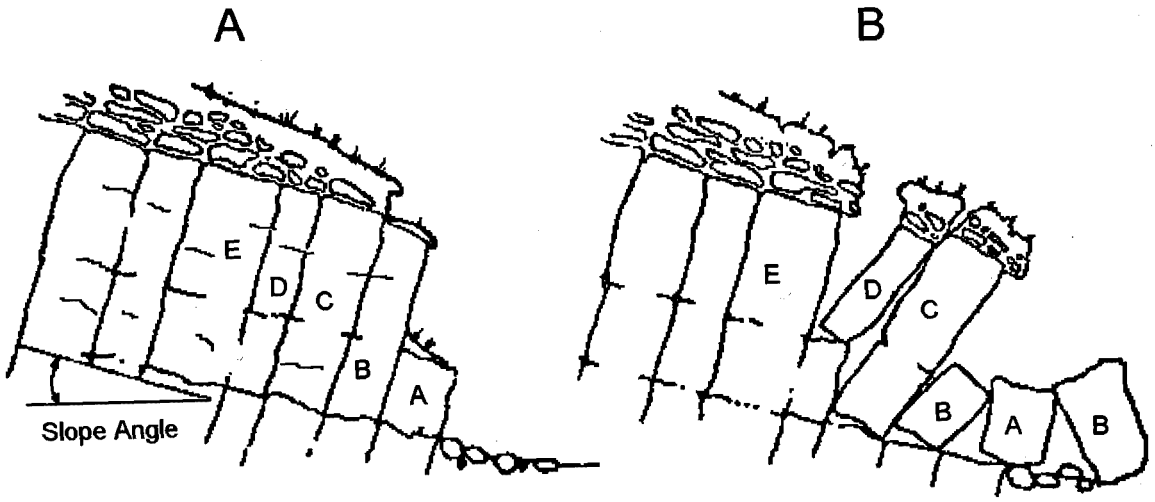

1.5b Rock Topple: A Pre failure; B, Post failure

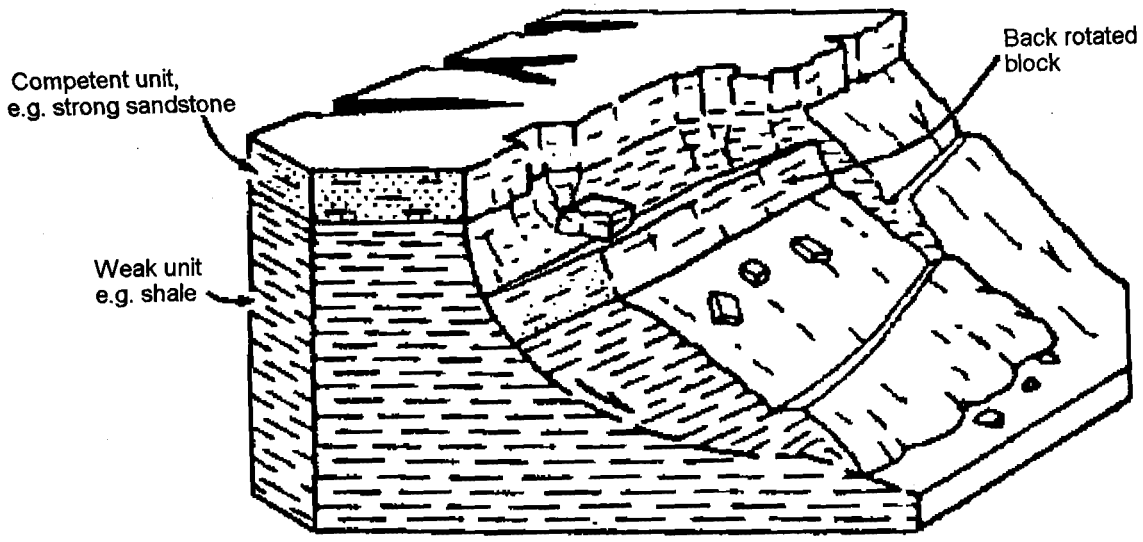

1.5c Rotational Slumping

Figure 1.5 **(a)** Rock Fall **(b)** Rock Topple and **(c)** Rotational slumping. All figures taken from Varnes (1978).

Varnes' (1978) classification will generally be used throughout this thesis, however, some modification is made under the category of 'flow' (section 1.6.3.3.; see also discussion in chapter 4). Because various types of slope movement can be recognised within different areas of the two complexes, the Coringa and Mt. Vulcan landslides fall within the category of 'complex' (see below).

1.6.3. Movement Types Related to Study

Both complexes have components of rock fall and rock topple; rotational sliding (rock and debris slumps) involving intact and/or disrupted Amuri limestone, and; components of earthslide in this study (see section 1.6.3.3) movements within Ashley Mudstone Homebush Sandstone lithologies.

1.6.3.1. Rock Fall and Rock Topple

1. Rock Fall (fig. 1.5 a): In this kind of movement, a mass of any size is detached from a steep slope or cliff along which little or no shear displacement occurs, and descends mostly through the air by free fall, leaping, bounding or rolling (Varnes, 1978; see also Whalley, 1984).
2. Rock Topple: Topple movements consist of the forward rotation of an exposed block about some pivotal point under the influence of gravity (fig. 1.5b). Topple movements can, in some cases, culminate in either falling or sliding, depending on the geometry of the topple block and the extent and orientation of any defects within the block.

In the two landslides presented in this study, small (generally less than 10 m^3) rock falls occur and have occurred from prominent Amuri Limestone escarpments. Rock topples, which can involve substantial masses (up to 25m^3) of rock, occur from the same escapements along rough, but persistent, joint planes. Topples subsequently develop rock fall type motions, due to the presence of closely spaced bedding planes and joint defects. These two slope movements have led to the development of substantial talus aprons at the base of escarpments at many points.

1.6.3.2. Rotational Sliding

In true slides, the movement consists of shear strain and displacement along one or several surfaces that are visible or may be reasonably inferred (Varnes, 1978). Rotational Slides[4] have a concave-upward slide surface and movement is due to forces that cause a turning moment about a point above the centre of gravity of the slide body (fig. 1.5c). This movement commonly produces a 'back-rotated' block where the top

---

[4]The commonest example of rotational sliding is termed 'slump' and the two terms are often used synonymously.

surface of the failed block tilts backward toward the slope. However, some blocks may display forward tilting.

Amuri limestone rock masses that display rotational slide movements can be clearly seen within the Mt. Vulcan and Coringa Landslide Complexes. Soil (debris) slumps can likewise be observed on both complexes.

1.6.3.3. Earthslide movements.

Earthslides and earthslide complexes can be seen on both the Coringa and Mt. Vulcan Landslide Complexes. Some of these bodies show evidence of current activity while others are assumed to be inactive or dormant at the present time. The terminology used in this thesis is based on, but differs slightly from, that of Varnes (1978) and Hutchinson (1988). In this thesis, the term 'earthslide' will be used to describe a slow moving lobate or elongate landslide that advances by displacement along discrete lateral and basal shear surfaces, and whose average grain size distribution shows more than 50% sand, silt and clay (ie., particles finer than 2 mm). Features termed 'earthslides' in this study would, under Varnes' (1978) classification be termed "slow earthflows" or under Hutchinson's (1988) morphological classification be termed "mudslides". Details of, and rationale for, this deviation from these 2 classifications are given in Chapter 4.

1.7. Characteristics of Earthslides

1.7.1. Morphologic Features

Earthslides generally occur along relatively gentle slopes or depressions and display basal and lateral shear failure along distinct and often slickensided planes of failure (Keefer and Johnson 1983). Slip surfaces within the moving mass however, are usually not visible or are short lived. The toe lies at the point most distant from the head, referred to as the 'distal margin' of the slide. The length of the earthslide (L_e) from head to toe is normally considerably greater than d, the earthslide depth (Fig. 1.6), producing d/L_e ratios less than 0.25. An earthslide may display either a tongue (elongate) or tear-drop (lobate) shape, depending on several factors including (i) the slope angle on which the earthslide is developed; (ii) the effective shear strength parameters (friction angle and cohesion) of the earthslide material; and, (iii) pore water pressure within the earthslide.

Material is provided to the earthslide from a 'zone of depletion', which forms the majority of the upslope portion of the slide. Material is constantly added to the depletion zone at the head of the slide by falls, shallow slides and minor earthslides. In the 'zone of accumulation' the surface of an earthslide bulges above the undisturbed ground on either flank. In profile this produces a sinusoidal form with the zone of

Figure 1.6 Idealised morphology of an earthslide (from Keefer & Johnson, 1983)

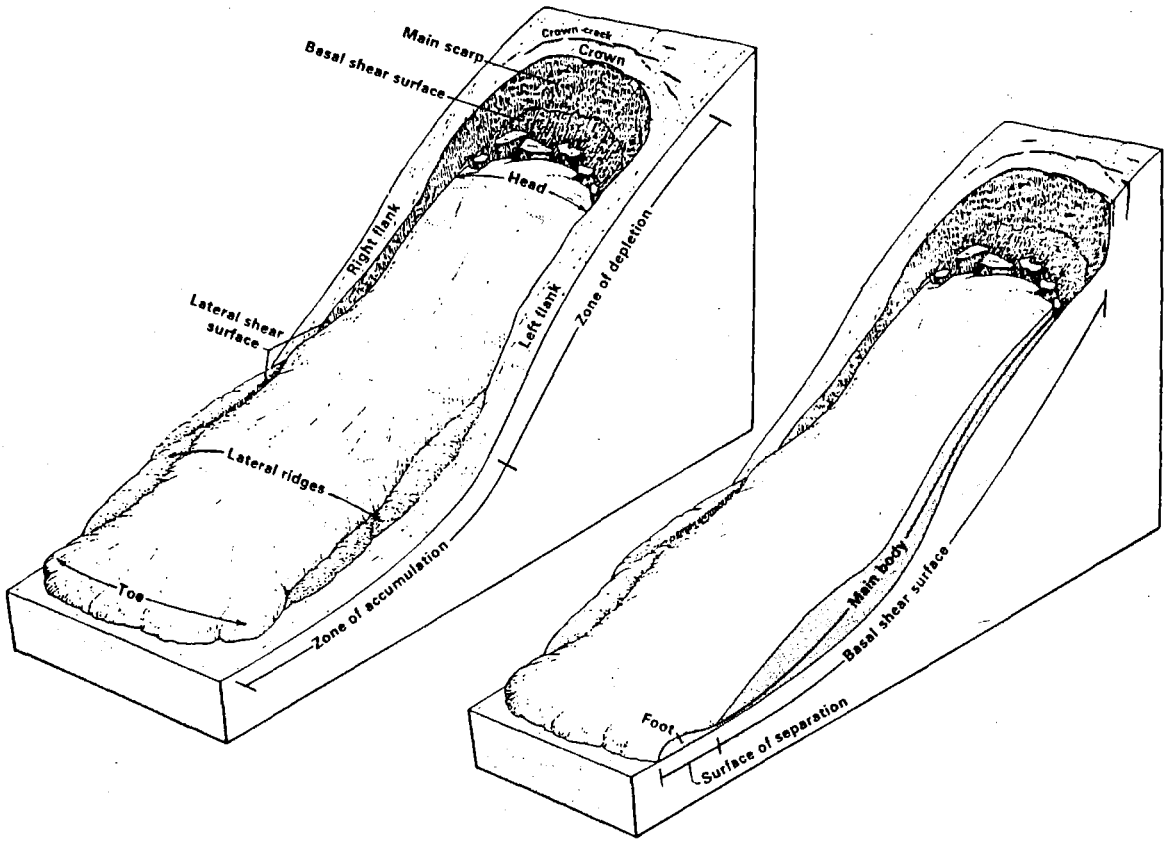

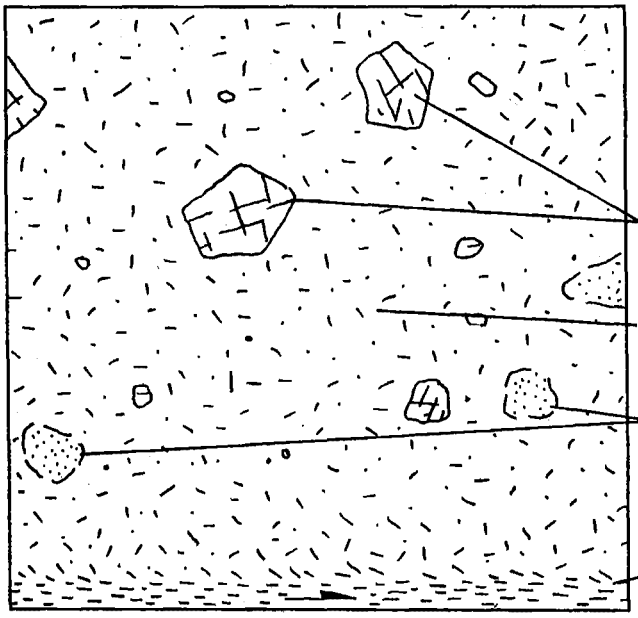

Figure 1.7 Typical earthslide fabric (modified from Brunsden, 1984; Hutchinson, 1988)

Boulder

General matrix

Lump

Basal shear zone

Clay particle orientation

depletion being concave upward and zone of accumulation convex upward. Between the accumulation and depletion zones, there may be a region where 'plug-like' movement (ie, movement of the slide as an essentially rigid body over a zone of shear) occurs. This region is known as the zone of transport or 'track zone' (Brunsden, 1984).

Slope inclinations on which earthslides occur can vary considerably depending on the climate of the region within which the earthslide is developed (see, for example, Prior et.al., 1968; Hutchinson, 1970; Hutchinson & Bhandari, 1971; Keefer & Johnson, 1983; Thomas & Kropp, 1989; Zhang et. al., 1991b). However, most slides generally occur on slopes of between 4° and 12°, but can in some instances form on slopes as shallow as 2° (Baily, 1972) or as steep as 25° (Smith 1974).

1.7.2. Distribution of Displacement

Earthslides advance chiefly by movement along discrete bounding shear surfaces (Hutchinson & Bhandari, 1971; Keefer & Johnson, 1983; Bovis, 1986; Hutchinson, 1988), of which there are two types. (a) basal shear, at the base of the sliding mass, and (b) 'lateral' or 'boundary' shears at the edges of the mass. When sufficiently large displacements take place along these shears, the adjacent clay particles become orientated along the direction of shear (Wu & Sangrey, 1978; fig 1.7), producing slickensides and striations subparallel to the ground surface in the orientation of movement. Along these surfaces the shear strength approaches, or is equal to, the residual strength (Skempton, 1964, 1985). Some internal deformation may be caused within the earthslide body by differential movement along discrete internal shear zones similar to those at the boundaries. Alternatively, internal deformation may be due a component of flow behaviour (see chapter 4). In true flow behaviour, the fastest displacements occur at the centre of the moving mass, with displacement lessening as the edges of the moving mass are approached.

1.7.3. Earthslide Complexes

Most earthslide deposits occur as parts of earthflow complexes (Keefer and Johnson, 1983). Complexes may consist of coalescing channels, they may cover large areas with hummocky disrupted topography, or may be a single sinuous channel. Within a complex a single earthslide may be formed by older deposits, but may not have the same boundaries as the older earthslides. Younger slides will commonly leave behind remnants of older slides as scarps and other features. Lateral shears formed by the younger slide can cut across older inactive shears, or they can follow these boundaries in part, or in whole. Many earthslide complexes are active only intermittently over many years or even several centuries (Hutchinson et al., 1974).

Figure 1.8 Velocity Behaviours of Earthslides. (a) from Hutchinson et. al. (1974); (b) from Campbell (1966)

(a) surge

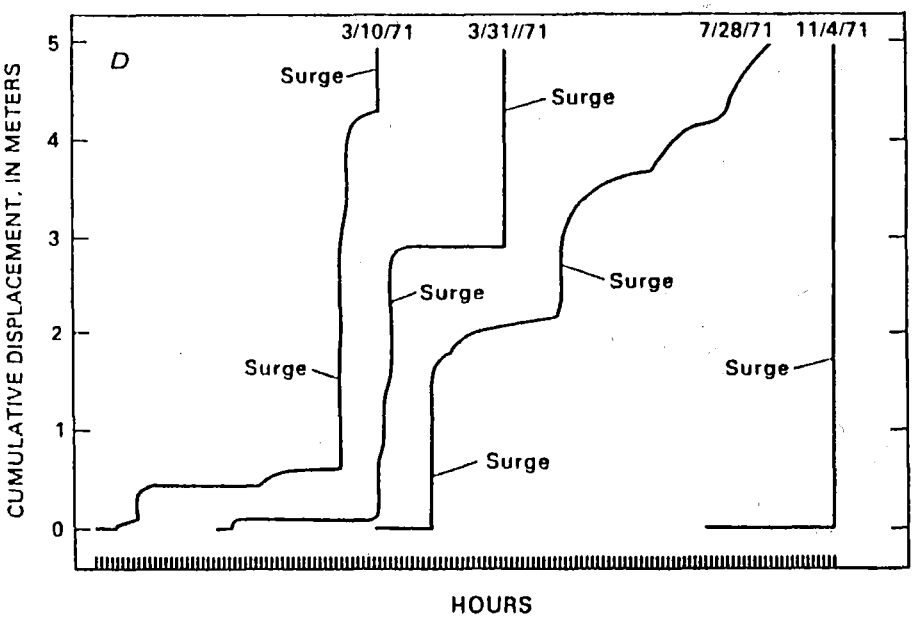

(b) relatively constant movement, periods of acceleration and deceleration

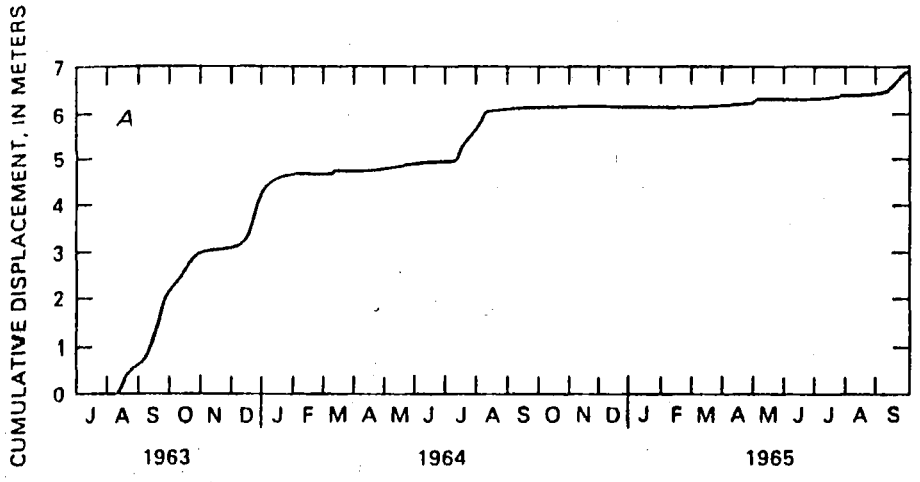

1.7.4 Composition

Earthslides generally consist of masses of accumulated debris in a softened clayey (usually a swelling clay; smectite, montmorillonite or chlorite) matrix. An idealised example of earthslide fabric is shown in figure 1.7. Earthslides are especially well developed on slopes containing stiff, well fissured clays, because of the ease with which such material breaks down to provide a good debris supply (Hutchinson, 1988). It should be noted however, that the character of the source material will be reflected in the composition of the earthslide.

1.7.5. Movement Characteristics

Earthslide movements are frequently highly seasonal, with the maximum displacement occurring during periods of high precipitation. Velocities can range from extremely slow to rapid (Varnes, 1978; see fig. 1.4(b)). Earthslides exhibit 2 basically different patterns of velocity behaviour (Keefer & Johnson, 1983). The more common pattern is one of slow movement, with relatively short periods of accelerated movement, that continues for several days, months, or years (figure 1.8 a); the less common pattern is a rapid surge of movement that lasts a few minutes. (figure 1.8 b).

In general, movement of an earthslides is reliant on the development of a forward thrust by the undrained rear part of the slide, where the basal shear surface is inclined steeply downwards (Hutchinson & Bhandari, 1971). This mechanism can enable sliding to occur on slopes considerably flatter than that indicated by back analysis, and is of particular significance where the inclination of the accumulation slide is low.

Chapter Two: Mt Vulcan Landslide Complex

2.1. Introduction

The Mt Vulcan Landslide Complex[1] (previously called 'Montserrat Landslide' by Wilson, 1963) covers an area of approximately 85 ha, and is located in Tertiary lithologies 9km southwest of Motunau beach (fig. 1). The complex has been renamed for two reasons: (i) the original station on which the complex was situated was the Mt. Vulcan station[2]; and, (ii) the complex is situated on the lower flanks of Mt Vulcan.

The Mt. Vulcan Landslide Complex displays a curved form (fig. 2.1.), and the mean slide direction near the head of the complex is nearly coast-parallel (~230°), while at the toe of the complex the direction of sliding is approximately perpendicular to the coast (~170°). The complex has a length from head to toe of 2400 m and displays a reasonably constant width (λ) from head to near the toe of about 500m. However, at the toe of the complex the width of the landslide is significantly narrower, having a value of λ equal to 300 m in this region.

Forms of slope movement observed within the complex are translational and rotational rock and/or soil slides, earthslides (as defined in chapter 1) and earthslide complexes. Slope movements which result in oversteepened rock blocks can be recognised at the downslope end of the complex.

2.1.1. Previous Work

The Mt. Vulcan Landslide Complex is shown on geological maps constructed by Wilson (1963), but these show no detail of the geomorphology of the landslide. Yousif (1987) described the landslide as a massive complex class VI slump-earthflow (using Varnes', 1978, classification scheme) but noted that rock slumps, debris slides, and earth and rock block slides occurred throughout the complex. Yousif (1987) indicated the landslide geomorphology in his study, however, this geomorphology was based entirely on aerial photographic interpretation.

---

[1]Smale et.al. (1974) used the phrase "landslide near Mt Vulcan" to describe a 4ha bedding plane failure located on the coast in this area. The term "Mt Vulcan Landslide Complex" as used in this study refers to the large complex slope movement as shown in figures 2.1 and 2.

[2]The complex is now situated on "Pacific Downs Station", which has been subdivided from the original Mt. Vulcan Station.

Figure 2.1. Vertical aerial photograph of Mt. Vulcan Landslide Complex, January 1992. Scale approximately 1:10 000. (courtesy of Mr. Ross Little, owner, Pacific Downs Station).

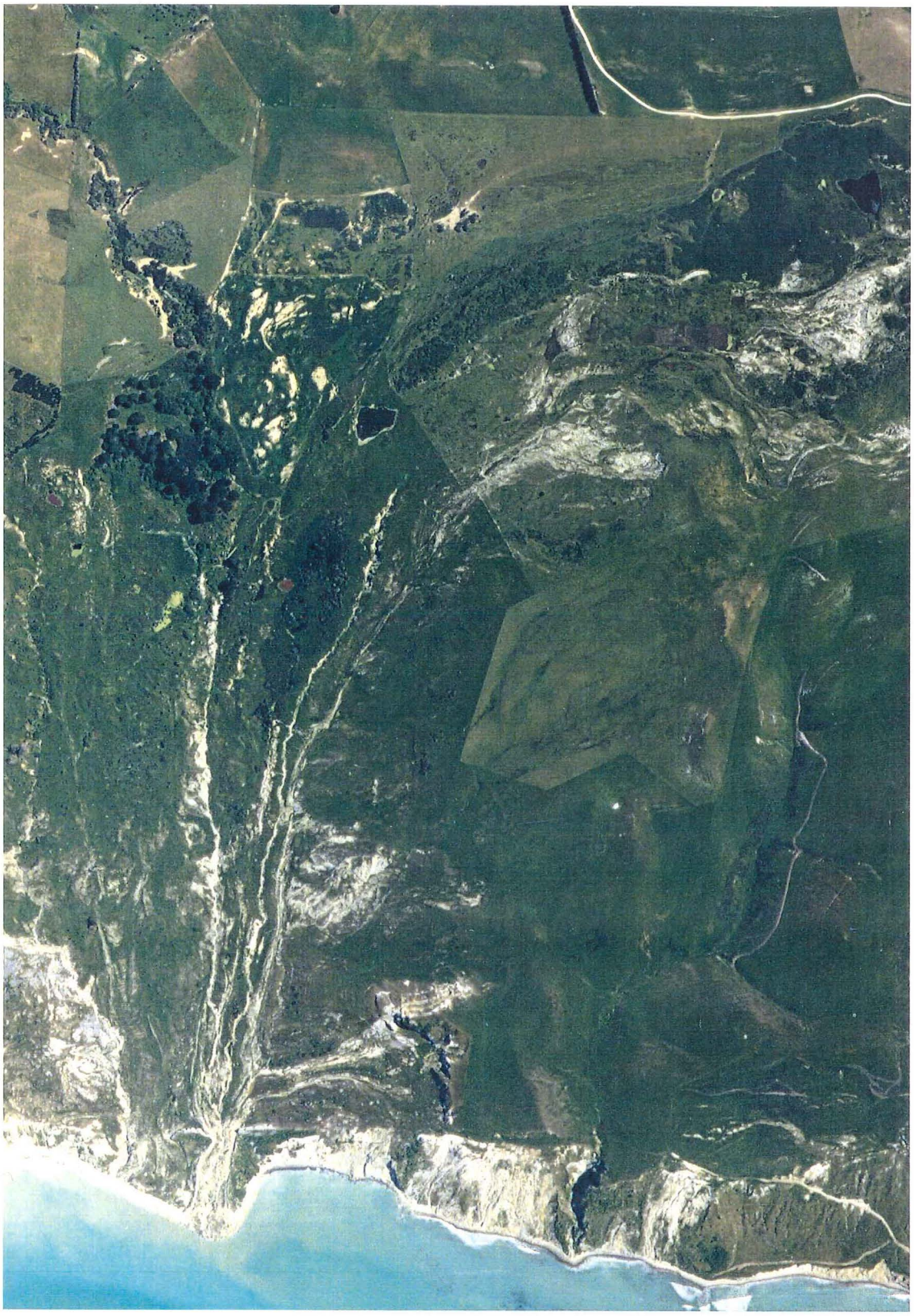

2.1.2. Chapter Objectives

The study of the Mt. Vulcan Landslide Complex comprised an initial engineering geological investigation into the nature, causes and probable development of the landslide complex. The objectives of the study were to (i) determine the geological setting of the failure; (ii) describe the geomorphology and determine areas of current activity within the complex; (iii) determine long-term movement rates (average movement rate over a period of 10 years or longer) for various areas of the complex; and (iv) derive a model for the evolution of the landslide. The particular portion of the complex herein referred to as 'Earthslide A' was examined in detail. Objectives here were to (i) describe the geomorphology of the earthslide; (ii) determine the geotechnical parameters of the slide material; (iii) conduct a theoretical stability analysis (back analysis) for the earthslide; (vi) determine failure mechanisms of the slide; and (vii) assess the pattern of probable future activity of the earthslide.

Methodology included:

1. Engineering Geological mapping at a scale of 1:2500 (fig. **2**). This map was compiled using aerial photographic interpretation and extensive field mapping.
2. Determination of long-term movement rates for various morphological units. This was achieved by determining the displacement of a recognisable feature on two sets of vertical aerial photographs.
3. Geotechnical analysis of the most obviously active downslope portion of the complex (Earthslide A), involving determination of Atterberg limits, bulk density, particle size distribution and effective shear strength parameters.
4. Stability analysis (back analysis) using the Infinite Slope (Skempton & DeLory, 1957) and the Infinite Rectangular Landslide (Hutchinson & Del Prete, 1985) Expressions to obtain values of effective residual shear strength at limiting equilibrium conditions for Earthslide A.

2.2. Local Geological Setting

2.2.1. Lithology

The downslope half of the Mt. Vulcan Landslide Complex is bounded at its western edge by calcareous glauconitic sandstones of the Omihi Formation (see chapter 1, fig. 1.3; also Appendix B) At the head and eastern boundary of the complex, a prominent (20-30 m high) lateral scarp of Amuri Limestone is apparent. The units stratigraphically below the limestone are the uppermost members of the Eyre Group (after Brown & Field, 1985), namely Ashley Mudstone/Homebush Sandstone. Massive Waipara Greensand (Stormont member; see Appendix B) is exposed along the northwestern lateral scarp (section 2.3.1.) near the head of the complex, while coarsely layered alternating strong and weak

greensand beds (Mt. Ellen member) are recognised at the toe of the landslide complex, directly under landslide debris.

Lithologies recognised within the material comprising the landslide debris are Ashley Mudstone/Homebush Sandstone, Amuri Limestone and Waipara Greensand. Ashley Mudstone was distinguished in the complex by a light brown, soft, dry to wet, silty clay/clayey silt; whereas the Homebush Sandstone lithology was identified by a light brown, dry to moist, loose sand; and the Waipara Greensand lithology was recognised as a brownish green, moist to wet, glauconitic sand. The Amuri Limestone lithology was identified as an unweathered to slightly weathered, very strong, white limestone. Ashley Mudstone (a soft silty clay) and Amuri Limestone make up the most common lithologies observed. Engineering geological descriptions of units are given in section 1.5.2 and Appendix B.

To the north of Mt. Vulcan Landslide Complex, lower members of the Eyre succession are exposed. Units exposed sequentially inland of the landslide complex are (i) Waipara Greensand, exposed immediate to the complex; (ii) Loburn Mudstone; (iii) Conway Formation, exposed in the core of the southwesterly plunging Montserrat Anticline (fig. **1**).

2.2.2. Tectonic Setting

The Mt. Vulcan Landslide Complex is situated on the eastern limb of Montserrat Anticline (fig. **1**). The Tertiary succession in the area immediate to the core of the anticline dips shallowly (5°-10°) to the southeast, but steepens to between 15° and 25° in the region of the landslide complex.

A number of faults are observed or inferred to be present in the area of the landslide complex (fig. **2**; **2B**). In particular, the Montserrat Fault (after Yousif, 1987) extends in an arc from near the toe of the complex up to near the summit of Montserrat (figs. **1**, **2**, **2b**). Wilson (1963) indicates the movement on this fault to be reverse, however, Yousif (1987) suggested that the fault may in fact be a regional slump feature. Cross-sectional construction near the toe of the complex and in the area to the west of the complex indicates that Wilson's position may be correct, however, further field mapping is needed to fully resolve this situation. Movement on the Montserrat Fault is inferred (section 2.5) to be partly responsible for the formation of the complex.

Numerous small crush zones can be observed within Amuri Limestone outcrop at the head of the complex, and on both the western and eastern boundaries of the complex at the toe. Two joint sets can be recognised in Amuri Limestone bounding the complex at its western edge. Joint set 1 has an orientation of about 100-110° and dips steeply at an

angle of 85-90°, while joint set 2 is orientated between 000 and 025° and also dips steeply, at approximately the same angles as observed for joint set 1.

2.3. Description of the Landslide Complex

The Mt Vulcan Landslide Complex was mapped in late 1993. The engineering geology of the complex is indicated in figure **2**, which was produced as a result of aerial photographic interpretation and extensive geomorphological and geological field mapping.

2.3.1. Morphological Units

The Mt. Vulcan Landslide Complex can de divided into 12 morphological units, based on the surface characteristics, location within the complex, type of movement, and current movement rate (fig. 2.2).

1. Crown Scarp: Approximately 70 m upslope from the head scarp, a small (1-3 m high) scarp is situated along a ridge crest. Open joints (joint set 2; see section 2.2.2) developed in Amuri Limestone to the southeast of the crown scarp suggest that this feature has developed as a response to stress relief, due to slumping and loss of support from material now incorporated into the landslide complex. Aerial photograph evidence (see fig.2.7) indicates that this feature has developed over the past 40 years (about) from a crown crack.
2. Head Scarp: Active retrogressive failure by slump activity (see point 5 below) has resulted in the formation of a prominent northwest-southeast trending scarp at the head of the complex. The head scarp ranges from less than one to about 10 m. in height. Lithologies exposed along the scarp from true left are (a) Amuri Limestone, (b) Ashley Mudstone/Homebush Sandstone (c) Waipara Greensand.
3. Southeastern Lateral Scarp (fig 2.3): This scarp extends from the southeast end of the head scarp and forms one boundary of the complex at the head of the landslide. The lateral scarp is situated in Amuri Limestone and has maximum height of over 20 m. The southeastern lateral scarp experiences retrogressive failure by back- or forward- slumping, toppling, and falling of limestone material along closely to widely spaced joints (joint set 2; section 2.2.2; previous page).
4. Northwestern Lateral Scarp (fig. 2.3): This unit is located within in situ Waipara Greensand, and displays a generally subdued appearance. The scarp extends southwest from the head scarp and forms the opposite boundary to the head of the complex from morphological unit 3.
5. Slumped Blocks: (i) At the northwestern end of the head scarp, a large slumped block of Ashley Mudstone/Homebush sandstone is apparent. Aerial photographic evidence shows that this block failed sometime in the period 1950-1974 (section 2.4.1). (ii) Smaller limestone rock slumps occur from the southeastern lateral scarp.

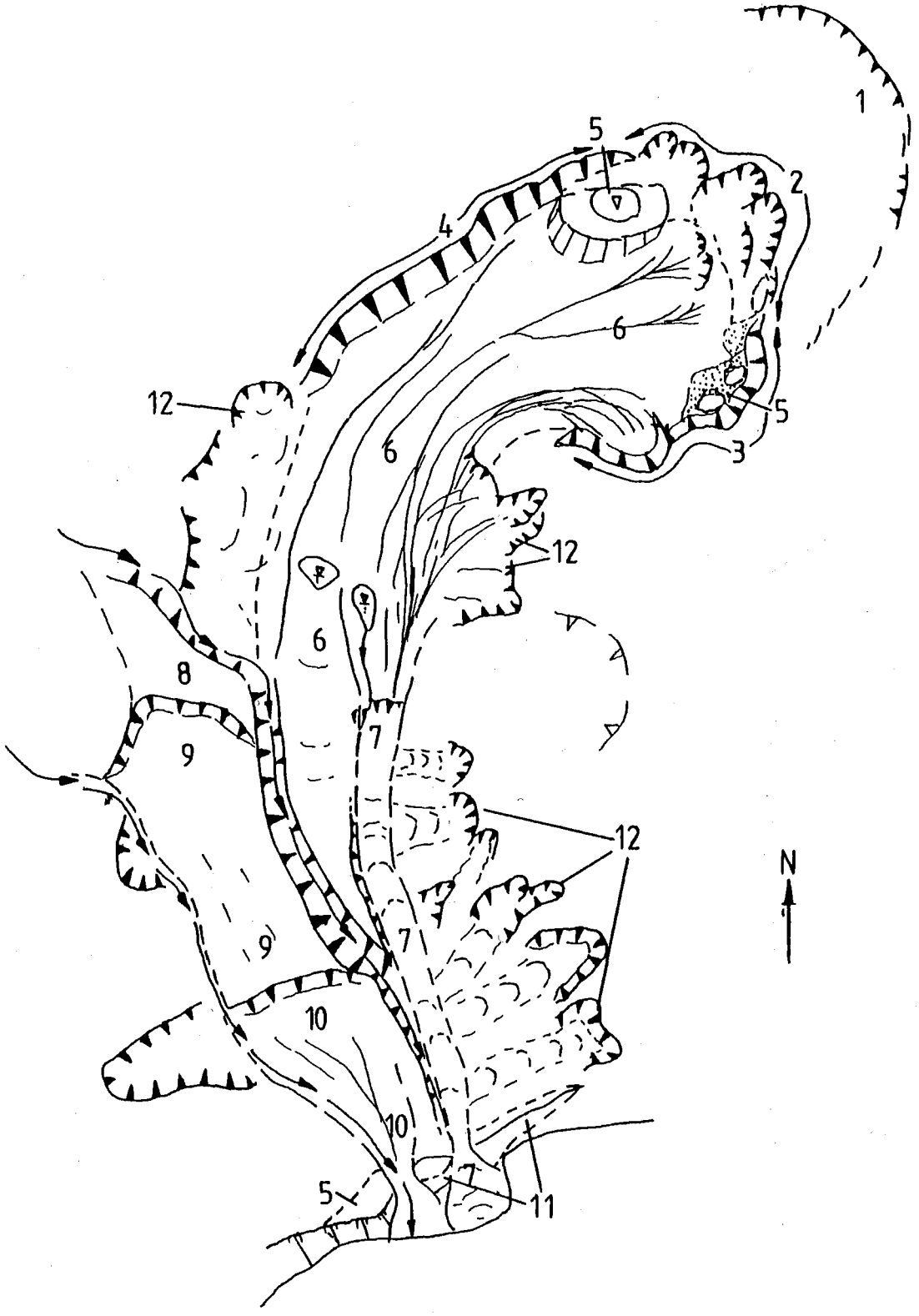

Figure 2.2 Morphological units of Mt. Vulcan Landslide Complex. Scale 1:12 500 (approx)

(1) Crown scarp; (2) Head scarp; (3) Southeastern lateral scarp; (4) Northwestern lateral scarp; (5) Slumped blocks; (6) Upper earthslide/flow complex; (7) Lower earthslide (Earthslide A); (8) Disrupted limestone debris (9) Older earthslide/flow debris; (10) Reactivated earthslide/flow debris; (11) Front-tilted toe blocks; (12) Feeder earthslide/flows.

Figure 2.3 Composite View from crown crack down the length of Mt. Vulcan Landslide Complex. Toe of complex is located adjacent to the whiteish bluff (limestone bluff) at centre of photograph in middle distance

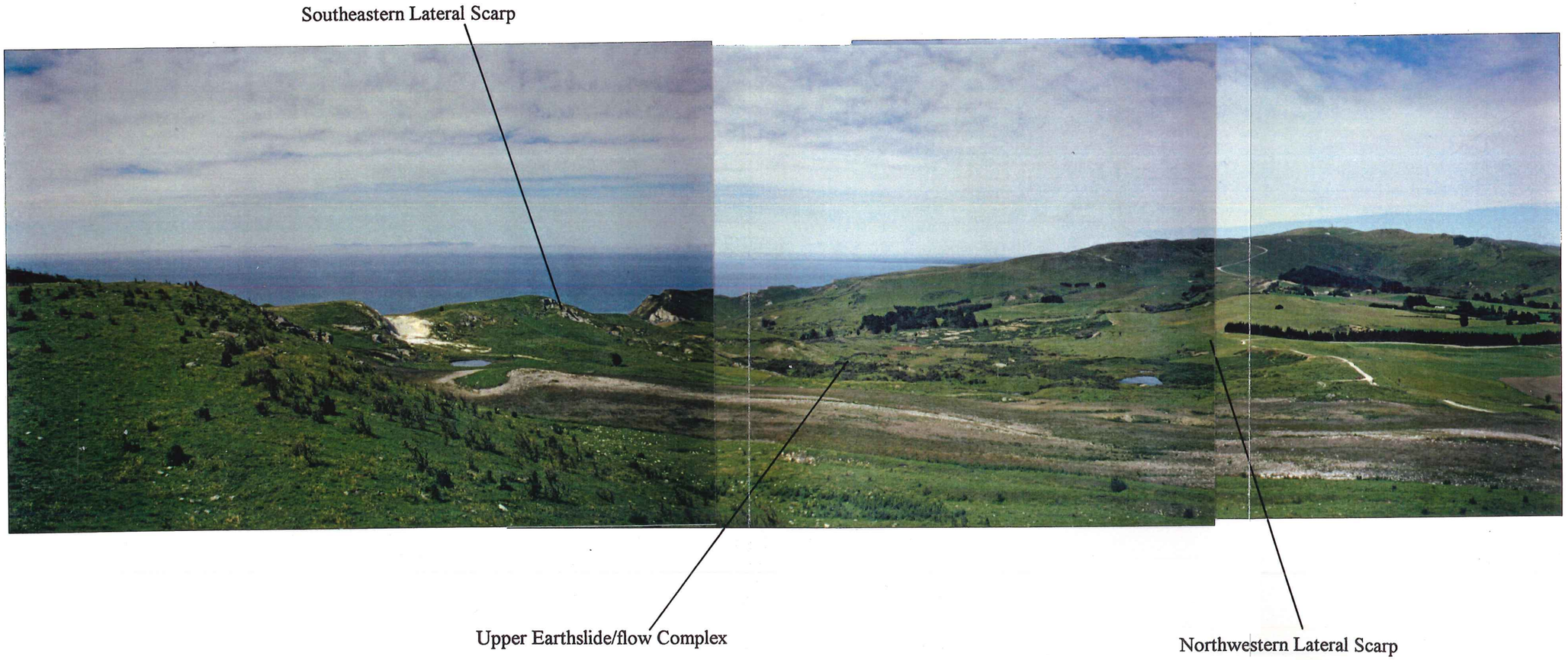

Differing rock slump blocks display various degrees of back- or forward- tilting. (iii) Large rock-block slumps can be observed on either side of the complex near the toe.

6. Upper earthslide/flow complex (fig 2.3): This morphological unit covers an area of about 25 ha and is characterised by hummocky disturbed ground, made up primarily of limestone and mudstone debris. Within the earthslide complex, movement directions and rates of movement are variable, with vegetated 'islands' displaying little or no movement, while other areas are moving at a rate sufficient for little or no vegetation to grow. Younger earthslide/flow features can be readily observed within the complex, which may be formed from older deposits, or material derived from the head scarp and/or feeder slide/flows.
7. Lower earthslide (Earthslide A; fig **2**): Earthslide A forms the eastern half of the downslope segment of the complex and moves in an approximately southerly direction. The slide is inferred to be sourced from the upper earthslide/flow complex, and displays a range of features indicative of active movement (fresh scarps, tension cracks and well-defined lateral bulges and shear zones; fig. 2.4; see section 2.6.1), particularly in the toe of the slide, where movement is inferred to be so rapid that vegetation is scarce. This morphological unit is examined in some detail in section 2.6.
8. Disrupted limestone debris: Blocks (up to 2.5 m diameter) of either internally intact or pervasively fractured Amuri limestone supported in a silty clay matrix can be observed near the eastern edge of the complex. It is likely that this material is derived from outcrop of Amuri Limestone immediately to the northwest of this morphological unit.
9. Older earthslide/flow debris: This unit forms the western half of the lower segment of the landslide complex. The upslope end of the unit is bounded by a prominent scarp composed of disrupted Amuri Limestone debris in a silty clay matrix. The older earthslide/flow debris can be recognised on aerial photographs, and is now well covered in vegetation and has degraded into an undulating slope.
10. Reactivated earthslide/flow debris: A series of small earthslide/flow features in the downslope section of the older earthslide/flow debris is interpreted as a sign of reactivation of the older debris in this area. This reactivation coincides with a steepening of slope gradient and a number of seepage points (fig. **2**).
11. Front-tilted toe blocks (fig 2.4): Near the toe of the complex, large displaced Amuri limestone blocks can be observed. These display typical seaward dips of about 50-60° (in situ limestone beds dip seawards between 15°and 25°)
12. Feeder Earthslides/flows: These features can be observed at various localities (fig. 2.4) and are generally relatively small slides that incorporate clay dominated material into the main body of the landslide complex

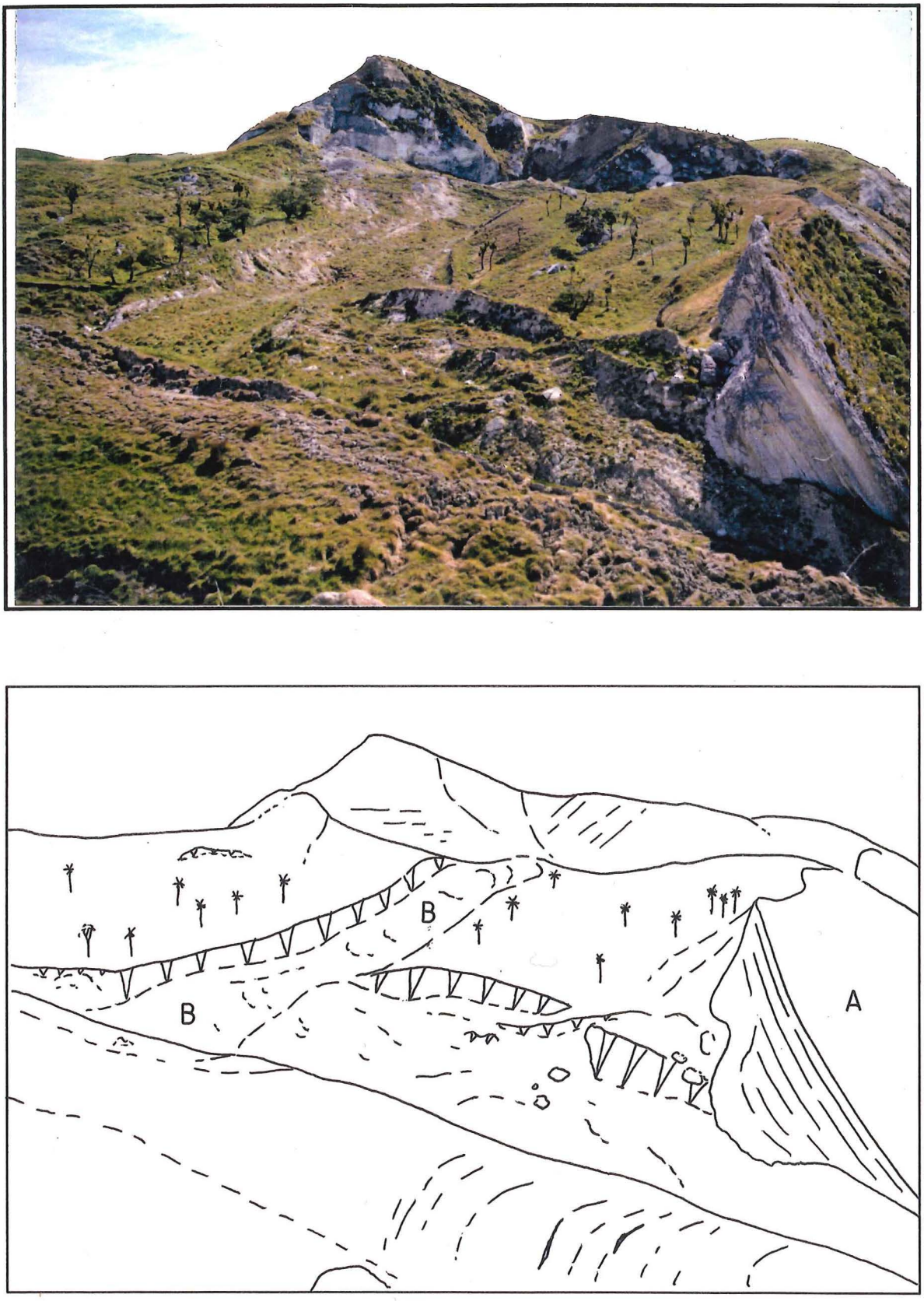

Figure 2.4. View of part of Earthslide A (bottom of photograph; note concave downslope tension cracks); (A) front tilted toe block (note characteristic oversteppening of bedding) and; (B) feeder earthslide near toe of complex. View looking approximately east from centre of complex

2.3.2. Composition of Debris

The debris comprising the Mt. Vulcan Landslide Complex can be divided into four distinct forms:

1. Earthslide[3] material, constituting an essentially massive matrix of sheared and highly deformed silty clay, containing sand (Homebush Sandstone, Waipara Greensand and sand-sized particles of Amuri Limestone) and limestone fragments of fine to very coarse gravel size. Earthslide material comprises morphological units 6 (upper earthslide/flow complex); 7 (lower earthslide); 9 and 10 (older and reactivated earthslide/flow debris respectively) and 12 (feeder earthslide/flows). The matrix generally comprises 65-85% of the soil mass in the earthslide complex and lower earthslide, while in the older and reactivated earthslide debris, the matrix constitutes about 50% of the soil mass.
2. Disrupted limestone, comprising of blocks (up to about 2 m diameter) of Amuri Limestone, either internally intact or pervasively fractured. Material between blocks is typically fine sand to chaotically arranged boulder-sized, generally well graded and matrix supported limestone fragments. The matrix is consists of silty clay, and typically comprises 25-35% of the soil mass. Disrupted Limestone comprises morphological unit 8, and in conjunction with large limestone blocks (note 3, below) forms the rock-block slumps (morphological unit 4) immediately below the southeastern lateral scarp.
3. Limestone megablocks (greater than 5 m diameter). These blocks are generally internally intact, and may be supported by disrupted limestone material (described in note 2, above). Amuri Limestone megablocks surrounded by disrupted limestone material forms morphological unit 5 (slumped blocks) while morphological unit 11 (front-tilted toe blocks) has little disrupted limestone material.
4. Greensand-rich material, occurring either as loose to stiff masses of intact sandstone or as individual particles within a softened brownish matrix (sourced from Ashley Mudstone; see section 2.6.3). Field mapping and soil sampling indicates that this lithology is present in: (i) the upper earthslide complex (morphological unit 6); (ii) the lower earthslide (morphological unit 7), (iii) both the older and reactivated earthslide/flow debris (morphological units 9 and 10); and (iv) feeder slide/flows located along the true right[4] (generally western) lateral margin of the complex (morphological unit 12).

---

[3]The term 'earthslide' differs from that of Varnes (1978) , and is defined in chapter 1, see also discussion in chapter 4

[4]The 'true' direction is taken facing downstream.

2.4. Movement Rates

As adequate aerial photographic evidence is available for the Mt. Vulcan Complex (ranging from 1950-1993; see Appendix B) it is possible to surmise the long-term movement rates for various morphological units. Two sets of aerial photographs cover the Mt. Vulcan Landslide Complex (taken in 1959 and 1974; see Appendix C) and aerial photographic interpretation indicates considerable change in the landslide morphology between the two photographic runs (fig. 2.5). Additionally, an aerial photograph was taken of the complex in 1992 (shown in fig. 2.1). However, limited geomorphic interpretation could be conducted on this photograph, due to the lack of a stereo-pair.

2.4.1. Head Scarp

Aerial photograph runs taken in 1950 and 1974 indicate that on-going retrogressive slumping of substantial blocks of limestone or soil (Ashley Mudstone/Homebush Sandstone and/or Waipara Greensand) is the main mechanism of scarp retreat. A recent example of slumping evidenced between the two aerial photograph runs occurred predominantly within Waipara Greensand at the northern end of the head scarp (Fig. **2** and 2.5). It is surmised that for the period 1950-1974 the scarp retreat was about 1.6 m/yr, although due to the nature of head scarp retreat, (periodic rock/soil block slumps) this retreat rate is subject to a large degree of variability. The indicated retreat rate for the period 1974-1992 was less than 0.5 m/yr.

2.4.2. Earthslide/Flow Complex

Directions of movement within the complex are variable: some areas of the complex display morphological features consistent with movement, while scrub-covered 'islands' display little or no evidence for movement. It was not possible, however, to measure the long-term rate of retreat for this morphological unit as (i) the unit has displayed a considerable change in surface morphology in the period covered by the aerial photographs (fig. 2.5); and, (ii) no feature could be recognised on both the 1950 and 1974 aerial photographic runs.

2.4.3. Older Earthslide/Flow Debris

On the basis of surface morphology, this morphological unit is surmised to be relatively stable. Long term movement rates determined from a prominent boulder located in this morphological unit indicated insufficient movement to recognise a displacement on the 2 sets of aerial photographs. As the minimum offset required to determine any change between the 2 sets of aerial photographs is in the order of 6 m, (Appendix B) a maximum rate of displacement 0.25 m/yr is indicated.

Figure 2.5 Interpretative changes in surface morphology of Mt. Vulcan Landslide Complex, 1950 to 1974. Scale for both A and B approximately 1:12 500.

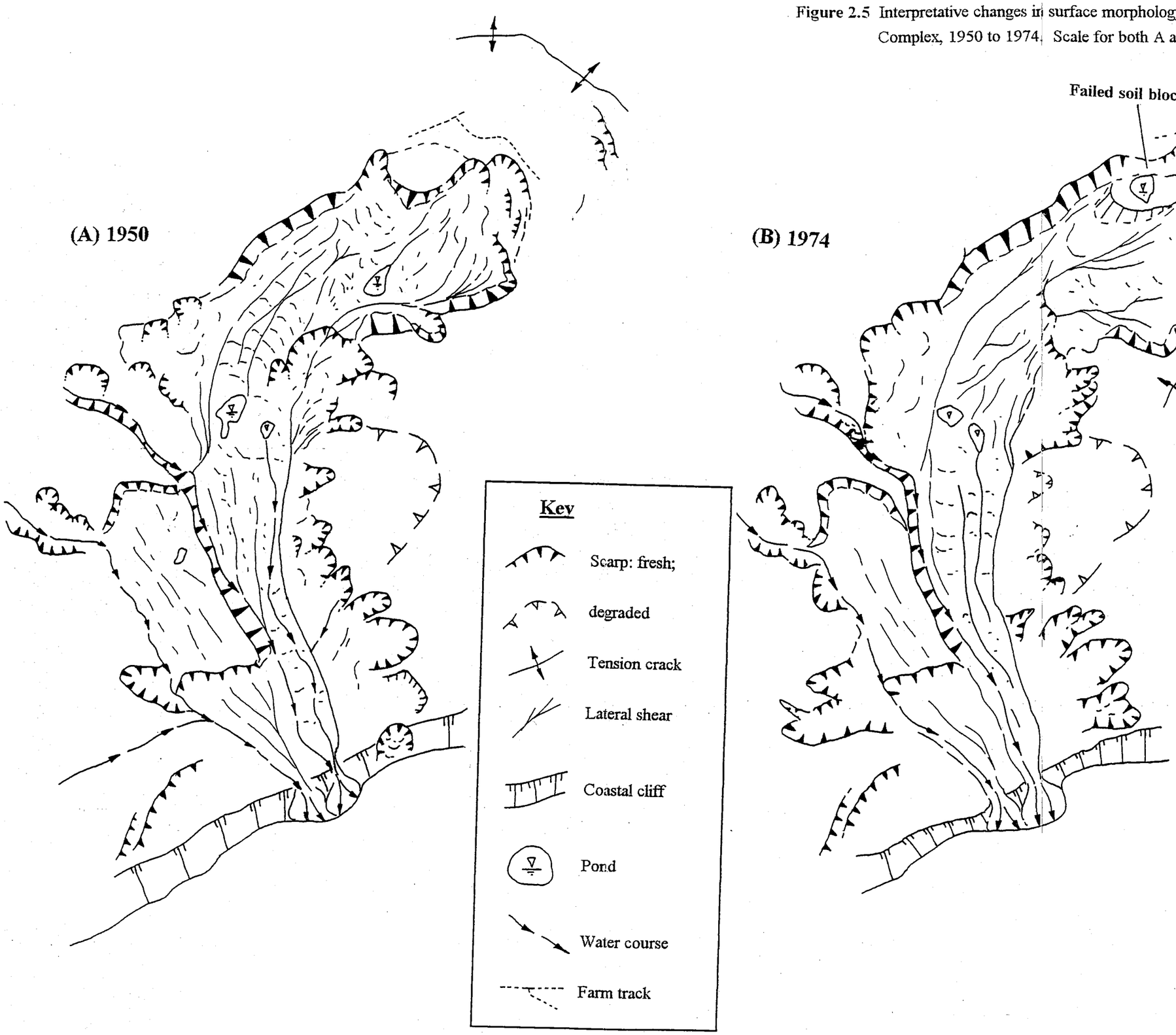

2.4.4. Reactivated Earthslide/Flow Debris

A series of scarps located in the older earthslide/flow debris (fig. 2 and 2.5) indicates that material comprising the older debris has been subject to reactivation. Long term movement rates determined for this morphological unit (again by recognition of a prominent boulder located in this unit on the two sets of aerial photographs) indicates a long-term movement rate of about 0.9 m/yr.

2.4.5. Earthslide A

Because of its surface morphology, Earthslide A is inferred to be the most active portion of the complex as a whole. However, due to the large time period between successive aerial photographic runs, and the substantial changes in surface morphology of the earthslide in this time, it was not possible to determine long-term movement rates.

2.5. Failure Mechanisms and Development of Landslide Complex

There is no means of quantifying the age of formation of the Mt. Vulcan Landslide Complex, however if it can be assumed that the head scarp retreat rate has maintained a rate in the past similar to the current rate (0.5 m/yr), over a landslide length (L) of 2400 m, the indicated age of formation of the complex would be about 5000 b.p. However, it is unlikely that head scarp retreat rate has remained constant with time (due to climatic and tectonic variation), and therefore a considerable margin of error is associated with this age. An age of 5000 b.p denotes the likely minimum age of formation of the complex. A maximum age is difficult to infer, although an age of formation of around 100 000 b.p is inferred for the Coringa Landslide Complex (see section 3.4) and it is possible that the Mt. Vulcan Complex has a similar age of formation.

The inferred development of the complex is as follows: (fig 2.6)

1. Initial thrust movement on the eastwardly dipping Montserrat Fault. It is inferred that movement on the fault plane in the area of the landslide complex (about 20m) is less than that further along the fault plane (calculated to be about 50 m).
2. Erosion (probably due to wave action) on the up-thrust side removed lateral support from the limestone, which was subject to a force from the upslope mass.
3. Failure along inferred closely spaced joints (joint set 2; see section 2.2.2) or possible crushed/sheared zones within Amuri Limestone allowed movement of the Ashley mudstone material A compressive force derived from mobilised Ashley mudstone material upslope caused a turning moment on limestone blocks on the upthrust side of Montserrat fault. Continued sliding /flowage from upslope effectively 'bulldozed; and pushed these blocks up into an oversteepened state.
4. Gradual headwards retreat of the slide, with slumps occurring at the head zone and slide/flow occurring downslope of this. The slide developed a curved form due to

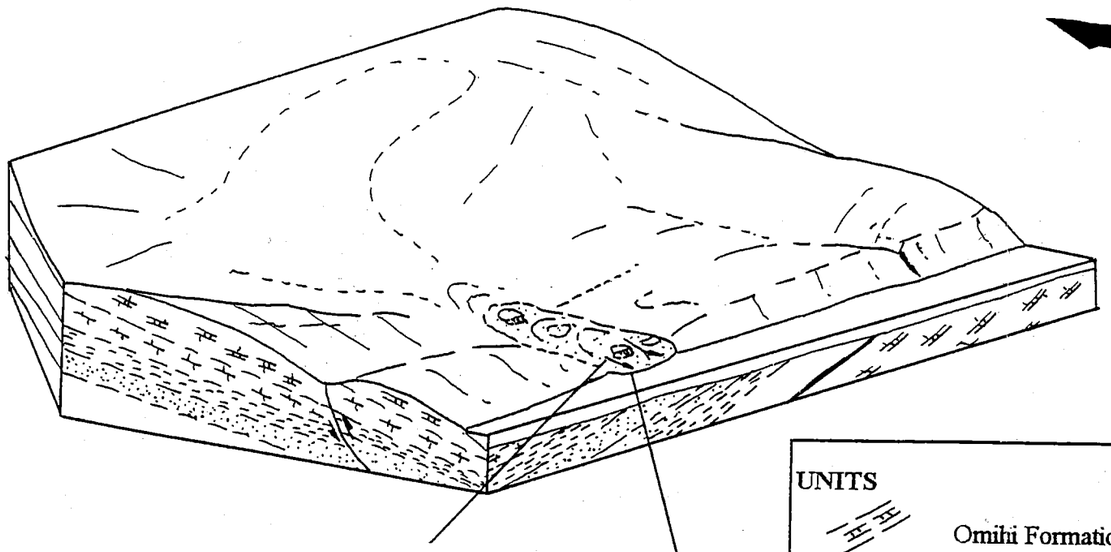

1. Uplift on Montserrat fault; development of minor earthslides/flows. Movement of front-tilted toe blocks (morphological unit 11).

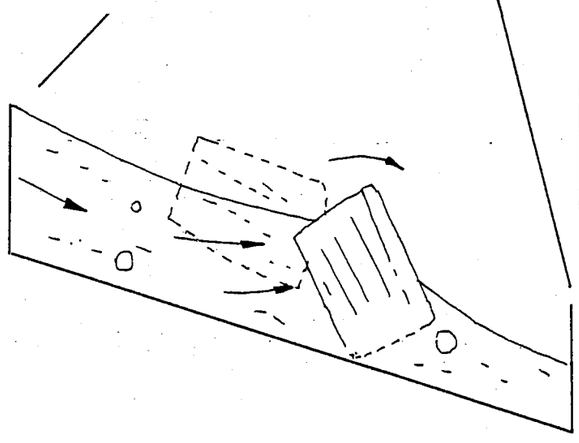

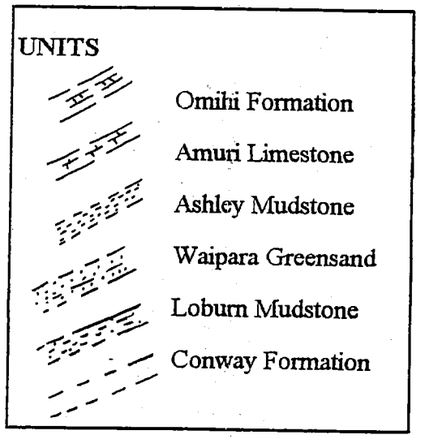

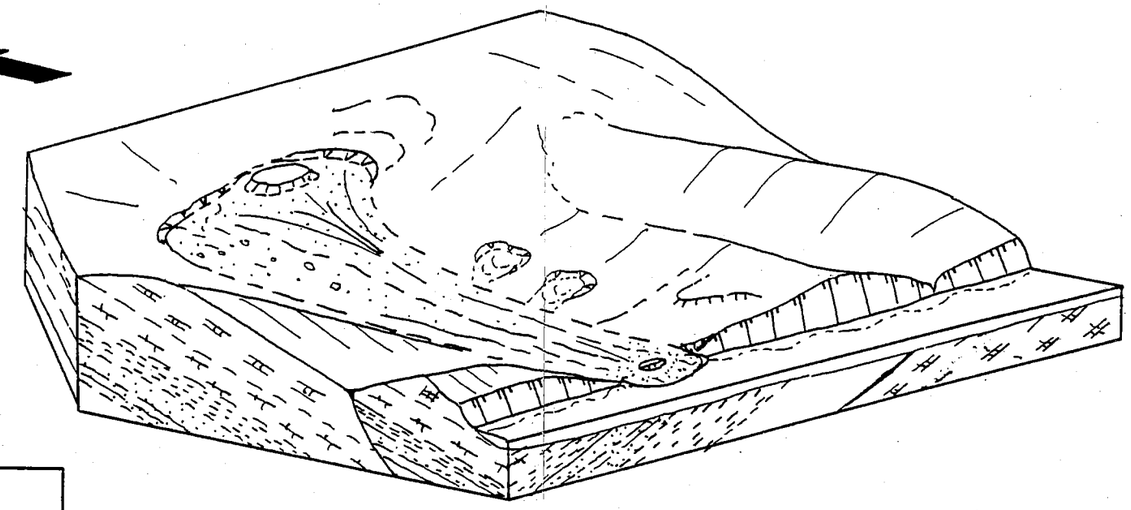

2. Gradual headwards retreat of by slumping, with subsequent slide motion occuring downslope. Movement and formation of older slide debris (morphological unit 9). Gradual swing of head zone to the east

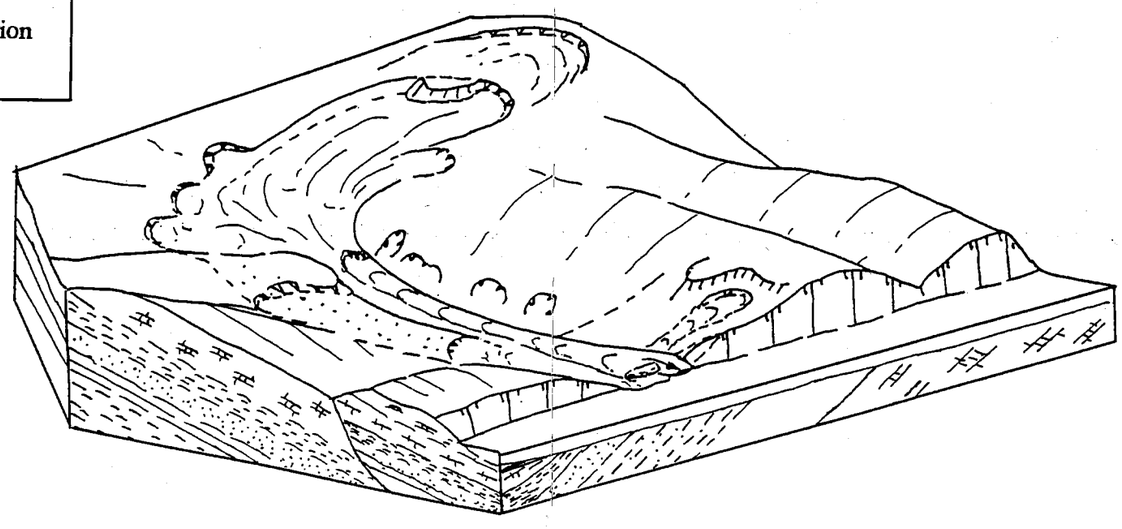

3. Development of Modern day morphology: note remnant material on western side of complexsion; development of upper earthslide/flow complex (morhological unit 6); Earthslide A (unit 7).

Figure 2.6 Interpretation of development of the Mt. Vulcan Landslide Complex
Arrow gives approximate north, scale 1: 25 000 (approx)
(note that for simplicity, diagrams are partly schematic)

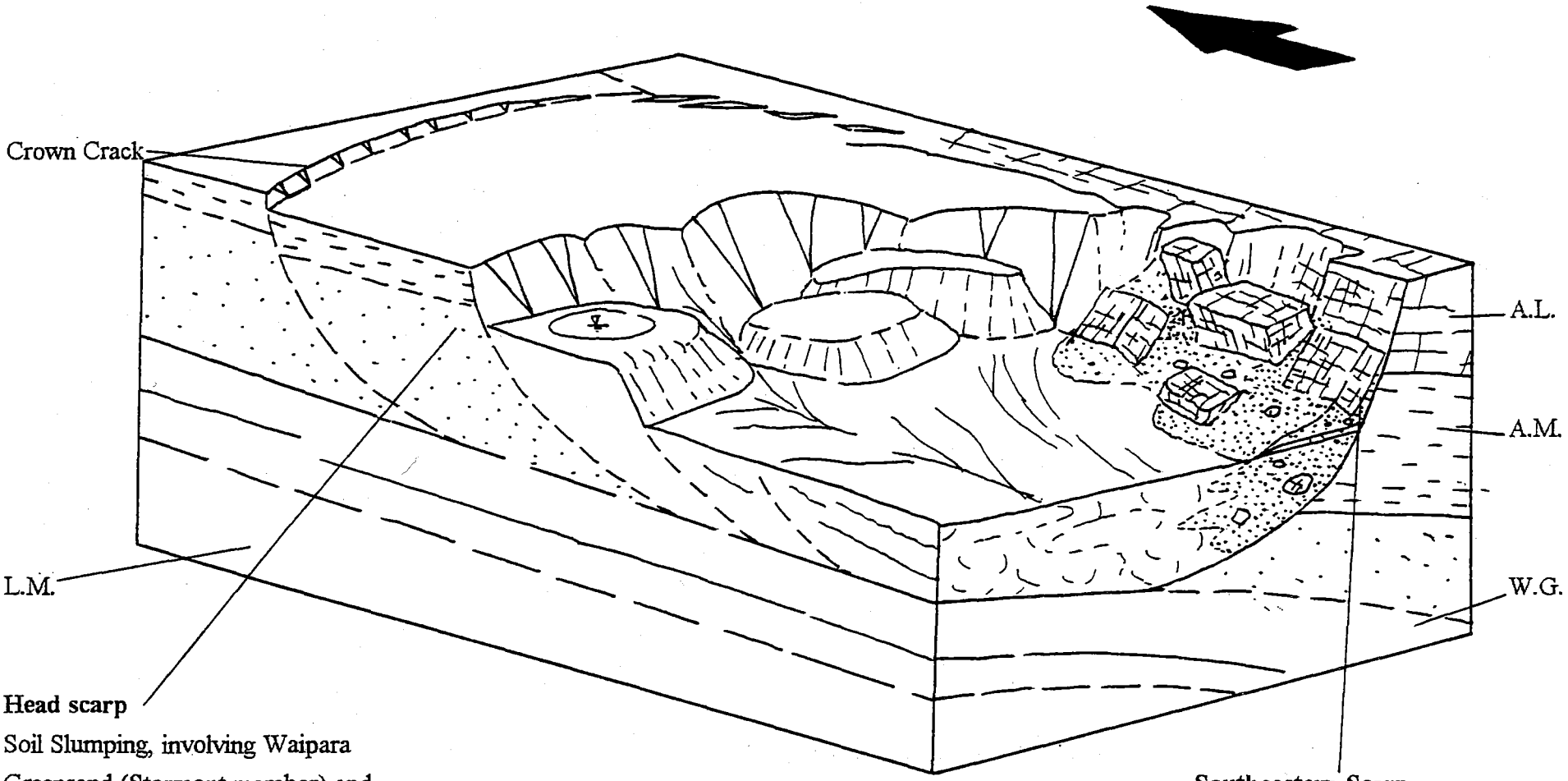

Figure 2.7. Schematic diagram of failure methods of Mt. Vulcan Landslide Complex. (Arrow shows approximate north; scale approx. 1:2750)

headwards migration following the bedding plane of the Amuri limestone ridge. A generally uniform dip direction of approximately southwest in the area of the complex is inferred to be responsible for the eastwardly curved form of the landslide. On the eastern side of the complex, topography controls mean that the dip direction is obliquely downslope (and therefore in an attitude likely to fail), whereas the character of topography on the west side of the complex means that the dip direction is into the hill. (an unfavourable attitude to produce failure; see fig 2.6)

5. As the head region rotated to a coast parallel attitude, and experienced a decrease in debris supply, it is inferred that remnant material was left on the outside of the curve (fig. 2.6). This material is represented by the older earthslide/flow debris.
6. Mobilisation of Ashley mudstone material from outcrop is inferred along the south eastern boundary of the landslide complex. Feeder slides/flows (morphological unit 12; section 2.3.1) and shallow slumping are evidence of this.

The head region of the complex is inferred to be primarily a deep-seated failure, whereas the lower half of the slide is likely to be a sliding/flow on a continuous slide plane, inferred to be located within Waipara Greensand. It is inferred that the Waipara Greensand is essentially massive near the top of the unit, while strong layers are located near the base of the unit. This inference is in keeping with the position of Brown & Field (1985). The upper member of the greensand unit (Stormont member; Brown & Field, 1985; see Appendix B) is inferred to fail at the head scarp by rotational slide-type movements. Strong to very strong decimetre thick layers near the base of Waipara Greensand (Stormont member; Brown & Field, 1985) are inferred to act as a rupture surface for the landslide. At the toe of the complex, reactivated earthslide/flow debris can be clearly seen overlying in situ beds of alternating weak and strong greensand (section 2.2.1).

The failure mechanism at the head scarp of the complex is inferred to involve rotational sliding of : (i) large blocks of Amuri Limestone from the southeastern lateral scarp, with or without a component of rotation, on convex upwards shear surfaces developed within Ashley Mudstone (fig. 2.7). Progressive downward and outward creep of failed blocks results in gradual destruction of the block, by fracturing of the failed block along closely spaced internal defects and; (ii) large soil blocks of the Mt. Ellen member of the Waipara Greensand, as evidenced in section 2.4.1.

2.6. Analysis of Earthslide A

2.6.1. Morphology

Earthslide A (morphological unit 7) originates near the inside corner of Mt. Vulcan Landslide Complex, and has a length from head zone to toe of approximately 1050 m.

The width is rather constant along the length of the slide, being approximately 90 m. On figure **2** it can be seen that the head zone of the earthslide is at an elevation of 145m, while the toe is at sea level. Over a earthslide length (L_e) of 1050 m, an average earthslide surface inclination (β) of about 8° is realised.

The head zone of Earthslide A is marked by a prominent scarp, and is located directly downslope of the earthslide/flow complex. Material from the complex is continually being fed from the head zone to the main body of the earthslide by small slumps and slides.

A track zone extends from the bottom of the head zone to the toe of the complex, at sea level. The movement direction within the track zone is approximately 180° near the head of the earthslide, and swings through to about 160° at about half way down the slide. This movement direction is then followed to the earthslide toe. While the average surface inclination (β) of the earthslide is about 8°, observed surface inclinations on the track zone range from near horizontal to over 12°. Approximately 200 m upslope from the end of the earthslide, the surface inclination steepens to about 10°.

At about 175 m from the earthslide toe, the track zone experiences a 'constriction' as it passes between two large front tilted limestone blocks (morphological unit 11). On either side of the constriction, the earthslide width (λ_e) is slightly less than 60 m wide whereas the value of λ_e within the constriction is only 25-30 m (fig. **3**). The earthslide bulges markedly upslope of the constriction, and as the slide moves through the constriction, it experiences a steep surface inclination, resulting in a sinusoidal cross-section (fig. 2.8). Vegetation downslope of the constriction is sparse, usually occurring as part of a disrupted 'raft' of material.

The surface of the earthslide is generally marked by hummocky, undulating ground, and in a few places by the development of tension cracks orientated across the earthslide (perpendicular to the sliding direction). These tension cracks are concave in the direction of sliding. Tension cracks of this type occur where the earthslide experiences a change in slope gradient (fig. 2.9; see also fig. 2.4)

No accumulation zone is apparent on the earthslide, due to rapid erosion at the toe by wave action. Wave action also provides an impetus for continuing movement of the earthslide.

2.6.1.1. Characteristics of Surface Boundaries

The lower earthslide is bounded at its eastern and western edges by well developed lateral shears. In several places, lateral bulges could also be observed. No information

Figure 2.8 Interpretive cross section through earthslide constriction near the toe of Earthslide A. Scale 1: 500 (approx)

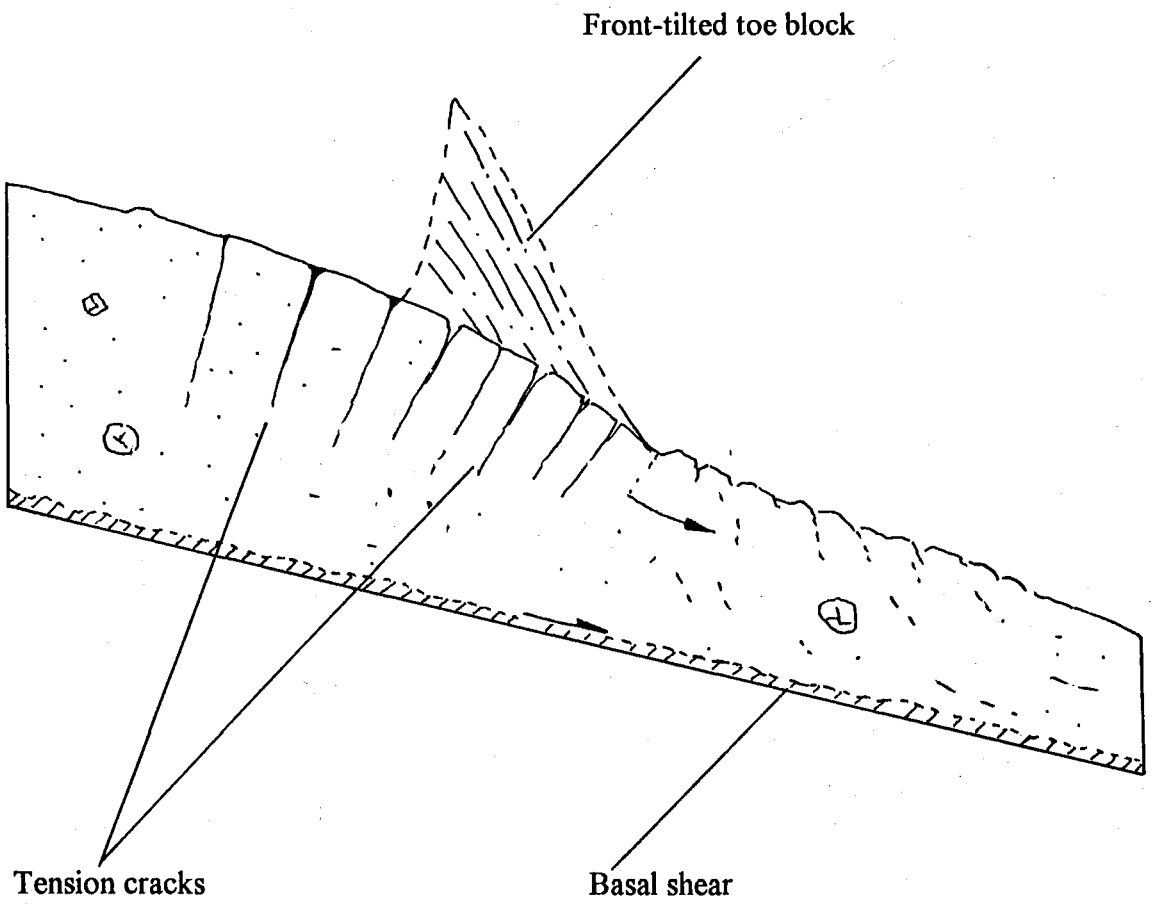

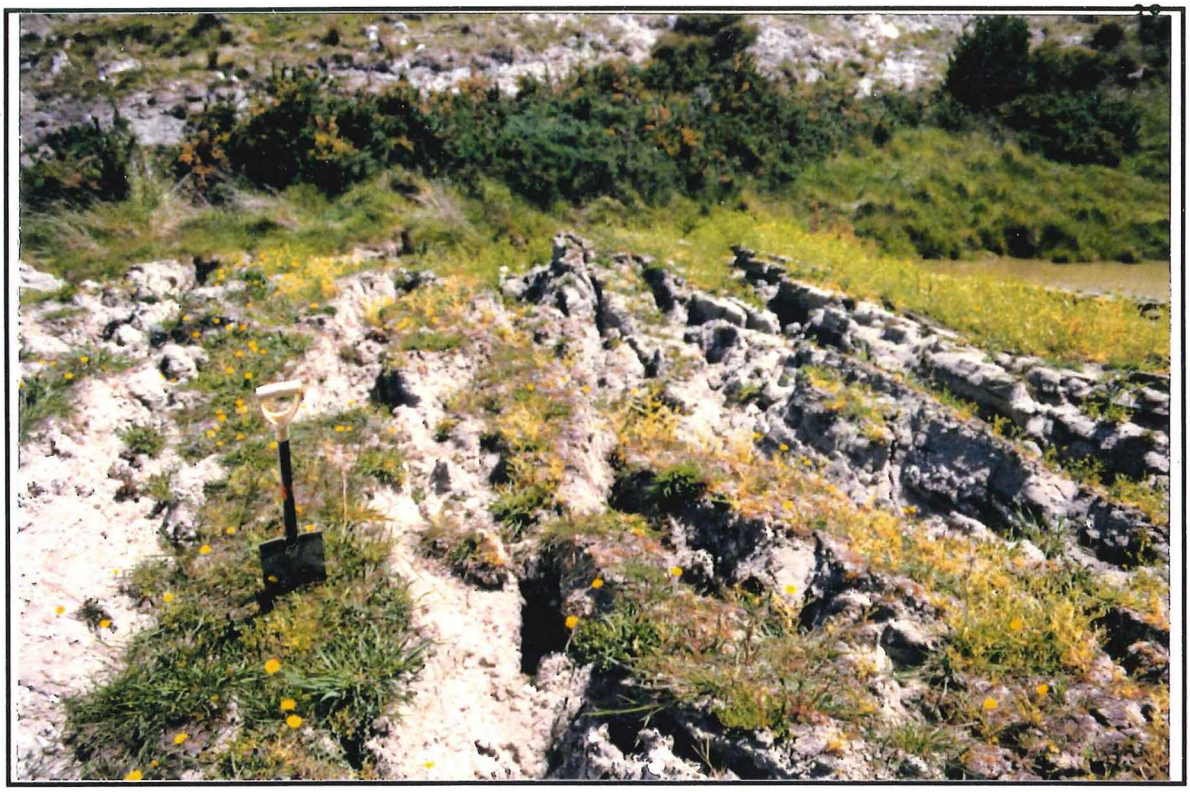

Figure 2.9 Transverse tension cracks, associated with a convex break in slope, Earthslide A, Mt. Vulcan Landslide Complex. Sliding direction left to right.

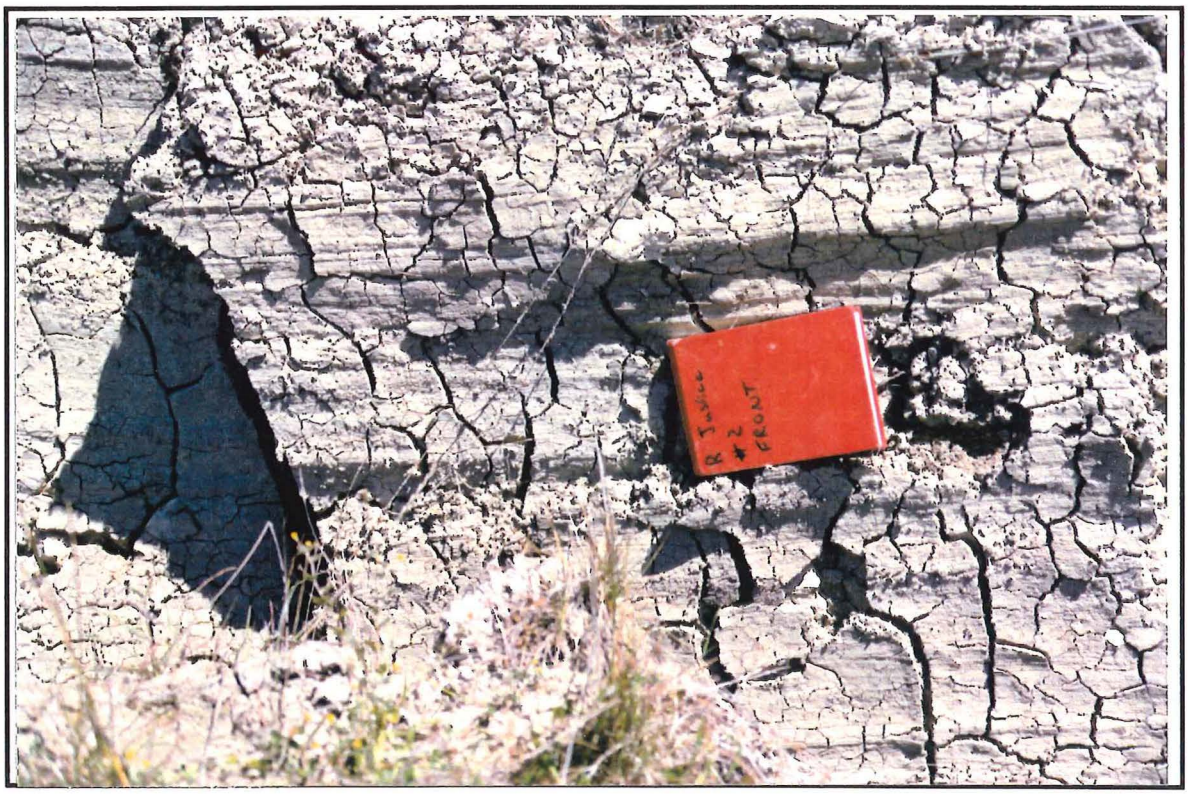

Figure 2.10 Striations and slickensides associated with eastern lateral shear, Earthslide A., Mt. Vulcan Landslide Complex (note shrinkage cracks typically associated with swelling clays). Notebook 18x13cm

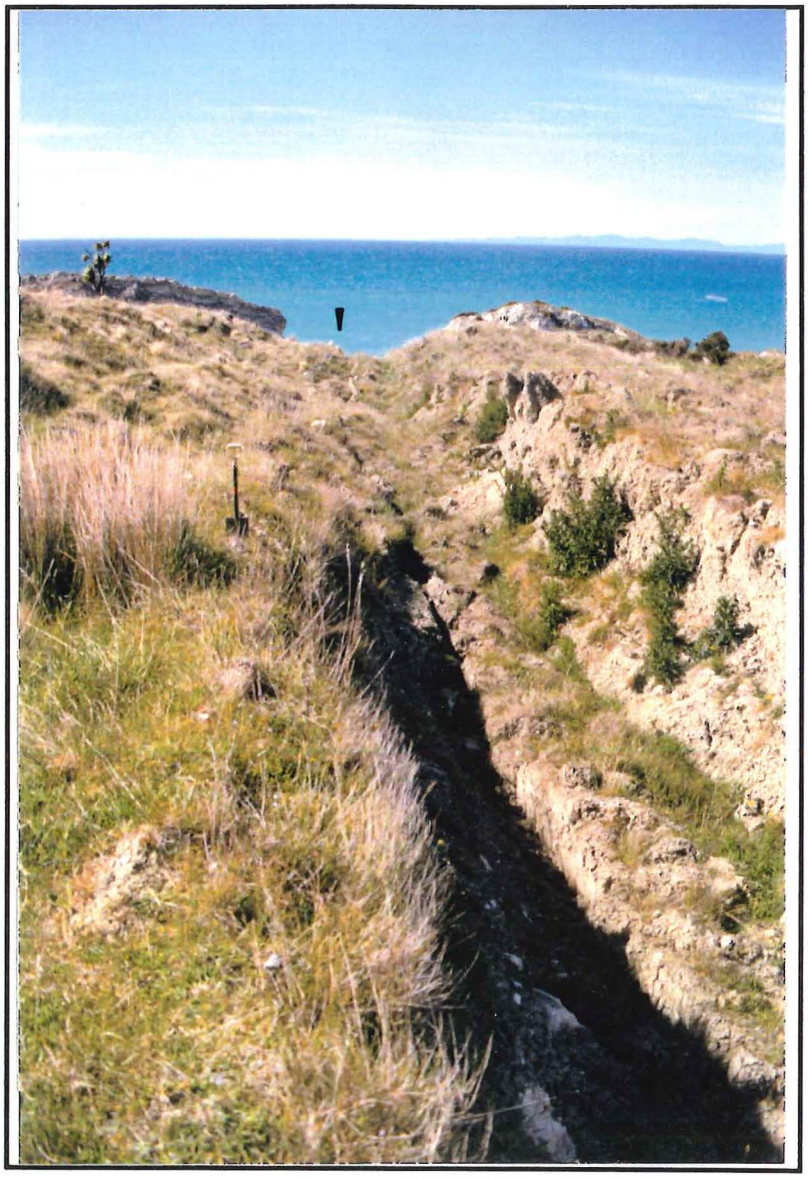

Figure 2.11 Fully developed Eastern Lateral shear (arrowed) and associated lateral bulge. Earthslide A, Mt. Vulcan Landslide Complex. Note front-tilted limestone blocks in middle distance.

could be obtained about the nature of the basal shear surface, due to the lack of subsurface data.

A Lateral Shears

Lateral shears bounding Earthslide 3 commonly display slickensides and striations subparallel to the ground surface in the orientation of movement (fig. 2.10). The most common features observed along the lateral shear zone of Earthslide 3 were tension cracks orientated approximately 45° clockwise or anticlockwise respectively from the trend of the underlying dextral or sinistral shear. Tension cracks commonly displayed an en-echelon arrangement. Shear segments along the lateral shear could also be observed, which have the same sense of shear as the main lateral shear, but are turned clockwise or anticlockwise from a few to about 20° from the main shear. Well developed, very linear shears could be noticed at various localities along the boundary of Earthslide 3. In particular, the downslope half of the earthslide was characterised by these well developed linear shears (fig. 2.11). Generally, a saturated zone of about 10 cm in width was associated with these lower lateral shears.

B Lateral Bulges

Lateral bulges of up to 1.5 m in height can be noticed at a number of localities along both lateral shear zones. The bulges are located immediately adjacent to, but on the displaced side of, the lateral shear zones (fig. 2.11). The length of these bulges ranged from about 30 m to over 100 m.

2.6.2. Composition of Earthslide Material

Material within the earthslide comprises a sheared and highly deformed matrix of mud (silty clay/clayey silt; see section 2.6.3.3), within which fine to coarse sand (Homebush Sandstone, Waipara Greensand and sand-sized particles of Amuri Limestone) and limestone gravels ranging in size from fine to very coarse occur. The matrix comprises 65-85% of the earthslide soil mass. Occasional 'lumps' of stiff brown clay (sourced from Ashley Mudstone), brownish green sand (sourced from Waipara Greensand) and larger blocks of intact Amuri Limestone (up to 2.5 m. diameter) can be observed within the earthslide material. Large blocks of Amuri Limestone are in evidence at the toe of the earthslide, having been exposed due to the erosion and removal of the surrounding finer material.

2.6.3. Geotechnical Analyses

A suite of geotechnical analyses were conducted on samples from the Earthslide A. Eight bulk samples were obtained from localities on the earthslide as shown on figure **2**. Note that near the earthslide constriction, the sample names have been omitted to retain a degree of clarification. MVL 1 is located on the true left lateral shear, and MVL 2 on

the right. All samples were, by the nature of acquisition, disturbed, and no attempt was made to obtain undisturbed samples. Results of the analyses performed are given in table 2.1

2.6.3.1. Natural Water Content, Atterberg Limits and Linear Shrinkage

A Water Content

The water content (w) of a soil is the ratio of the mass of water to the mass of solids in the soil (Kenney, 1984; Craig, 1992; see Appendix D). Water contents were determined for the eight sample localities on the Earthslide A. It can be seen (table 2.1) that samples of lateral shear material showed significantly higher water contents (40-50%) than those of general earthslide debris (30-35%).

B Atterberg Limits

"Atterberg limit" is a collective term that encompasses both the plastic and liquid limits. The upper and lower limits of the range of water content over which a soil exhibits plastic behaviour are defined as the liquid limit (w_L) and the plastic limit (wP) respectively. The difference between w_L and wP is defined as the plasticity index (Ip)

Liquid limits for material comprising the lower earthslide were in the range 65-78%, while plastic limits ranged between 29% and 38%. Correspondingly, Ip values ranged between 34% and 42%.

2.6.3.2. Bulk Density and Soil Unit Weight

The bulk density (ρ) is the ratio of the total soil mass to the total volume. Because of the nature of acquisition of soil samples, samples used in the analysis of the bulk density were recompacted before the experiment was performed. Bulk densities were found to range between 1654 and 1976 kg/m^3, with an average value of ρ equal to 1792 kg/m^3.

Soil unit weight (γ) is calculated from the expression $\gamma=\rho g$, where g is the acceleration due to gravity (9.8 m/s^2; Craig 1992). Accordingly, values of γ for the lower earthslide range between 1.62 and 1.93 kN/m^3, while the average soil unit weight is equal to 1.76 kN/m^3.

2.6.3.3. Grainsize Analysis

Analysis of grainsizes were performed using wet and/or dry sieving and pipette analysis for mud fractions. Tests were performed in accordance with NZS 4402 (see Appendix

Sample Name	Moisture Content (%)	Index Properties			Linear Shrinkage (%)	Bulk Density (kg/m^3)	Particle Size			Effective shear parameters (ring shear analysis)	
		Liquid Limit (%)	Plastic Limit (%)	Plasticity Index (%)			Sand Fraction (%)	Silt Fraction (%)	Clay Fraction (%)	Residual friction Angle (°)	Residual Cohesion (kPa)
MVL 1 (lsz)	51.6	77.5	38.2	39.3		1704	25	33	42	13.1	0
MVL 2 (lsz)	49.5	68.2	36.5	31.7	14.52		22	46	32	13.6	0.5
MVL 3 (ed)	32.9	51.9	29.3	18.6	9.56	1666	23	51	26	14.7	0.5
MVL 4 (lsz)	48.7	67.5	25.3	42.2	15.55	1654	18	42	40	13.2	0.5
MVL 5 (lsz)	52.3	78.5	36.6	41.9	12.89	1765				13.6	0
MVL 6 (ed)	34.6	72.6	38.5	34.1		1876	48	39	13	22.6	0
MVL 7 (lsz)	39.8	65.2	29.1	36.1		1627	15	38	47	13.0	0
MVL 8 (lsz)	43.5	70.2	32.5	37.7	13.56					13.2	0

Table 2.1 Material Properties, Earthslide A, Mt. Vulcan Landslide Complex
(lsz = lateral shear zone material, e.d. = general earthslide debris)

D). Particle size analyses were conducted for six samples from Earthslide A, of which MVL 1,2,4 and 8 constituted lateral shear zone material, while samples MVL 3 and 6 comprised general earthslide debris. In general, it was found that lateral shear samples had sand contents ranging from 15-25%, silt contents ranging from 33-42% and clay contents ranging from 32-47% (fig. 2.12). One particle size distribution determined for general earthslide debris (MVL 3) showed similar results to the lateral shear samples, while the other sample (MVL 6) had notably more sand (48%) and less clay fraction (13%).

2.6.3.4. Residual Strength Testing (Ring Shear Apparatus)

When sufficiently large displacements take place along lateral shears bounding earthslides, the clay particles immediate to the shear surface become orientated with their long axes in the direction of shear (Wu & Sangrey, 1978; Bromhead, 1986). This rearrangement produces a shear strength approaching, or equal to, the residual strength (ϕ'_r; Skempton, 1964). The Bromhead Ring Shear Apparatus conducts a continuous shear strength test within an annular, ring shaped test sample for the determination of ϕ'_r (Law, 1987). The sample is sheared by differential rotation and shear stress is measured for a series of normal stress conditions. Details of the test procedure and setup are given in Appendix D.

Ring shear analysis of the eight sample localities on the Earthslide A produced two results (see examples in fig. 2.13):

1. samples of lateral shear zone material (MVL 1,2,4,5,7 and 8) yielded effective residual friction angles ranging between 13.0 and 13.6°, with an average value of 13.3°. Effective residual cohesion was found to be very low, and assumed to be 0.
2. samples of general earthslide debris with high sand or silt contents (see section 2.7.3.3) showed significantly higher residual friction angles.

However, measured values for Earthslide A tend to indicate that c'_r =0 and ϕ'_r =13.3° are realistic residual strength parameters for later analyses.

2.6.3.5. X-ray Diffraction Analysis

X-ray diffraction (XRD) analysis was performed on only one sample from Earthslide 3 (MVL 3). It was assumed from field observations that the clay mineralogy of earthslide 3 was comprised mostly of smectite, and XRD analysis was used only to confirm this assumption.

Both random and orientated mounts (see Appendix D) of the sample (MVL 3) were prepared. These were subsequently run through a diffractometer, treated with ethylene glycerol, run again and lastly heated to 550°C and re-run. Diffraction plots are shown in figure 2.14. The major clay mineral that can be identified on these diffraction plots is Ca-

Figure 2.12. Particle size distributions, Earthslide A

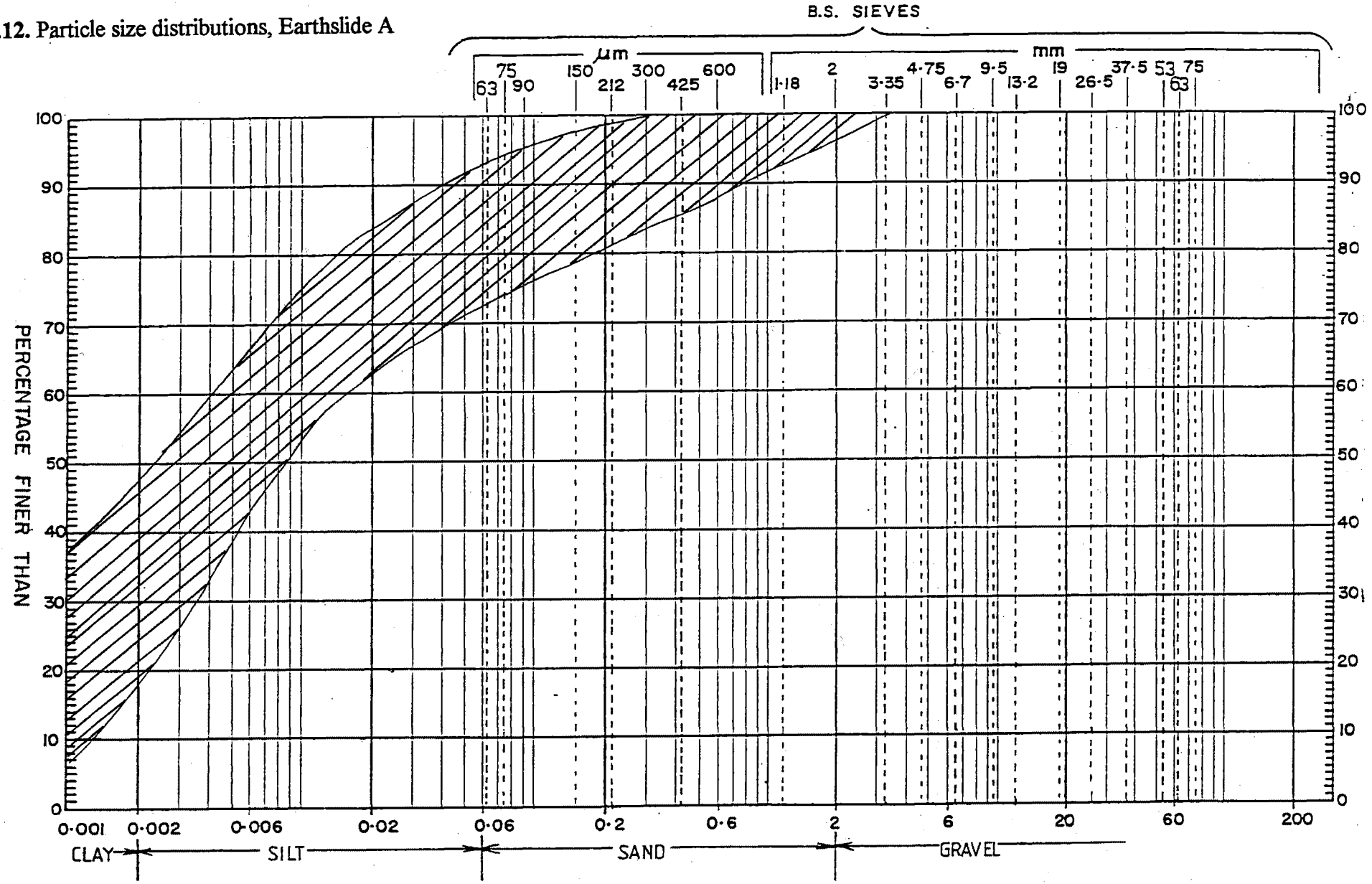

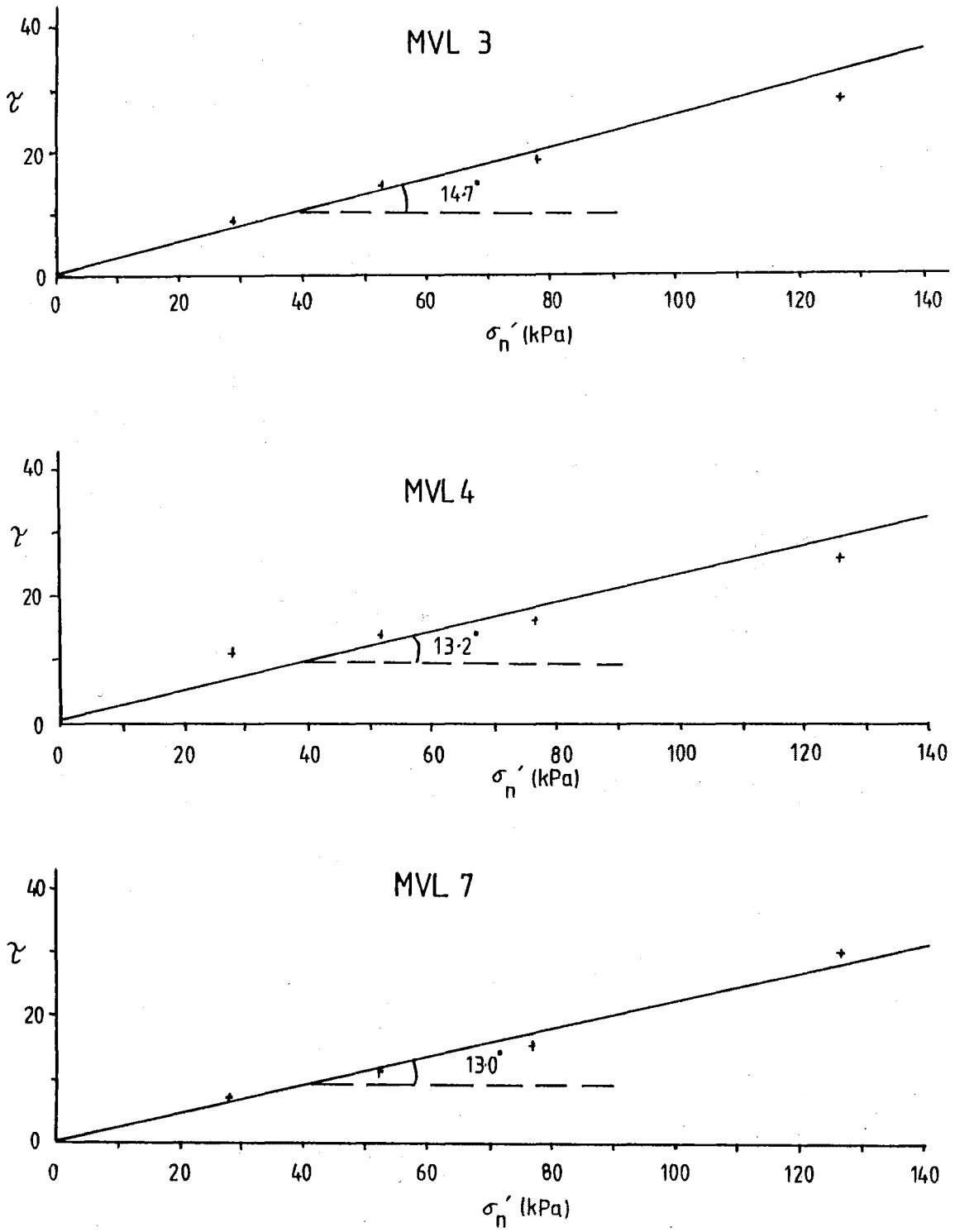

Figure 2.13. Examples of residual strength measurement for samples MVL 3, 4 and 7.

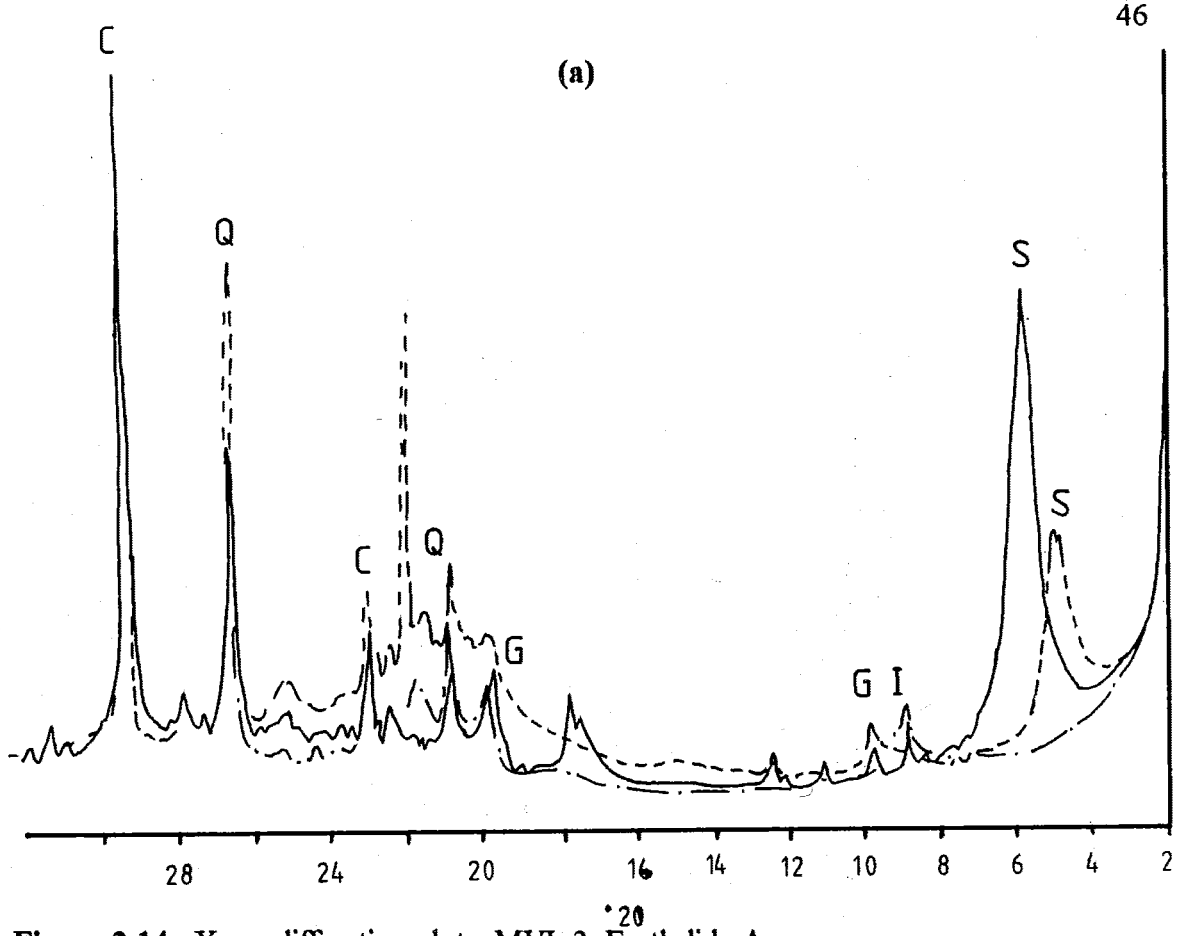

Figure 2.14. X-ray diffraction plots, MVL 3, Earthslide A
(a) Random (whole sample) mount; **(b)** Preferentially orientated (clay fraction) mount. S = smectite, G = glauconite, I = Illite, Q = Quartz C = Calcite. Note that feldspar peaks are located off diffraction plots. Untreated mount shown as a solid line, glycolated mount shown as a dashed line, fired mount shown as a dash-dot.

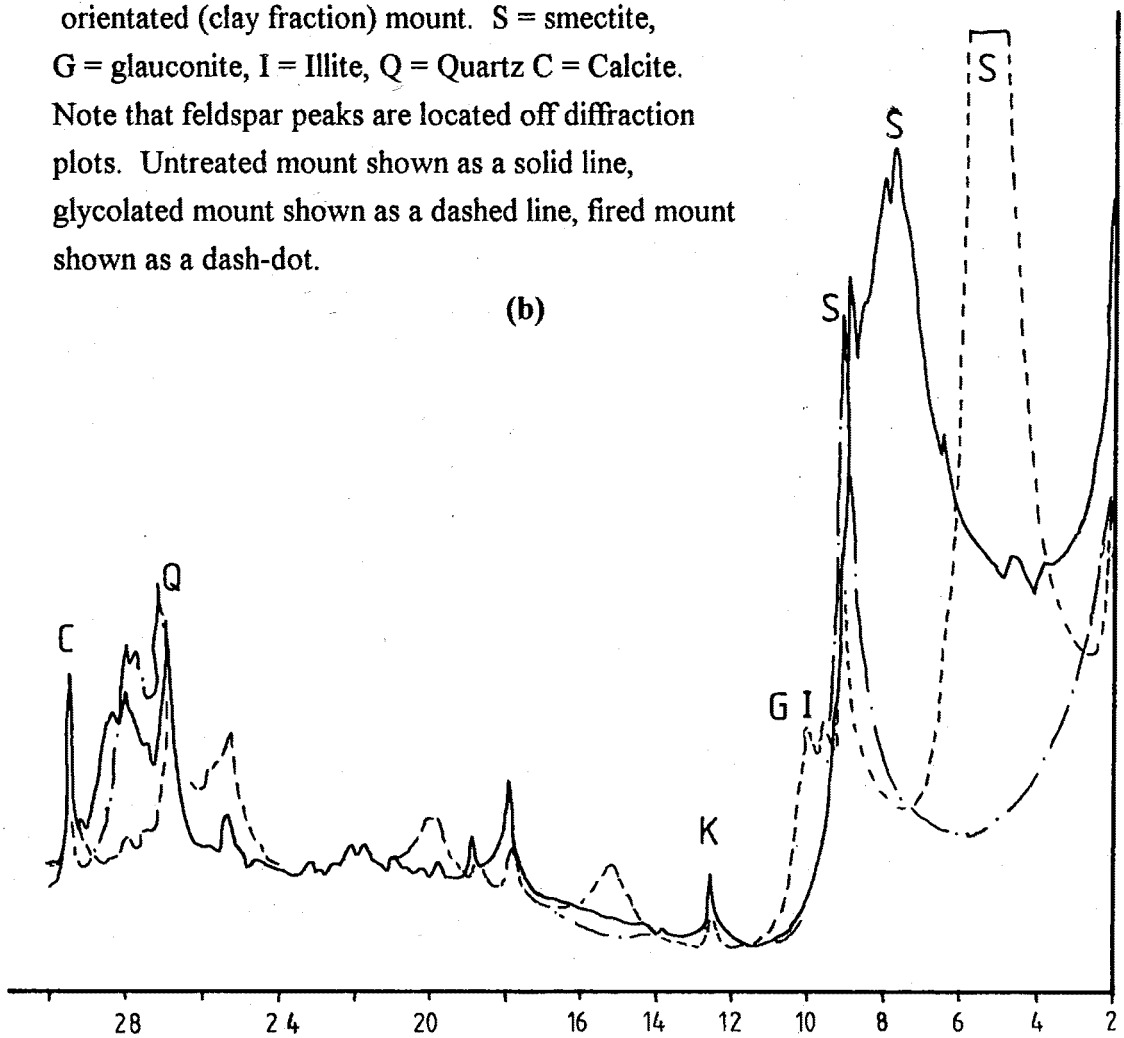

Mg Smectite. Minor amounts of montmorillonite group minerals and glauconite also occur. Non clay minerals identified in the random mount include quartz, calcium and feldspar.

2.6.4. Stability Analysis

2.6.4.1. The Infinite Slope Expression

The Infinite Slope Expression (Skempton & DeLory, 1957) is a simple two-dimensional analysis, that is, effects of lateral earth pressure perpendicular to the direction of sliding are disregarded. For a slope of constant gradient where the basal shear surface is known, or assumed to be parallel to the ground surface and which is formed of a material with a Mohr-Coulomb failure criterion (see, among others, Skempton & Hutchinson, 1969; Wu & Sangrey, 1978; Craig, 1992; also Appendix H) the factor of safety (F_2; Two dimensional factor of safety) is given by (Skempton & DeLory, 1957; Morgenstern & Sangrey, 1978; Graham, 1984; Bromhead, 1986; Mostyn & Small, 1987):-

$$F_2 = \frac{c' + (\gamma - \gamma_w m) z \cos^2 \beta \tan \phi'}{\gamma z \sin \beta \cos \beta} \qquad (2.1)$$

where c' is the effective cohesion, γ is the soil unit weight, γ_W is the unit weight of water, m is the ground water level in terms of landslide thickness (z) β is the landslide inclination and ϕ' is the effective friction angle. For clay soils under residual conditions, $c' = c'_r$ (residual cohesion) and can be assumed to be 0 (see 2.6.3.4), and $\phi' = \phi'_r$ (residual friction angle). Therefore, the infinite slope expression simplifies to:-

$$F_2 = \frac{(\gamma z - \gamma_w m z) \tan \phi'}{\gamma z \tan \beta} \qquad (2.2)$$

For known values of γ, γ_W, z, m and β, and for limiting equilibrium conditions (F_2 = 1.00) equation (2.2) can be rearranged to produce:-

$$\phi'_r = \tan^{-1}\left(\frac{\gamma \tan \beta}{\gamma - \gamma_w m}\right) \qquad (2.3)$$

2.6.4.2. The Infinite Rectangular Landslide Expression

The infinite rectangular landslide expression is based on the infinite slope expression of Skempton & DeLory (1957), but includes additional terms that account for lateral earth pressure acting on the sides of the moving mass. For a channelised landslide of constant surface inclination where the lateral shear surface is known, or assumed, to be parallel to the ground surface F_3 (three dimensional factor of safety) is given by the equation:-

$$F_3 = \frac{1}{\sin \beta}\left\{\left(\frac{2}{\lambda} + \sec \beta\right)\frac{c'}{\gamma z} + \left[\frac{K}{\lambda}\left(1 - m^2 \frac{\gamma_w}{\gamma} \cos^2 \beta\right) + \cos \beta \left(1 - m \frac{\gamma_w}{\gamma}\right)\right] \tan \phi'\right\} \qquad (2.4)$$

where K is the coefficient of lateral earth pressure and λ is the landslide width. (After Hutchinson & Del Prete, 1985; Prof. J.N. Hutchinson, pers. comm., 1993; see Appendix H). Where the effective cohesion (c') is equal to 0, and ϕ' is equal to ϕ'_r (ie., residual conditions) equation (2.4) simplifies to:-

$$F_3 = \frac{1}{\sin\beta}\left[\frac{K}{\lambda}\left(1 - m^2\frac{\gamma_w}{\gamma}\cos^2\beta\right) + \cos\beta\left(1 - m\frac{\gamma_w}{\gamma}\right)\right]\tan\phi' \qquad (2.5)$$

For limiting equilibrium conditions, F_3 = 1.00, and hence, equation (2.5) can be simplified and rearranged to produce:-

$$\phi'_r = \tan^{-1}\left(\frac{\sin\beta}{\frac{K}{\lambda}\left(1 - m^2\frac{\gamma_w}{\gamma}\cos^2\beta\right) + \cos\beta\left(1 - m\frac{\gamma_w}{\gamma}\right)}\right) \qquad (2.6)$$

2.6.4.3. Results of Stability Analysis

As equations 2.3 and 2.6 do not contain the variable z (earthslide thickness) no assumption needs to be made regarding the thickness of the lower earthslide. However, as ground water levels for the lower earthslide are not known, values of m ranging from 0.3 to 1 are used. The average slope inclination (β) of 8° is used. For the Infinite Rectangular Landslide Equation a value of K (coefficient of lateral earth pressure) equal to 0.67 is used (see Appendix H). Results of stability analysis for Earthslide A using equations 2.3 and 2.6 are given in table 2.2.

Ratio of height of phreatic surface above basal shear zone to earthslide thickness (m)	Infinite Slope Expression (F_2)	Infinite Rectangular Landslide Expression (F_3)
1.0	19.6	18.9
0.9	16.7	16.6
0.8	15.5	15.3
0.7	14.0	13.8
0.6	12.7	12.6
0.5	11.7	11.6
0.4	10.8	10.7
0.3	10.1	10.0

Table 2.2 Required values of effective residual friction to produce limiting equilibrium conditions (F= 1.0) at various water levels. Analysis using the Infinite Slope and Infinite Rectangular Landslide Expressions

2.6.4.4. Comparison of Results

It can be seen that the infinite slope expression provides slightly higher required values of ϕ'_r to place the earthslide in a state of limiting equilibrium than the infinite rectangular landslide expression, with either K equal to 0.67. This is due to the fact that, assuming no deformation occurs in the 'rectangular' landslide mass, lateral earth pressure will tend to act as a stabilising influence. At high values of m, significantly different values of ϕ'_r are calculated by the 2 stability analysis equations. However, at low m values, the infinite slope and infinite rectangular landslide expressions give little difference in the calculated value of ϕ'_r.

In section 2.6.3.4, it was found that the residual friction angle was 13.3°. Infinite Slope and Infinite Rectangular analysis indicate that a water level of m slightly over 0.6 is required to produce limiting equilibrium conditions on Earthslide A for the calculated residual friction angle. Two streams entering the earthslide near its head zone are inferred to supply sufficient water to maintain constantly high (over 0.6 m) ground water levels in the slide for most, if not all, of the year.

2.7. Summary and Conclusions

2.7.1. Mt. Vulcan Landslide Complex

The Mt. Vulcan Landslide Complex has been renamed in this study from the 'Montserrat Landslide' of Wilson (1963). The complex is categorised under Varnes' (1978) classification scheme as a bedding controlled slump/earthslide complex (class VI) and covers an area of approximately 85 ha, located in Tertiary Lithologies 9km southwest of Motunau beach. The complex has a landslide length (L) from head to toe of approximately 2400 m, and a relatively constant width (λ) of 500 m. However, at the toe, the landslide width is reduced to about 300 m. The mean direction of sliding near the head of the complex is 230°, which swings through to approximately 170° near the centre of the complex.

Mt. Vulcan Landslide Complex can be divided on the basis of surface morphology, failure style and likely current activity into 11 morphological units. Forms of slope movement recognised within these morphological units include falls, topples, back or forward rotational slumping and earthsliding (defined in chapter 1). Earthslide A comprises the most obviously active portion of the complex, and is located near the eastern lateral boundary in the downslope half of the landslide complex.

The composition of the landslide complex material is highly dependant on the particular morphological unit. In general, four categories of material can be recognised: (i) highly

deformed soft smectitic silty clay (sourced from Ashley Mudstone) with some sand and/or gravel (earthslide debris), (ii) blocks of Amuri Limestone supported in a chaotically arranged gravelly silty clay (disrupted limestone debris) (iii) large blocks (greater than 5 m diameter) of internally intact limestone (Limestone megablocks); and, (iv) loose to compact glauconitic sand (sourced from Waipara Greensand).

Rates of movement were determined for several morphological units comprising the landslide complex. Head scarp retreat rates were found to be variable through the period covered by aerial photography, which an average retreat rate of 1.6 m/yr between 1950 and 1974, while the period 1974-1992 indicated retreat rates of less than 0.5 m/yr. While movement rates were determined for the older earthslide/flow debris, lack of recognisable features and changes in surface morphology between the two sets of aerial photographs made determination of movement rate impossible for a number of units.

An age of formation of the complex proved difficult to determine, with a substantial range of ages (from about 5000 b.p. to about 100 000 b.p) possible. The formation of the complex is inferred to be related to uplift and subsequent erosion of material along the Montserrat fault, inferred to cross the complex near the toe. The failure mechanism for the main body of the complex (ie, all materials except earthslide deposits) is inferred to involve slumping of large blocks of Amuri Limestone from the eastern lateral scarp, with or without a component of rotation, on convex upwards shear surfaces developed within Ashley Mudstone. Progressive downward and outward creep failed blocks results in gradual destruction of the block, by fracturing of the failed block along closely spaced internal defects.

2.7.2. Earthslide A

Earthslide A originates near the inside corner of Mt. Vulcan Landslide Complex, and has a length (L_e) from head zone to toe of approximately 1100 m. The width (λ_e) is rather constant along the majority of the length of the slide, being approximately 90 m. The head zone is located at about 145 m a.m.s.l, while the toe is at sea level, producing an average earthslide surface inclination (β) close to 8°.

The earthslide moves primarily by sliding on discrete slickensided lateral shears. Lateral shears display a range of features, depending on the degree of development of the shear at the ground surface. Features range from en-echelon tension cracks, typically located near the head of the earthslide to sublinear, fully developed lateral shear planes, generally in the downslope regions of the slide. Lateral bulges can be observed at many localities along the boundaries of the earthslide. Bulges were typically located on the inside (displaced side) of the lateral shear. Prominent lateral bulges were observed on either

side of the earthslide immediately upstream and downstream of a constriction formed by two front tilted limestone blocks located near the toe of the earthslide.

Material comprising the lower earthslide consists of a sheared and highly deformed silty clay matrix (comprising 65-85% of the mass) within which fine-coarse sand and fine-coarse Amuri Limestone gravels occur. Occasional 'lumps' of stiff brown clay and brownish green sand and larger blocks of intact Amuri Limestone can be observed within the earthslide material. Particle size analyses established that, for examined samples, the sand fraction was generally less than 20%, although some samples showed sand fractions as high as 63%. The silt fraction generally composed from 35% to 55% of analysed samples, while the clay fraction comprised 20-50%. X-ray diffraction analysis indicates that the major clay mineral comprising the matrix is a calcium-magnesium smectite, although smaller quantities of illite and glauconite were present.

No short term movement rates were determined, and due to the large time period between successive aerial photographic runs, it was not possible to obtain a long-term movement rate.

Geotechnical analysis of the earthslide material ascertained that the water content of the material involved in the earthslide varies from 34 to 52%, with average values of plastic and liquid limit ranging between 29-39% and 48-84% respectively. Values of linear shrinkage ranged from 9.5% to 15.6%. The average remoulded bulk density was found to be about 1715 kg/m^3, corresponding to an average soil weight of 16.8 kN/m^3. Ring shear analysis indicated that, for lateral shear material, the effective shear parameters (residual friction angle; ϕ'_r, and cohesion; c'_r) were close to 13.3° and 0 kPa, respectively.

Stability analysis for the lower earthslide was attempted using both the infinite slope equation of Skempton & DeLory (1957) and the infinite rectangular landslide equation (see Hutchinson & Del Prete, 1985). It was found that for the determined residual friction angle, a water level of just over m equal to 0.6 is required to produce limiting equilibrium conditions on Earthslide A.

Chapter Three: Coringa Landslide Complex

3.1. Introduction

3.1.1. Landslide Description

Coringa Landslide Complex (figure 3.1) is a large slump/earthflow complex (under Varnes' (1978) classification scheme), involving an area of approximately 50 hectares and is located in Tertiary lithologies about 3.5 km inland from Motunau township (figure 3.1). The complex has a length (L) from head to toe of over 1400m and a width (W) ranging from 550 m near the toe to 125m near the head. The landslide complex[1] has developed as a depression between two prominent northeast-southwest trending lateral scarps and displays translational and rotational rock and/or soil slide-type movements and earthslide (as defined in chapter 1; see also chapter 4) features.

3.1.2. Previous Work

Coringa Landslide Complex is shown on geological maps produced by Taylor (1950) and Wilson (1963), but neither map includes detail of the geomorphology of the landslide. Wilson's figure 9 (page 30 in his work) is of the complex, and the failure is described as "slumping on bentonite". The definition of the term 'slumping', however, is not made clear by Wilson.

Yousif (1987) labelled the failure as the "Inland Motunau Slide". Yousif's study was largely of a reconnaissance nature, but included some morphological detail of the complex. Yousif thought the failure to be a bedding controlled slump[2]-earthflow complex.

Barrell (1989) conducted the first investigation of the complex from a strictly engineering geological point of view, although his study was largely of a reconnaissance nature. The objectives of Barrell's study were to determine the geological setting of the failure; to describe landslide geomorphology and determine short-term movement rates; to derive a model for the evolution of the landslide; and to assess the potential for rapid

---

[1]the term "Coringa Landslide Complex" as used in this study refers to the entire complex slope movement as outlined in fig 3.1. Individual parts of the complex will be referred to under their morphological names, as defined in section 3.3.1.

[2] defined as in Varnes' (1978) classification scheme

Figure 3.1 Oblique view of Coringa Landslide complex. Photograph looking approximately north.

movement of the landslide debris to dam the Motunau River. Coringa Landslide Complex was labelled by Barrell as a bedding-controlled slide-slump-earthflow complex, similar to the terminology adopted by Yousif (1987).

3.1.3. Chapter Objectives

The objectives in this chapter are to re-examine the geological setting and geomorphology of the failure, and re-derive a model for the development of the complex. The particular portion of Coringa Landslide Complex termed "Earthflow 3" by Barrell (1989), but termed 'Earthslide 3' in this study (see chapter 1; also chapter 4) is examined in detail. Objectives here are to (i) describe surface morphology and characteristics of displacement boundaries; (ii) provide data on short-term (yearly) and long-term (average over greater than 10 years) movement rates; (iii) ascertain the effect of rainfall on the movement rate of the earthslide; (iv) determine the geotechnical parameters of material involved in the earthslide; (v) provide subsurface data for the earthslide portion of the landslide complex; (vi) conduct a theoretical stability analysis (back analysis) for the earthslide; (vii) determine failure mechanisms of the slide; and (viii) assess the pattern of probable future activity of the earthslide.

3.2. Local Geological Setting

3.2.1. Lithology

Coringa Landslide Complex is bounded at its eastern edge by a prominent (20-30 m high) lateral scarp of Amuri Limestone[3] (fig **3**). The units stratigraphically below the limestone are the uppermost members of the Eyre Group (after Brown & Field, 1985), namely Ashley Mudstone/Homebush Sandstone. The complex is bounded at its western edge by a less prominent lateral scarp, composed partly of displaced Amuri Limestone, Waipara Greensand and other lithologies, and partly of in situ Waipara Greensand.

Lithologies recognised within the landslide debris are Ashley Mudstone/Homebush Sandstone, Amuri Limestone and Waipara Greensand. The Ashley Mudstone lithology was distinguished in the complex by a light brown, soft, dry to wet, silty clay/clayey silt; whereas the Homebush Sandstone lithology was identified by a light brown, dry to moist, loose sand; and the Waipara Greensand lithology was recognised as a brownish green, moist to wet glauconitic sand. The Amuri Limestone lithology was identified as a generally unweathered to slightly weathered, very strong, white limestone. Ashley mudstone and Amuri Limestone form the most common lithologies observed. Remnants

[3]Stratigraphy and engineering geological descriptions of soil and rock units are given in Appendix B, see also section 1.*.*

of Scargill siltstone are also apparent within the landslide complex, resting directly on back-tilted megablocks of Amuri Limestone.

Exposed at the upstream end of the toe of the complex, directly under earthslide debris, is a dark bluish grey clay, inferred to be Loburn Mudstone. A similar lithology was intersected at depth in boreholes emplaced within Earthslide 3, and is inferred to underlie the earthslide. Borehole information indicates that this lithology is also present in the earthslide mass, occurring as stiff lumps of non-in situ bluish grey clay within a softened brownish silty clay matrix (of Ashley Mudstone origin; see section 3.6.2).

To the west of Coringa Landslide Complex, lower members of the Eyre succession are exposed. Units exposed sequentially upstream (westward) of the landslide complex are (i) Waipara Greensand (carbonaceous layers of generally less than 20 cm in thickness were identified within this unit); (ii) Loburn Mudstone; (iii) Conway Formation, and; (iv) Broken River Formation (fig. **1**). Barrell (1989) distinguished Claverley Sandstone (defined by Barrell as a 'grey moderately indurated very fine to medium sandstone') between Conway Formation (a light/dark grey stiff silty fine/medium sand) and Loburn Mudstone. Claverley Sandstone unit and not previously been recognised south of Conway River (Brown & Field, 1985). I find Barrell's distinction dubious due to the locality, and similarity in lithology between Claverley Sandstone and Conway Formation. As a consequence, I have not shown the position of Claverley sandstone on figures **1** or **3**. Approximately 1.5 km. upstream of the landslide complex, Torlesse supergroup rocks are exposed in the core of Montserrat Anticline (fig. **1**).

To the east of Coringa Landslide Complex, are a number of raised late Quaternary marine terraces. The oldest (and therefore the highest elevation) terrace in the succession has been assigned an age of 120 ka by Yousif (1987).

3.2.2. Structural and Tectonic Setting

The Coringa Landslide Complex lies on the eastern limb of the Montserrat anticline (fig. **1**). The Tertiary sequence in the area immediately adjacent to the landslide complex strikes approximately northeast-southwest and dips shallowly to the southeast, typically between 15° and 30°, but can locally be as steep as 55°.

Numerous faults are observed or inferred to be present in the area of the landslide complex (fig. **3**). In particular, 2 eastward dipping faults (the Evesham and Coringa faults after Barrell, 1989) are conjectured (both by Barrell and from field work conducted as part of this study) to run beneath the complex. The faults are inferred to be reverse in movement and to result in uplift and subsequent exposure of Loburn Mudstone at the toe of the landslide complex. The faults are likely to be directly

responsible for formation and subsequent movement of the landslide complex (section 3.4.).

3.3. Description of the Landslide Complex

3.3.1. Morphological Units

Coringa Landslide Complex was initially mapped in detail by Barrell (1989). The engineering geology of the complex is indicated in figure **3**, which was produced partly as a result of Barrell's work supplemented to a large extent by aerial photographic interpretation and further field mapping by myself in 1993.

The Coringa Landslide Complex (as defined in section 3.1) can be divided into 9 morphological units (Barrell, 1989; fig. 3.2) based on the surface morphology and the type(s) of movement present in each:

1. Older landslide debris. This geomorphological unit is composed of earthslide/flow deposits and highly fractured limestone blocks. The movement is considered (Barrell, 1989; this study) to be very old, as the morphology of the area is subdued; there were no features in this area that have been interpreted in this study (or Barrell's) to indicate current activity.
2. Slide Block. (fig 3.3). A large faulted and fractured slide block composed principally of Waipara Greensand and Loburn Mudstone is evident on the western lateral scarp near the head region of the complex. It is inferred (Barrell, 1989) that this block slid in a westward direction from the hanging wall of the Coringa fault during the early stages of formation of the landslide complex.
3. Displaced Blocks. This area is composed of very large limestone blocks that have relaxed and/or subsided along joint planes, and have subsequently slid on the underlying Ashley Mudstone. Joints in the area are generally open 1-3 m, while bedding is approximately the same as that for in situ limestone, typically 10° to 15° to the east-southeast. The boundary between this displaced and in situ Amuri Limestone is indicated on figure **3** (map volume) by a dashed line running southeast from the eastern lateral scarp.
4. Upper basins. (fig 3.3) These are two extensive, bedding controlled benches which are drained by minor earthslides that incorporate regolith derived from the benches and talus aprons of the eastern lateral scarp (Barrell, 1989).
5. Eastern Lateral Scarp (fig. 3.3). This prominent scarp has been formed by retrogressive failure of limestone blocks by falling, toppling or sliding. Limestone material is constantly being fed by these failures to talus aprons which conceal the bottom of the scarp.

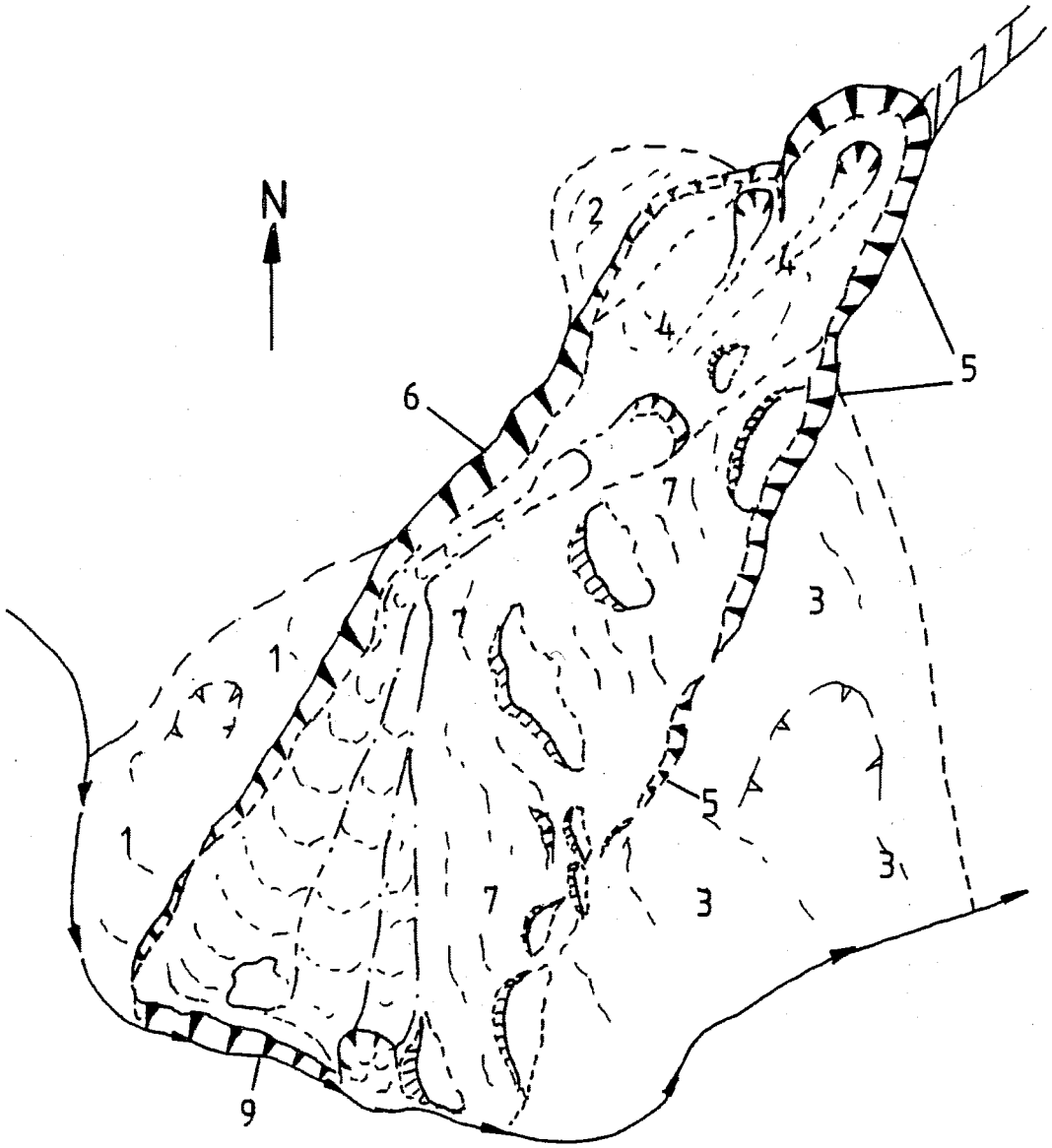

Figure 3.2 Morphological units of Coringa Landslide Complex. (1) Older Landslide Debris; (2) Slide Block; (3) Displaced block zone; (4) Upper basins; (5) Eastern Lateral scarp; (6) Western Lateral scarp (7) slumped block zone; (8) Earthslide complex; (9) Toe Complex. Scale 1:9000 (approx.)

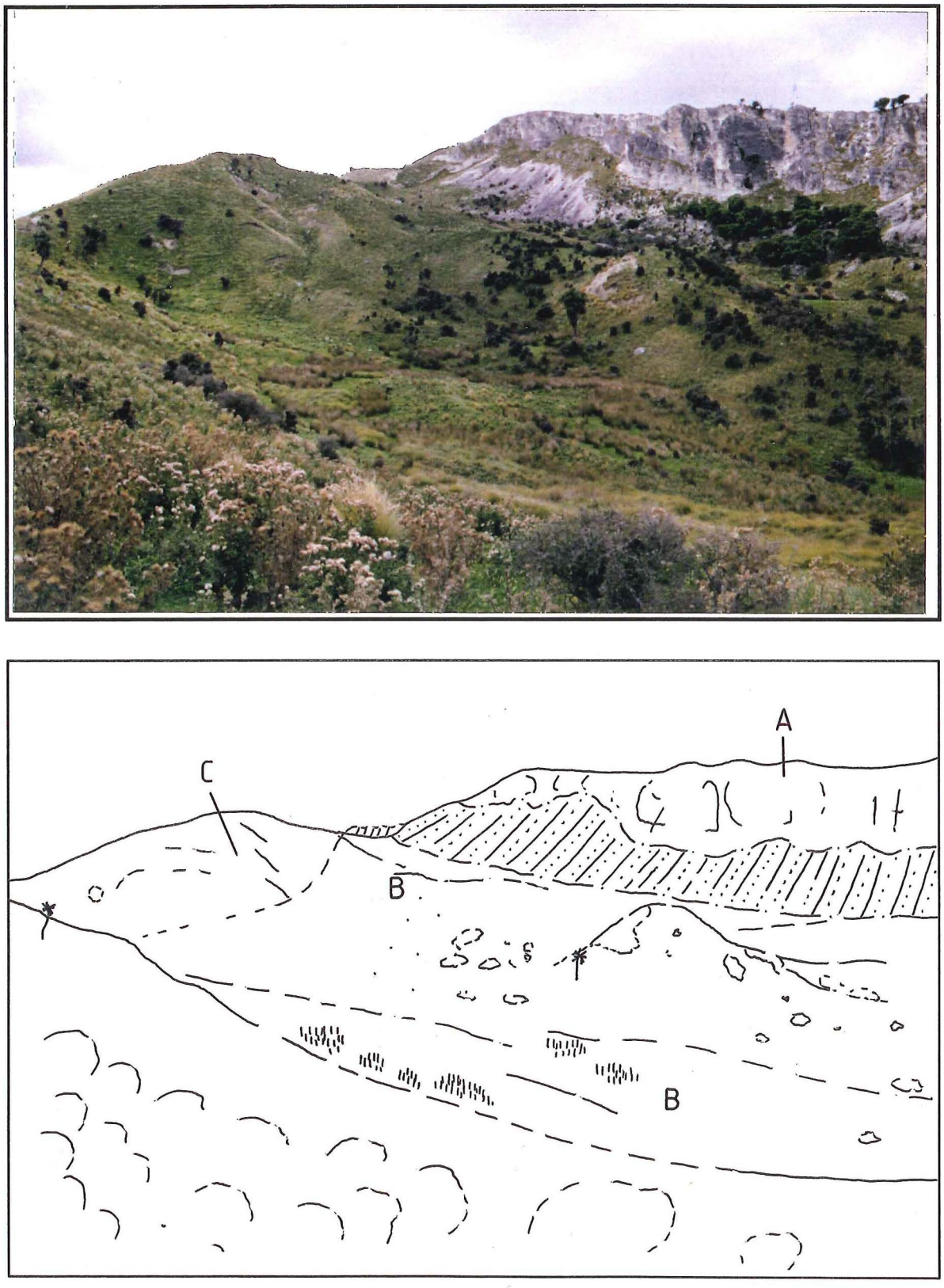

Figure 3.3 (A) View of the head of the eastern lateral scarp (morphological unit 5), (B) Upper basins (unit 4) and (C) slump block (unit 2); taken from western lateral scarp.

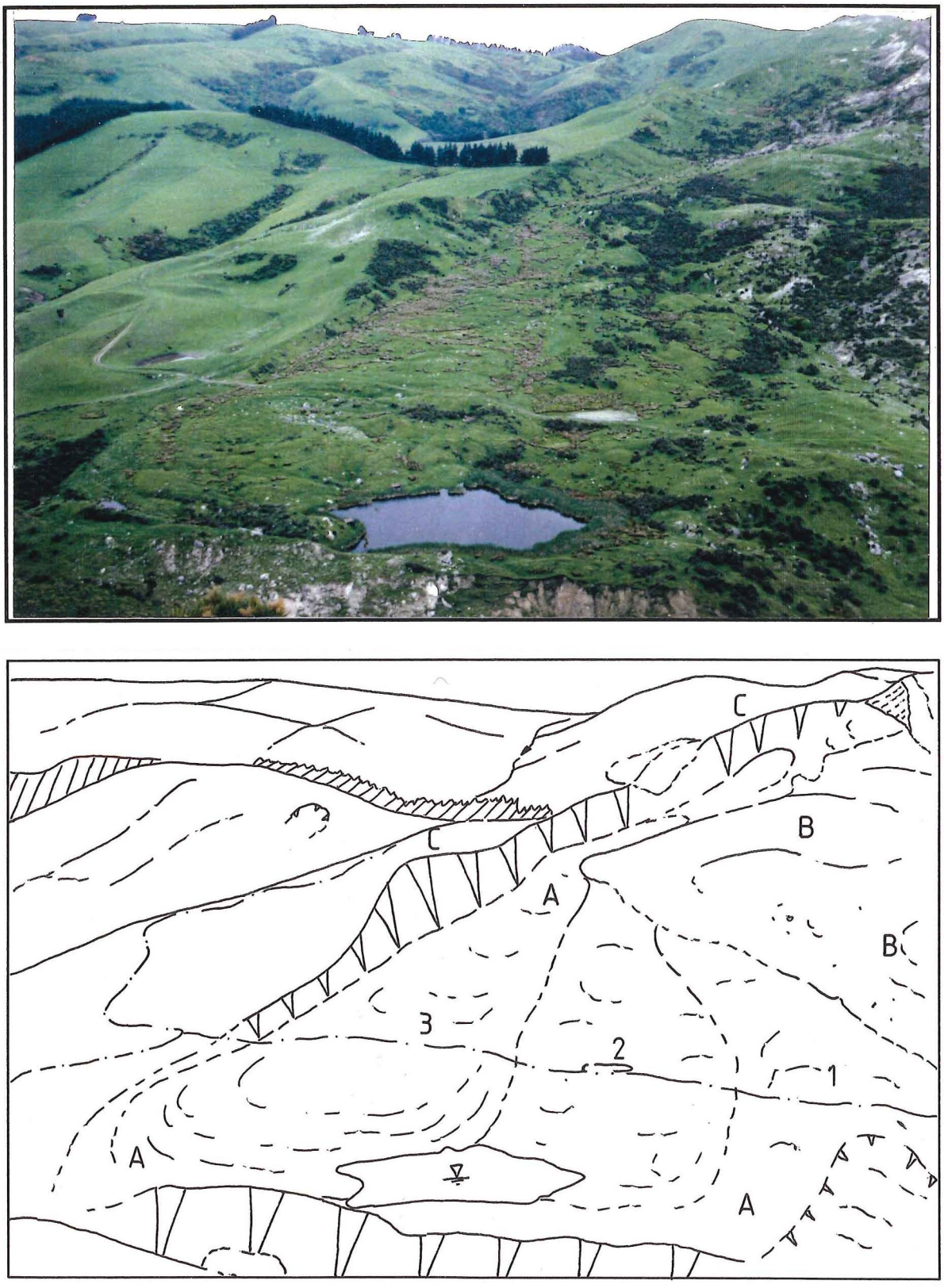

Figure 3.4. View of (A) earthslide complex (morphological unit 8) showing earthslides 1,2 and 3 (as defined in text); (B) part of slumped block zone (unit 7); and (C) western lateral scarp (unit 6)

6. Western Lateral Scarp. This lateral scarp is comprised of remnant slide block material, as well as in situ Waipara Greensand. The slide blocks are composed of Waipara Greensand and Loburn Mudstone or disrupted Amuri Limestone.
7. Slumped Blocks (partly shown in fig 3.4). This area is comprised of large, chaotically arranged limestone blocks (up to several 10's of metres in length), that have slid generally south-southeast from the eastern lateral scarp on underlying Ashley Mudstone. Rotational slide-type movements (as defined by Varnes, 1978) are evident, with some blocks displaying back tilting while others display a component of forward rotation.
8. Earthslide complex (fig. 3.4). Three major earthslides can be identified using morphological criteria. Earthslide 3 is the most obviously active, demonstrating such features as fresh scarps (both lateral and transverse), bulging ground and displacement of fences and fence posts. Earthslides 1 and 2 show no sign of recent movement and both have comparatively subdued morphology. Earthslide 2 has a significant proportion (30 - 40%) of Waipara Greensand blocks at the surface, whereas the other flows are dominated by limestone blocks (Barrell, 1989).
9. Toe complex. The landslide toe comprises earthslide deposits with occasional Amuri Limestone and Ashley Mudstone/Homebush Sandstone blocks. Erosion is taking place at the toe complex due to the action of the Motunau River, resulting in on-going slumping and movement of material exposed in this area.

3.3.2. Composition of Landslide Complex

The landslide debris can be divided into 3 distinct forms:

1. Earthslide material, constituting an essentially massive matrix of sheared and highly deformed silty clay/clayey silt, that contains sand (Homebush Sandstone, Waipara Greensand and sand-sized particles of Amuri Limestone) and limestone gravel ranging in size from fine to very coarse. The matrix can comprise as little as 40% of the soil mass on the flanks of the earthslide complex, but within Earthslide 3 the matrix can constitute up to 90% of the total mass (section 3.5.4.3). Occasional larger blocks of intact Amuri Limestone (up to 2.5 m in diameter) are present within the earthslide material. Earthslide material comprises morphological units 4 (upper basins); 8 (earthslide complex); 9 (toe complex) and partly comprises morphological unit 1 (older earthslide/flow debris).
2. Disrupted limestone, which consists of blocks (up to about 5 m diameter) of Amuri Limestone, either internally intact or pervasively fractured (fig. 3.5). Material between blocks is typically fine sand to chaotically arranged angular boulder sized-limestone fragments in a matrix of silty clay. This matrix is generally well graded and clast supported, and typically comprises 25-45% of the soil mass. Disrupted limestone material comprises part of morphological unit 1 (older earthslide/flow debris).

Figure 3.5 Typical disrupted limestone material from slumped block zone (notebook is 18x13cm).

3. Amuri Limestone megablocks (greater than 5 m diameter). These blocks are generally internally intact, and may or may not be surrounded by disrupted limestone material (described in note 2, above). Amuri Limestone megablocks comprise morphological unit 3 (displaced block zone), while morphological unit 7 (slumped block zone) is comprised of occasional megablocks surrounded by disrupted limestone material.

Late Quaternary marine terrace deposits (bored limestone boulders, rounded Torlesse gravels) were found by Barrell (1989) resting on displaced and relaxed Amuri Limestone megablocks (morphological unit 3) above the western lateral scarp of the landslide complex. Similar remnants were found in the older debris area (morphological unit 1), slumped block region (morphological unit 7) and earthslide complex (morphological unit 8) of Coringa Landslide Complex. Identical deposits were found in the same areas during field mapping conducted as part of this study. Barrell assigned these remnants to his Vulcan terraces 1 or 2 on the basis of elevation, thereby placing an age of 105-120 ka (based on the dates presented in Yousif; 1987) for these deposits.

3.4. Interpretation of Landslide Development and Failure Mechanisms

Remnant marine terrace deposits found on the landslide complex place a maximum age on the formation of the complex. At about the time represented by the remnant marine deposits, the area about and east of the present day landslide was progressively elevated by movement on the Coringa and Evesham fault systems (Barrell, 1989; fig.3.6). Subsequently, slumping of limestone occurred in the area between the two faults within Waipara Greensand and Ashley Mudstone, with earthslides developing downslope of the slump region (fig. 3.6 (2)). This phase of development is represented by the older debris. Movement of the slide block observed near the head of the western lateral scarp probably occurred about this time. Movement on the Coringa and Evesham faults effectively increased the width of the complex during its development, with the result that the debris represented by this earliest slope movement is now westwardly displaced some distance from the eastern lateral scarp (fig. 3.6).

As uplift along the fault systems continued, earthslides 1 and 2 are likely to have developed, with their head zones located within the upper basins. The slumped block zone developed along the eastern lateral scarp of the landslide complex. The failure mechanism for this morphological unit is inferred to involve slumping of large rock/soil blocks of Amuri Limestone and Ashley Mudstone, with or without a component of rotation, on convex upwards shear surfaces developed within Ashley Mudstone (fig. 3.7a) Progressive downslope (ie, southeastward) sliding of the failed blocks as part of the main body (see below) of the complex resulted in gradual destruction of the blocks

Figure 3.6 Interpretation of landslide development (modified from Barrell, 1989). (note that for simplicity, diagrams are partly schematic)

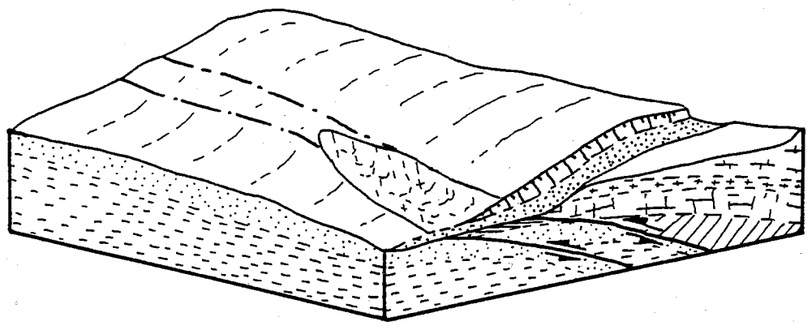

1. Uplift on Evesham and Coringa faults; minor earthslides/flows between the 2 faults

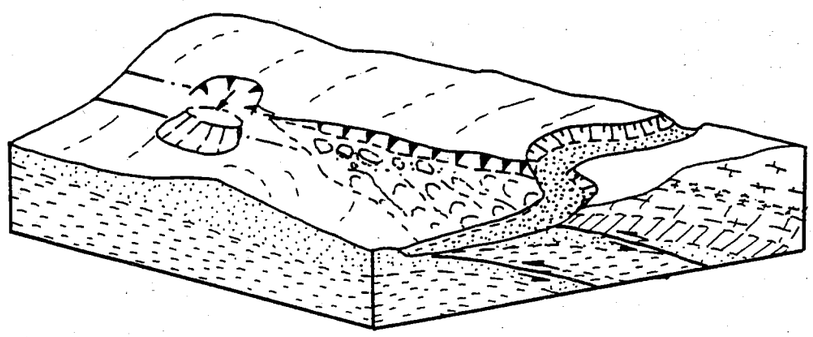

2. Formation of older landslide debris (morphological unit 1). Movement of slide block (morphological unit 2)

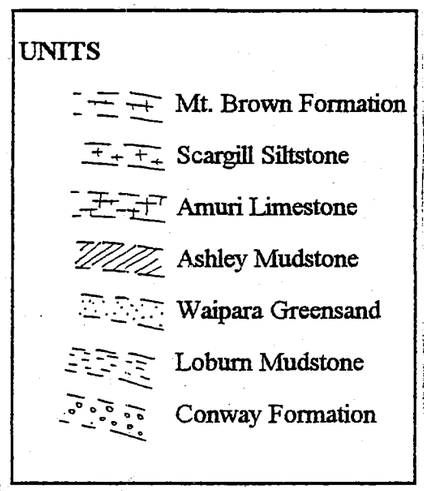

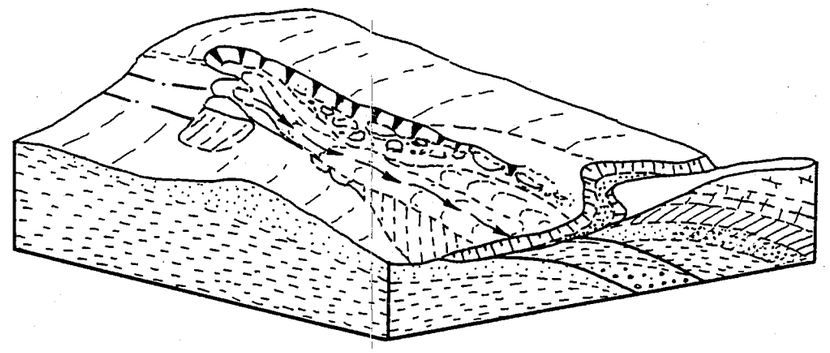

3. Formation of Earthslides 1 and 2; note, head zones located within the upper basins of the complex. On-going developement of displaced and slumped block zones (morphological unit 3 and 7 respectively)

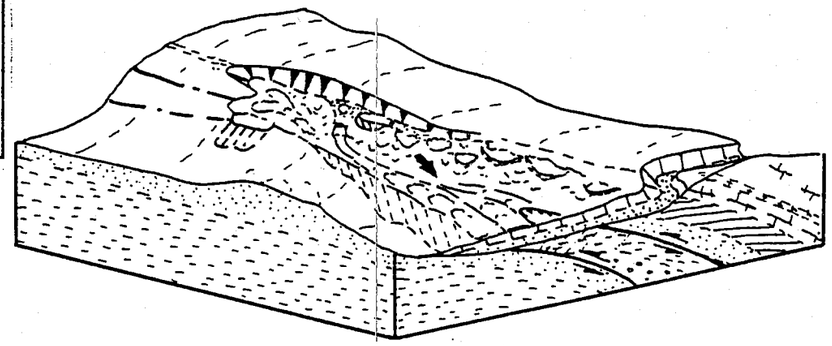

4. Development of Modern day morphology: removal of lateral support by erosion; development of Earthslide 3.

Figure 3.7 Interpretative failure model along **(A)** eastern lateral scarp and **(B)** head zone of Coringa Landslide Complex. Arrows show approximate north. Scale approximately 1:2500

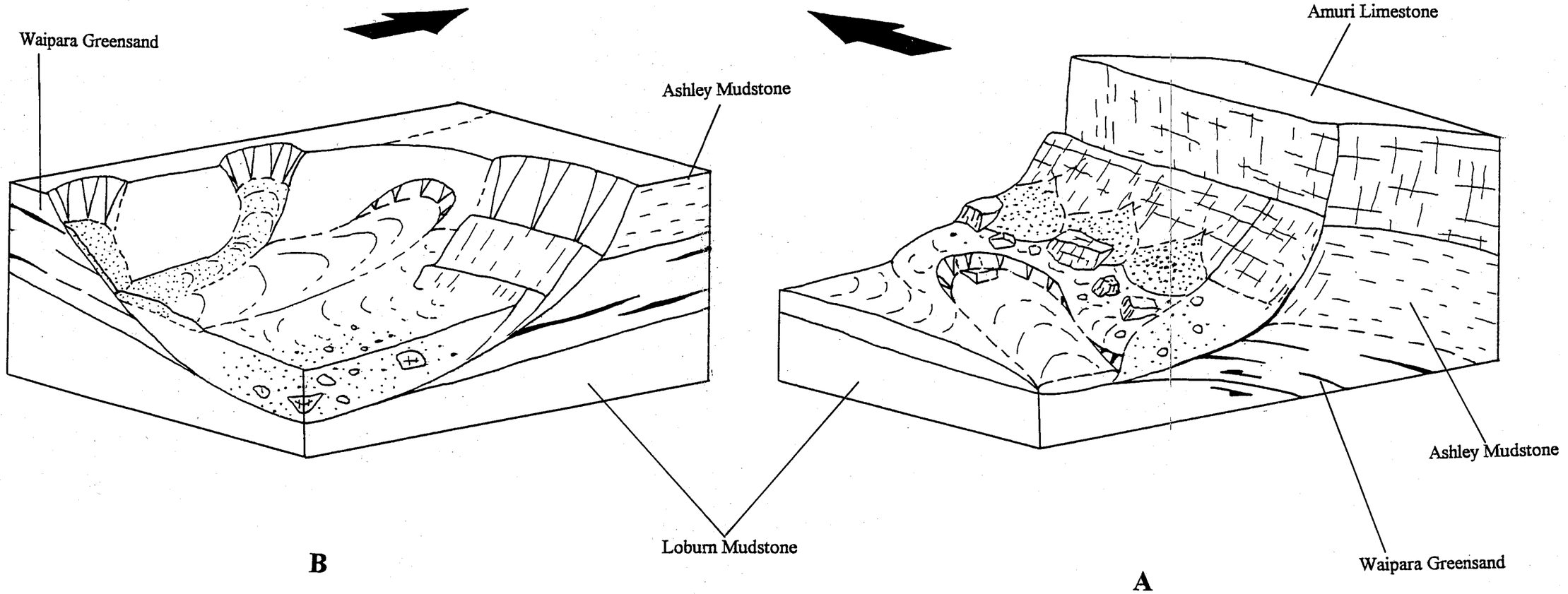

by internal fracturing along closely spaced defects. It is inferred that the toe of the slumped block zone progressively over-rode the older earthslides 1 and 2.

The development of the main body (effectively the area between the western and eastern lateral scarps; fig. 3.2) of the landslide complex is likely to involve the periodic deep seated movement of the main slide mass in response to the removal of support at the toe by the action of the Motunau River (see Barrell, 1989 for further discussion). Barrell interpreted that the surface of rupture of the main body of the complex (ie., to the west of Coringa Fault) is located at the Waipara Greensand/Ashley Mudstone contact. However, I infer that the complex is likely to have its base at a lower depth than interpreted by Barrell (1989), likely to be at the Waipara Greensand/Loburn Mudstone contact. This inference is supported by 2 facts: (i) stiff Loburn Mudstone, inferred to be in situ, was intersected at depth in boreholes on Earthslide 3; and (ii) material derived from Waipara Greensand can be observed within the complex. While some of this material is derived from shallow slumps and slides along the western lateral scarp (greensand material from this source is incorporated into the earthslide complex), other greensand material within the complex is not. In the area immediate to the complex, bedding dips southeastward, thereby providing a gradient for bedding-controlled movement of the complex, governed by the relatively low effective residual friction angle of Loburn Mudstone (fig. **3**).

It is likely that the displaced block zone (morphological unit 3) has experienced on-going failure of blocks as the combined result of uplift along the Coringa and Evesham faults, and the down-cutting action of the Motunau Gorge. Failure in this unit is inferred to involve parting along widely spaced joints developed within the Amuri Limestone due to stress relief, and ensuing subsidence and partial displacement on the underlying Ashley Mudstone.

The rock/soil slump failure mechanism for the slumped block zone may also be used to explain the source for Earthslide 3 in that material derived from Ashley Mudstone was effectively 'bulldozed' ahead of slump blocks which failed near the middle of the eastern lateral scarp (fig. 3.7a). This silty clay material has subsequently become reactivated, forming the youngest earthslide feature on the complex. The earthslide deposits developed near the western edge of the complex are inferred to slide over in situ Loburn Mudstone, uplifted between the two fault strands underlying the complex (fig. **3**; section 3.5.2.)

Active failure at the head of the complex is considered in this study to involve a different mechanism to that along the eastern lateral scarp. Head scarp failure is likewise considered to involve the initial slumping of Ashley Mudstone and Waipara Greensand

and the subsequent sliding material (fig. 3.7b) either at, or close to, the Waipara Greensand/Loburn Mudstone contact. Discontinuous carbonaceous layers within the Waipara Greensand may act as low friction failure planes helping to initiate failure at the head of the slide.

3.5. Analysis of Earthslide 3

Earthslide 3 (figures **3**, and **4**) comprises an elongate body located adjacent to the western lateral scarp and is the most obviously active portion of the Coringa Landslide Complex. This section (i) describes the earthslide composition and morphology; (ii) presents and discusses the nature and rate of surface movements and the influence of precipitation; (iii) outlines geotechnical characteristics of the earthslide material; (iv) provides subsurface data for the earthslide portion of the landslide complex, and (v) provides a theoretical stability analysis (back analysis) for the earthslide.

3.5.1. Earthslide Morphology

Earthslide 3 is elongate in nature, having a length from head zone to toe of approximately 790 m, a minimum width of about 20m near the head of the slide, and a maximum width at the toe of 155 m (fig. **4**). The earthslide has a surface inclination (β) ranging from 0° to 10° at the steepest section immediately east of BH 3. Inclinations on the back slope (or head zone) are considerably steeper, from 30° to 40°. The elevation at the head of the slide is 150 m a.m.s.l., whereas the toe has an elevation of 70 m a.m.s.l. Over an earthslide length (L_e) of 790 m, an average slope gradient of close to 6° is realised.

The head zone is located in an area of active slumping adjacent to the slumped block region of the complex (morphological unit 7). Material is constantly being fed from the head zone to the main earthslide body by small slumps, slides and 'feeder' earthslides. It is notable on figure **4** that the head zone is relatively small in comparison with the size of the earthslide. The implications of this are further discussed in chapter 4, section 4.5.5.2.

A track zone extends from the bottom of the head zone to a distance approximately one third of the length of the earthslide. In the track zone, the slide steepens and narrows, being only about 20 m wide. The direction of movement in the track zone is about 235°. Below the track zone, however, the direction of movement swings through to 190° before straightening to 205°, producing a noticeable 'bend' in the earthslide. This feature is considered a critical region within the slide, because the movement of the earthslide may be partly or wholly governed by the earthslide bend (chapter 4, section 4.5.2). Morphological features of the earthslide bend are described in section 3.5.1.2.

The earthslide gradually widens as it moves downslope from the bend, increasing from a width of about 48 m to approximately 155 m at the toe. The surface of the earthslide generally displays an undulating, or hummocky, appearance within this region. The zone of accumulation extends from the toe complex to about 140 m up the earthslide. This zone is marked by bulging and hummocky ground, which is likely to be due partly to complex internal deformation (possibly flow[4] behaviour), and partly to the presence of multiple basal thrust surfaces. The zone of accumulation also partly forms the toe complex at the base of Earthslide 3 (see section 3.3). Active erosion of the toe complex occurs due to the action of the Motunau River, providing on-going impetus for movement of the earthslide mass.

3.5.1.1. Characteristics of Movement Boundaries

A. Basal Shear

The basal shear, when intersected in boreholes, was easily recognised by the presence of a zone of saturated, very soft brown clay, immediately above a very stiff blue/grey clay. The penetration resistance of the auger was significantly reduced within this saturated layer. Furthermore, small lumps of blue/grey clay occurred within, and immediately above, this zone. Limited information is available on the earthslide thickness, but borehole data (fig. **4.C**) implies a minimum thickness of about 2 m. at the top of the track zone. A maximum thickness of 8-9 m. is inferred in the toe region, based on the depth of earthslide material observed at the toe.

B. Lateral Shears

Lateral shears bounding Earthslide 3 commonly display slickensides and striations subparallel to the ground surface in the orientation of movement (fig. 3.8). The most common features observed along the lateral shear zone of Earthslide 3 were tension cracks orientated approximately 45° clockwise or anticlockwise respectively from the trend of the underlying dextral or sinistral shear. Tension cracks commonly displayed an en-echelon arrangement (fig. 3.9).

Remnants of Riedal shears, formed at the early stages of displacement of the earthslide, could also be recognised (fig. **4**). Riedal shears have the same sense of displacement as the underlying lateral shear, and are typically orientated about $\phi/2$ and $90°-\phi/2$ from the trend of the main shear (Naylor et.al., 1986; Sylvester, 1988). Typically, Riedal shears observed on Earthslide 3 had an offset of 15°-20° from the trend of the lateral shear. Shear segments along the lateral shear could also be observed, which have the same sense of shear as the main lateral shear, but are turned clockwise or anticlockwise from a

[4]discussed in chapter 4.

Figure 3.8 Exposed striations and slickensides on eastern lateral shear of Earthslide 3 (lens cap is about 7 cm diameter)

Figure 3.9. En-echelon tension cracks, eastern lateral scarp, Earthslide 3 (bottom of photograph at right of page; hammer is about 30 cm long)

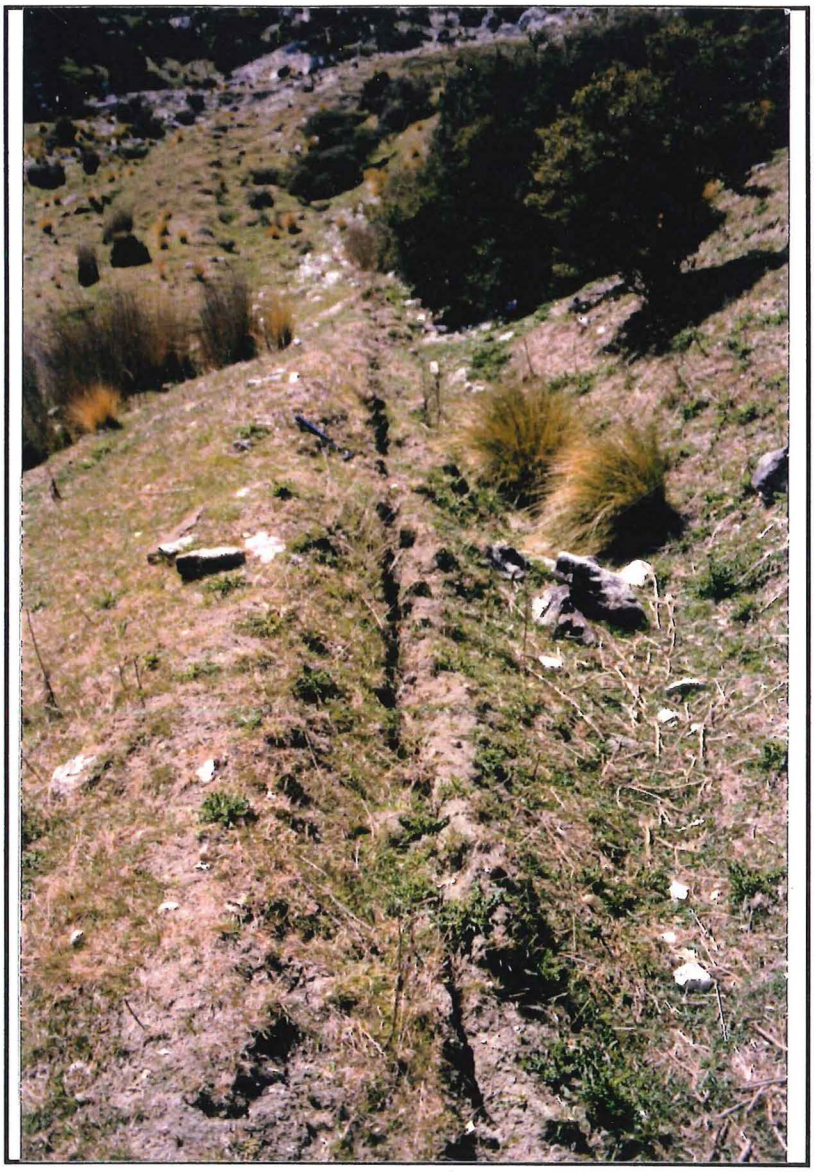

Figure 3.10 Fully developed lateral shear, eastern lateral scarp near the head zone of Earthslide 3.

few to about 20° from the main shear (fig. **4**). Well developed, very linear shears could be noticed at various localities along the boundary of Earthslide 3 (fig. 3.10).

The eastern lateral scarp (a sinistral shear) displays a pronounced left-step at the bottom of the earthslide. This step has resulted in the formation of an extensional, or 'pull-apart' basin (fig. **4**, 3.12). With subsequent precipitation and slope runoff, this depression has become water-logged, resulting in the formation of a large pond (fig. **4**). Aerial photographic evidence indicates that the pull apart basin had not formed by 1950, while the subsequent aerial photographic run, taken in 1974 clearly shows the extensional feature.

C. Lateral Bulges

Lateral bulges of up to 2.5 m in height can be observed at various intervals on both sides of the earthslide. Usually, the bulges are in evidence immediately adjacent to the lateral shears of the earthslide, although a lateral bulge was observed immediately downslope of the earthslide bend, and is associated with a discrete internal shear. For lateral bulges adjacent to lateral shears, 2 different morphologies can be recognised: 'type I' bulges typically display slickensided shear surfaces on their outer flanks (figure 3.11a), and are the more common lateral bulge observed; 'type II' lateral bulges display slickensided shear surfaces on the inner flank of the ridge (fig. 3.11b). Lateral bulges observed on Earthslide 3 have lengths ranging from 70-140 m, while the lateral bulge observed immediately downslope of the earthslide bend has a length of approximately 50 m.

3.5.1.2. Features in the Earthslide Bend

A distinct bend in the direction of sliding occurs at about 1/3*L* from the head zone. The direction of movement above the bend is approximately 235°. Within the bend, the direction of movement swings through to 190° before straightening to 205° below the bend (fig. **4**). The earthslide is at its steepest at the top of the bend, descending at an angle of about 10°. Below the bend, the inclination of the slide ranges between horizontal and 6°. A three dimensional terrain model of the earthslide bend is shown figure 3.12.

Noticeable internal shears can be observed within the bend. The most prominent of these internal shears can be seen in figures **4** extending in an arc from the western lateral scarp to about half-way across the slide. Immediately below the steepest section of the bend, a number of large (up to 2.5 m. high) transverse pressure bulges have formed (fig.**4**, 3.12). These transverse bulges have a length of generally less than 30 m and are orientated across the earthslide, approximately 60° to the direction of sliding.

(a) Type I lateral bulge (note lateral shear plane, arrowed, on outside of bulge)

(b) Type II bulge (note lateral shear plane, arrowed, on inside of bulge)

Figure 3.11 (a) Type I lateral bulge (b) Type II lateral bulge

Figure 3.12. 3 dimensional terrain model of the earthslide bend.
(scale approximately 1: 1200)

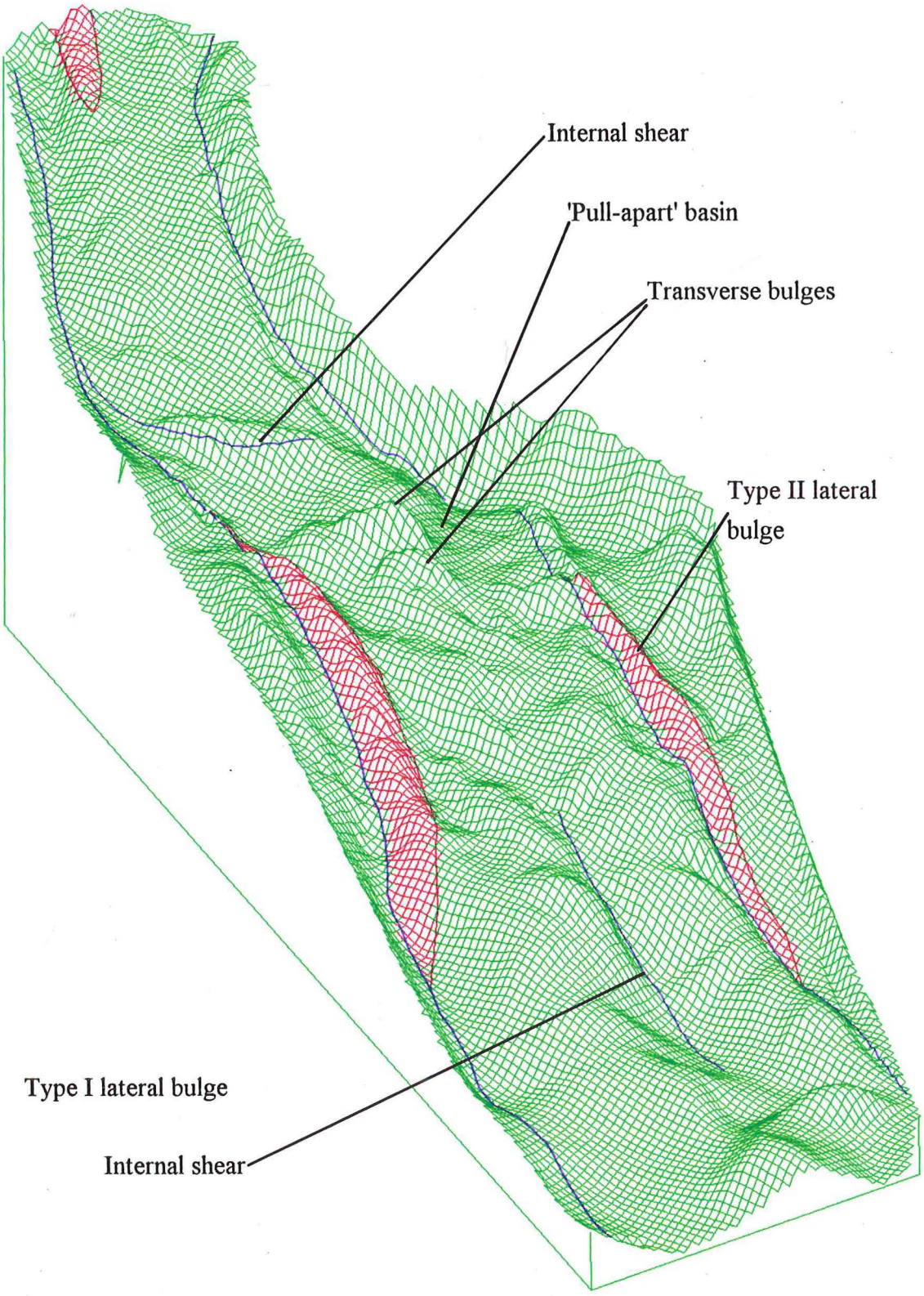

It can be seen in figures 4 and 3.12 that lateral bulges have formed immediately upstream and downstream of the earthslide bend. Directly below the bend, a type I lateral bulge is apparent along the western lateral scarp, while the eastern lateral scarp displays a type II bulge. Above the bend, a prominent type I bulge is apparent along the western lateral shear.

3.5.2. Composition of Earthslide Material

Material within the earthslide comprises a sheared and highly deformed matrix of mud (silty clay/clayey silt; see section 3.5.4), within which fine to coarse sand (Homebush Sandstone, Waipara Greensand and sand-sized particles of Amuri Limestone) and limestone gravels ranging in size from fine to very coarse occur. X-ray diffraction analysis indicates that the clay mineral comprising the majority of the matrix is a calcium-magnesium smectite (see section 3.5.4.5). The matrix generally comprises over 60% of the earthslide soil mass, but can comprise as little as 40% of the mass on the flanks of the earthslide, or as much as 90% of the mass along lateral shears. Occasional fragments of stiff brown (Ashley Mudstone) or blue-grey silty clay (Loburn Mudstone) and larger blocks of intact Amuri Limestone (up to 2.5 m. diameter) can be observed within the earthslide material.

At the toe of the earthslide, deformed bands of a stiff blue grey clay can be seen. This material can also be observed directly under earthslide material and is likely to be in situ Loburn Mudstone. As mentioned before, this lithology also occurs as lumps within the earthslide mass.

3.5.3. Earthslide Movement Rates

The movement rates of Earthslide 3 are analysed from two perspectives: (i) 'long-term' rate, ie, rate of displacement of the slide over a period of more than 10 years, and; (ii) the rate and nature of displacement over a yearly interval, or 'short-term' movement rate.

3.5.3.1. Long Term Movement Rate

The determination of long term movement rate for the earthslide was attempted using differing sets of aerial photographs by attempting to record the displacement of a recognisable feature common on both sets. However, this had limited success for Earthslide 3, due to the relatively large scale of both sets of photographs and the fact that on one set only half of Earthslide 3 is photographed. Nevertheless, a long-term movement rate was able to be determined for the track zone of the earthslide: Located within the earthslide bend is a strainer post displaced from the upslope fenceline (fig. 4). The post was emplaced in 1969 (Mr Dick Carmicheal, pers. comm, 1993), and has subsequently moved close to 55 m, thus providing an average movement long-term movement rate for this portion of the slide of about 2.3 m per year.

3.5.3.2. Short Term Movement Rates

A. Subsurface Data

Limited subsurface investigations were conducted on Earthslide 3 using a simple hand auger. Logs of boreholes are shown in figure **4**(C). The boreholes were subsequently fitted with Casagrande piezometers to measure ground water pressures. The holes also provided information on the depth to the basal shear surface of the landslide. No information could be gained from the boreholes in regard to the vertical displacement profile of the earthslide but it is assumed that the majority of displacement observed at the surface occurs at the basal shear zone.

B. Surface Data

A surface monitoring network was installed on Earthslide 3, with the intention of observing both horizontal and vertical surface displacements over the period of one year. Positions of monitoring points are shown in figure **4**. Points initially emplaced for Barrell's (1989) study were incorporated into the monitoring network. Barrell's monitoring points are denoted by a P, followed by a number (for example, P14). Points installed in March 1993 are denoted by a letter (which refers to the particular line the monitoring point is in), and a single number (eg., C5).

The positions of points within the monitoring network were surveyed using an E.D.M. theodolite (see Appendix E) stationed on a control point (IT1) at the western edge of the landslide complex. Stability of the control point was achieved in exactly the same way as outlined in Barrell (1989), that is, by triangulation with established survey marks located outside of the landslide area (see Appendix C). During the course of monitoring, triangulation confirmed negligible movement of the control point. Resurveys were conducted approximately bi-monthly.

C. Results of Surveying

The results of each survey are given in Appendix F and are shown diagrammatically on figure **5.** Tables 3.1 and 3.2 provide a summary of data presented in Appendix F.

(i). Movement of points emplaced by Barrell (1989)

It is noticeable that points located on the active earthslide show considerable displacements in the 4 years between the two surveys (table 3.1). Points 11-14 have moved on average 3.7 m. from their March 1989 positions, while point 5, Barrell's only point located on the narrowest part of the earthslide (ie, at the bottom end of the track zone) shows a movement vector of over 8 m. Therefore, for the period March 1989-March 1993 (a period of almost exactly 4 years), the average velocity for the region

immediate to points 11-14 was 0.93 m/yr, while the track zone has had an average velocity of approximately 2 m/yr.

POINT	Horizontal displacement	Average displacement	Movement direction	Vertical displacement
P1	5.042	1.008	193.211	-0.190
P2	3.743	0.749	208.751	-0.648
P3	0.060	0.012	209.889	0.011
P4	6.779	1.356	233.560	-1.003
P5	8.512	1.702	187.292	0.924
P6	0.645	0.129	155.814	-0.083
P10	0.941	0.188	206.130	-0.087
P11	3.705	0.741	204.785	-0.395
P12	3.627	0.725	208.112	-0.251
P13	3.541	0.708	208.874	-0.587
P14	4.022	0.804	217.234	-0.661

Table 3.1 Horizontal and Vertical displacements of points installed in 1989 at March 1993 (displacements in m., direction given in degrees)

It is evident on figure **6** that the direction of displacement of monitoring points between 1989 and 1993 is in the same direction as for the monitoring period March 1993 - 1994, with the exception of point 5. Notable too is the substantial rise in the elevation of point 5. The reason for the rise in R.L. and change in direction of point 5 is probably due to a component of internal deformation occurring in this area.

Points 1 and 2 are located on either side of a curved internal shear within the earthslide bend (discussed in section 3.5.1.2). It is evident from data presented in table 3.1 that this internal shear has components of both dextral strike slip and normal faulting, with P2 being downthrown relative to P1, while P1 is offset dextrally relative to P2. From evidence presented in table 3.1, this internal shear accommodates on average about 30 cm/yr differential movement in the horizontal direction and 9 cm/yr in the vertical direction.

(ii) Correlation with Precipitation

The amount of monthly precipitation from January 1986 to March 1994 (NIWA, 1994a) indicates that there was considerably less than average monthly rainfall during the 6 months of Barrell's survey (fig. 3.13). During this time, the maximum displacement recorded by monitoring points on Earthslide 3 was approximately 5 cm (Barrell, 1989). Therefore, this period of low rainfall from about June 1987 to June 1989 resulted a period of extremely slow movement of Earthslide 3. However, substantial displacement of monitoring points emplaced by Barrell was noted at the first survey of this study (fig. **6** and table 3.1). Periods or months displaying an above average rainfall in the years between March 1989 and March 1993 were, on a yearly basis:

1. June and October 1989
2. August 1990
3. January-February, April, June-July, November - December 1991
4. May -September 1992

D. Movement of points emplaced in March 1993

Horizontal and Vertical displacements for the year of monitoring are given in figure **6**. Table 3.2 gives total horizontal and vertical displacements between the first and last surveys.

Station	Horizontal vector magnitude	Vertical vector magnitude	Station	Horizontal vector magnitude	Vertical vector magnitude
A1	0.2300	-0.103	P14	1.1165	-0.217
A2	0.2989	-0.092	D1	0.1568	0.065
A3	0.3745	-0.168	D2	1.2302	0.026
A4	0.3563	-0.155	D3	1.1232	0.054
A5	0.3994	-0.174	D4	0.0319	0.105
A6	0.0477	0.043	P1	1.4563	-0.081
B2	0.3896	-0.079	P2	1.2804	-0.107
B3	0.4612	-0.103	E1	0.1632	0.130
B5	1.1076	-0.089	E2	1.7519	-0.138
B9	1.4032	0.022	E3	2.0331	-0.097
C1	0.1677	0.046	E4	0.0403	0.106
C2	0.7663	-0.020	P4	1.7555	-0.387
C3	0.7845	0.010	P5	1.6353	-0.253
C4	0.7848	-0.053	P6	0.1638	0.008
C5	0.0818	0.028	BH1	1.4491	-0.099
P10	0.2376	-0.018	BH2	1.5719	1.472
P11	1.2409	-0.151	BH3	1.6285	-0.200
P12	1.2122	-0.100	BH4	0.9020	-0.150
P13	1.1725	-0.205	BH5	0.8571	0.030

Table 3.2 Horizontal and Vertical displacements of monitoring points, March 1993 -March 1994. (note: boreholes installed May-June 1993)

It is evident in figure **6** that points in the downslope region of Earthslide 3 ('A' line, B2 and B3) have moved on average 0.28 m, but show somewhat erratic horizontal movement vectors (compared with those observed further upslope), and show a generalised tendency to experience a rise in elevation during times when the earthslide is in a state of acceleration, followed by a subsequent decrease in elevation during periods of low movement rate. It is also notable that A3, A4 and A5 have been displaced by a greater amount than points A1,2 or 6.

Points located in line C, and point B5, show a lesser degree of inflation at times of earthslide acceleration and show larger horizontal displacements without the same degree

Figure 3.13 Monthly precipitation, January 1986-December 1991, showing periods of monitoring of movement rates on Earthslide 3.

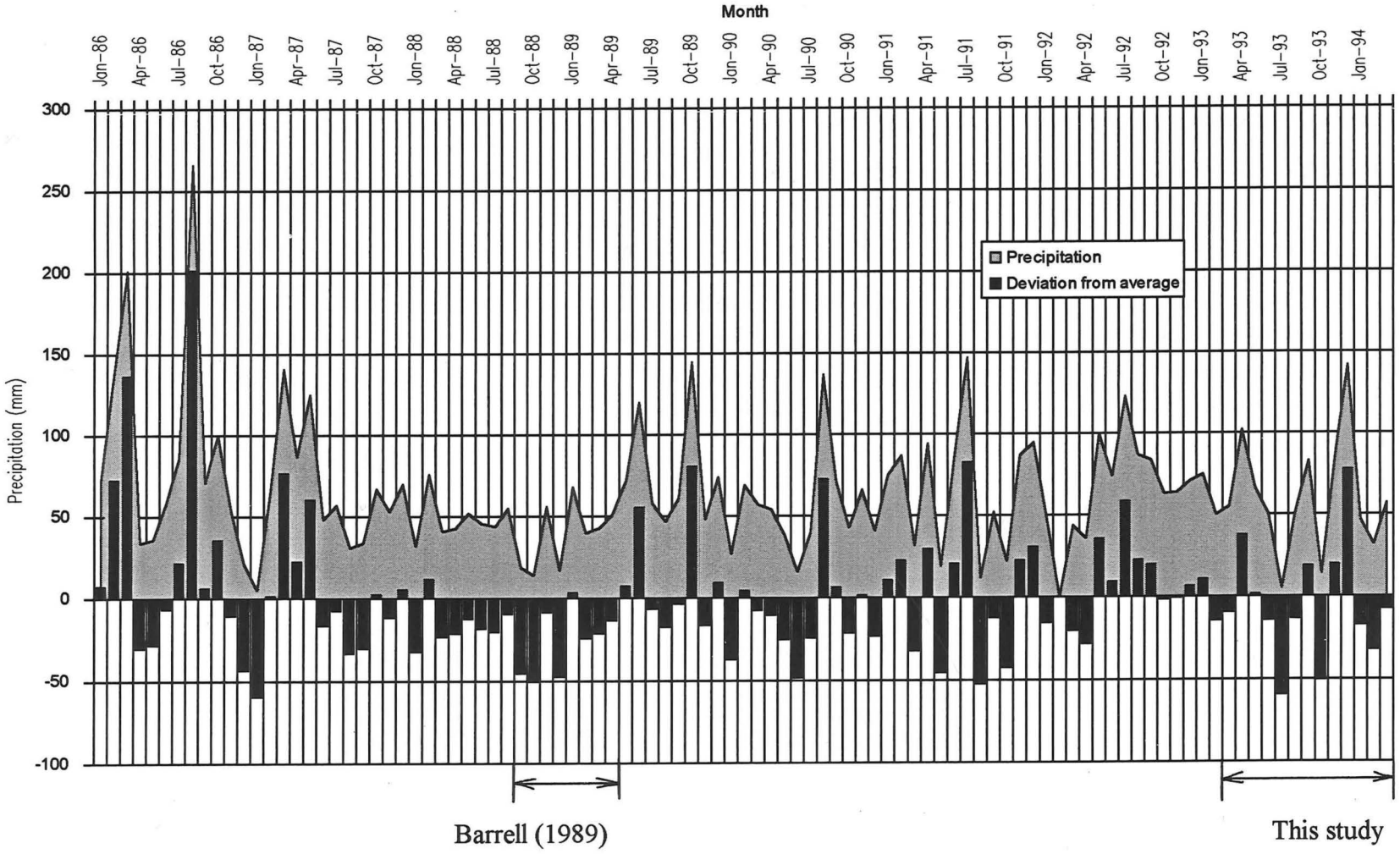

Figure 3.14 Cumulative and total displacement of monitoring points, Earthslide 3.

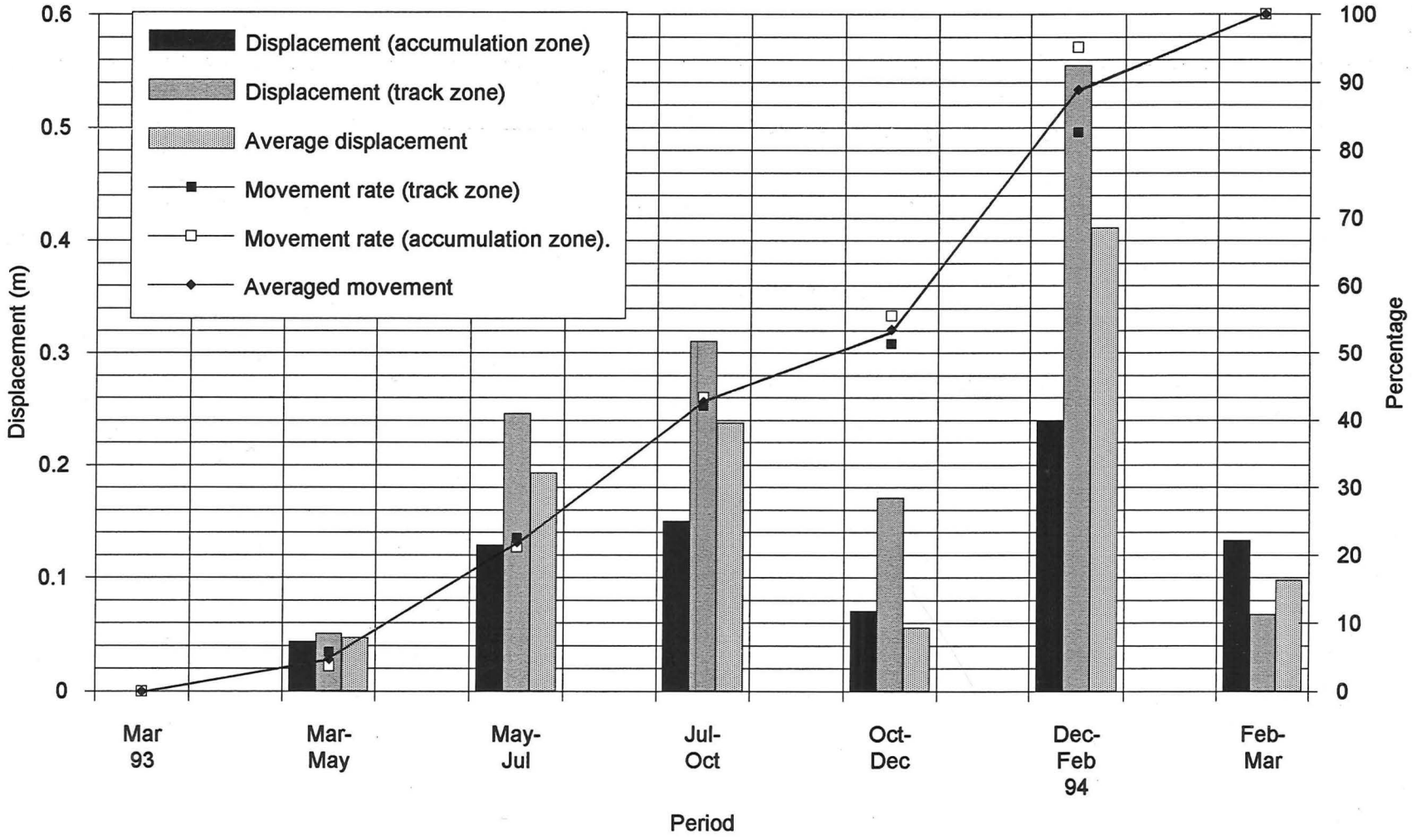

Figure 3.15 Weekly rainfall, Motunau Beach, March 1993-March 1994.

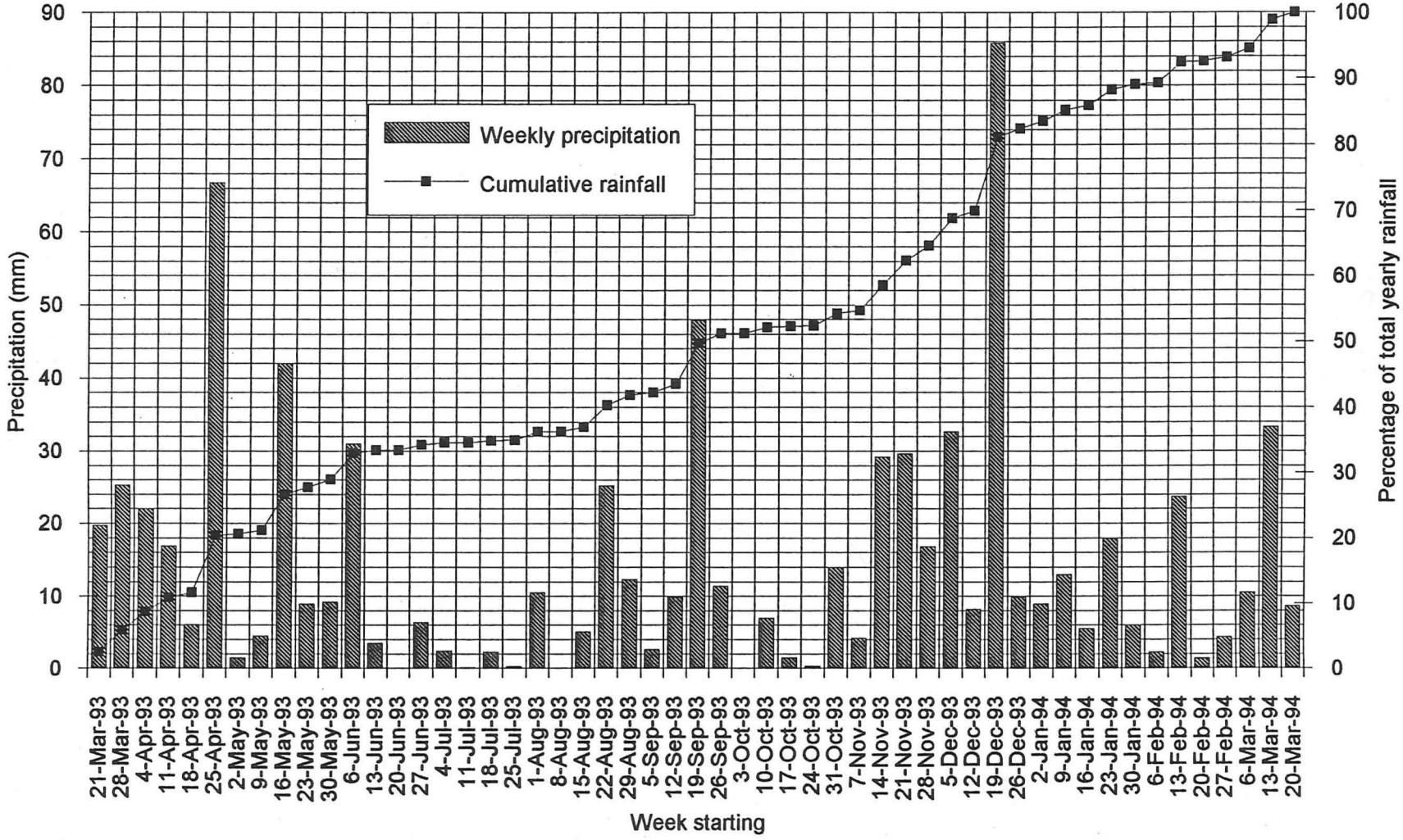

Figure 3.16 Borehole water levels and monthly precipitation, July 1993-March 1994

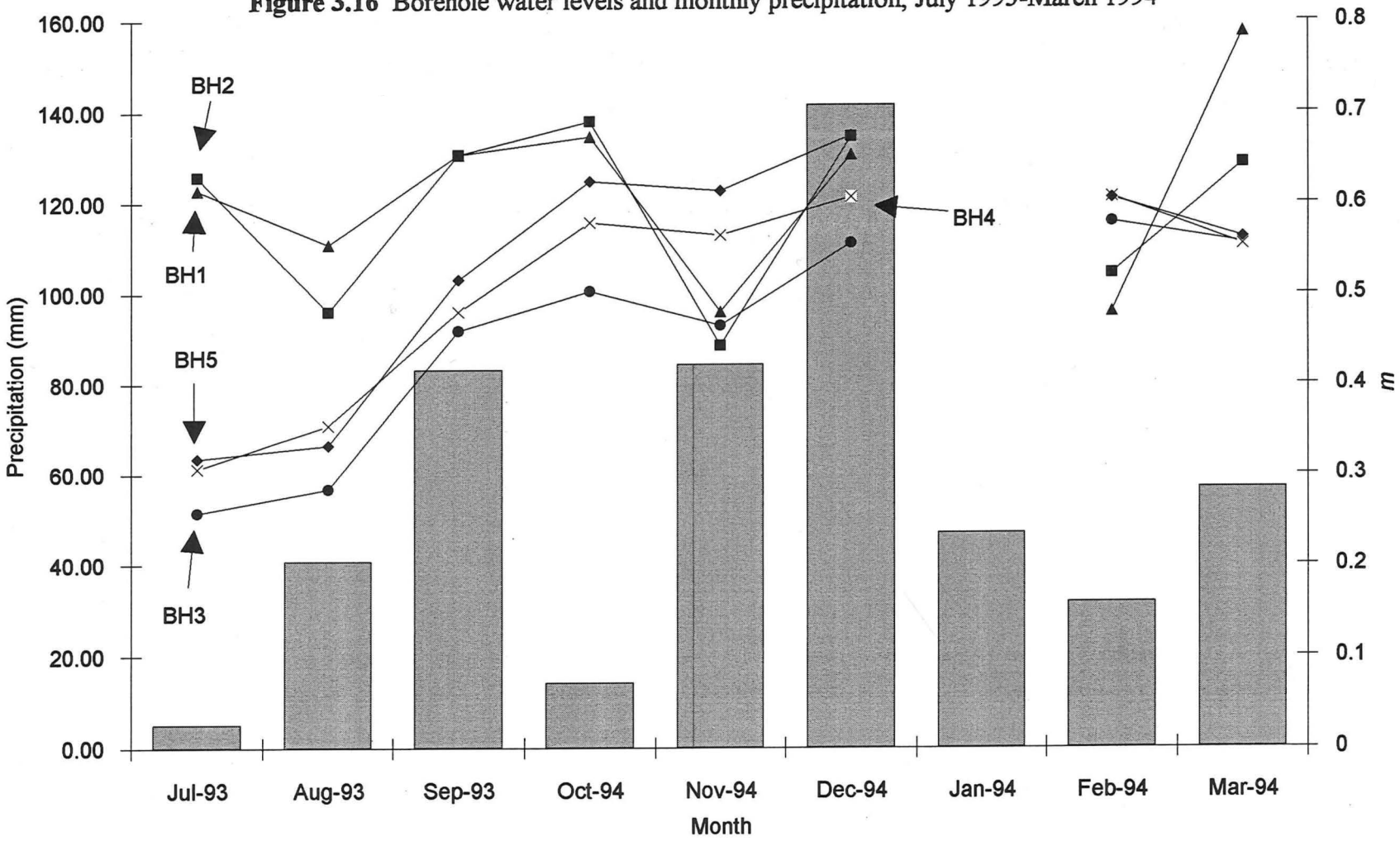

of erratic movement directions observed in points B2, B3 and line A. However, points P11-P14 show almost linear horizontal displacements, and show a constant decrease in elevation with displacement, regardless of the overall state of motion of the earthslide. Similarly to P11-P14, the two points of D line located on Earthslide 3 also show near linear horizontal displacements, but show some degree of inflation at times of accelerated movement rate.

Monitoring points located within the track zone above the earthslide bend (E2, E3, P5 and B9) show the greatest displacement, with an average of 1.7 m. Points E2 and E3 show the greatest net displacement on Earthslide 3, with an average between these 2 points of about 1.9 m/yr. However, this displacement is still less than the long-term movement rate in this area, indicated by the displaced strainer post which gives an average annual movement rate of 2.3 m/yr for this part of the earthslide (see section 3.5.3.1). Similarly to monitoring points P11-P14, points E2, E3, P5 and B9 show a steady decrease in elevation with time.

E. Timing of Movements

The first resurvey, conducted on 11 May 1993, in general showed little displacement (fig. 3.14) of monitoring points from the initial survey, conducted on 22 March 1993. A steady increase in the amount of displacement was recorded in the 2 subsequent surveys, on 22 July and 3 October. The resurvey conducted in December showed that movements of points had slowed; however, dramatic displacement was subsequently recorded in the January 1994 survey. The following (and last) resurvey at the end of March 1994 showed little displacement of monitoring points from their January positions (fig. 3.14).

Therefore, two major periods of movement of Earthslide 3 can be recognised initially (fig.3.14):

1. late May-early October 1993: this period accounted for approximately 40% of the total displacement observed.
2. early December - late January 1994: this shorter time interval realised approximately 38 % of the total observed movement

The remaining 22 % of displacement occurring between March 1993 and March 1994 occurred at times of relatively slower movement rate, that is, pre May 1993, early October - early December 1993 and post- January, 1994.

F. Characteristics of Displacement

Figure 3.14 shows that the characteristics of movement between the track and accumulation zones of the slide are somewhat different. It is noticeable that at the 4th resurvey (conducted in early December 1993) points within the track zone of the slide

(P11-P14, P1, P2, D1, D2, E1, E2, P5, B5 and B9) had achieved 57 % of the total observed displacement, whereas at the same stage points within the accumulation zone ('A'-line, B2, B3, 'C'-line) had only realised 49% of the total observed movement. Similarly, at the 5th resurvey (early February 1994) the head of the slide had attained 95% of the observed yearly movement, while the toe of the slide had only achieved 84% of the observed displacement

Therefore, displacement near the head of the slide is characterised by short periods of relatively rapid movement rate interspersed with periods of relative inactivity. In contrast, displacement near the toe of the earthslide is generally more uniform, with movement occurring at a slower rate, but for relatively longer periods, than observed further upslope.

3.5.3.3. Influence of Precipitation on Short Term Movement Rate

Daily rainfall data was recorded at a NIWA station located at Motunau township. Data from this station is likely to closely reflect the actual rainfall at Coringa due to the proximity of the two sites.

A. Rainfall Patterns for Year starting 21 March 1993

Total rainfall for the year starting 21 March 1993 was 768.4 mm (NIWA, 1994b), and is shown by week in figure 3.15. The week starting 19 December 1993 had the maximum rainfall, with approximately 85 mm, while several weeks from late June to late July 1993 had zero or only a few millimetres of rain. Periods of higher rainfall for the year starting 21 March are (i) late March-early June, (ii) mid August-early October and (iii) early/mid November 1993-early January 1994 (fig. 3.15). A correlation is achieved between the yearly rainfall pattern and earthslide movement rates (see chapter 4, section 4.5.2.3)

B. Ground Water Levels

Casagrande type piezometers (Appendix C) were installed in boreholes BH1-BH5. Water levels in the boreholes were recorded approximately monthly, at each resurvey, and generally once in between successive surveys. The maximum value of m (ie., ground water level expressed as a function of earthslide depth, z), detected in boreholes 1 to 5 was close to 0.8, while the minimum value is less than 0.3 (fig. 3.16). However, it can be seen in figure 3.16 that no strong correlation existed between measured ground water levels and the amount of precipitation. This lack of correlation is likely to be due to a combination of one of more of the following factors: (a) inadequate emplacement of the piezometer setup; (b) complex groundwater response patterns, due to changes in horizontal stress states (effecting a change in the void ratio of the soil); (d) overly long response times, due to the soil permeability and type of piezometer used (ie. Casagrande

measurement, and/or (d) disruption to the instruments caused by displacement of the earthslide mass.

3.5.4. Geotechnical Analyses

A number of geotechnical analyses were performed on the material involved in Earthslide 3. Laboratory tests included: (i) Natural moisture content; (ii) Atterberg limits; (iii) Linear shrinkage; (iv) Bulk density; (v) Whole sample and clay fraction X-ray diffraction analysis for determination of the mineralogy of the material; (vi) Pipette analysis for grainsize distribution (vii) Ring shear analysis for residual cohesion intercept and friction angle values; (viii) Repeated reversal direct shear tests for residual cohesion intercept and friction angle values, and; (ix) Permeability (falling head) tests. Full explanations and procedures of each test are given in Appendix C.

Nine sample localities were dug on Coringa near at the beginning of September 1993 (fig. 4). Sites CL 1, 4, 6 and 8 were located in general earthslide debris, while sites CL 2, 3, 5, 7, and 9 comprised disturbed clay from lateral shear zones. Sub-surface soil samples, and samples of material inferred to be in the basal shear zone were provided from boreholes BH1-5. Because of the method of emplacement of the boreholes (by hand auger) only disturbed samples of the basal shear could be obtained.

3.5.4.1. Natural Moisture Content, Atterberg Limits and Linear Shrinkage

A. Moisture Content

Moisture contents for soil samples from Earthslide 3 showed moisture contents ranging from 32% to 43%, with the exception of sample BH1@0.85m. Bh1 was emplaced in a wet area of the earthslide and it is inferred that the high moisture content is due to the infiltration of surface water. Samples derived from basal and lateral shear zones typically showed much higher moisture contents, approximately 48 to 55%.

B. Atterberg Limits

Samples analysed on Earthslide 3 showed liquid limits of between 57.3 and 84.3%, while plastic limits were between 29.6 and 38.5%. Plasticity indices correspondingly ranged Plasticity indices correspondingly ranged between 23 and 46%. The analysed sample of material underlying Earthslide 3 (ie. Loburn Mudstone) showed a w_l equal to 78.5% and a wp of 33%.

C. Linear Shrinkage

The amount of linear shrinkage was determined for 5 samples from Earthslide 3. Values ranged from 9.4 to 16.2%. Linear shrinkage in Loburn Mudstone was slightly over 10%.

Sample Name	Moisture Content (%)	Index Properties			Linear Shrinkage (%)	Bulk Density (kg/m^3)	Particle Size			Permeability (k) (mm/s)	Effective shear parameters	
		Liquid Limit (%)	Plastic Limit (%)	Plasticity Index (%)			Sand Fraction (%)	Silt Fraction (%)	Clay Fraction (%)		Residual friction Angle (°)	Residual Cohesion (kPa)
BH1@0.85m(2)	53.4	65.5	31.0	34.5	12.78	1721	52	29	18	$2.54x10^{-6}$		
BH1@1.80m	38.9	76.0	36.8	39.2								
BH2@1.44m	42.5	64.5	34.6	29.9	9.93	1567				$1.96x10^{-6}$		
BH2@3.51m(1)	48.4	76.5	35.9	40.6			10	47	43		12.7	0
BH3@2.90m(1)	49.1	72.5	36.8	35.7			11	44	45		12.8	0.5
BH4@1.42m	35.9	56.4	32.9	23.5		1581	13	53	34			
BH5@3.57m	41.4	67.5	31.0	36.5	13.87	1633						
BH5@4.68m	31.6	57.3	32.6	24.7	9.41							
CL 1	42.2	74.0	38.5	35.5	13.98		23	52	25	$2.00x10^{-6}$	22.9	1.5
CL 2 (l.s.z)	51.2	76.5	36.2	40.3			14	47	39		13.1	0.5
CL 3 (l.s.z)	48.2	84.3	38.2	46.1	15.23	1674	15	44	41		13.1	0
CL 4	33.4	69.7	32.1	37.6						$2.77x10^{-6}$	22.3	0
CL 5 (l.s.z)	55.3	77.3	36.2	41.1	14.94		9	48	43		12.8	1
CL 6(2)	36.5	44.1	29.6	14.5		2004	63	23	14			
CL 7 (l.s.z)	49.8	72.6	33.5	39.1							12.9	1
CL 8	32.4	73.1	31.9	41.2	16.20	1732	56	24	20	$2.76x10^{-6}$	26.0	0
CL 9 (l.s.z)	54.3	70.1	37.6	32.5			16	49	35		13.4	0
Loburn Mudstone (BH3 & 4)	41.7	78.5	33.0	45.5	10.25	1993						

Table 3.3 Summary Data of Geotechnical Analyses, Earthslide 3, Coringa Landslide Complex.
(1) basal shear zone material; (2) high Waipara Greensand content; (l.s.z) lateral shear zone material

3.5.4.2. Bulk Density and Soil Unit Weight

Recompacted bulk densities for Earthslide 3 range from 2004 kg/m^3 for CL 6 to 1521 kg/m^3 for BH4@1.42m, with an average value of 1693 kg/m^3. Soil unit weights (γ, kN/m^3) are given by the equation $\gamma = \rho g$, where g is the acceleration due to gravity (9.8 m/s^2; Craig, 1992). Values of γ for material comprising Earthslide 3 correspondingly range between 19.9 kN/m^3 and 14.9 kN/m^3. Accordingly, the average soil weight for Earthslide 3 is about 16.6 kN/m^3.

3.5.4.3. Grainsize Analysis

Analyses were performed on 11 samples from Earthslide 3 and results are given in table 3.3 and expressed diagrammatically in figure 3.17. It can be seen that two major groupings of grainsize occur, (a) minor (<20%) sand fraction, and (b) major (>50%) sand fraction. Samples that have a high sand fraction (CL 6, CL 8 and BH1@0.85m) were located near the head of the slide, and reflect the influence of feeder flows and slides originating in Waipara Greensand along the western lateral scarp of Coringa Landslide Complex.

3.5.4.4. Permeability Tests (Falling Head Test)

The falling head test is the most common method of establishing the permeability of fine-grain soils. Details of the test are given in Appendix D. Values of k (coefficient of permeability) for material comprising Earthslide 3 range from 1.96×10^{-6} to 2.77×10^{-6} mm/s, in keeping with expected values for a non-fissured silty clay (Craig, 1992).

3.5.4.5. Measurement of Residual Shear Strength

Residual shear strengths; effective residual friction angle, ϕ'_r, and effective residual cohesion, c'_r were determined for 5 samples from Earthslide 3 using both ring shear analysis and repeated reversal direct shear analysis. Samples comprised remoulded material from lateral shear zones.

A. Ring Shear Analysis

The Bromhead Ring Shear Apparatus conducts a continuous shear strength test within an annular, ring shaped test sample (Law, 1987). The sample is sheared by differential rotation and shear stress is measured for a series of normal stress conditions. Details of the test procedure and setup are given in Appendix D.

Results

Measured values of effective friction angle for Earthslide 3 fall into three groups (fig.318):

1. Basal shear samples (BH2@3.51m; BH3@2.90 m) provided a value of ϕ'_r of 12.9°. These samples had *CF* (clay fraction) values of 43-45%.

Figure 3.17. Particle size distributions, Earthslide 3

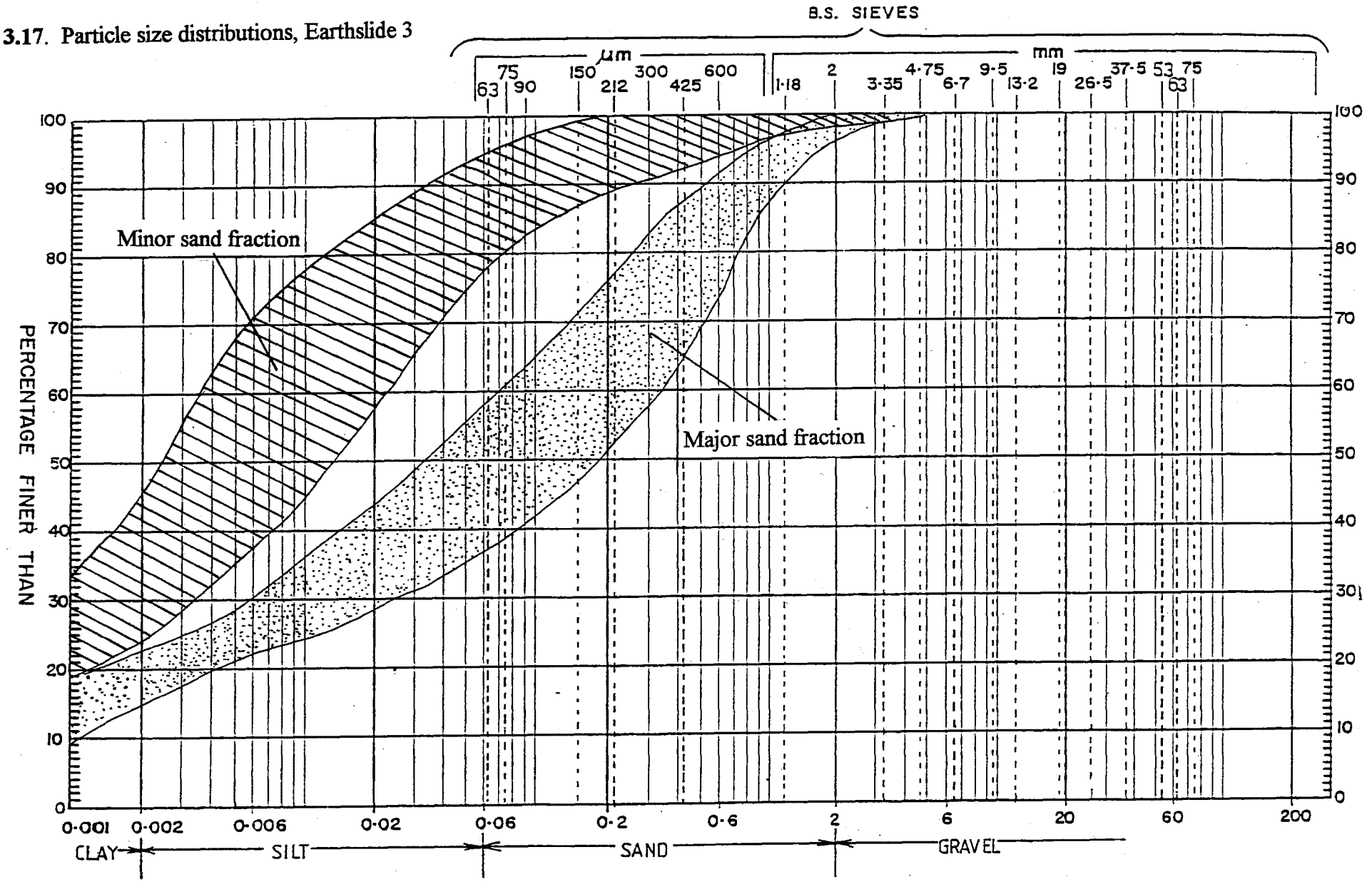

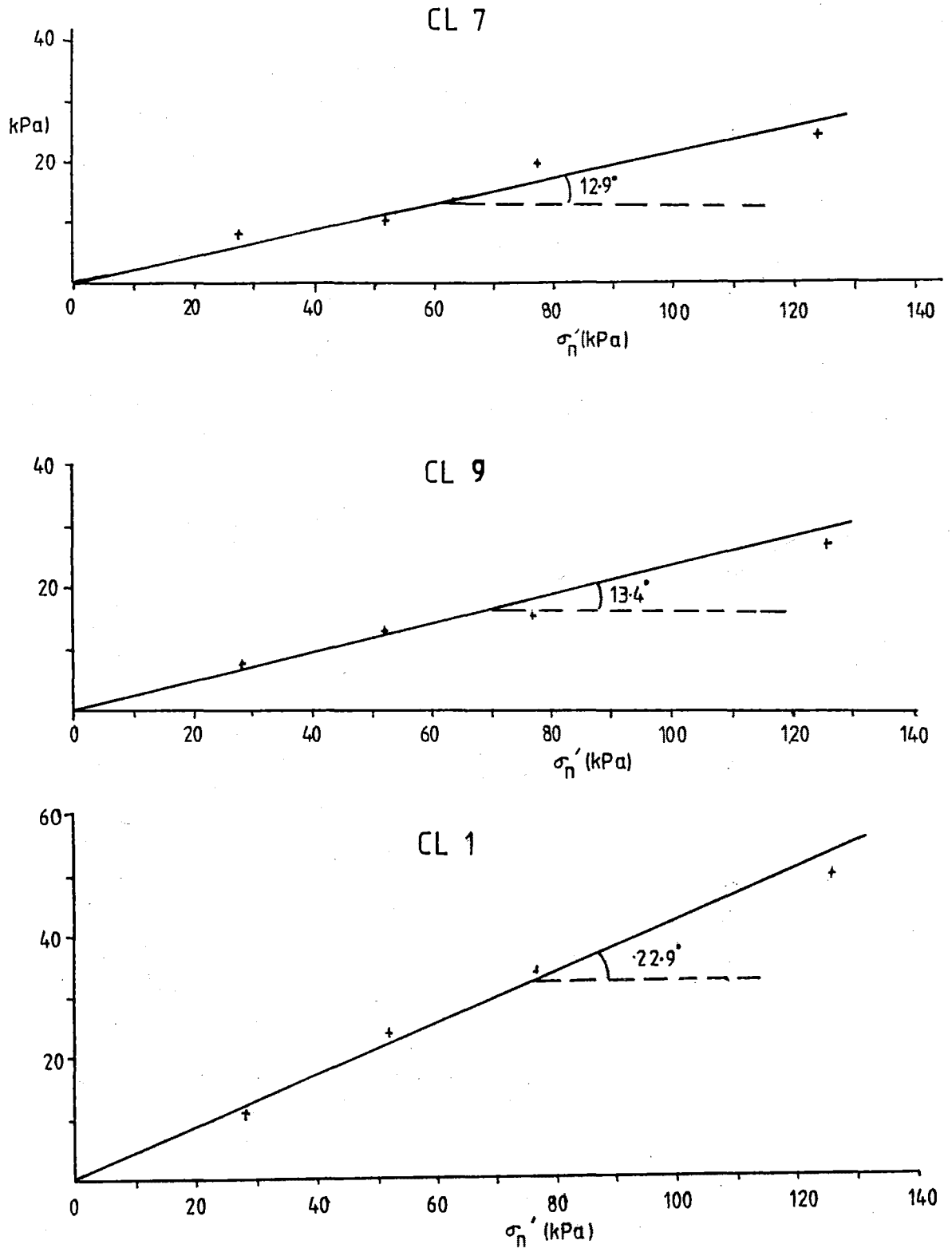

Figure 3.18 Results of ring shear analysis for samples CL 1, 7 and 9; obtained from Earthslide 3 (see fig. 4 for locations)

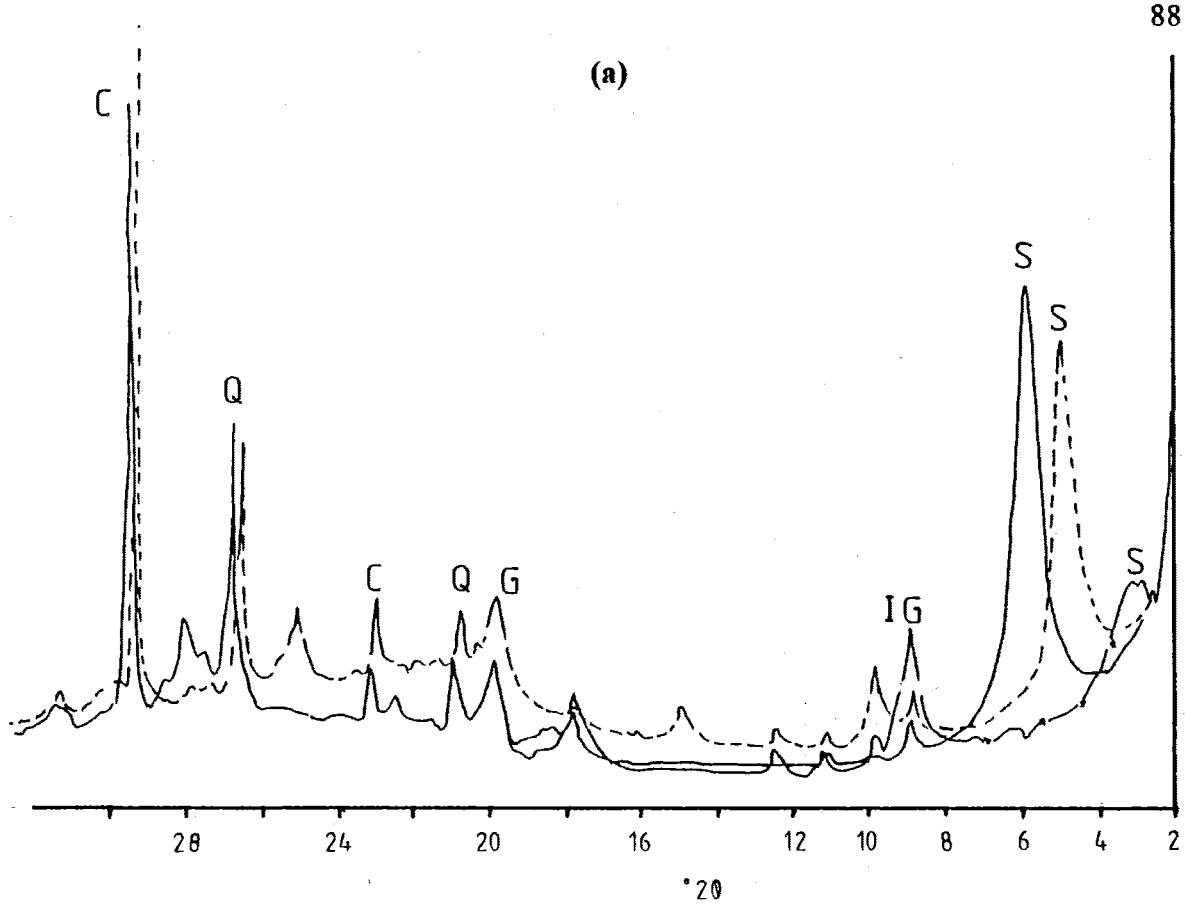

Figure 3.19 X-ray diffraction plots, BH4@1.42m, Earthslide 3
(a) Random (whole sample) mount; **(b)** Preferentially orientated (clay fraction) mount.S = smectite, G = glauconite, I = Illite, Q = Quartz C = Calcite. Note that peaks consistent with feldspar minerals are located off plots. Untreated mount shown as a solid line, glycolated mount shown as a dashed line, fired mount shown as a dash-dot.

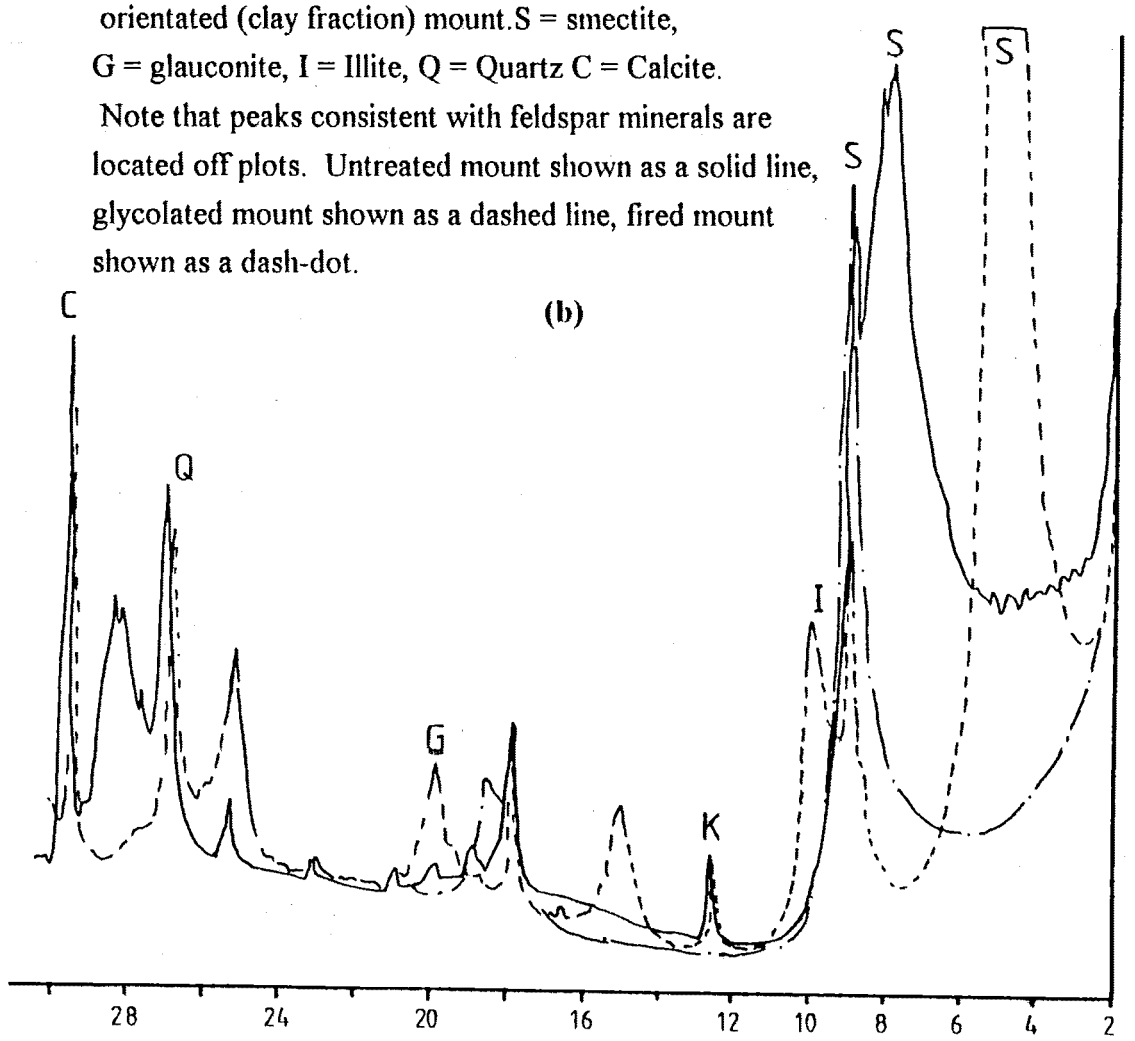

2. Lateral shear samples (CL 2,3,5,7 and 9) supplied values of effective friction angle between 12.8° and 13.5°. These samples had clay fractions of 38-45%
3. Samples with a relatively high sand and/or silt content (CL 6 and 8) showed values of residual friction angle as high as 26°.

However, measured values for Earthslide 3 tend to indicate that c'_r =0 and ϕ'_r =13° are realistic residual strength parameters for later analyses.

B. Direct Shear Analysis

One repeated reversal direct shear test was performed on material from CL 5, to provide an alternative method of obtaining the residual friction angle. Results from this test were not satisfactory, due to the fact that the maximum displacement able to be generated by the shear box was less than that required to produce an adequate shear plane in the clay sample. As such, true residual conditions could not be achieved, even with a number of reversals.

3.5.4.6. X-ray Diffraction (XRD) Analysis

X-ray diffraction analysis was performed on only one sample from Earthslide 3. Due to the characteristics of exposures of clay within the earthslide it was assumed that the clay mineralogy of Earthslide 3 was comprised mostly of smectite, and XRD analysis was in actuality only used to confirm this assumption.

Both random and orientated mounts (see Appendix E) of the sample (BH4@1.42m) were prepared. These were subsequently run through the diffractogram, treated with ethylene glycerol, run again and lastly heated to 550°C and re-run. Diffraction plots are shown in figure 3.19. The major clay mineral that can be identified on these diffraction plots is Ca-Mg Smectite. Minor amounts of illiite, glauconite and kaolinite also occur. Non clay minerals identified in the random mount include quartz, calcium and feldspar.

3.5.5. Stability Analysis

A stability analysis of Earthslide 3 was performed using both the Infinite Iandslide Expression and the Infinite Rectangular Landslide Expression (see section 2.6.4). For Earthslide 3, the failure surface is assumed to be sub-parallel to the ground surface, and to occur at shallow depth compared to the length if the slide (fig. **4**). The slide has the ratio z/L equal to 0.0065 ($z \cong 5$ m, L = 775 m), thus the Infinite Landslide and Rectangular Landslide Expressions can be applied with negligible error (Skempton & Hutchinson, 1969).

Earthslide 3 has a height difference from head to toe of approximately 80 m, which produces an average gradient (β) of nearly 6°. The maximum value of β (close to 10°) occurs in the area around BH2. The average depth to the basal shear surface is about 5

m, while γ (soil bulk density) = 16.4 kN/m^3 (section 3.5.4.2); and γ_w (bulk density of water) = 9.8 kN/m^3 (Craig, 1992).

3.5.5.1. The Infinite Slope Expression

It was demonstrated in Chapter 2, section 2.7.4 that, for clay soils under residual conditions (c'_r = 0) and assuming that the slope is in a state of limiting equilibrium (F_2=1, where F_2 is the two dimensional factor of safety) that the effective residual friction angle (ϕ_r') is given by

$$\phi_r' = \tan^{-1}\left(\frac{\gamma \tan\beta}{\gamma - \gamma_w m}\right) \qquad (3.1)$$

where m is the ratio of the height of ground water above the basal failure plane to earthslide thickness. Therefore, by varying the values of β and m, a range of effective residual friction angles needed to place the earthslide in a state of limiting equilibrium can be calculated (table 3.4).

Slope Gradient (β)	Ratio of height of ground water above basal failure plane to earthslide thickness (m)					
	1.0	0.9	0.8	0.7	0.6	0.5
9.0	21.5	19.0	17.0	15.2	13.9	12.7
8.5°	20.4	18.0	16.0	14.4	13.1	12.0
8°	19.3	17.0	15.1	13.6	12.4	11.3
7.5°	18.1	16.0	14.2	12.8	11.6	10.6
7.0°	17.0	14.9	13.2	11.9	10.8	9.9
6.5°	15.8	13.9	12.3	11.1	10.1	9.2
6.0°*	14.6	12.8	11.4	10.2	9.3	8.5
5.5°	13.5	11.8	10.5	9.4	8.5	7.8
5.0°	12.3	10.7	9.5	8.6	7.8	7.1
4.5	11.1	9.7	8.6	7.7	7.0	6.4

Table 3.4 : Infinite Slope Analysis; Required values of ϕ'_r to produce a limiting equilibrium state on Earthslide 3 (F_2 = 1.00), assuming residual conditions (c'_r = 0). * average earthslide gradient

3.5.5.2. The Infinite Rectangular Landslide Expression

While the infinite slope analysis can model the conditions existing within Earthslide 3, the slide is laterally confined, and therefore the factor of safety of the earthslide will be influenced to some degree by the effects of lateral earth pressure. In the infinite rectangular landslide expression (after Hutchinson & Del Prete, 1985), ϕ'_r is given by:

Slope Gradient (β)	Ratio of height of phreatic surface above basal failure plane to landslide thickness (m)											
	1.0		0.9		0.8		0.7		0.6		0.5	
K	*0.6*	*0.3*	*0.6*	*0.3*	*0.6*	*0.3*	*0.6*	*0.3*	*0.6*	*0.3*	*0.6*	*0.3*
9.0°	21.3	21.4	18.69	18.8	16.7	16.8	15.0	15.1	13.7	13.8	12.6	12.6
8.5°	20.2	20.3	17.71	17.8	15.8	15.9	14.2	14.3	12.9	13.0	11.9	12.0
8.0°	19.1	19.2	16.71	16.8	14.9	15.0	13.4	13.5	12.2	12.3	11.2	11.3
7.5°	17.9	18.0	15.71	15.8	14.0	14.1	12.6	12.7	11.4	11.5	10.5	10.6
7.0°	16.8	16.9	14.69	14.8	13.1	13.2	11.8	11.9	10.7	10.8	9.8	9.8
6.5°	15.6	15.7	13.68	13.8	12.2	12.2	10.9	11.0	9.9	10.0	9.1	9.2
6.0° (ave. β)	14.5	14.6	12.65	12.7	11.2	11.3	10.1	10.2	9.2	9.2	8.4	8.5
5.5°	13.3	13.4	11.62	11.7	10.3	10.4	9.3	9.3	8.4	8.5	7.7	7.8
5.0°	12.1	12.2	10.59	10.7	9.4	9.5	8.4	8.5	7.7	7.7	7.0	7.1
4.5°	10.9	11.0	9.55	9.6	8.5	8.5	7.6	7.7	6.9	6.9	6.3	6.4

Table 3.5. Infinite Rectangular Landslide Expression: Required values of ϕ'_r to produce a state of limiting equilibrium (F_3 = 1.00) with K = 0.67 and 0.3, and; $c'_r = 0$

Note: F_3 is the three dimensional factor of safety.

$$\phi'_r = \tan^{-1}\left(\frac{\sin\beta}{\frac{K}{\lambda}\left(1-m^2\frac{\gamma_w}{\gamma}\cos^2\beta\right)+\cos\beta\left(1-m\frac{\gamma_w}{\gamma}\right)}\right) \qquad (3.2)$$

where the variables β, γ, γ_w and m are defined as in equation (3.1); K is the coefficient of lateral earth pressure, and λ is the width of the moving landslide mass. For Earthslide 3 the maximum value of K is taken as 0.67, and the minimum value is taken as 0.3 (equal to K_a; see Appendix G). The average value of λ is close to 60 m. Again, by varying the values of β, m and K, a range of effective friction angles can be calculated that place the slide in a state of limiting equilibrium (Table 3.5).

3.5.5.3 Results

The infinite rectangular landslide expression provided consistently higher values of ϕ'_r than the infinite slope expression. This is due to the fact that, assuming no deformation occurs in the 'rectangular' landslide mass, lateral earth pressure will tend to act as a stabilising influence. The degree of the stabilising influence is governed by the amount to which K approaches K_a (coefficient of active earth pressure) or K_p (coefficient of passive earth pressure). However, it can be seen in tables 3.4 and 3.5 that the difference in values of ϕ'_r required for limiting equilibrium using the 2 methods of stability analysis is only slight. Therefore, for the encountered value of λ, it is noted that (i) the value of F is not greatly affected by lateral earth pressure and (ii) the main factors governing the value of ϕ'_r are the values of β, γ and m.

The maximum water level detected in boreholes was about 0.8 m. Infinite slope and Infinite Rectangular Slope analysis require that, for this water level, at the average gradient of the earthslide, a maximum angle of effective residual friction of 11.4° is needed to place the slide in a state of limiting equilibrium. In section 3.5.4.5, it was found that the angle of effective residual friction for the slide was about 13°. Stability analysis indicates that for friction angles of this order, movement would cease if the ground water level fell below 0.9 m. Monitoring evidence (section 3.5.3.2) and measured ground water levels indicate that the earthslide displays movement at values of m less than 0.9.

3.6. Summary and Conclusions

3.6.1 Greater Coringa landslide Complex

Coringa Landslide is a large class VI slump/earthslide complex, (under Varnes' (1978) classification scheme) involving an area of approximately 50 hectares, located at the stratigraphic top of the Eyre Group (after Brown and Field, 1985) on the eastern limb of Montserrat Anticline. The complex has a length from head to toe of nearly 1400m and a width ranging from 550m near the toe to 125m near the head. The lithologies involved in the failure are highly deformed soft smectitic silty clay (Ashley Mudstone) loose to firm sand (Homebush sandstone), loose to compact glauconitic sand (Waipara Greensand) and strong to very strong Amuri Limestone.

Nine morphological units can be recognised within the complex, based on the current activity of the area and the type of slope movement involved. Forms of slope movement involved in Coringa Landslide Complex include falls, topples, back or forward rotational slumping and earthsliding (defined in chapter 4). Earthslide 3 comprises the most obviously active portion of the complex.

A model of landslide evolution is proposed, and it is postulated that the complex is as old as 105 ka -120 ka. Evolution of the complex is likely to have been controlled by movement on the Coringa and Evesham fault systems, inferred to be underlying the complex. Two different failure mechanisms of the complex can be recognised:

1. Along the eastern lateral scarp, failure is inferred to involve slumping of rock/soil material on concave upwards shear surfaces developed within Ashley Mudstone.
2. It is postulated that the development of the main body (effectively the area between the western and eastern lateral scarps) of the landslide complex is likely to involve periodic deep seated movement, in response to the removal of support at the toe of the complex by the action of the Motunau River. It is inferred that the surface of rupture of the complex is located at or near the Waipara Greensand/Loburn Mudstone contact.

The source area for Earthslide 3 is inferred to have resulted from a displaced mass of Ashley Mudstone material bulldozed ahead of a slumped block derived from the eastern lateral scarp. This material has subsequently become reactivated.

3.6.2 Earthslide 3

Earthslide 3 comprises an elongate body located adjacent to the western lateral scarp of Coringa Landslide Complex. The earthslide has a length from head zone to toe of slightly less than 800m, with a width ranging from about 20m near the head of the slide to over 150 m at the toe. The average inclination of the slide is about 6° on the frontal

slope, but varies from horizontal to a maximum of slightly less than 10°. The earthslide is noticeably 'bent' at about 250 m from the head. The direction of movement above the earthslide bend is 235°, while below the bend, the movement direction is approximately 190°.

The earthslide moves primarily by sliding on discrete slickensided basal and lateral shears. Limited data is available on the depth of the basal shear, but a minimum depth of slightly over 2 m is probable near the head of the slide. A maximum depth of the basal shear of 8-9 m is inferred in the accumulation zone from the observed height of the earthslide toe.

Lateral shears display a range of features, depending on the degree of development of the shear at the ground surface. Features range from Riedal shears (in the early stages of formation of the lateral shear) to en-echelon tension cracks, to almost linear, fully developed lateral shear planes. A pronounced left-step and associated pull-apart basin can be recognised on the eastern lateral shear (a sinistral shear) within the earthslide bend.

Lateral bulges can be observed at many localities along the boundaries of the earthslide. Two different types were noted for Earthslide 3. Type I bulges are located on the inside of the lateral shear zone, while type II bulges are located on the outside of the lateral shear. Lateral bulges of both types have formed immediately upslope and downslope of the earthslide bend. Also located within the earthslide bend, immediately downslope of the maximum surface inclination of the earthslide, are a series of prominent transverse bulges, displaying a maximum height of about 2.5 m.

Material comprising Earthslide 3 consists of a sheared and highly deformed light brownish matrix of silty clay within which lumps of stiff blue/grey and light brown clay, sand and limestone fragments occur. Particle size analyses established that, for examined samples, the sand fraction was generally less than 20%, although in areas of the earthslide sourced from Waipara Greensand, the sand fraction could be as high as 63%. The silt fraction generally composed from 25 to 55% of analysed samples, while the clay fraction comprised 20-40%. X-ray diffraction analysis indicates that the main clay mineral comprising the matrix is calcium-magnesium smectite.

The water content of the material involved in the earthslide varies from 32 to 43%, with average values of plastic and liquid limit ranging between 29-39% and 57-84% respectively. The average remoulded bulk density was found to be about 1670 kg/m^3, which corresponds to an average soil weight of 16.4 kN/m^3. Ring shear analysis discovered that, for lateral shear material, the effective shear parameters (residual friction

angle; ϕ'_r; and cohesion; c'_r), were 13.0° and 0 kPa, respectively. Analyses conducted on basal shear samples provided only a slightly lower value of residual friction angle of 12.8°.

In the year of monitoring between March 1993 and March 1994, points near the toe of the earthslide had moved an average of 0.28 m, but showed erratic movement directions with time. Monitoring points located further upslope (to D-line, in the middle of the earthslide bend) showed faster displacement rates than at the toe (points P11- P14 averaged 1.18 m) and showed almost constant decrease in elevation with time. The two points of D line located on Earthslide 3 also show near linear horizontal displacements, but show some degree of inflation at times of accelerated movement rate. Points further upslope of D-line showed displacement patterns similar to those observed for P11-P14. Earthslide movements were non-constant through the year of monitoring, with periods of accelerated movement between late May 1993 - early October and early December - late January 1994 accounting for 78% of the observed displacement.

Infinite Slope and Infinite Rectangular Slope analysis require that, for the observed maximum level of the water table at the average gradient of the earthslide, a maximum angle of effective residual friction of 11.4° is needed to place the slide in a state of limiting equilibrium.

Chapter Four: Earthslides: Terminology, Morphology and Mechanisms of Movement

4.1. Introduction

Chapter 4 is intended to provide a synthesis and review of data presented in chapter 2 on Earthslide A (Mt. Vulcan Landslide Complex) and chapter 3 on Earthslide 3 (Coringa Landslide Complex). Observations made in these two chapters are compared and contrasted with literature sources. Rationale of the terminology used in this study is presented.

It should be noted that in this chapter, the earthslides examined within the Mt. Vulcan and Coringa Landslide Complexes are referred to simply as 'Earthslide A' and 'Earthslide 3' respectively.

4.2. Terminology

The terms 'mudflow', 'debris flow', mudslide', 'earthslide', 'flow slide' and even 'mud glacier' have been used by different authors to describe essentially the same phenomena (Brunsden, 1984). Varnes (1978) employs the term "earthflow", while Hutchinson (1988) uses the term "mudslide".

Varnes' (1978) classification of flow is based on the velocity distribution of the displaced mass. In flows, the distribution of velocities of the mass takes the form of that observed in viscous fluids, hence the movement can be described as a form of flow of the sliding mass. The fastest velocities (and therefore, the largest displacements) generally occur in the centre of the moving mass, with displacement becoming increasingly smaller as the edges of the moving mass are approached (see fig. 4.5). However, it is evident from sections 2.6.1.1 and 3.5.1.1 that the landslides analysed in this study move by displacement along discrete lateral shear surfaces, and most probably move along a discrete basal surface. Furthermore, on Earthslide 3, displacement distributions across the moving mass were found to be more or less constant (section 3.5.3.2) which is essentially a 'slide' movement. This situation was previously recognised on similar features in England studied by Hutchinson (1970) and Hutchinson & Bhandari (1971), and subsequently led U.K. workers to reclassify these types of slope movement as 'mudslides' (Hutchinson, 1988 & pers. comm, 1993).

The definitions of the prefixes 'mud-', 'earth-' and 'debris-' are poorly defined in Hutchinson (1988) as it is not specified what grain size distribution is required for the use of a particular term. Varnes (1978) makes a partial distinction between the terms 'debris' and 'earth' on the basis of particle size: (i) 'debris' is restricted to those materials which have 20-80% coarse particles (greater than 2 mm), (ii) 'earth' is used for those soils in which about 80% of the fragments are smaller than 2mm. The term' mud' is not specifically defined by Varnes (1978) Therefore, I have made the following changes in nomenclature from that of Varnes (1978):

1. 'mud-': this term is reserved for those materials whose average grain size distribution consists of more than 50% silt and clay (ie., particles finer than 0.06 mm), with a major clay fraction.
2. 'earth-': this term is used for those soil masses whose average grain size distribution is comprised of more than 50% sand, silt and clay (ie., particles finer than 2 mm).
3. 'debris': this term is reserved for those materials which contain greater than 50% gravel-sized clasts (i.e., above 2mm diameter).

Particle size distributions for Earthslide 3 and Earthslide A show a range of grainsizes, depending on the relative influence of various source materials (section 4.4.2). While some of the grainsize distributions of measured samples clearly fall within the above definition of 'mud', others (because of significant sand content) are clearly 'earth'. However, as the average grainsize distribution for both slides would have an average of more than 50% sand, silt and clay (sections 2.6.3.3 and 3.5.4.3), the prefix 'earth-' is the more appropriate.

In New Zealand, the terms 'earthflow' (Trotter et.al., 1992) or 'creeping earthflow' (Northey et. al., 1974) are more widely used than 'earthslide' (or 'mudslide') to describe the type of slope movement outlined in sections 2.6 and 3.5. However, the distinction between 'flow'- and 'slide'-type movements is an important one, as mechanisms of mobilisation and movement, and rates of movement, between the two types can be significantly different. Bovis (1986) took a similar position to the one adopted in this study, suggesting that some of the slope movements termed 'earthflows' (Bovis, 1985) in the interior plateau of Southwest British Columbia would be more appropriately named as 'earthslides'.

The changes to existing terminology outlined on the previous page may warrant a review and reorganisation of this particular area of landslide classification, but such a review is beyond the scope of this study.

4.3. Morphological Characteristics

4.3.1 General Morphology

An earthslide may display either a tongue (elongate) or tear-drop (lobate) shape, depending on the slope angle on which the earthslide is developed (fig.4.1). Elongate slides display smaller λ/L ratios (λ = slide width; L = landslide length) than lobate slides. Figure 4.1 shows the slope inclination (β) to L ratios for both Earthslide 3, and Earthslide A, in comparison to earth and mudslides described in the literature. It can be clearly seen that both earthslides are elongate and fall well within the theoretical curves described by the Infinite Rectangular Landslide Equation (sections 2.6.4.2, 3.5.5.2; see also Appendix H).

Elongate forms of earthslides tend to develop where the slope angle approaches the angle of 'ultimate stability'[1] for the debris involved (Hutchinson, 1988), whereas lobate forms are associated with low angle zones of accumulation (3 to 4°; Brunsden, 1984). Infinite rectangular slope analysis indicates that for Earthslide 3 with m (ratio of ground water level to landslide thickness)= 0.7, K (coefficient of lateral earth pressure)= 0.67, λ_e (earthslide width)=60 m, ϕ'_r (effective residual friction angle)=13°, c'_r (effective residual cohesion) =0 and F_3 (three-dimensional factor of safety)=1.0, the angle of ultimate stability (β_u) is about 7.75°, whereas, using similar values (except for λ_e=90 m) for earthslide A the value of β_u is equal to 7.9°. In sections 2.6.1 and 3.5.1. it was noted that the average earthslide gradients were about 6° and 8° for Earthslide 3 and Earthslide A respectively. Therefore, the average inclination of Earthslide 3 closely approaches its ultimate value β_u, while Earthslide A is inclined at about its ultimate stability angle. The implications of these calculated values of β_u are discussed in more detail in sections 4.6.2 and 4.6.3.

Elongate earthslides possess three distinct morphological units: a source (or head zone), a track and a lobe or accumulation zone (Brunsden, 1984). On both the earthslides examined in this study, the head zone comprises an area in which active slumping and minor earthflow/slides occur from a relatively steep head scarp. The track on the Earthslide A (fig. 2) consists of a relatively straight channel (mean slide direction near the head was 180°, while near the toe it was 155°), while the track of Earthslide 3 is noticeably bent (mean slide direction above the bend is 235°: this swings through to 190° in the bend before straightening to 205°). The width of the track zone varies considerably between the two earthslides, with Earthslide A having an average width (λ_e) of 90 m, while Earthslide 3 has a value of λ_e ranging from 20 (above the earthslide bend) to 50 m. No accumulation zone was noted on Earthslide A, which is likely to be due to

[1]calculated using back analysis.

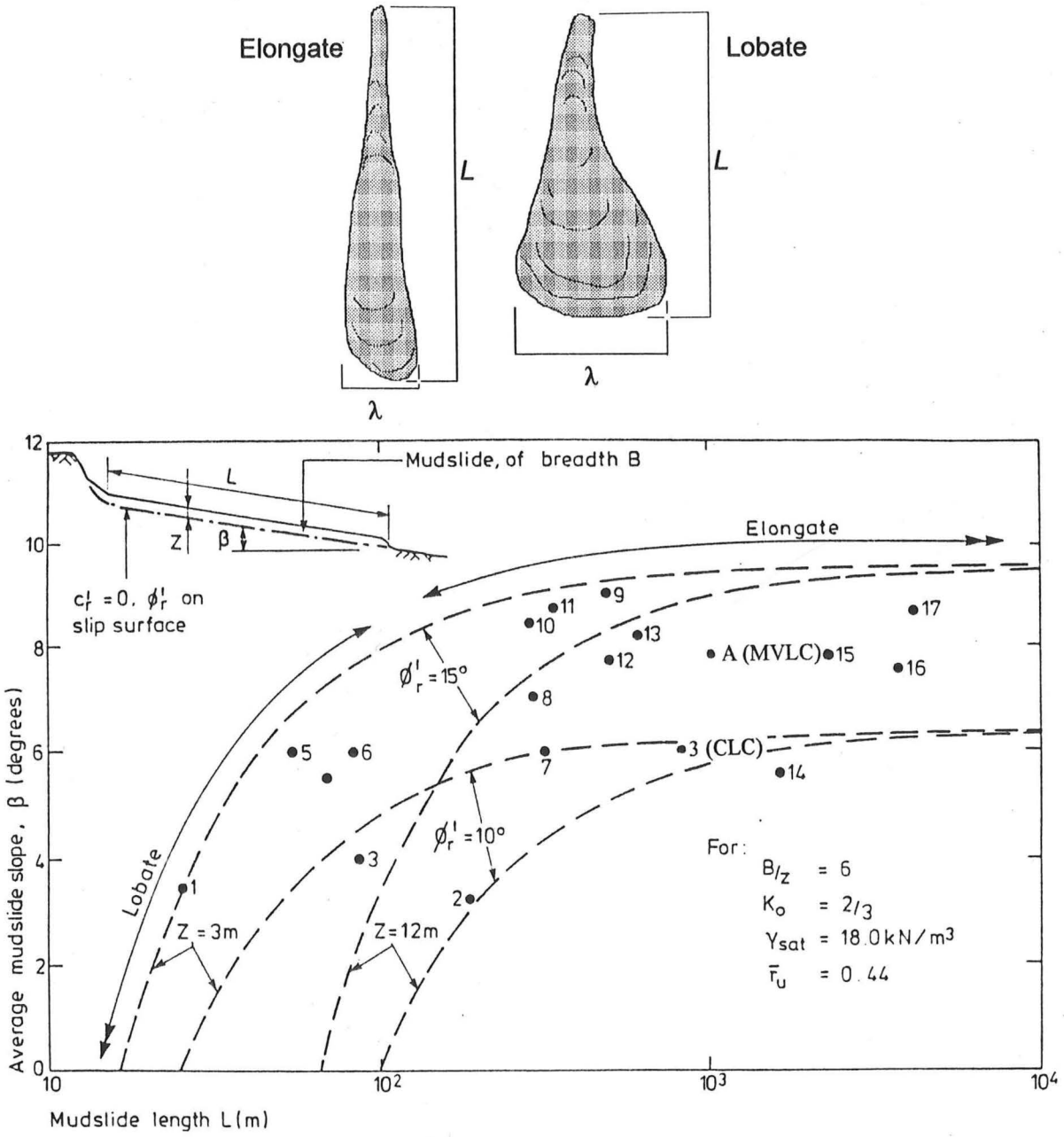

Figure 4.1 Comparison of observations on lobate and elongate mudslides with theoretical curves obtained from three-dimensional analysis (see Hutchinson & Del Prete, 1985). 1. Irvine (1963); 2. Conway 1974; 3. Bhandari & Hutchinson, 1982; 4. Hutchinson & Bhandari, (1971); 5. Hutchinson (1970); 6 Prior (1977); 7. Campbell (1966); 8,9. D'Elia & Tancredi (1979); 10. Bovis (1985); 11. Manfredini et al. (1981); 12. Hutchinson & Del Prete (1985); 13. Del Prete & Petley (1982); 14. Zaruba & Mencl (1982); 15. von Moos (1953); 16. Crandell & Varnes (1961) 17. Van Dine (1980). 3 (CLC) Earthslide 3, Coringa Landslide Complex; A(MVLC) Earthslide A, Mt. Vulcan Landslide Complex. Modified from Hutchinson (1988).

the steep earthslide gradient and rapid erosion at the toe of the slide by wave action. However, an accumulation zone is evident on Earthslide 3, indicated at the ground surface by a region of hummocky, bulging ground which extends for about 150 m up the slide.

4.3.2. Features of Earthslide Boundaries

4.3.2.1. Basal Shears

It has been shown by several authors that most of the displacement observed at the ground surface occurs at, or close to, the basal shear surface. For example, on the Beltinge mudslide in Kent, England, Hutchinson (1970) found that 89-95% of the displacement measured at ground surface took place within 200 mm of the basal shear surface. Similarly, Zhang et. al. (1991b) found that, for a particular earthslide on Raukumara Peninsula in the North Island, internal deformation accounted for less than 25% of the total surface movement, while the remaining 75% of movement was the result of displacement along the basal shear plane. Likewise, for the Mikonui Earthflow near Kaikoura, Grocott (1977) found that the "earthflow" mass moved at a rate comparable with ground survey stations to a depth just above the basal failure plane. It was impossible to measure the amount of total displacement occurring along the basal shear surface of either of the earthslides examined in this study, due to the lack of suitable instrumentation (because of financial constraints). However, the basal shear zone when intersected at depth in boreholes on Earthslide 3 was represented by a softened and highly deformed wet clay layer, and it is assumed that the majority of displacement occurs within this zone.

At the toe of Earthslide 3 deformed bands of blue grey silty clay were noticed, and it is inferred that these bands represent the daylighting of multiple basal thrust surfaces within the accumulation zone of the slide. Multiple basal surfaces are ideally arranged like imbricate thrust surfaces (Hutchinson, 1970; Keefer & Johnson, 1983; see fig. 4) and result in the shortening and thickening of material involved in the earthslide.

4.3.2.2. Lateral Shears

Structures formed at the ground surface along the lateral shear zone are analogous to those developed along strike-slip faults (Fleming & Johnson, 1989). Lateral shears on Earthslide 3 displayed an almost complete range of structures, from Riedal shears (orientated at approximately $45°-\phi$ and $90°-\phi/2$ from the trend of the underlying shear) to en echelon tension cracks to linear, slickensided shear planes at the fully developed state. The offset of Riedal shears from 15 to 20° for Earthslide 3 indicates that the peak shear strength for the earthslide material is about 30°. Earthslide A typically only displayed features associated with a well developed shear surface, that is, a distinct linear striated,

slickensided shear plane, although in places en echelon tension cracks could be observed. These well developed shears may indicate movement of the earthslide is continual. Shear segments, ranging from a few to several tens of metres in length, could be noticed on both earthslides.

Fleming and Johnson (1989) comment that the tension cracks and shear segments are ephemeral features; they are created and destroyed with continuing displacement of the landslide. These structures are ultimately replaced by a through-going lateral shear. Furthermore, Fleming & Johnson (1989) indicate that persistent structures are associated with zones of compression or extension along the zone of shear. A persistent pull-apart basin (an extensional structure) can be observed on earthslide 3, associated with left step on the eastern lateral shear (a sinistral shear; see section 3.5.1.1). Aerial photographic evidence indicates that this pull apart basin was formed some time in the period 1950-1974 (see Appendix C).

4.3.2.3. Internal Shears

Internal shears, inferred to be acting as zones of differential movement, can be observed at a number of localities on both earthslides. An arcuate internal shear can be noticed near the western lateral shear zone on Earthslide 3, at the head of the earthslide bend (fig. 4). Evidence from monitoring points P1 and P2, located on either side of the shear indicate that the shear acts as a zone of differential movement, with the northeastern side of the shear moving downslope at a faster rate than southwestern side (P1 was displaced down gradient by 1.3 m, while P1 was displaced 1.4 m). Monitoring evidence also suggests that the northeastern side is being up-thrust relative to the south (P1 decreased in elevation by about 8 cm, while P2 experienced a decrease of nearly 11 cm). This thrust movement would therefore be associated with a compressional movement state along the western lateral shear at this point.

4.3.2.4. Lateral Bulges

These bulges can be commonly observed at the sides of the moving earthslide mass. Keefer & Johnson (1983) and Fleming & Johnson (1989) note that lateral bulges can be either (i) pushed up as a pressure ridge due to lateral earth pressure (deformational bulge); (ii) remnant material left in place during remobilisation, after formerly overriding an existing ground surface (depositional bulge); or (iii) overflow of earthslide material onto the adjacent ground surface.

On both earthslides, lateral bulges could be recognised flanking the moving mass of the slide. It was observed that two different types existed. 'Type I' bulges display slickensided shear surfaces on their outer flanks, and are the more common lateral bulge observed; 'type II' lateral bulges display slickensided shear surfaces on the inner flank of

the ridge. It is inferred that type I (fig 4.2a) lateral bulges display typical features associated with pressure bulges described in Keefer & Johnson (1983), and are therefore 'deformational' (after Fleming & Johnson, 1989) bulges. Type II (fig. 4.2b) bulges are inferred to form as a result of overflow of material onto existing ground surfaces and are therefore 'depositional' bulges .

Examination of many deformational bulges indicates that their amplitudes are the cumulative result of growth during several episodes of landsliding (Fleming & Johnson, 1989). Monitoring evidence from P14 (the only point located on a type I bulge) on Earthslide 3 did not confirm this hypothesis however. The vertical displacement March 1989-March 1993 indicated a decrease in elevation. This decrease in elevation is due to the earthslide gradient, that is, a down-gradient movement will naturally result in a lower elevation.

Crosta et. al., (1992) noted that lateral bulges are liable to form immediately upstream and downstream of obstacles along the path of an earthslide. On Earthslide 3, lateral bulges have formed on up- and down-slope sides of the earthslide bend (section 3.5.1.2.), while bulges and regions of no-flow or 'dead-zones' (Crosta et. al., 1992) and lateral bulges can be observed in the region of the constrictive 'neck', near the toe of Earthslide A (section 2.6.1; see fig. 4.3). These observations therefore provide further field evidence for Crosta et. al's (1992) experimental study. The obstacle in the path of movement would have the effect of disrupting the downslope movement vector of the earthslide, resulting in increased lateral pressure immediately adjacent to the obstacle, the expression of which would be the formation of deformational (or type I) lateral bulges.

Figure 4.2 a

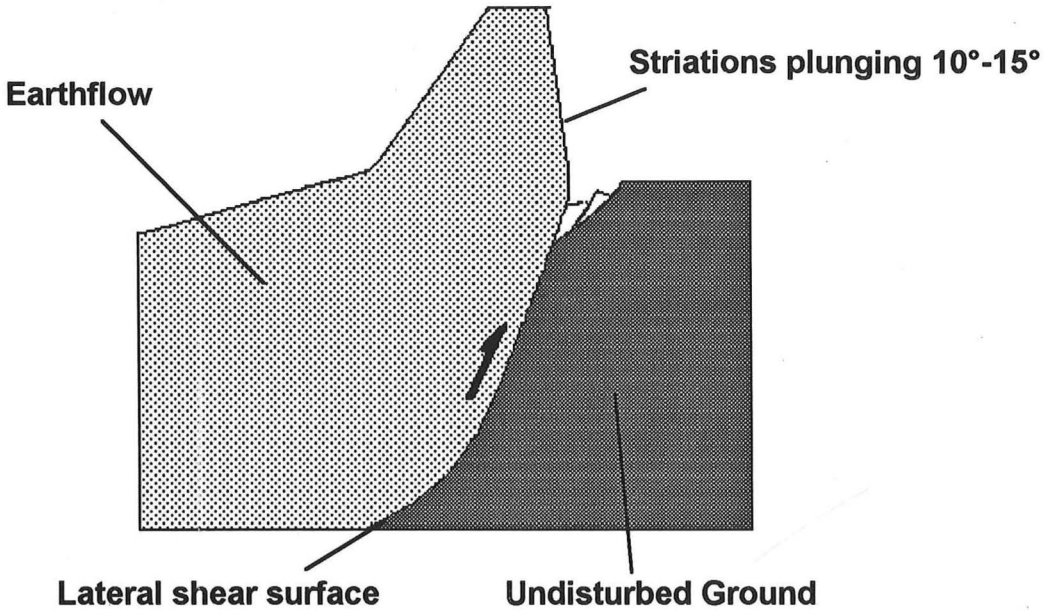

Figure 4.2b

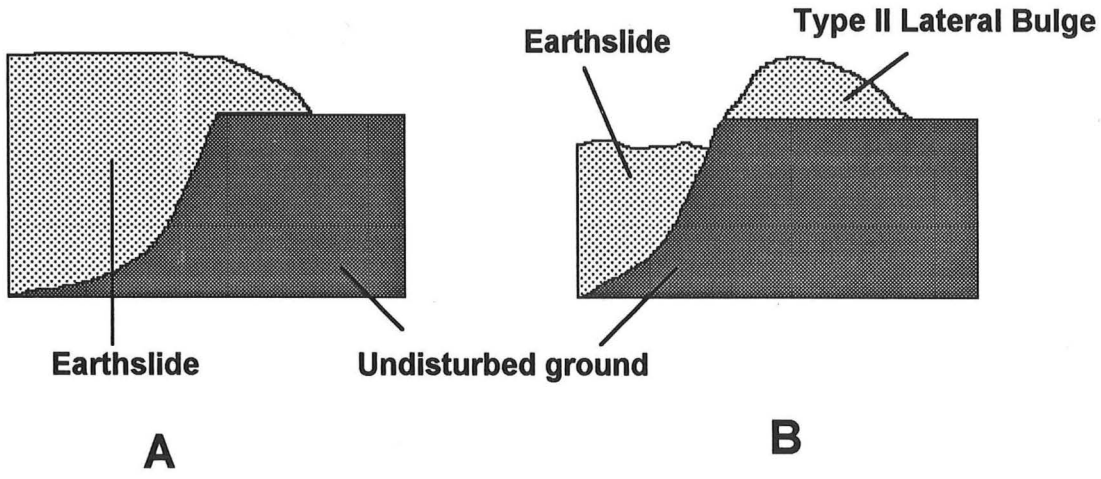

Figure 4.2. (a) Formation of Deformational (Type I) bulge (modified from Keefer & Johnson, 1983) (b) Formation of Depositional (Type II) bulge.

Figure 4.3a

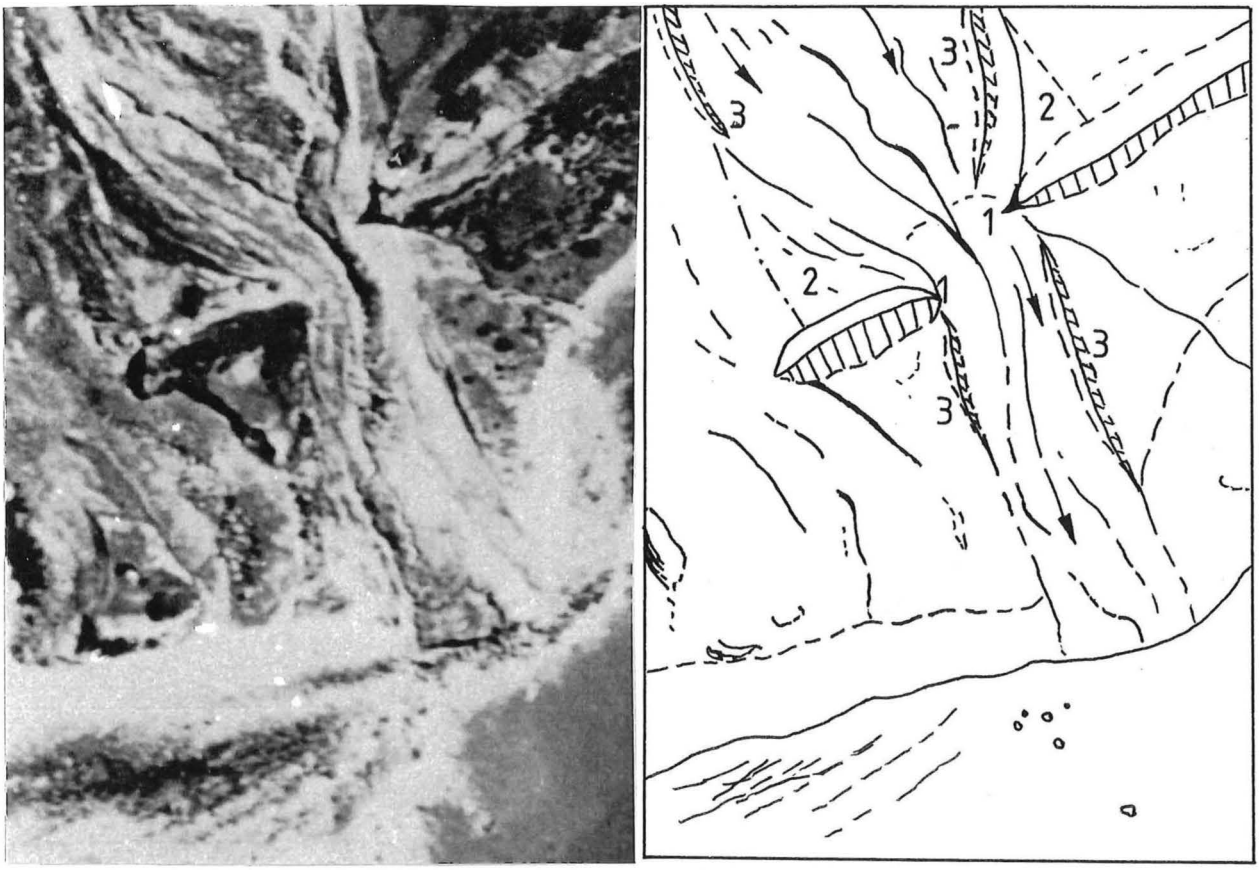

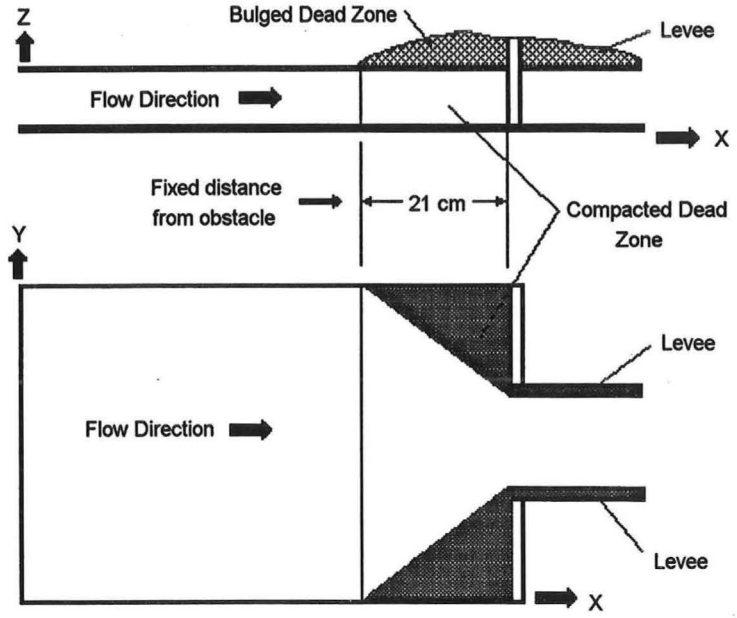

Figure 4.3b

Figure 4.3 Comparison of field (4.3a) and experimental (4.3b) responses to earthslide obstacles. Fig 4.3a shows slide behaviour in the region around the constrictive 'neck' of Earthslide A (1) earthslide consticting; (2) dead zones; (3) lateral bulges. Fig 4.3b from Crosta et. al., (1992).

4.3.2.5. Transverse Cracks and Bulges

Transverse tensional cracks and bulges within the track zone generally reflect both the pattern of movement and the general slope form of the earthslide profile (Brunsden, 1984). In addition, transverse cracks and bulges reflect the degree of obstruction to movement. Transverse tension cracks were noticed at several points on the Earthslide A, while large transverse bulges were noted on Earthslide 3.

A. Transverse Cracks

Tension cracks generally occur at steep, convex breaks of slope and are therefore associated with regions of extending flow (see section 4.5.2.1). Tension cracks noted on Earthslide A were generally semi-arcuate in plan, and concave downslope (see chapter 2; fig 2.12).

B. Transverse Bulges

Large transverse bulges have formed within the bend of Earthslide 3, immediately downstream of the steepest section of the slide. There are three likely explanations for the formation of these bulges:

1. 'standing wave': This situation is analogous to the formation of rapids within a river or stream. As the earthslide descends from its steepest inclination, some obstacle is intercepted at depth, which disturbs the downslope vector of movement, causing complex internal deformational patterns, the surface expression of which is the formation of transverse bulges.
2. surface expression of compressive flow behaviour (see section 4.5.2.1)
3. passive thrusting as a result of undrained loading. The earthslide is at its steepest at the top of the bend, and an undrained loading may consequently be created immediately downhill of the steepest inclination (Prof. J.N Hutchinson, pers.comm.). The transverse bulges would therefore be the surface expression of forward thrusting generated directly downslope from the region of undrained loading.

Of these three hypotheses, (2) and (3) are considered in this study to be the more likely modes of formation, due to the inferred failure mechanism of the landslide complex (failure at or near the Loburn Mudstone/Waipara Greensand contact). Therefore, an abrupt variation in the basal surface is unlikely. Additional suggestions of an area of undrained loading in this area are given in sections 4.5.2.3 and 4.6.3.

4.4. Materials and Geotechnical Properties

4.4.1. Earthslide Composition

Earthslides usually occur in saturated clays of all types from soft intact clays to stiff fissured clays which have become progressively softened, weathered or broken up by movement (Brunsden, 1984). The clay may be lightly or heavily overconsolidated. In

general, it was found that the material comprising the earthslides examined in this study consisted of a deformed and sheared sandy silty clay matrix within which gravel sized particles occur. The matrix generally comprised greater than 60% of the slide mass.

4.4.2. Sources of Debris Supply

There are likely to be 4 main sources of debris supply for both earthslides examined:-

1. Incorporation at the head zone of material (by falls, slides or slumping) of silty clay material. For Earthslide A, this material is likely to be derived from the earthslide/flow complex, which comprises the head region of the Mt. Vulcan Landslide, while for Earthslide 3, this material is likely to involve a reactivation of displaced and slumped material.
2. 'Feeder' earthslides. Small earthslides, located predominantly within Ashley Mudstone can be observed entering both earthslides at various localities, while shallow slides located within Waipara Greensand enter Earthslide 3 at various localities along the western lateral scarp of the Coringa Landslide Complex (see figs. **3** and **4**).
3. Basal Incorporation. Lumps of blue grey clay intercepted in boreholes emplaced on Earthslide 3 (figure **4.C**) are likely to be derived from Loburn Mudstone, which underlies the earthslide. This material has been incorporated into the earthslide mass by the process of 'basal incorporation' (Hutchinson, 1970). Fragments of harder clay or limestone gravels near the boundary of the earthslide effectively act as scrapers, scouring in situ material and amalgamating it into the moving body. It is inferred that a similar mechanism is operating on the Earthslide A.
4. Earthslide A experiences reactivation of older earthslide/flow debris located immediately west of the earthslide. Small slumps and slides of the topographically higher older debris along the western edge of the slide incorporates material into the moving slide mass.

4.4.3. Geotechnical Properties

Geotechnical properties for material comprising Earthslides A and 3 are summarised in table 4.1. It can be seen that the material properties determined for the 2 earthslides in this study have very similar values (because they are sourced from the same lithological unit, which is inferred to show little lateral variation) and also have similar values to those reported in other studies. In fact, Brunsden (1984) states that (p383) "there is a remarkable consistency in the values [of earthslide material properties] in the reported literature". A significant aspect of the geotechnical properties noted as part of this thesis are the relatively low clay fraction (*CF*) values. Samples from both Earthslide A and Earthslide 3 generally had a major proportion of silt. It could be assumed that this high silt content would reflect in a relatively higher residual friction

Site	w_L (%)	w_P (%)	I_p (%)	CF (%)	ϕ'_r (°)	γ (kN/m^3)	Clay Minerals
Earthslide 3, Coringa Landslide Complex	44-84	27-37	15-45	14†-45	13	1.54-1.96	Ca-Mg Smectite Glauconite
Earthslide A, Mt. Vulcan Landslide Complex	48-79	29-38	18-43	13†-47	13.3	1.62-1.93	Ca-Mg Smectite Glauconite
Literature Values*	56-80	22-36	20-30	40-70	11-16	1.6 - 2.0	Smectite Illite Kaolinite

Table 4.1 Earthslide material properties, Earthslide 3, Coringa Landslide Complex, lower earthslide, Mt. Vulcan Landslide Complex, where w_L = liquid limit, wP = plastic limit, I_p = Plasticity Index, CF = Clay Fraction, ϕ'_r = effective residual friction angle and γ = soil unit weight. † high Waipara Greensand Content. Samples from lateral and basal shear zones of both slides had typical CF values of 40-45%. * Literature values taken from values reported in Hutchinson (1969, 1970), Prior & Stevens (1972), Hutchinson et.al.(1974), Grocott (1977), Zaruba & Mencl (1982), Keefer & Johnson (1983), Brunsden (1984), Thomas & Kropp(1989), Bertini et.al (1992), Deganutti & Gasparetto (1992) and Marden et.al., (1993).

angle. However, Skempton (1985) and Fell and Jefferey (1987) note that for sand-'bentonite' mixtures (and therefore essentially the same material as involved in both earthslides) in the ring shear apparatus, three differing mechanisms of residual plane development are possible, depending on the value of *CF*: (i), at low *CF* (0-25%), turbulent or rolling shear; (ii) at high *CF* (>50%) sliding shear, and; (iii) for intermediate values of *CF*, a transition between the 2 types (see Appendix D). It is inferred that the values of residual friction obtained in this study reflect behaviour at the lower end of the transition between sliding and turbulent shear (Appendix D). Therefore, there is sufficient clay fraction in analysed samples to govern the residual friction angle, and hence the 'effective soil' is essentially a clay in terms of its geotechnical properties.

4.5. Displacement Behaviours

4.5.1 General

Earthslides display a marked seasonal pattern closely related to the incidence of wet and dry periods (Hutchinson, 1970; Brunsden, 1984). Surface monitoring conducted on Earthslide 3 revealed that the movement was generally slow (as defined by Varnes, 1978;

see chapter 1, fig 1.4b), with periods of accelerated movement that continue typically for a few months. This behaviour matches the more common earthslide displacement behaviour noted by Keefer & Johnson (1983; see chapter 1, fig 1.9). As no short-term surface monitoring was conducted on Earthslide A, no assumptions can be made regarding the surface movement behaviour.

4.5.2. Earthslide 3 (Coringa Landslide Complex)

4.5.2.1. Long Term Displacement Rate

A long-term rate of movement could be determined only for the track zone of the earthslide. A displaced fence post now located at the upslope end of the earthslide bend gave an average displacement of about 2.3 m/yr (chapter 3, section 3.5.3.1).

4.5.2.2. Displacement 1989-1993

The maximum displacement recorded by Barrell (1989) in his 6 months of monitoring from September 1988 to March 1989 was approximately 5 cm. It was noted in section 3.5.3.2 that Barrell's monitoring was conducted in a period of low rainfall (see fig 3.13). However, at the first survey of this study, considerable displacement of monitoring points emplaced by Barrell was calculated. The average displacement for the period March 1989-March 1993 of points in the track zone was about 2 m/yr (and consistent with the poorly constrained long-term movement rate for this part of the slide), while points emplaced at the bottom of the track zone had mean displacements of 0.93 m/yr. Months of high precipitation in the period March 1989-March 1993 are inferred to be responsible for the large majority of movement observed. These months are (i).June and October 1989; (ii) August 1990; (iii) January-February, April, June-July, November-December 1991; (ii) May-September 1992 (see chapter 3, fig. 3.13).

4.5.2.3. Displacement March 1993-March 1994

It was found that movement rates of monitoring points were non-constant through the year March 1993-March 1994, with periods of accelerated movement between late May-early October (1993) and early December-late January (1993-1994) accounting for 78% of the observed displacement. These accelerations correlate well with periods of increased precipitation (April-May 1993 and December 1993) and/or reduced evapotranspiration rates (July-August 1993; see fig. 4.4). While intervals between successive resurveys were insufficiently short[2] to adequately determine the 'lag-time' between a significant rainfall event (ie., where sufficient rain falls to potentially alter the

[2]A shorter time interval between successive resurveys would have allowed a more accurate assessment of the 'lag-time'. Financial constraints, however, prohibited this.

Figure 4.4 Correlation between weekly precipitation and recorded surface movement rates, Earthslide 3, Coringa Landslide Complex. Inferred displacement pattern shown as a dashed line Rainfall data from NIWA (1994b)

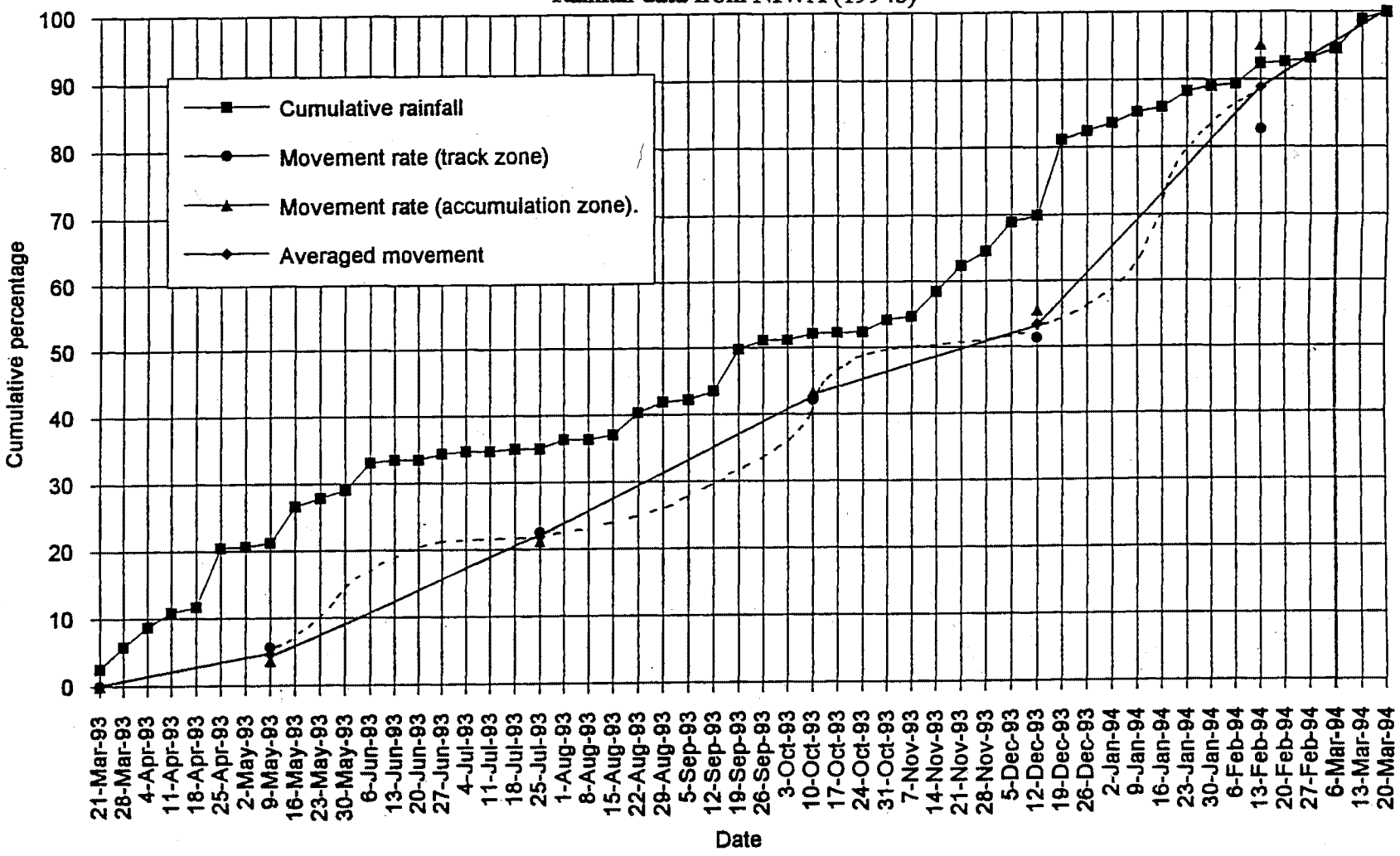

stability of the slide) and the onset of movement (or acceleration) of the slide, a lag time of 2-4 weeks is inferred (shown as a dashed line on fig. 4.4). However, it is most likely that the lag time is affected by ground water levels, with pre-existing high water levels before a rainfall event having a shorter lag time, and low levels having a longer lag time. Ground water levels measured on Earthslide 3 provided inconclusive data, due to reasons explained in section 3.5.3.3.

4.5.2.4. Characteristics of Displacement; Head and Accumulation Zones

It is noticeable that at the fourth resurvey (conducted in early December 1993) the track of the slide had achieved 57% of the total observed displacement, whereas at the same stage the accumulation zone had only realised 49% of the total observed movement. Similarly, at the fifth resurvey (early February 1994) the head of the slide had attained 95% of the observed yearly movement, while the toe of the slide had only achieved 84% of the observed displacement (fig 4.4). Therefore, displacement in the track zone of Earthslide 3 is characterised by short periods of accelerated movement interspersed with periods of relative inactivity. In contrast, displacement near the toe of the earthslide is generally more uniform, with movement occurring at a slower rate, but for relatively longer periods than observed further upslope.

These observations are in keeping with Hutchinson (1970), who showed that in general the mudslide track moves, with a slight lag, during times of water surplus, but accumulation lobes showed lag-times of 1-4 months. Similarly, Brunsden (1984) notes that (p. 410) "Track movements are ... more likely to reflect the seasonal and short-term rainfall conditions. Accumulation lobe movements commonly lag behind rainfall, the effect of which is filtered out through the complex loading and supply mechanisms." Brunsden goes on to note that failures of accumulation lobes are likely to be sudden and "vigorous", with no readily discernible pre-failure creep, and therefore essentially a stick-slip behaviour. No such failure was measured, or inferred likely to happen, for the accumulation zone of Earthslide 3. Rapid failure of the accumulation zone is unlikely, due to the erosive action of the Motunau River, which continually removes support at the toe of the earthslide, thereby allowing the accumulation zone to slide at a slow, constant rate.

It is assumed that because Earthslide A experiences rapid erosion at the toe by wave activity and as a result, has no accumulation zone, the displacement rates along the length of the slide are more or less constant.

4.5.3. Movement Patterns

4.5.3.1. Longitudinal Behaviour of the Slide Mass

In longitudinal profile, 3 different types of movement of the slide mass are theoretically possible, depending on the longitudinal deformation rate (from Savage & Smith, 1986):

1. where tensile longitudinal stresses occur, and therefore, generally at the head of the earthslide or at convex breaks in slope, 'extending flow' (or extending slide) behaviour is apparent. Normal fault scarps and tension cracks orientated approximately perpendicular to the slide direction are evident at the surface within this region. Both earthslides are inferred to have a region of extending flow near their respective heads. However, figure 2.9 shows the typical inferred surface expression of extending flow at a concave break in slope on Earthslide A.
2. in domains of longitudinal compressive stress, 'compressive flow' behaviour occurs. Within compressive flow regions, thrust surfaces, transverse bulges and thrust fault scarps can be observed. No region of compressive flow is indicated on Earthslide A, however, the accumulation zone and centre of the earthslide bend (at a concave break in slope) on Earthslide 3 are found to be regions of compressive flow (see 4.5.2.3).
3. 'plug-flow' wherein the slide body moves as a rigid body over the basal shear zone, at a rate given by the basal slide velocity. Within the basal shear zone, flow behaviour is theorised by Zhang et. al. (1991a). Plug flow is most likely to occur within the track zone (or zone of transport) of an earthslide, and can be observed on both slides in this study.

If the dimensions of an earthslide or particular zone remain constant even though movement continues, the earthslide or particular zone can be said to be in a 'steady state' (Zhang et. al., 1991 b). Mathematically, the criterion for steady state behaviour requires a constant cross-sectional area perpendicular to the slope (A), with time (t), or $\frac{\partial A}{\partial t} = 0$.

Conversely, unsteady behaviour occurs where $\frac{\partial A}{\partial t} \neq 0$. Regions of plug flow of the earthslide may approximate steady state conditions. Unsteady state conditions may, depending on the rate of sediment influx at the head of the slide and/or the rate of erosion at the toe of the slide, result where extending ($\frac{\partial A}{\partial t} < 0$; relative decrease in elevation with time) or compressive ($\frac{\partial A}{\partial t} > 0$; relative increase in R.L. with time) flow occur.

Figure 4.5 Schematic examples of possible movement patterns (A) true slide; (B) true flow; (C) rigid plug; (D) complex sliding block; (E) complex slide-plug. The columns show details of movement in plan, long- and cross-section (modified from Brunsden, 1984)

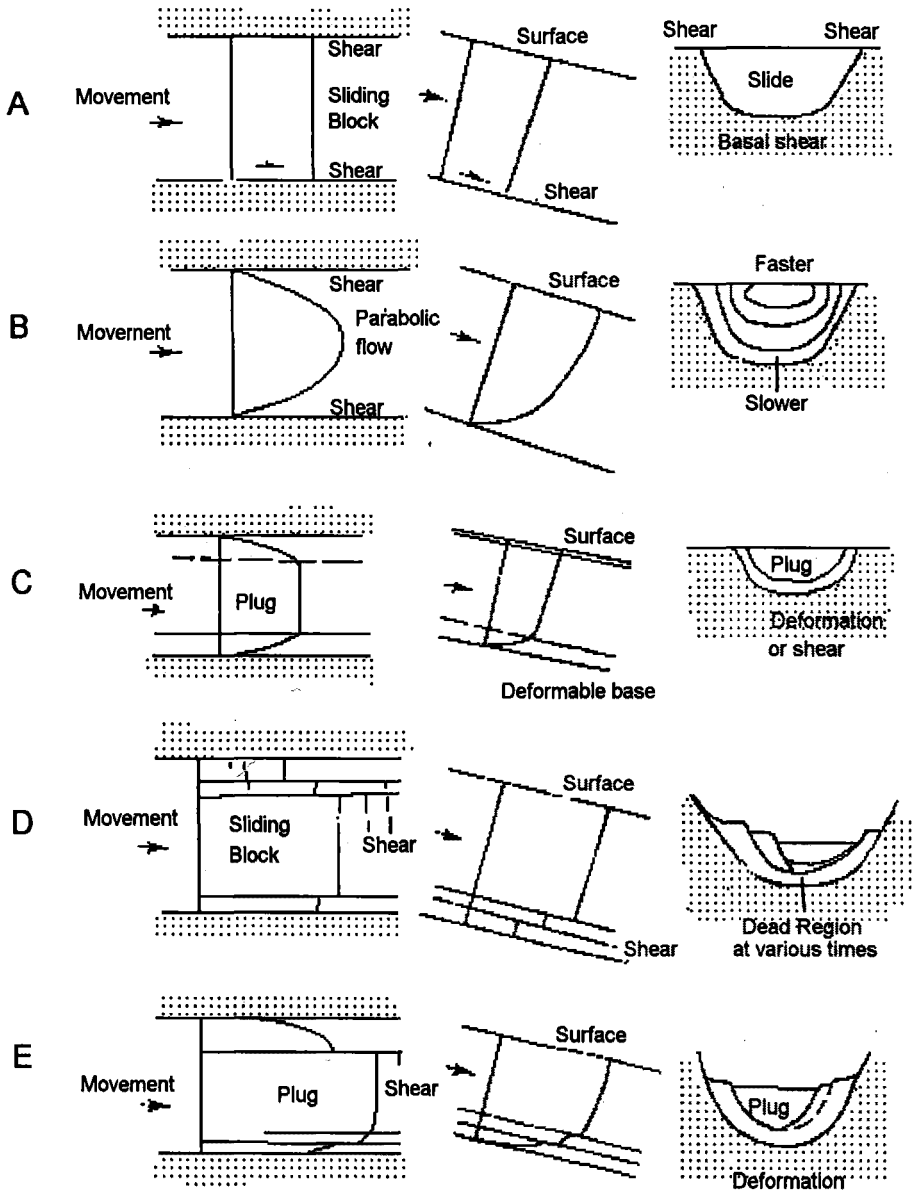

4.5.3.2. Edge Displacements

Observations made by Hutchinson, (1970) and Hutchinson & Bhandari, (1971) demonstrated that mudslide (and earthslide) movements approximate plug-flow. However, more recent studies have shown that while slide- or plug flow-type movement is the major displacement mechanism, movement patterns may be complicated by the presence of complex lateral shearing or internal deformation of the slide mass and the topography on which the earthslide is developed. Figure 4.5 shows examples of characteristic displacement patterns.

Surface Monitoring and limited subsurface information for Earthslide 3 indicated that plug-flow and/or true sliding are the predominant movement types within the track zone (note, for example, the near constant displacement of points P11-P14 indicated on fig. **5**). However, discrete internal shears above and below the earthslide bend may indicate that some form of complex block-slide/plug flow behaviour is occurring in this region, while displacement characteristics for A-line suggest that some form of internal deformation (possibly flow behaviour) is acting in the accumulation zone.

4.5.3.3. Movement Patterns of Earthslide 3 (Coringa Landslide Complex)

Evidence presented in section 3.5.3.2 indicated that monitoring points in the accumulation zone of Earthslide 3 (A-line, B2 and B3; see figs. **4** and **5**) showed somewhat erratic horizontal movement vectors (compared with those observed further upslope), and a generalised tendency to experience an rise in elevation during times when the earthslide is in a state of acceleration, followed by a subsequent decrease in elevation during periods of low movement. It is also notable that A3, A4 and A5 have been displaced by a greater amount than points A1,2 or 6 (fig. **5**). These several factors indicate that: (i) complex internal deformations (due to internal flow and/or shearing) occur in this area, resulting in variable directions of movement; (ii) during times of accelerated movement, this portion of the earthslide experiences a compressive force derived from the upslope earthslide mass, which has the tendency to 'inflate', or swell, the accumulation zone. During times of decreased movement the compressive force is dissipated, allowing the toe region of the earthslide to relax, or 'deflate', and; (iii) a component of internal deformation (probably due to flow behaviour) acts in this region, with the result that displacement rates across the slide are non-uniform.

Points located in line C, and point B5, show a lesser degree of inflation at times of earthslide acceleration and show larger horizontal displacements without the same degree of erratic movement directions observed in points B2, B3 and line A. This movement is inferred to indicate that this region is effectively at the downslope end of the track zone, and the movement characteristics noted in monitoring points reflect a transitional state

between steady state, plug flow further upslope and unsteady state, compressional flow further downslope in the accumulation zone.

Points P11-P14, located at the downslope end of the earthslide bend, show almost linear horizontal displacements, and show a constant decrease in elevation with displacement, regardless of the overall state of motion of the earthslide. The decrease in elevation in this area is more to be a function of slope inclination (ie, a decrease in elevation due to downslope movement), rather than an actual deflation. These characteristics are inferred to reflect a region of steady state behaviour.

The two points of D line located on Earthslide 3 also show near linear horizontal displacements, but show some degree of inflation at times of accelerated movement rate. This unsteady behaviour is inferred to be a response to the development of an area of undrained loading that is likely to occur immediately upslope of D-line (postulated in section 4.3.2.5; see also 4.6.3).

Points located further upslope than D-line (E1-E4 and points P5 and P6) like points P11-P14 show nearly linear horizontal displacements and a constant decrease in elevation with time. This decrease in R.L. is, as for P11 - P14, likely to be due to a function of slope gradient, rather than a deflation.

4.6. Mechanisms of Earthslide Movement

4.6.1. General

According to the Mohr-Coulomb failure criterion, modified by Terzaghi's theory of effective stress (see, among others, Skempton & Hutchinson, 1969; Wu & Sangrey, 1978; Graham, 1984), an increase in pore water pressure (u) results in a reduction of the shear strength acting across the earthslide basal failure plane. If this reduction results in an effective shear strength less than the shear stress acting on the earthslide, mobilisation will occur. Pore water pressure increases can occur by either (a) a rise in the groundwater level due to increased precipitation and/or a decrease in the rate of evapotranspiration; or (b) undrained loading of (generally) the head of the earthslide by debris discharged onto the rear of the slide from feeder slides, slumps or other earth- or mud- slide/flows. Undrained loading is of particular significance where the inclination of the accumulation slide is low (Hutchinson & Bhandari, 1971).

Because clays in general are materials of low permeability (typical k values in the range 10^{-5} to 10^{-9} m/s; see section 3.5.4.4) it could be expected that earthslides would show slow piezometric responses by infiltration to surface recharge, and hence very delayed movement rates. However, more rapid piezometric responses can be attained, due to

tension cracks and shear zones at the surface of the earthslide serving as zones of high hydraulic conductivity (Bovis, 1985).

4.6.2. Earthslide A, Mt. Vulcan Landslide Complex

Stability analyses performed using the infinite slope expression and the infinite rectangular landslide expression (section 2.6.4) indicate that, for the maximum water level (m=1), a minimum effective residual friction angle (ϕ'_r) of only 19.6° and 18.9° is required respectively. Residual friction angle tests indicated that the material constituting Earthslide A has a value of ϕ'_r =13.3°, and similar values of ϕ'_r are indicated by stability analysis when m=0.6. Although not measured, ground water levels in Earthslide A are inferred to be over 0.6 m for most, if not all, of the year; this inference is based on the fact that two water courses enter the slide near its head zone, thereby supplying sufficient water to keep the slide in a state of movement. Therefore, Earthslide A is considered in this study to be in a state of motion for most or all of the year. This is consistent with the similarity of the earthslide gradient (β; about 8°) to the calculated angle of ultimate stability (β_u; equal to 7.9°).

It is postulated therefore, that the controlling influences on movement of Earthslide A are (i) the similarity between β and β_u; (ii) rapid erosion at the toe by wave action; and (iii) consistently high ground water levels.

4.6.3. Earthslide 3, Coringa Landslide Complex

Infinite Slope analysis requires that, for the observed maximum level of the water table (m =0.7) at the average gradient of the earthslide (6°), a maximum angle of effective residual friction of 10.24° is needed to place the slide in a state of limiting equilibrium. From the geotechnical analyses performed, the angle of residual friction (ϕ'_r) was found to be close to 13°. However, back analysis indicates that, for residual friction angles of this order, movement should cease if the water table falls below 0.9 m. Surface monitoring (section 3.5.3.2.) indicates, however, that the slide is active at substantially lower water levels than m=0.9.

It is therefore obvious that the earthslide demonstrates activity at higher friction angle values and/or lower water levels than calculated by either the infinite slope or infinite rectangular slope expressions. This then provides almost conclusive evidence that an area of undrained loading is controlling the stability of Earthslide 3. From evidence presented in sections 4.3.2.5 and 4.5.2.3, it is likely that this region of undrained loading has developed near the top of the earthslide bend, where the slide is at its steepest, rather than at the head of the slide. Surface evidence for this undrained loading is given by the development of transverse pressure bulges, which may be associated with subsurface thrusting.

4.6.3.1. Characteristics of Momentum Transfer

Monitoring on the Dome Earthflow Complex, located on Raukumara Peninsula in the North Island over a 10 year period, indicated that there was some mechanism acting that transferred "information" of head zone disturbances from point to point within the earthflow at a rate 40-170 times faster than the particle velocity (Zhang et. al., 1991b). Zhang et al. suggested that the kinematic and diffusion behaviours of earthflow movements in Iverson's (1986a and b) unsteady, non-uniform landslide motion theory may be used to explain this information transfer.

Iverson (1986b) introduced the dimensionless landslide Peclet number (P_e) in his theoretical study. In broad terms, the Peclet number represents the importance of advective transfer relative to diffusive transfer of "sediment flux perturbations" (Iverson, 1986b; Zhang et al, 1991b), or head zone disturbances. Advective transfer is essentially kinematic wave transfer, that is, disturbances at the head zone are transferred downslope as a wave that moves 5-50 times faster than the speed at which the sediment moves (Iverson, 1986b) Diffusive transfer is essentially the transfer of head zone disturbances from the head to points throughout the slide mass.

Three ranges of value of P_e were recognise by Iverson (1986b):
(i) for $P_e > 10^{-1}$, head zone disturbances spread rapidly outward by diffusion. This is essentially a plastic behaviour phenomenon.
(ii) for $P_e > 10^2$, the response to head scarp disturbances is slow and wave-like, and the disturbance moves downslope at a speed predicted for that of ideal kinematic waves (Zhang et al, 1991b). This behaviour is consistent with highly viscous material..
(iii) for ($0.1 \leq P_e \leq 10$) the response to head scarp disturbances shows a more even blend of plastic and viscous response styles. Values of P_e of this order would be expected for many slow, persistently moving landslides (Zhang et. al., 1991 b).

The landslide Peclet number is given by the expression (subscript d denotes datum-state):

$$P_e = \frac{L}{z_d} \frac{\tan\beta_d \rho_s - \tan\phi(\rho_s - \rho_w)}{\tan\beta_d \tan\phi(\rho_s - \rho_w) + \rho_s} Y \qquad (4.1)$$

where L=earthslide length, z=earthslide thickness, β=earthslide inclination, ϕ=angle of internal friction (assumed to be ϕ'_r), ρ_S= saturated soil density, ρ_W=density of water, and;

$$Y = \frac{(n+1)^2(n+2)}{(n+2)(n+a)^2 + (1-a)^2 n} \qquad (4.2)$$

where a is the ratio of the rigid body thickness (T) to the landslide thickness z_d, ie, $T=az_d$, and n is the power-law index (equals unity for a Newtonian substance; Zhang. et. al., 1991b).

The use of equation 4.2 is reliant on the fact that the earthslide is in a steady state, and surface monitoring on Earthslide 3 indicates that the track zone of the slide is in this situation. It should be noted that Zhang et al's (1991b) study was based on a long period (10 years) of surface monitoring, which established a near constant ratio of single peg movement in each survey period to total peg movement over the whole study period. As the surface data for earthslide 3 only covers one year, no assumptions can be made regarding the long-term ratio of single-to total-peg movement.

The physical and geotechnical parameters established for Earthslide 3 are (section 3.5) L=790 m, β_d=6.0°, z=5 m (average), ϕ'_r=13°, and T = about 4.5 m (a is therefore about 0.9). The saturated soil density was not calculated for earthslide 3, as it was of no use in back analyses equations (sections 2.6.4 and 3.5.5), however, it is assumed $\rho_s \cong 1.9$ t/m^3. The density of water is 1.0 t/m^3, and assuming Newtonian behaviour, Y is found in equation 4.2 to be 1.65. Therefore, using equation 4.1, the landslide Peclet number is found to be P_e=1.09.

The calculated value of P_e (1.09) is at the lower end of the intermediate range calculated by Iverson, and is slightly less than the P_e value (2.67) calculated for the Dome Earthflow Complex by Zhang et.al. (1991b). The value of P_e calculated for Earthslide 3 indicates that the response to head scarp disturbances is a blend of plastic and viscous styles, however, because the P_e value is at the low end of the range diffusion (transfer of head zone disturbances from the head to points throughout the slide mass) may be more important mechanism of head zone disturbance transfer than advection (kinematic wave propagation).

4.6.3. Probability of Future Movements

4.6.3.1. Earthslide A, Mt. Vulcan Landslide Complex

Given the facts that (i) abundant debris is supplied to the earthslide from the upper earthslide/flow complex, (ii) sufficient water is supplied to the slide via water courses; (iii) for reasonable values of m, the earthslide is inclined at about its angle of ultimate stability (β_u); and (iv) wave action produces rapid erosion at the toe, it is probable that Earthslide A will continue to move at about current rates indefinitely. Substantial material is available for incorporation into the earthslide body, and active retrogressive slumping at the head zone of the Mt. Vulcan Landslide Complex ensures an on-going supply of this material.

4.6.3.2. Earthslide 3, Coringa Landslide Complex

No record in the past of movement rate vs precipitation for Earthslide 3 exists prior to Barrell's (1989) study, which itself was conducted for only 6 months in a period of low

movement (and rainfall). Therefore, it is impossible to compare past yearly rates of movement with the present known rate. However, the inferred source of debris supply for the earthslide (remobilisation of mud-rich landslide material from exposure; see section 3.4.) implies that there is only a limited amount of material available. It is estimated that the remaining available material has a volume of about $1.5x10^5$ m^3 (this was done assuming the remaining material formed a wedge-shaped three dimensional object, with length of about 200m, width of about 100 m, and height of 15 m). If the average width (λ_e=60 m), depth (z=5 m) and average velocity (v=1.2 m/yr) of Earthslide 3 are taken, then a volume of about 360 m^3 is transferred downslope per year. If it is assumed that all the earthslide mass is derived from the material at the head zone (essentially an incorrect assumption; some material is derived from feeder earthslides), then the available material would be depleted after 400-450 years (equal to $1.5x10^5$ m^3 divided by 360 m^3/yr). However, it is unlikely that the present movement rates would be maintained for all of this time interval. The usual pattern would be one of slowly reducing movement rates with time, and eventual dormancy

4.7. Potential Hazard Mitigation Procedures

Both the earthslides outlined in this study are of very low risk, and therefore there are potentially only three options:

1. do nothing: This has been the policy of both landowners in the past, and involves little more than periodical replacement of fences that cross the earthslides.
2. Reforestation: Marden et.al (1992) note that average movement rates on reforested earthslides (0.2-0.5 m/yr) on the Raukumara Peninsula (North Island) are only about 10% of those on unforested earthflows (3-5 m/yr), implying an order of magnitude reduction in movement rate. This option has some merit on Earthslide 3, Coringa Landslide Complex, as a rapid surge of the accumulation zone (see section 4.4.1.4), while thought unlikely (Barrell, 1989, this study), may temporarily dam the Motunau River, initially causing flooding upstream, and after breach of the slipped mass, flooding downstream. Assuming that a similar order of magnitude applies for the 2 slides analysed in this study, displacement rates on Earthslide 3, Coringa Landslide Complex would be theoretically less than 0.1 m/yr. However, Zhang et.al's (1991) studies and Marden et. al's (1993) review were based on fast moving earthslides, with magnitudes of displacement much larger than those observed and inferred on earthslide 3. It is possible that potential displacements after any reforestation may be significantly different to those described by Marden et al (1993)
3. Drainage measures. As the fundamental mechanism controlling movement on Earthslide 3 is the development of an area of undrained loading in the earthslide bend, drainage of this area would theoretically stop or reduce movement. On Earthslide A, control by diversion of streams entering the slide near its head would have the effect of stopping, or reducing rates of, movement.

4.8. Conclusions

Two earthslides were examined in this study. Earthslide A is part of the Mt. Vulcan Landslide Complex, while Earthslide 3 comprises part of the Coringa Landslide Complex. In this study, the term 'earthslide' is used to describe a slow moving lobate or elongate landslide that advances by displacement along discrete lateral and basal shear surfaces and whose average grain size distribution is comprised of more than 50% sand, silt and clay. Both earthslides examined in this study are elongate features and it was found that Earthslide 3 has an average surface inclination slightly less than its ultimate stability angle, while Earthslide A has an average surface inclination of about its ultimate stability angle.

Both earthslides move by plug-flow or sliding on lateral and basal shear surfaces. No information is available on the characteristics of the basal shear surface on the Earthslide A, however, borehole information for Earthslide 3 implies that the basal shear zone comprises a softened and highly deformed zone of 300-500 mm in thickness. Multiple basal shear surfaces are inferred to be underlying the toe of Earthslide 3. Lateral shears on both earthslides exhibited features ranging from Riedal shears at the early stages of development, through to a linear, slickensided shear at the fully developed state. A pull apart basin associated with a region of extension along the sinistral (eastern) shear of Earthslide 3 is inferred to be the only persistent feature observed along the boundaries of either earthslide.

Lateral bulges noted on both earthslides are inferred to form in 2 different ways. Type I bulges are postulated to form as a pressure ridge (deformational bulge), while type II bulges are inferred to form as a result of remnant material left after overriding an existing ground surface (depositional bulge) On both earthslides, lateral bulges have formed immediately upstream and downstream of regions of constricted movement.

Monitoring evidence shows that the accumulation zone of the Earthslide 3 tends to inflate at times of movement, as a response to increased pressure from the moving upslope slide mass. During times of deceleration, the accumulation zone tends to 'deflate'. These factors indicate that the accumulation zone of Earthslide 3 acts as a region of non-steady state behaviour. Points located further upslope showed faster displacement rates than at the toe and showed almost constant decrease in elevation with time, indicating a region of steady state behaviour. The similarity in the amount of offset of points across the earthslide suggests that in this region the majority of displacement occurs along the lateral shear zones, and the earthslide is in a region of plug-flow or slide movement.

Movement rates of Earthslide 3 were non-constant through the year of monitoring, with periods of accelerated movement between late May 1993-early October and early December-late January 1994 accounting for 78% of the observed displacement. These accelerations correlate well with periods of increased precipitation April-May 1993 and December 1993. A 'lag-time' of between 2 and 4 weeks is postulated between a significant rainfall event (ie., where sufficient rain falls to potentially alter the stability of the slide) and the onset of movement (or acceleration) of the slide.

Combined evidence from surface morphology, surface displacement patterns and back analysis indicates that an area of undrained loading is most likely to be effecting the movement rates of Earthslide 3. It is thought that this area of undrained loading occurs near the top of the earthslide bend. However, back analysis conducted for Earthslide A show that an undrained loading is not necessary to produce movement on the earthslide. Rather, movement rates are controlled by the relatively steep inclination of the slide, and the continual erosion of the earthslide toe by wave action.

Momentum transfer calculations performed for Earthslide 3 indicate that sediment-flux perturbations at the head zone are transferred downslope by components of diffusion and advection (transfer of disturbances from the head zone by a kinematic wave) behaviour. Due to the low value of P_e, it was postulated however, that diffusion transfer (transfer of disturbances from the head zone to points within the earthslide) may the dominant component.

Both earthslides are postulated to maintain current displacements for some further period of time, although Earthslide 3 may reach a state of dormancy as the debris supply is exhausted. Dormancy could be achieved in 400-450 years, although a large margin of error is associated with this figure. The remedial options include reforestation, which is inferred to produce a order of magnitude decrease in the displacement rate or drainage and/or stream control. These options are particularly applicable to Earthslide 3, as rapid movement of the slide may lead to the temporary damming of the Motunau River.

Chapter Five: Summary and Conclusions

5.1. Mt. Vulcan Landslide Complex

The Mt. Vulcan Landslide Complex is categorised as a bedding controlled slump/earthslide complex (class VI), covering an area of approximately 85 ha, and is developed in lower Tertiary lithologies 9km southwest of Motunau Beach. The complex has a length from head to toe of approximately 2400 m, and a relatively constant width of 500 m. However at the toe, the landslide width is reduced to about 300 m. The mean direction of sliding near the head of the complex is 230°, which changes to approximately 170° in the downslope half of the complex.

The Mt. Vulcan Landslide Complex is situated at the stratigraphic top of the Eyre Formation on the eastern limb of the northeast-southwest trending Montserrat Syncline, and is located specifically within Ashley Mudstone/Homebush Sandstone and Waipara Greensand lithologies. Forms of slope movement recognised within the complex include rock falls, rock topples, back or forward rotational slumping and earthsliding. On the basis of surface morphology, failure style and likely current activity, the complex can be divided into 12 morphological units. Areas of former activity were recognised at the western side of the complex, while areas of current activity include the head region and associated earthslide/flow complex. Earthslide A comprises the most obviously active portion of the complex. Four types of material can be recognised within the Mt. Vulcan landslide Complex: (i) highly deformed soft smectitic silty clay with some sand and/or gravel, (ii) blocks (up to approximately 5 m diameter) of Amuri Limestone supported which may or may not be supported in (iii) chaotically arranged gravelly silty clay; and (iv) loose to compact glauconitic sand.

Rates of movement were determined for several morphological units comprising the landslide complex. Head scarp retreat rates were found to be variable through the period covered by aerial photography, with an average retreat rate of 1.6 m/yr between 1950 and 1974, and retreat rates of less than 0.5 m/yr for the period 1974-1992. While movement rates were determined for the older earthslide/flow debris, lack of recognisable features and changes in surface morphology between the 2 sets of aerial photographs made determination of movement rate impossible for a number of morphological units.

An age of formation of the complex proved difficult to determine, however, the inferred minimum age is about 5000 years, while the inferred maximum age is about 100 000 years.

The formation of the complex is inferred to be related to uplift and subsequent erosion of material along the Montserrat fault, conjectured to cross the complex near the toe. The head region of the complex is inferred to be primarily a deep-seated failure, whereas the lower half of the slide is likely to be a sliding/flow on a continuous slide plane. It is inferred that this plane comprises a strong cemented greensand layer, at or near the top of the Mt. Ellen member, the lower unit of Waipara Greensand.

The failure mechanism for the main body of the complex (ie, all materials except earthslide deposits) is inferred to involve initial slumping of soil (Ashley Mudstone and the Stormont member of Waipara Greensand) or rock (Amuri Limestone) from the scarps at, or near the head of the complex. Translational slide and earthslide movements are subsequently developed downslope from the head from the eastern lateral scarp, with or without a component of rotation, on convex upwards shear surfaces developed within Ashley Mudstone.

5.2. Coringa Landslide Complex

Coringa Landslide is a large slump/earthslide complex (class VI) involving an area of approximately 50 ha, and is located at the stratigraphic top of the Eyre Group on the eastern limb of Montserrat Anticline. The complex has a length from head to toe of nearly 1400m and a width ranging from 550m near the toe to 125m near the head.

Forms of slope movement involved in the complex include falls, topples, back or forward rotational slumping and earthsliding. Nine morphological units can be recognised within the complex based on the current activity of the area and the type of slope movement involved. Areas of ancient movement were recognised along the western lateral scarp of the complex, while current activity occurs within Earthslide 3.

A model of landslide evolution is proposed, and it is postulated that the complex is as old as 100 000 b.p. Evolution of the complex is inferred to have been controlled by movement on 2 eastwardly dipping thrust faults, conjectured to be underlying the complex. Two different failure mechanisms of the complex can be recognised (i) slumping of rock/soil material on concave upwards shear surfaces developed within Ashley Mudstone along the eastern lateral scarp (ii) periodic deep seated movement, in response to the removal of support at the toe of the complex by the action of the Motunau River. It is inferred that the surface of rupture of the complex is located at or near the Waipara Greensand/Loburn Mudstone contact.

5.3. Earthslide Studies

The analysis of Earthslide A (within the Mt. Vulcan Landslide Complex) and Earthslide 3 (part of the Coringa Landslide Complex) formed the main objective of this project. In this thesis,

the term 'earthslide' is defined as a slow moving lobate or elongate landslide that advances by displacement along discrete lateral and basal shear surfaces and whose average grain size distribution shows more than 50% sand, silt and clay combined.

Earthslides commonly display lobate or elongate shapes, depending on the ratio between the angle of ultimate stability (β_u; calculated by stability analysis equations) and the earthslide inclination (β). Both earthslides examined in this study are clearly elongate features and it was found that for observed or inferred maximum water levels, Earthslide 3 (Coringa Landslide Complex) had an average surface inclination slightly less than its ultimate stability angle, while Earthslide A (Mt. Vulcan Landslide Complex) had an average surface inclination of about its ultimate stability angle.

Earthslide A and Earthslide 3 display surface morphology consistent with similar features documented in the literature. While both slides exhibited head and track zones, no accumulation zone exists on Earthslide A due to rapid erosion of debris at the toe by wave action. However, an accumulation zone is in evidence on Earthslide 3.

Both earthslides move by plug-flow or sliding on lateral and basal shear surfaces. No information is available on the characteristics of the basal shear surface on the Earthslide A (Mt. Vulcan Landslide Complex), but borehole information for Earthslide 3 (Coringa Landslide Complex) implies that the basal shear zone comprises a softened and highly deformed zone of 300-500 mm in thickness. Multiple basal shear surfaces are inferred to underlie the toe of Earthslide 3. Lateral shears on both earthslides exhibited features ranging from Riedal shears at the early stages of development, through to a linear, slickensided shear at the fully developed state. A pull apart basin associated with a region of extension along the sinistral (eastern) shear of Earthslide 3 is inferred to be the only persistent feature observed along the boundaries of either earthslide.

Lateral bulges noted on both earthslides form in two different ways. Type I bulges form as a pressure ridge (deformational bulge), while type II bulges form as a result of remnant material left after overriding an existing ground surface (depositional bulge) On both earthslides, lateral bulges have formed immediately upstream and downstream of regions of constricted movement.

Monitoring from September 1988- March 1989 of the earthslide showed that the earthslide was near a state of dormancy at that time. However, significant displacement was observed during the recent year of monitoring, with a maximum displacement of about 2 m recorded. Movement rates of Earthslide 3 (Coringa Landslide Complex) were variable through the year

of monitoring, with periods of accelerated movement between late May 1993-early October and early December-late January 1994 accounting for 78% of the observed displacement. These accelerations correlate well with periods of increased precipitation in April-May 1993 and December 1993. A 'lag-time' of between 2 and 4 weeks is postulated between a significant rainfall event (ie., where sufficient rain falls to potentially alter the stability of the slide) and the onset of movement (or acceleration) of the slide.

Regions of compressive, extensional and plug flow could be observed on both earthslides. Tensional cracks occurring at convex breaks in slope on Earthslide A (Mt. Vulcan Landslide Complex) are inferred to be the surface expression of extensional flow. Monitoring evidence for Earthslide 3 (Coringa Landslide Complex) shows that the accumulation zone of the slide tends to inflate at times of movement, as a response to increased pressure from the moving upslope slide mass. During times of deceleration, the accumulation zone tends to 'deflate'. These factors strongly indicate that much of the accumulation zone of Earthslide 3 acts as a region of non-steady state behaviour as the cross-sectional area of the slide is not constant with time. There is also evidence to suggest a component of internal deformation in this area. Monitoring points located in the track zone showed faster displacement rates than at the toe and showed almost constant decrease in elevation with time, indicating a region of steady-state behaviour. The similarity in the amount of offset of points across the earthslide suggests that in this region the majority of displacement occurs along the lateral shear zones, and the earthslide is in a region of plug-flow or slide movement.

Combined evidence from surface morphology, surface displacement patterns, geotechnical analysis and back analysis indicates that an area of undrained loading is most likely to be effecting the movement rate of Earthslide 3, Coringa Landslide Complex. It is perceived that this area of undrained loading occurs within the bend in movement direction of the slide. However, stability analysis conducted for Earthslide A on the Mt. Vulcan Landslide Complex indicates that an undrained loading is not necessary to produce movement on the earthslide. Rather, movement rates are controlled by the relatively steep inclination of the slide, inflows of water near the head zone of the slide and the continual erosion of the earthslide toe by wave action.

Momentum transfer calculations performed for Earthslide 3 indicate that sediment-flux perturbations at the head zone are transferred downslope by components of diffusion and kinematic wave behaviour. Due to the low value of the calculated Peclet number, however it was postulated, that diffusion may the dominant behavioural component.

Both earthslides are postulated to maintain current displacements for some further period of time, although Earthslide 3 may reach a state of dormancy as the debris supply is exhausted. Dormancy could be achieved in 400-450 years, although a large margin of error is associated with this figure. The remedial options include reforestation, which is inferred to produce a order of magnitude decrease in the displacement rate or drainage and/or stream control. These options are particularly applicable to Earthslide 3, as rapid movement of the slide may lead to the temporary damming of the Motunau River.

5.4 Recommended Further Investigations

5.4.1 Mt. Vulcan Landslide Complex

The investigation of the complex in this study comprised an initial (or reconnaissance) study. Therefore, detailed study is warranted. In particular, it is recommended that following investigations be executed:

1. Subsurface investigations by drilling at various locations within and immediately adjacent to the complex.
2. Subsurface monitoring of Earthslide A and the Upper earthslide/flow complex, including examination of ground water levels and subsurface deformation profiles.
3. Surface movement rates of the Upper earthslide/flow complex and Earthslide A. Due to the probable fast displacements of Earthslide A, especially near the toe, a number of semi-unique monitoring options could be attempted, including time-lapse photography of movement across lateral shear zones.
4. Detailed monitoring of head scarp retreat rates.
5. Detailed monitoring of the behaviour of the crown scarp and associated features.

5.5.2 Coringa Landslide Complex

It is recommended that

1. Regular surveys be maintained on Earthslide 3 to determine more conclusively (i) the lag-time between a significant rainfall event and the onset of acceleration of the earthslide, and; (ii) which regions of the slide demonstrate permanent steady or unsteady state behaviour. Long term surveying is justified to monitor earthslide movement rates determine and to determine the overall long term behaviour of the slide.
2. A drilling program be undertaken. This program would have two aspects: (i) subsurface investigation of the larger complex (ii) emplacement of further boreholes on Earthslide 3.
3. Subsurface instrumentation on Earthslide 3, involving inclinometer and piezometer installation to determine subsurface deformation profiles and ground water levels.
4. Subsurface investigations by trenching in the region of development of transverse bulging, to fully resolve whether an area of undrained loading occurs within this area.

References

Andrews, P.B. 1963. Statigraphic nomenclature of the Omihi and Waikari Formations, North Canterbury. *N. Z. Jour. Geol. Geophys.* 228-256.

Andrews, P.B.; B.D. Field; G.H. Browne and J.M. McLennan 1987. *Lithostratigraphic Nomenclature for the Upper Cretaceous and Tertiary Sequence of Central Canterbury, New Zealand.* New Zealand Geological Survey Record 24.

Bailey, R.G. 1972. *Landslide Hazards Relating to Land Use Planning in Teton National Forest, Northwest Wyoming.* Ogden, Utah, U.S. Dept. of Agriculture, Forest Service. 131 pp

Barrell, D. 1989. *Engineering Geological Investigations at Coastal Motunau, North Canterbury* Unpub MSc thesis, University of Canterbury.

Bell, D. H. and J.R. Pettinga. 1983. Presentation of Geological Data. *IPENZ, Proc. Technical Groups,* vol. 9 no. 4.

Bell, D. H. and J.R. Pettinga. 1992. Engineering geological assessment of slope instability for rural land-use, Hawke's Bay, New Zealand. in Bell. D. H. (ed) *Landslides.* Proc. 6th Intl. Symp. Landslides: 1467-1480

Bertini, T., F. Cugusi, B. D'Elia, G. Lanzo and M. Rossi-Doria. 1992. Slow movement investigations in clay slopes in Bell. D. H. (ed) *Landslides.* Proc. 6th Intl. Symp. Landslides: 329-334

Bhandari, .K. and J.N. Hutchinson 1982. Coastal mudslides in the Oligocene clays of Bouldnor Cliff, Isle of Wight. in Sheko, A (ed.) *Landslides and Mudflows* Reports of Alma-Ata. Intl. Seminar Oct. 1981:176-199

Blong, R.J. and G.O. Eyles. 1989. Landslides: extent and economic significance in Australia, New Zealand and Papua New Guinea. in Brabb, E.E. and B. L. Harrod (eds.) *Landslides: Extent and Economic Significance.* Proc. 28th Intl Geol. Cong: Symp. Landslides, Washington, D.C:343-356

Bovis, M. J. 1985. Earthflows of the Interior Plateau, southwest British Columbia. *Can. Geotech. J.*. v 22: 313-334

Bovis, M. J. 1986. The morphology and mechanics of large-scale slope movement, with particular reference to southwest British Columbia. in Abrahams, A. D. (ed.). *Hillslope Processes*. Binghampton Symp. Geomorphology. Int. Ser. no. 16: 319-341

Brindley, G. W. and G. Brown. 1984. *Crystal Structures of Clay Minerals and their X-ray Identification*. 2nd ed. Mineralogical Society. 495 pp.

Bromhead, E.N. 1986. *The Stability of Slopes*. Surrey University Press 374 pp.

Browne, G.H. and B.D. Field. 1985. *The lithostratigraphy of late Cretaceous to Early Pleistocene rocks of Northern Canterbury, New Zealand*. New Zealand Geological Survey Record 6.

Brunsden, D. 1984. Mudslides. in Brunsden, D. and D. B. Prior (eds.). *Slope Instability*. Wiley. pp 363-418

Campbell, A.P. 1966. Measurement of movement of an earthflow. *Soil & Water* 2 no. 3: 23-24.

Campbell, R.H. 1975. *Soil Slips, Debris Flows and Rainstorms in the Santa Monica Mountains and Vicinity, Southern California*. U.S.G.S. Prof. Paper 851 United States Government Printing Office, Washington. 51 pp.

Carlson, J. R., J. A Grant-Mackie and K. A. Rogers (1980). Stratigraphy and sedimentology of the Coalgate area, Canterbury, New Zealand. *N. Z. Jour. Geol Geophys* 23:192-197.

Carter, R.M. and L. Carter 1982. The Motunau fault and other structures at the southern edge of the Australian-Pacific plate boundary, offshore Marlborough, New Zealand *Tectonophysics* 88: 133-159.

Conway, B.W. 1974. The Black Ven landslip, Charmouth, Dorset. *Inst. Geol. Sci.* rept no 74/3: 1-16

Craig, R.F. 1992. *Soil Mechanics* 5th ed. Van Nostrand Reinhold. 427 pp

Crandell, D. R. and D. J. Varnes 1961. *Movement of the Slumgullion earthflow near Lake City, Colorado.* USGS Prof. Paper 424B:136-139

Crosta, G. B., W. Z. Savage and F. Guzzetti 1992. Modelling flow development near obstructions of mass movements in earth materials. in Bell. D. H. (ed) *Landslides.* Proc. 6th Intl. Symp. Landslides: 53-58

Crozier, M.J. 1969. Earthflow occurence during high intensity rainfall in Eastern Otago (New Zealand). *Eng. Geol.* 3:325-334

Cruden, D. M. 1991. A simple definition of a landslide. *Bull. Intl.Assoc.Eng.Geol.* 43: 27-29

Cruden, D.M. and W.M. Brown III. 1992. Progress towards the World Landslide Inventory. in Bell. D. H. (ed) *Landslides.* Proc. 6th Intl. Symp. Landslides: 59-64

D'Elia, B. and G. Tancredi. 1979. Colate permanenti e tempranee: confronto tra due casi. *Geologia Applicata e Idrogeologia.* (Italian, with English summary), 14:23-29

Deganutti, A.M. and P. Gasparetto 1992. Some aspects of a mudslide in Cortina, Italy. in Bell. D. H. (ed) *Landslides.* Proc. 6th Intl. Symp. Landslides: 373-378

Del Prete, M. and D. J. Petlry. 1982. Case history of the main landsldie at Craco, Basilicata, south Italy. *Geologia Applicata e Idrogeologia*, 17:291-304

Einstein, H.H. 1988. Landslide risk assessment procedure. in Bonnard, C. (ed.) Proc. 5th Intl. symp. *Landslides*, Lausanne. A.A Balkema 1075-1090.

Eslinger, E. and D. Pevear. 1988. *Clay Minerals for Petroleum Geologists and Engineers.* SEPM short course no. 22.

Field, B. D. and G.H. Browne. 1989. *Cretaceous and Cenozoic Sedimentary Basins ans Geological Evolution of the Canterbury Region, South Island, New Zealand.* NZGS Basin series 2. 92 pp

Fell, R. and R.P. Jeffrey. 1987. Determination of drained shear strength for slope stability analysis. in Walker, B.F and R. Fell 1987 (eds.) *Soil Slope Instability and Stabilisation.* A.A. Balkema: 53-71.

Fleming, R.W and A. M. Johnson. 1989. Structures associated with strike-slip faults that bound landslide elements. *Engineering Geology* 27, nos 1-4: 39-115

Graham, J. 1984. Methods of Stability Analysis. in Brunsden, D. and D. B. Prior (eds.). *Slope Instability*. Wiley. pp 171-216

Grocott, G.G. 1977. *Landslide Investigations, Main North Line Railway, South Island, New Zealand.* Unpub. MSc thesis, University of Canterbury.

Hansen, M. J. 1984. Strategies for classification of landslides. in Brunsden, D. and D. B. Prior (eds.). *Slope Instability*. Wiley. pp 1-24.

Hutchinson, C.S. 1974. *Laboratory handbook of Petrographic Techniques*. J. Wiley & sons. 527 pp

Hutchinson, J.N. 1969. A reconsideration of the coastal landslides at Folkstone Warren, Kent. *Geotechnique* 19 no 1: 6 - 38

Hutchinson, J.N. 1970. A coastal mudflow on the London Clay cliffs at Beltinge, North Kent *Geotechnique* 20 no.4: 412-438

Hutchinson, J.N. and R.K. Bhandari. 1971. Undrained loading, a fundamental mechanism of mudflows and other mass movements. *Geotechnique* 21 no. 4: 353-358

Hutchinson, J.N., D.B. Prior and N. Stephens. 1974. Potentially dangerous surges in an Antrim Mudslide. *Q. J. Eng. Geol.* Vol 7.: 363-376

Hutchinson, J.N. and M. Del Prete. 1985. Landslides at Calitri, Southern Apennines, reactivated by the earthquake of 23rd November 1980. *Geologia Applicata e Idrogeologia* 20: 9-38

Hutchinson, J. N. 1988. General Report: Morphological and geotechnical parameters of landslides in relation to geology and hydrogeology. in Bonnard, C. (ed). *Landslides*. Proc. 5th Intl. Symp. Landslides.: 3-35.

IASPEI (1994) *Field Guide to New Zealand Active Tectionics*. Roy. Soc. N.Z. Misc. series 27.

Iverson, R.M. 1986a. Unsteady, non-uniform landslide motion: 1. Theoretical dynamics and the steady datum state. *J. Geol.*, 94:1-15

Iverson, R.M. 1986b. Unsteady, non-uniform landslide motion: 1. Linearized theory and the kinematics of transient response. *J. Geol.*, 94:349-364

Irvine, B.M. 1963. *Ralston Creek Landslide, Jefferson County, Colorado.* Univ. of Colorado Studies, Series in Geogr., no 2.

Keefer, D.K. and A.M. Johnson. 1983. *Earth Flows: morphology, mobilisation and movement.* U.S. Geol Survey Prof. Paper 1264: 1-56

Kenney, C. 1984. Properties and behaviours of soils relevant to slope instability. in Brunsden, D. and D. B. Prior (eds.). *Slope Instability.* Wiley. pp 27-65

Law, C.C. 1987. *Geomechanics Manual No 4. Ring shear, vane shear, variable normal load direct shear, and core samples for plain direct shear tests.* Dept. Earth Sciences. University of Waikato 16 pp.

Marden, M., C. J. Phillips, R. J. Jackson, X.B. Zhang, and J. Ekanayake. 1993. A decade of earthflow research and inter-related studies in the North Island of New Zealand. in Walling, D.E., T.R. Davies and B. Hasholt (eds.) *Erosion, Debris Flows and Environment in Mountain Regions.* Proc. Symp. Intl. Assoc. Hydrological Sciences, Chengdu, China. IAHS pub no. 209. pp. 263-273.

Mason, B. H. 1941. The Geology of the Mt. Grey District, North Canterbury. *Trans. Roy. Soc. N. Z.* 71(2):103-127.

Moon, C.F. and K. B. White. 1985. A comparison of liquid limit test results. (Technical Note) *Geotechnique* 25 no.1:59-60

Morgenstern, N. R. and D. A. Sangrey. 1978. Methods of stability analysis. in Schuster, R. L. and R. J. Krizek (eds.) *Landslides, Analysis and Control.* TRB Sp. Rep. 176. 155-171.

Morris L. J. 1986 *Engineering Geological Investigations of the Wharanui Earthflow, Northeast Marlborough.* Unpub. MSc thesis, University of Canterbury.

Mostyn, G.R. and J.C. Small. 1987. Methods of stability analysis. in Walker, B.F and R. Fell. 1987 (eds.) *Soil Slope Instability and Stabilisation*. A.A.Balkema: 71-121.

Naylor, M.A., G. Mandl and C. H. K. Sijpesteijn. 1986. Fault geometries in basement-induced wrench faulting under different initial stress states. *Jour. Struct. Geol.* 8 no. 7. pgs 737-752.

New Zealand Geological Survey (NZGS). 1973. *Quaternary geology - South Island, 1:1 000 000. (1st ed.)*. N Z G S misc. series map 6. Department of Scientific and Industrial Research, Wellington.

National Institute of Water and Atmospheric Research (NIWA) 1994(a). Monthly rainfall data for station H33001 - Motunau and H3003 - Motuiti, January 1986 - March 1994. unpub data, Wellington, N.Z..

National Institute of Water and Atmospheric Research (NIWA) 1994(b). Daily rainfall data for station H3003 - Motuiti, January 1993 - March 1994. unpub. data, Wellington, N.Z.

Nicol, A, & Wise (1993) Paleostress adjacent to the Alpine Fault of New Zealand: fault, vein and styoloite data from the Doctors' Dome area. *Jour. Geophys. Reasearch* 97: 17,685-17,692

Northey, R.D., J.G. Hawley and P.R. Barker. 1974. Classification and mechanisms of slope failures in natural ground. NZ Geomech Soc. Proc. Symp. Stability of Slopes in Natural Ground. Nelson, 1974 pp 3.1-3.8

Manfredini, G. S. Martinetti, R. Ribacci, V. M. Santoro, M. Sciotto and T. Silvestri. 1981. An earthflow in the Sinni Valey (Italy). Proc. 10th Intl. Conf. Soil Mech. and Found. Eng., Stockholm, 2:457-462.

Prior, D.B. and Stephens, N. 1972. Some movement patterns of temperate mudflows:examples from north-east Ireland. *Geol. Soc. Am. Bull.* 83:2533-2544.

Prior, D.B. 1977. Coastal mudslide morphology and processes on Eocene clays in Denmark. *Geografisk Tidsskrift*, 76:14-33

Schuster, R.L. 1978. Introduction. in Schuster, R.L. and R. J. Kriizek (eds.) *Landslides, Analysis and Control* TRB Sp. Rep. 176.

Skempton, A. W. and F. A. DeLory. 1957. Stability of natural slopes in London Clay. Proc. 4th Intl. Conf. Soil Mechanics and Foundation Engineering, London. vol 2: 378-381

Skempton, A. W. 1964. Long-term stability of clay slopes. Fourth Rankine Lecture. *Geotechnique* XIV 77 - 102

Skempton, A. W. and J. N. Hutchinson. 1969. Stability of natural slopes and embankment foundations. *Proc 7th Intl Conf Soil Mechanics and Foundation Engineering,* Mexico. vol 3:291-340

Skempton, A. W. 1985. Residual strength of clays in landslides, folded strata and the laboratory. *Geotechnique* 35 no. 1

Sharpe, C.F.S. 1938. *Landslides and Related Phenomena.* Columbia. Univ. Press, New York. 137 pgs.

Smale, D., G. J. Van der Lingin and D.H. Bell. 1982. A bedding plane landslide near Mt Vulcan, North Canterbury. *N.Z. Jour. Geol. Geophys* v25: 397-404

Smith, R.K. 1974. *Earthflows in the Poverty Bay-East Coast Region. Report on Project Na/Hy/5.* National Water and Soil Conservation Organisation, N.Z. Progress Report 18: 19 pp

Sowers, G. F. and D. L. Royster. 1978. Field Investigation. in Schuster, R.L. and R.J. Krizek (eds.) *Landslides, Analysis and Control.* TRB Sp. Rep. 176.

Standards Association of New Zealand. (NZS 4402: 1986). *Methods of Testing Soils for Civil Engineering Purposes.* Standards Association of New Zealand.

Stapledon, D. 1992. Geological Modelling in landslide investigation. in Bell. D. H. (ed) *Landslides.* Proc. 6th Intl. Symp. *Landslides.* (in prep)

Sylvester, A.G. 1988. Strike-slip faults. *Geol. Soc. Am. Bull.* 100. pgs. 1666-1703

Taylor, S. R., 1950: *The Geology of the Stonyhurst District, North Canterbury, New Zealand.* unpub. MSc. thesis, Geology dept, University of Canterbury.

Thomas, M. R. and A. L. Kropp. 1989. Earthflow evaluation and control: a case history. in Watters, R. J. (ed.) *Engineering Geology and Geotechnical Engineering*. A.A. Balkema, Rotterdam. 420 pp.

Trotter, C.M., E.J. Pinkney and H.G. Tod. 1992. Weathering and strength loss at an earthflow site. in Bell. D. H. (ed) *Landslides*. Proc. 6th Intl. Symp. Landslides: 1489-1495.

Van Dine, D.F. 1980. Engineering geology and geotechnical study of Drynoch landlside, British Columbia. *Geol. Surv. Canada.* paper 79-31:1-34.

Varnes D. J. 1978. Slope Movement Types and Processes. in Schuster, R. L. and R. J. Krizek (eds.) *Landslides, Analysis and Control* TRB Sp. Rep. 176

von Moos, A. 1953. The subsoil of Switzerland. Proc. 3rd. Intl. Conf. Soil Mech. and Found. Eng., Zurich 3:252-264.

Warren, G. and I. Speden. 1978. The Piripauan and Haumurian stratotypes (Mata series, Upper Cretaceous) and correlative sequences in the Haumuri Bluff district, South Marlborough. *N. Z. Geol. Surv. Bull* 92

Whalley, W.B. Rockfalls. in Brunsden, D. and D. B. Prior (eds.). *Slope Instability*. Wiley. pp 217-256

Williams, J. W. (1989) Foreward. in Brabb, E.E. and B. L. Harrod (eds.) *Landslides: Extent and Economic Significance*. Proc. 28th Intl. Geol. Cong: Symp. Landslides, Washington, D.C:XIII

Wilson, D.D (1963) *Geology of the Waipara Subdivision*. DSIR bull. no. 64. 122p.

Wilson, S.D. and P.E. Mikkelson. 1978. Field Instrumentation in Schuster, R. L. and R. J. Krizek (eds.) *Landslides, Analysis and Control.* TRB Sp. Rep. 176.

WP/WLI (International Geotechnical Societies' UNESCO Working Party on World Landslide Inventory), 1990a. A suggested method for reporting a landslide. *Bull. Intl. Assoc. Engineering Geology*, 41: 5-12

WP/WLI (International Geotechnical Societies' UNESCO Working Party on World Landslide Inventory), 1990b. Suggested nomenclature for landslides. *Bull. Intl. Assoc. Engineering Geology*, 41: 13-16

WP/WLI (International Geotechnical Societies' UNESCO Working Party on World Landslide Inventory), 1993. A suggested method for describing the activity of a landslide. *Bull. Intl. Assoc. Engineering Geology*, 47: 53-57

Wu, T.H. and D. A. Sangrey. 1978. Strength properties and their measurement. in Schuster, R.L. & R.J. Krizek (eds.) *Landslides, Analysis and Control* TRB Sp. Rep. 176: 139-154

Wykeham Farrance Engineering Ltd (a). *The Bromhead Ring Shear WF25850. Instruction Manual.*

Wykeham Farrance Engineering Ltd (b). *Stepless Shearbox Apparatus WF25302. Instruction Manual*

Yousif, H. S. 1987. *The Applications of Remote Sensing to Geomorphological Neotectonic Mapping in North Canterbury, New Zealand.* unpub. Phd. thesis, University of Canterbury.

Zaruba, Q and V. Mencl. 1982. *Landslides and their Control* (2nd ed.) Elsevier, Amsterdam.

Zhang, X., C. Phillips and A. Pearce. 1991 (a). Internal deformation of a fast moving earthflow, Raukumara Peninsula, New Zealand. *Geomorphology*, 4: 145-154.

Zhang, X., C. Phillips and A. Pearce. 1991 (b). Surface movement in an earthflow complex, Raukumara Peninsula, New Zealand. *Geomorphology*, 4: 261-272.

Appendix A: New Zealand Geological Time Scale, Upper Cretaceous-Quaternary

SYSTEM	t (m.y.)	SERIES	STAGE	SUBSTAGE	International Equivalent
Quaternary	0.001	Hawera	Aranuian		Holocene
	0.07		Otirian Oturian Waimean Terangian Waimaungan Waiwheran		Pleistocene
	0.25				
	0.28		Porikan		
	0.45	Wanganui	Castlecliffian	Putikian Okehuan	
	1.79		Nukumaruan	Marahauan Hautawan	
			Waitotaran	Mangapanian Waipipian	Pliocene
	5.00		Opoitian		
Tertiary		Taranaki	Kapitean Tongaporutuan		Miocene
	10.50				
	14.00	Southland	Waiauan Lillburnian Clifdenian		
		Pareora	Altonian Otaian		
	22.50	Landon	Waitakian Duntroonian Whaingaroan		Oligocene
	36.00	Arnold	Runangan Kaiatan Bortonian		Eocene
	53.50	Dannevirke	Porangan Heretaungan Mangaorapan		
			Waipawan Teurian		Paleocene
Upper Mesozoic	65.00	Mata	Haumurian Piripauan		Cretaceous
		Raukumara	Teratan Mangaotanean Arowhanan		
	95.00	Clarence	Ngaterian Motuan Urutawan Korangan		

Appendix B: General

B.1 Extent of study area

The area as shown on figures 1.1 and **1** (map volume) is shown on NZMS 260, N34, 'Motunau'. The area runs north from the coast at 579050N, 250400 E to 579400 N, 250400 E. From this point, the edge of the study area runs approximately coast-parallel to 580000N, 251100E, before running directly east to 580000N, 251450E. From this point, the edge of the study area runs directly south to the coast at 579570N, 251450 E

B.2 Aerial photography

1. Coringa Landslide Complex. Coringa Landslide Complex is covered by aerial photographic runs 1821 no. 52-55 (1950) and SN 3685 26-28 (1974)
2. Mt. Vulcan Landslide Complex. The complex is covered by aerial photographic runs 1823, no 4-8 (1950) and SN 3685; 23-25

B.2.1 Determination of long-term movement rates using aerial photography

Long-term movement rates were determined for various morphological units of the Mt. Vulcan Landslide Complex. The technique involved the recognition of the same feature on both sets of aerial photographs, and determining the distance to a known stationary object (for example, head scarp retreat rates were measured by determining the distance of the head scarp from a farm track; see chapter 2, fig. 2.5).

Margin of Error

SN 3685 was found to have a scale of 1:25 000, whereas run 1823 was found to have a scale of 1:17777. This was determined using a standard formula

$$S = \frac{f}{H - h}$$

where S =scale, f = focal length; H =flying height and h= height of ground surface

The major source of error arrives from measuring inaccuracies. The standard error in measuring was determined to be ±2% (assuming a measuring inaccuracy of ±0.25 mm). Therefore, for the typical distances involved in determination of movement rates (a maximum of about 300 m), the typical measuring error is about 6 m.

Figure C.1 Engineering Geological Field Desciptions of Soil Material (from Bell & Pettinga, 1983)

WEATHERING

	TERM	GRADE	SOIL DESCRIPTION
5	Completely Weathered (CW)	V	completely discoloured and altered, no trace of original fabric
4	Highly Weathered (HW)	IV	mostly altered and weakened, little trace of original fabric
3	Moderately Weathered (MW)	III	large discoloured portions of original soil separated by more altered material, significantly weakened
2	Slightly Weathered (SW)	II	minor discolouration of some parts of the original soil, no loss of strength
1	Unweathered (UW)	I	original soil with NO discolouration, loss of strength or other effects due to weathering

0 NOTE * in coarse-grained soils record weathering grade of DOMINANT fraction here and qualify weathering grade of subordinate and/or minor fractions if appropriate

STRENGTH

	TERM	FIELD CRITERIA
1	loose	can be removed from exposure in disaggregated form by hand
2	compact	only removed from exposure by implement, material readily disaggregated by physical means
3	+cemented	only removed from exposure by implement, material does not disaggregate
4	hard	may be removed from exposure with difficulty by implement or hand, softened on immersion in water and may be remoulded
5	stiff	indented by thumb pressure, but not moulded by fingers; softened on immersion in water, and may be remoulded
6	firm	moulded or indented only by strong finger pressure, easily moulded after immersion in water
7	soft	easily indented or moulded by finger pressure
8	very soft	exudes between fingers when squeezed
9	spongy	readily compressed by finger pressure, but cannot be remoulded

+ may require description as rock material

UNIFIED SOIL CLASSIFICATION SYSTEM

			FIELD IDENTIFICATION	GROUP SYMBOL	TYPICAL NAMES
COARSE-GRAINED SOILS	GRAVELS (<50% larger than 2mm)	clean gravels	wide range in grain size and substantial amounts of all interm. sizes	GW	well graded GRAVELS
			predom. one size or a range of sizes with some interm. sizes missing	GP	poorly graded GRAVELS
		gravels with fines	non-plastic fines (see ML below)	GM	poorly graded SILTY-GRAVELS
			plastic fines (see CL below)	GC	poorly graded CLAYEY-GRAVELS
	SANDS (<50% smaller than 2mm)	clean sands	wide range in grain sizes and substantial amounts of all interm. sizes	SW	well graded SANDS
			predom. one size or a range of sizes with some interm. sizes missing	SP	poorly graded SANDS
		sands with fines	non-plastic fines (see ML below)	SM	poorly graded SILTY-SANDS
			plastic fines (see CL below)	SC	poorly graded CLAYEY-SANDS

			SHINE	DILATANCY (1)	TOUGHNESS (1)		
FINE-GRAINED SOILS SILTS AND CLAYS	LIQUID LIMIT <50		none to very dull	quick to slow	none	ML	INORGANIC SILTS with slight plasticity
			moderate	none to very slow	medium	CL	INORGANIC CLAYS of low to medium plasticity
			none to very dull	slow	slight	OL	ORGANIC SILTS & CLAYS of low plasticity
	LIQUID LIMIT >50		dull	slow to none	slight to medium	MH	INORGANIC SILTS of high plasticity
			very glossy	none	high	CH	INORGANIC CLAYS of high plasticity
			moderate to v. glossy	none to very slow	slight to medium	OH	ORGANIC CLAYS of medium to high plasticity
HIGHLY ORGANIC SOILS			identified by colour, odour, spongy feel and fibrous texture			Pt	PEAT and other highly organic soils

PROCEDURES FOR FINE-GRAINED SOILS OR FRACTIONS (1)

DILATANCY (reaction to shaking) -

1) Prepare pat of moist soil, adding water to make soft - but not sticky.

2) Place pat in palm of hand, shake horizontally by striking vigorously against other hand

Positive Reaction: appearance of water on surface of pat, which becomes glossy. When squeezed between fingers, water and gloss disappear, pat stiffens and may crumble

TOUGHNESS: (consistency near plastic limit) -

1) Mould sample to consistency of putty, adding water or air drying as required

2) Roll to thin (3mm) thread, fold and reroll repeatedly until thread crumbles at plastic limit

3) Knead together and continue until lump crumbles

Diagnosis: a tough thread and stiff lump indicate high plasticity, a weak thread and lump low plasticity clays

GROUP SYMBOL CODINGS FOR USCS

COLUMN 1		COLUMN 2	
G:1	C:4	W:1	C:4
S:2	O:5	P:2	L:5
M:3	Pt:6	M:3	H:6

BOUNDARY CLASSIFICATIONS specify, enter 0.0

WEATHERING TERM | **WATER CONTENT TERM** | **STRENGTH TERM** | **COLOUR** | **FABRIC** | **SOIL NAME** | **USCS SYMBOL**

	TERM	FIELD CRITERIA
1	Dry	looks and feels dry; fine-grained soils usually hard, powdery or friable; coarse-grained soils may run freely through hands
2	Moist	soil feels cool and may be darkened in colour, particles tend to adhere in coarse-grained materials, fine-grained soils may be softened
3	Wet	soils feel cold and are darkened in colour, free water forms on hands when sample is disturbed
4	Saturated	restricted to wet soils below the water table or the static water level in excavations or drill holes

WATER CONTENT

1: light / 2: dark

1	pinkish	1	pink
2	reddish	2	red
3	yellowish	3	yellow
4	brownish	4	brown
5	olive	5	olive
6	greenish	6	green
7	bluish	7	blue
8	whitish	8	white
9	greyish	9	grey
		0	black

COLOUR

1: finely layered (<25 mm)
2: coarsely layered (25-100 mm)
3: massive
4: other (specify)

FABRIC

***SUBORDINATE FRACTION** 20-50% volume visual estimate

DOMINANT FRACTION >50% volume visual estimate

*** MINOR FRACTION** <20% volume visual estimate

1	coarse	gravelly
2	medium	gravelly
3	fine	gravelly
4	coarse	sandy
5	medium	sandy
6	fine	sandy
7	silty	
8	clayey	
9	peaty	

	SOIL TYPE TERM		PARTICLE SIZE (mm)	GRAPHIC LOG
1	coarse	gravel	> 60	
2	medium	gravel	20-60	
3	fine	gravel	2-20	
4	coarse	sand	0·6-2·0	
5	medium	sand	0·2-0·6	
6	fine	sand	0·06-0·2	
7	silt		0·002-0·06	
8	clay		< 0·002	
9	peat		NA	

PARTICLE SIZE

WITH SOME

1	coarse	gravel
2	medium	gravel
3	fine	gravel
4	coarse	sand
5	medium	sand
6	fine	sand
7	silt	
8	clay	
9	peat	

Figure C.2 Engineering Geological Field Descriptions of Rock Material (from Bell & Pettinga, 1983)

WEATHERING

	TERM	GRADE	ROCK DESCRIPTION
6.	* residual soil (RW)	VI	discolouration and complete transformation to soil; original fabric destroyed
5.	completely weathered (CW)	V	discolouration and transformation to soil; original fabric largely preserved
4.	highly weathered (HW)	IV	material pervasively altered with discolouration and loss of strength; fabric preserved; lithorelicts
3.	moderately weathered (MW)	III	penetrative discolouration and alteration of rock material, with some loss of strength
2.	slightly weathered (SW)	II	slight discolouration of rock fabric; no loss of material strength
1.	unweathered (UW)	I	no discolouration or loss of strength, or any other effects due to weathering

STRENGTH

	TERM	POINT LOAD STRENGTH INDEX Is(50)	FIELD ESTIMATION OF STRENGTH
1.	extremely strong (ES)	more than 10	can only be chipped with geological hammer
2.	very strong (VS)	3 to 10	several hard blows required to break hand specimen
3.	strong (S)	1 to 3	few firm blows of hammer required to break specimen
4.	moderately strong (MS)	0·3 to 1	breaks readily with one blow of hammer
5.	moderately weak (MWk)	0·1 to 0·3	broken by hand only with difficulty; small thin pieces broken by finger pressure
6.	weak (Wk)	0·03 to 0·1	broken by hand; pieces 25 mm or more broken by finger pressure
7.	* very weak (VWk)	less than 0·03	crushed or remoulded by hand (grades into soil materials)

* may require description as soil material

GEOLOGICAL CLASSIFICATION

CRYSTAL OR GRAIN SIZE	SEDIMENTARY (†)		IGNEOUS (†)					METAMORPHIC (†)	
	CLASTIC	CHEM/ORGANIC		Silicic	Intermed.	Mafic	Ultramaf.	FOLIATED	MASSIVE
very coarse 64 mm	CONGLOMERATE (1) AGGLOMERATE (2) BRECCIA (3)		INTRUSIVE	(27) (28) GRANITE GRANODIORITE	(29) (30) SYENITE DIORITE	(31) GABBRO	(32) (33) PERIDOTITE DUNITE	GNEISS (34) SCHIST (35) PHYLLITE (36) SLATE (37) MYLONITE (38)	HORNFELS (39) MARBLE (40) QUARTZITE (41) AMPHIBOLITE (42)
coarse 2 mm									
medium 0·06 mm	SANDSTONE (4)	Calcareous LIMESTONE (9) Siliceous CHERT (10) OTHER (11)							
fine	SILTSTONE (5)	Carbonaceous COAL (12) OTHER (13)	EXTRUSIVE	(19) (20) (21) RHYOLITE OBSIDIAN DACITE	(22) (23) TRACHYTE ANDESITE	(24) (25) DOLERITE BASALT	(26) SERPENTINITE		(†) OTHERS: Specify (43)
	MUDSTONE (6)	Ferruginous LATERITE (14) OTHER (15)							
very fine 0·002 mm	CLAYSTONE (8)	Saline ROCK SALT (16) GYPSITE (17) OTHER (18)							

TUFFS (7)

Mode of Occurrence

WEATHERING TERM | STRENGTH TERM | COLOUR | FABRIC | ROCK NAME

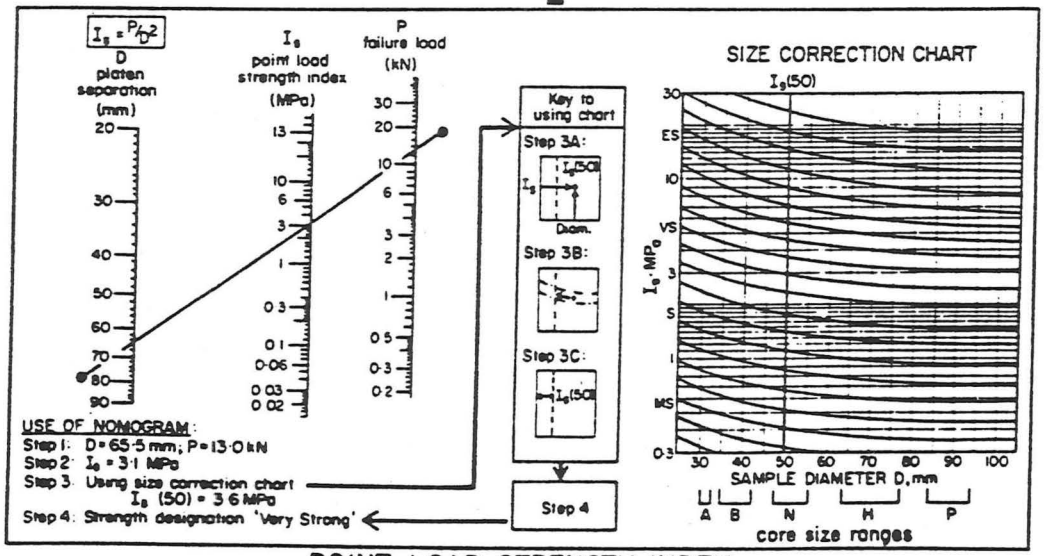

POINT LOAD STRENGTH INDEX

COLOUR

1: light
2: dark

1: pinkish	1: pink
2: reddish	2: red
3: yellowish	3: yellow
4: brownish	4: brown
5 olive	5: olive
6 greenish	6: green
7 bluish	7: blue
8: whitish	8: white
9: greyish	9 grey
	0 black

FABRIC

1 finely layered (< 25 mm)
2 coarsely layered (25 - 100 mm)
3 massive
4 other (specify)

Appendix C: Descriptions of Engineering Geological Units

Descriptions of units follows the method of Bell and Pettinga (1983; see previous pages) which is shown in figures C.1. Note that some lithostratigraphic units have been assigned the suffix "-stone", even though in some cases their strength is not sufficient to warrant the used of this term in the engineering sense (see Bell & Pettinga, 1983).

1. **Torlesse Supergroup**: Slightly weathered; strong/very strong; grey/dark grey; finely/coarsely layered SANDSTONE/MUDSTONE. A Permian to Cretaceous age is generally accepted for the formation of this supergroup.

2. **Eyre Group** (Brown & Field, 1985)

   (A) Broken River Formation (after Andrews et al, 1987)
   Unweathered/slightly weathered; light grey; massive/coarsely layered fine quartz SANDSTONE. In the study area, the thickness of the unit is indicated by Brown & Field (1985) to be about 140m, while Barrell (1989) estimates the thickness at 110m. Haumurian ages are indicated by micro- and macrofossil evidence for the majority of the formation (Brown & Field, 1987). The formation is interpreted as non-marine to marginal marine at the base, becoming fully marine towards the top.

   (B) Conway Formation (Brown & Field, 1985; modified from Warren & Speden, 1978).
   Unweathered/slightly weathered; dry/moist; loose/compact; light/dark grey; massive, fine silty fine/medium SAND (SM). Barrell (1989) suggested a minimum thickness of 30 m for this unit, however, the unit is considerably thicker than this at other localities (see Brown & Field, 1985). A largely Haumurian age is indicated for this unit. The depositional environment for the Conway Formation is interpreted by Warren & Speden (1978) to be a barred submarine depression.

   (C) Loburn Mudstone (after Mason, 1941)
   Unweathered; stiff; dark bluish grey; massive; clayey SILT, with some sand (ML). The formation exhibits a gradational contact with the underlying Conway Formation. A thickness of 50-70m (Yousif, 1987) is attained over much of the study area. Fossil evidence indicates a Teurian age for this unit. Brown & Field (1985) indicate a similar paleodepositional environment to that of Conway Formation.

(D) Waipara Greensand

Slightly weathered; dry; compact coarsely layered brownish green medium SAND, with some silt. Brown & Field (1985) indicate that the Waipara Greensand can be divided into 2 members. The lower Mt. Ellen member typically shows alternating weak and strong coarsely bedded layers, whereas the upper Stormont member consists of essentially massive compact sand. In the area around Coringa Landslide Complex, layers of carbonaceous mud (Pt) evident and the lower Mt. Ellen member is inferred to be absent or of small thickness, while in the area around the Mt. Vulcan Landslide Complex, both members are inferred to be present. A Teurian age is indicated by foraminifera (Yousif, 1987). Barrell (1989) suggested a probable thickness of about 40 m for the whole formation, and a similar thickness is inferred in this thesis. Waipara Greensand is interpreted to have formed in a shallow marine environment.

(E) Ashley Mudstone (after Mason, 1941)

Ashley Mudstone: dry/moist; soft; light brown; massive silty CLAY, with some sand (CH). The base of the formation is dated as Teurian to Waipawan, while foraminifera establish an age of Kaiatan near the top of the unit (Yousif, 1987). Brown & Field (1985) indicate that the depositional paleoenvironment for Ashley Mudstone was likely to have been bathyal. Severe slope movement in many areas does not allow quantitative measurement of the thickness of the unit.

(F) Homebush Sandstone (after Carlson et al, 1980)

Slightly weathered/unweathered; loose/compact; yellowish grey; massive fine SAND (SP). Brown & Field (1985) indicate an age for this unit of no younger than Bortonian. A near-shore paleoenvironment is indicated for this unit. In many areas, Homebush Sandstone is noted to show a complex deformational relationship with the underlying Ashley Mudstone. Brown & Field (1985) infer that large areas of overpressureised sand became mobilised immediately subsequent to deposition, intruding into the underlying mudstone as sand dikes, sills etc.

3. **Amuri Limestone**

Slightly weathered/unweathered; strong/moderately strong; greyish white; massive; LIMESTONE. In the study area, the thickness of Amuri Limestone is about 50 m. Brown & Field (1985) indicate a Whaingaroan age for the limestone is the Motunau area. The environment of deposition is inferred to be pelagic.

4. **Motunau Group** (Brown & Field, 1985)

   (A) Omihi Formation

   Slightly weathered, Moderately strong/strong light brownish grey massive sandy LIMESTONE/calcareous SANDSTONE. Yousif (1987) indicates a thickness for this unit ranging from 0-60m in the study area, and suggests an age for the formation of between Waitakian and Duntroonian.

   (B) Scargill Siltstone (after Andrews, 1963)

   Slightly weathered; moderately strong; light brown; finely/coarsely layered; SILTSTONE. In the study area, this unit is noted to have a thickness of about 15 m (Barrell, 1989).

   (C) Mt. Brown Formation

   Slightly weathered; moderately strong; light brownish grey; calcareous medium SANDSTONE, coarsely layered at bottom of formation, becoming massive near centre. Foraminiferal and macrofossil determinations indicate Otain to Waiauan ages (Brown & Field, 1985). Barrell (1989) indicates that the thickness of this unit is about 300 m, while other workers note that the Mt. Brown Formation has a stratigraphic thickness of only 75 m.

Appendix D: Geotechnical Testing

Geotechnical tests were conducted within the Geology Department, University of Canterbury. Tests were conducted (as far as possible) using standard techniques outlined in NZS 4402. Methodology is discussed below, and results are given in tables D.1 (Earthslide 2, Coringa Landslide Complex) and D.2 (Earthslide A, Mt. Vulcan Landslide Complex)

D.1. Natural Water Content, Atterburg Limits and Linear Shrinkage

D.1.1 Moisture Content

(NZS 4402: Test 2.1 Determination of the water content)

The water content (w) of a soil is defined as the ratio of the mass of water to the mass of solids in the soil and is determined by weighing a sample of the soil, drying (normally for a period of 24 hrs) and subsequently reweighing.

D.1.2 Atterberg Limits

"Atterberg limit" is a collective term that encompasses both the plastic and liquid limits. Depending on its water content, a soil may exist in the liquid, plastic, semi-solid or solid state. The water contents at which the transitions between states occur vary from soil to soil. Most fine grained soils exist naturally in the plastic state (Craig, 1984). The upper and lower limits of the range of water content over which a soil exhibits plastic behaviour are defined as the liquid limit (w_L) and the plastic limit (wP) respectively. The water content range itself defines the plasticity index (Ip), ie.:

$$I_p = w_L - w_P \qquad \text{(D1)}$$

Samples used for the determination of Atterburg limits were firstly wet sieved, and only that portion of the sample that passed a 425 μm BS sieve was used in the tests.

A. Liquid Limit

(NZS 4402 Test 2.2 Determination of the liquid limit)

The sieved test soil was mixed with distilled water to form a thick paste. NZS 4402 recommends that the soil paste then be stored for 24 hours to re-equilibrate. However, Moon & White (1981) note that there is little, if any, difference between values of liquid limit established in a '24 hour' test and an 'immediate' test, and hence, soil samples were generally not stored for any period in this study.

Liquid limits were measured using the Casagrande method. Repeat determinations were made until two successive determinations gave the same number of blows, and the water of the content of the sample established. The test was repeated four times at differing water contents. The water content of the four samples was then plotted against the corresponding logarithm of the number of blows and the line of best fit plotted.

B. Plastic Limit

(NZS 4402 Test 2.3 Determination of the plastic limit)

For the determination of the plastic limit the sieved test soil was mixed with distilled water until it became sufficiently plastic to be moulded into a ball. Part of the soil (about 2.5 g) was formed into an approximately 6 mm diameter thread. The thread was then rolled on a glass plate until its diameter was reduced to about 3 mm. The thread is subsequently remoulded and the procedure repeated until the soil shears both longitudinally and transversely when it is rolled to a diameter of 3 mm. The test is then repeated using four other sub-samples and the average water content taken to determine the plastic limit.

D.1.3 Linear Shrinkage

(NZS 4402 Test 2.6 Determination of the linear shrinkage)

The sieved test soil is mixed with distilled water until the soil mass has a water content approximately equal to the liquid limit. The soil is then placed in a standard linear shrinkage mould (dimensions given in NZS 4402) and air dried until shrinkage has largely ceased. The specimen is then fully dried in an oven at 105°C. The mean length of the oven dried specimen is recorded.

Linear shrinkage (*ls*) is calculated from:-

$$ls = \left(1 - \frac{l_{dry}}{l_{mould}}\right) \times 100\% \qquad \text{(D2)}$$

where l_{dry} = length of oven dried specimen and l_{mould} = internal length of mould (150mm)

D.2. Determination of Bulk Density

(NZS 4402 Test 2.7 Determination of the solid density of soil particles
Test 2.72 Method for medium and fine soils)

The 'bulk density' (ρ) of a soil is the ratio of the total mass to the total volume. Due to the nature of sample acquisition, bulk densities determined were for recompacted samples. Samples were placed in a container of known cross-sectional area, height and mass. The mass of soil and the container was measured, the container mass subtracted and the result was divided by the calculated soil volume.

D.3. Determination of Particle Size Distribution

NZS 4402: Test 2.8 Determination of the particle-size distribution

D.3.1 Wet Seiving method

Test 2.81. Standard method by wet seiving

This method covers the quantitative determination of the particle size distribution in a soil mass down to the fine sand size. Seives of appropriate size are stacked, and soil material washed through the stack. Soil material was manipulated through the seive stack by a rubber scraper, so as not to crush grains. Collections of grains were made from each seive, and measured in relation to the known total sample weight.

D.3.2 Pipitte Analysis

Test 2.8.3 Standard method for fine soils (pipette method)

Pipette analysis is based on the assumption that different size particles settle at different rates (Stokes' Law). The soil sample was intially wet sieved with a 0.063 mm (4Φ; Φ= - $\log_{10}$ (particle size in mm)) seive and placed in a sedimentation column. After stirring, subsamples of a specific volume were extracted from the mud suspension at a specified depth at a specified time. Each sample measures the proportion measures the percentage of material finer than the size that is calculated by Stoke's Law to have settled to the specified depth at that time. Samples were taken at 20 sec (4Φ); 2 min (4.5Φ); 4 min (5 Φ); 8 min (5.5Φ); 15 min (6.0Φ); 30 min (7.0Φ); 2 hrs (8.0Φ); and 8 hrs (9.0Φ). The subsamples were then dried at less than 65°, weighed and a cumulative percentage of the mud range obtained.

D.3.3 Results

A. Earthslide 3 (Coringa Landsldie Complex)

Analyses were performed on 11 samples from Earthslide 3, results are given in table D.1 and expressed diagrammatically in figure D.1.

Earthslide A, (Mt. Vulcan Landslide Complex)

Analyses were performed on 6 samples from Earthslide A, results are given in table D.2 and expressed diagrammatically in figure D.2.

D.4. Determination of Residual Friction and Cohesion

D.4.1 Ring Shear Testing

The Bromhead Ring Shear Apparatus conducts a continuous shear strength test within an annular, ring shaped test sample, for determination of residual shear strength parameters; effective residual friction angle, ϕ'_r, and effective residual cohesion, c'_r

Figure D.1 Particle size distributions, Earthslide 3

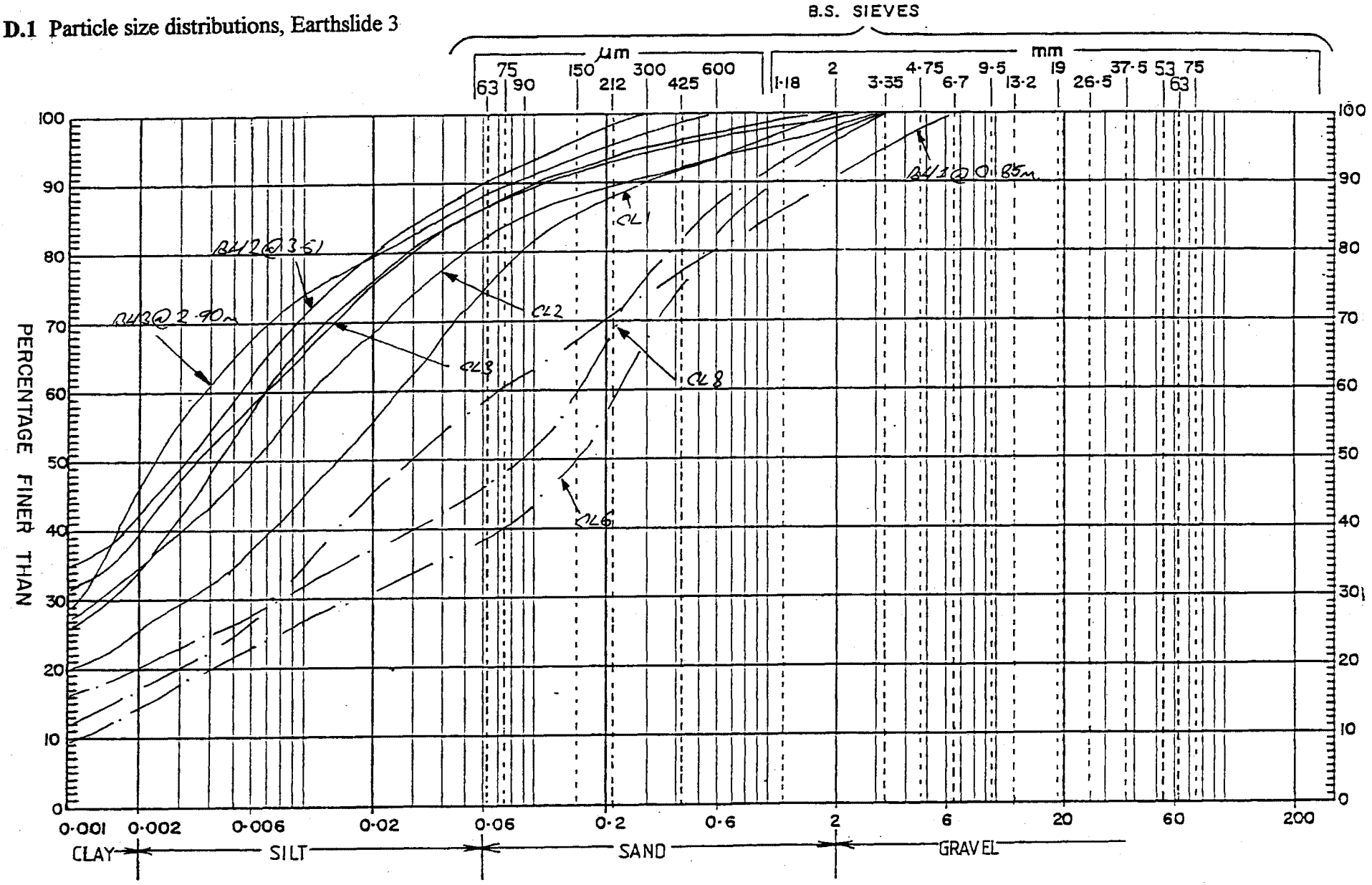

Figure D.2. Particle size distributions, Earthslide A

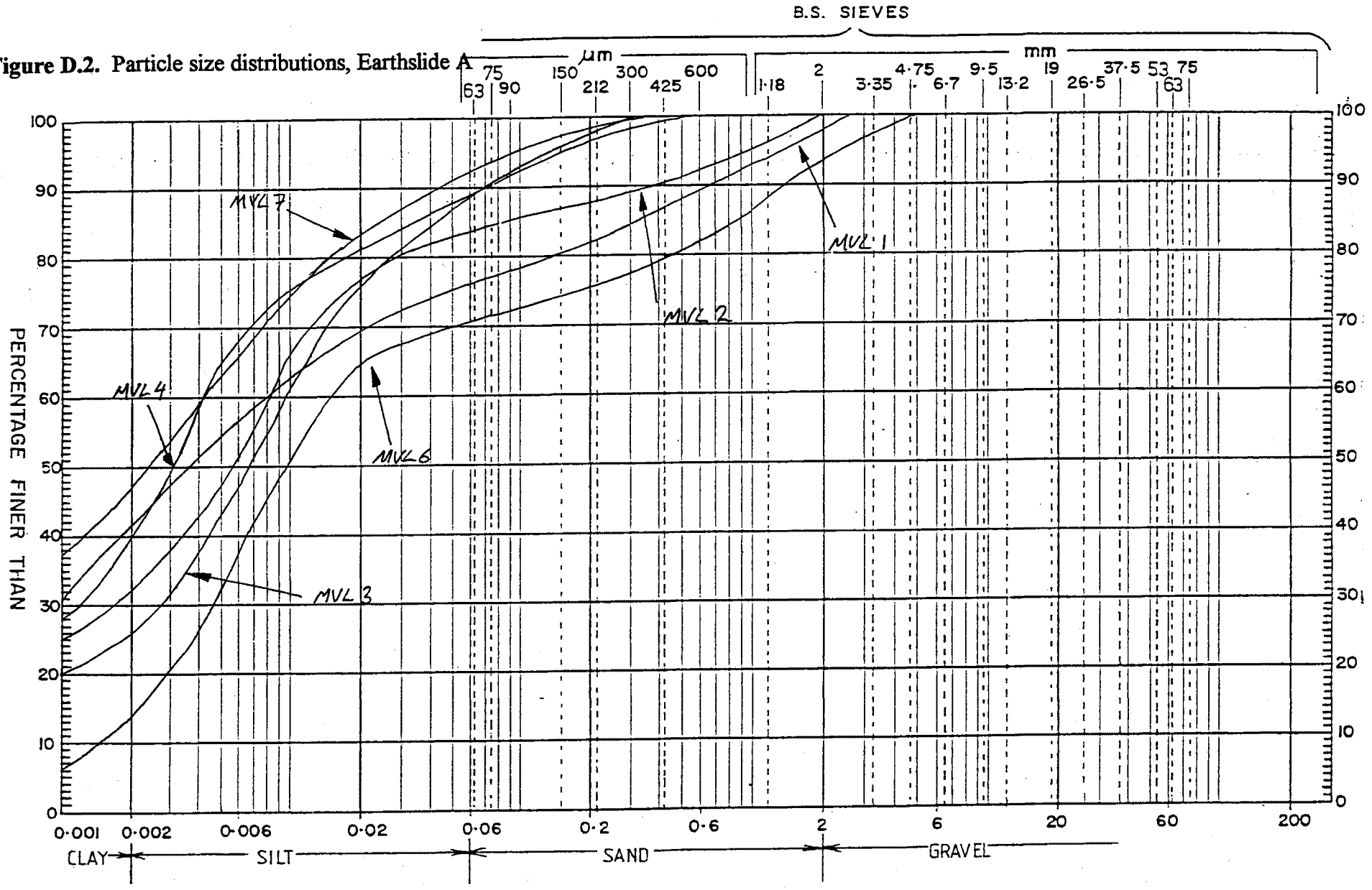

(Law, 1987). The test is conducted on a remoulded soil sample loaded into a ring of area approximately 4000 mm^2 and thickness 5 mm, between roughened porous bronze platens. The small sample thickness ensures perfect and rapid pore water dissipation even with very impervious clay rich samples (Law, 1987). The sample is sheared by differential rotation and shear stress is measured for a series of normal stress conditions. Normal stress is applied by means of a counter balanced 10:1 ratio lever loading system. For samples analysed in this study, a maximum normal stress of about 150 kPa was used (note that the calculated maximum field normal stress is equal to $\rho gh \cong 100$ kPa, with ρ = 2 kN/m^3, $g \cong 10$ m/s^2 and $h = 5$ m).

The seived soil sample is kneaded into the shearing ring and levelled off flush with the top of the container. The shearing ring is then placed in the apparatus, and a normal load applied via the loading arm. A record was made of the consolidation of the specimen.

A shear plane is subsequently formed within the specimen by rotating the top of the shearing ring by manual means. 3 full rotations are generally enough to duplicate residual conditions (Bromhead, 1986).

The sample was subsequently differentially sheared in the machine by means of a worm-drive. A record was made of the displacement of strain gauges on the machine with time.

D.4.2 Mechanisms of Shear Development

Bromhead (1985) notes that for sand-'bentonite' mixtures under the ring shear apparatus, 3 different types of shear development can 3 differing mechanisms of residual plane development are possible, depending on the value of *CF*. The 3 mechanisms are: (i), at low *CF* (0-25%), turbulent or rolling shear ('sand-type behaviour'; Skempton, 1985); (ii) at high *CF* (>50%) sliding shear ('clay-type behaviour';Skempton, 1985), and; (iii) for intermediate values of *CF*, a transition between the 2 types (fig. D.3).

D.4.3 Earthslide 3

7 ring shear analyses were conducted on samples obtained from both the basal shear and lateral shear zones. As well, 3 samples were conducted on material obtained from the earthslide mass. These samples generally had high sand contents. Results are given in table D1 and are shown on the following pages.

D.4.4 Earthslide A

Ring shear analyses were conducted on all of the 8 sample obtained from the Earthslide A. Results are given in table D.2 and shown on the following pages.

Figure D.1 Ring shear tests on sand-bentonite mixtures (from Skempton, 1985)

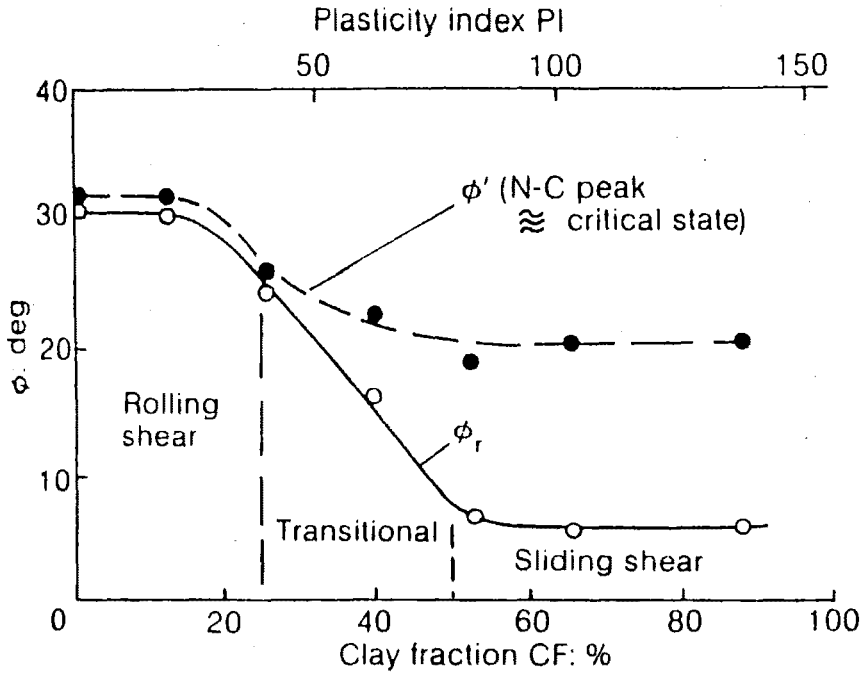

Normally consolidated at $\sigma' = 350$ kPa
PI/CF = 1·55

EARTHSLIDE 3 (CORINGA LANDSLIDE COMPLEX)

BH1@3.51m

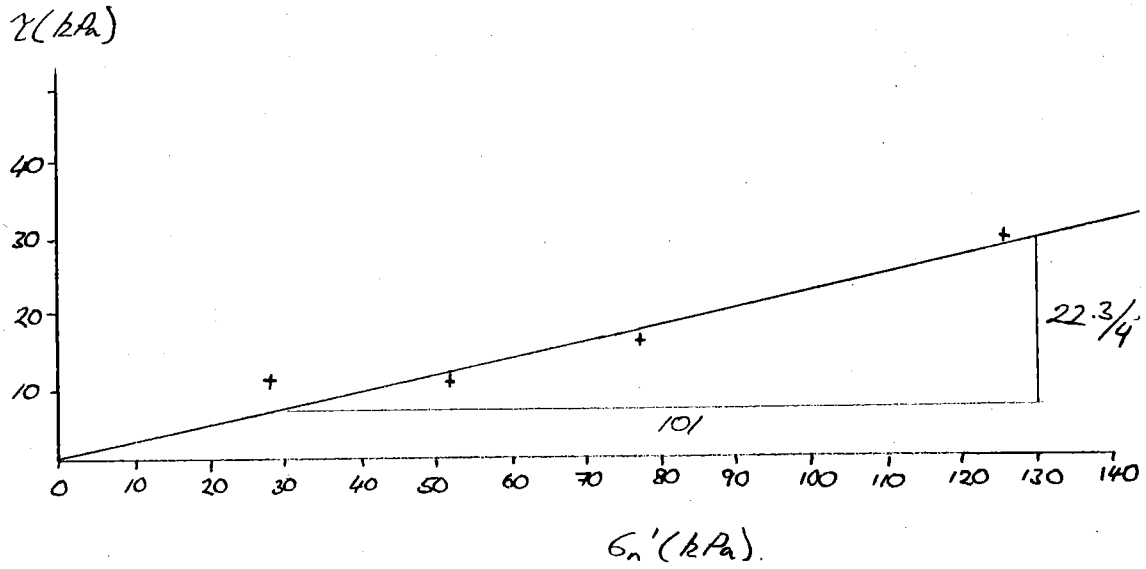

$c'_r = 0$, $\phi'_r = 12.7°$

DESCRIPTION: Wet, soft/very soft light brown silty CLAY (CH)

BH3@2.90m

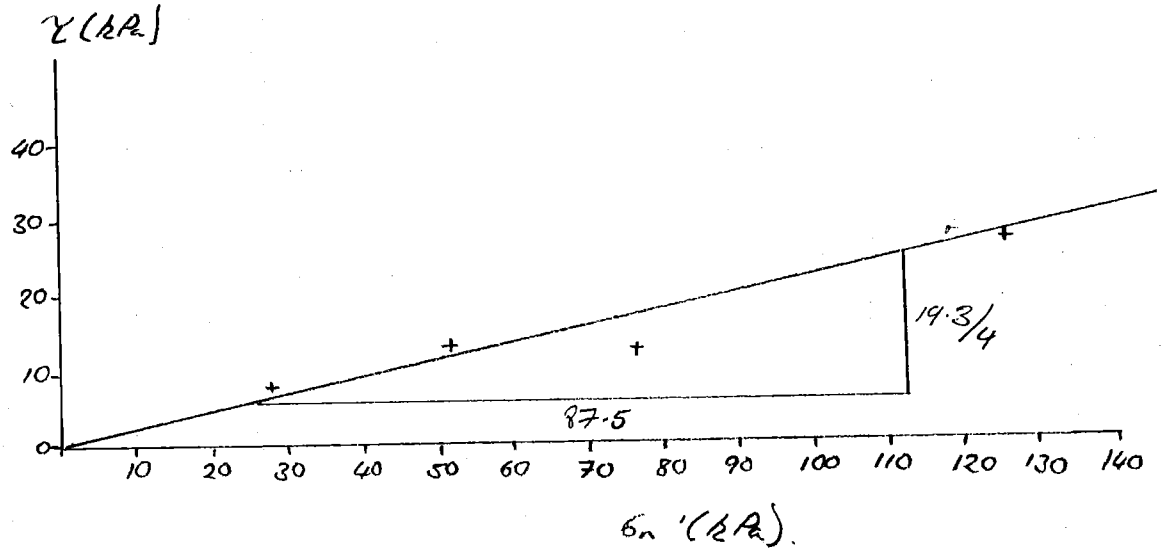

c'_r =0.5 kPa, ϕ'_r = 12.8°

DESCRIPTION: As above

CL 1

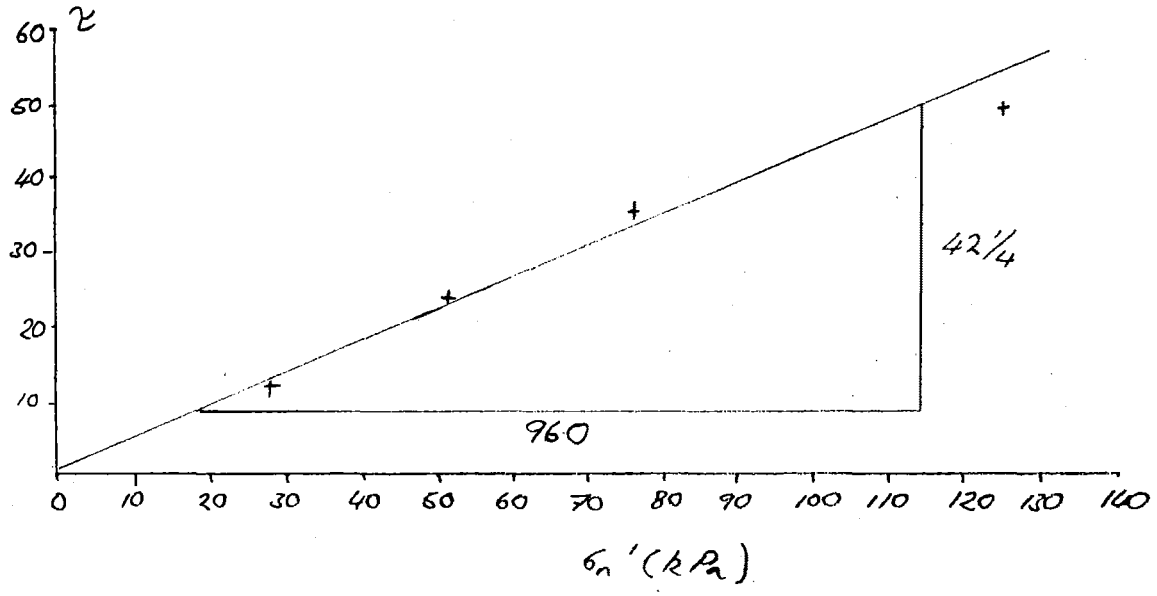

c'_r = 1.5 kPa, ϕ'_r =22.9°

DESCRIPTION: Moist, loose/compact greenish brown sandy SILT, with some clay.

CL2 (lateral shear zone)

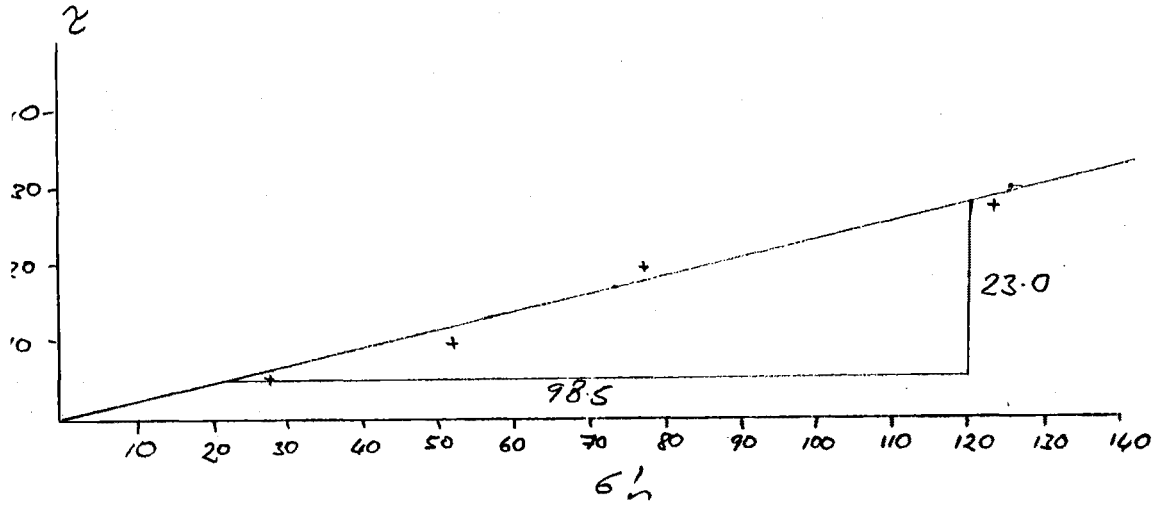

c'_r =0.5 kPa, ϕ'_r = 13.1°

DESCRIPTION: Moist/wet, soft, light brown silty CLAY, with some sand (CH).

CL 3

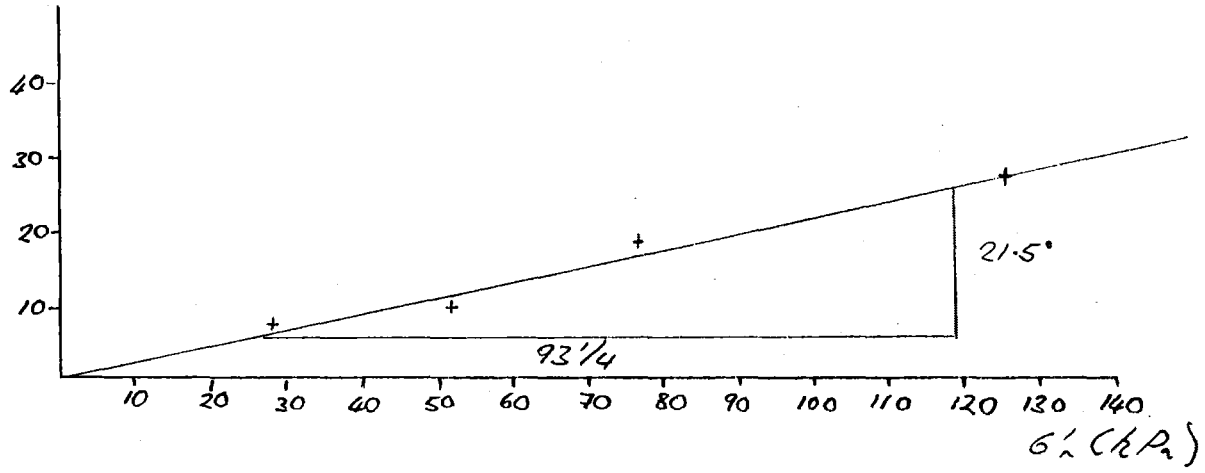

$c'_r = 0$, $\phi'_r = 13.1°$

DESCRIPTION: Moist/wet, soft, light brown silty CLAY CH)

CL 4

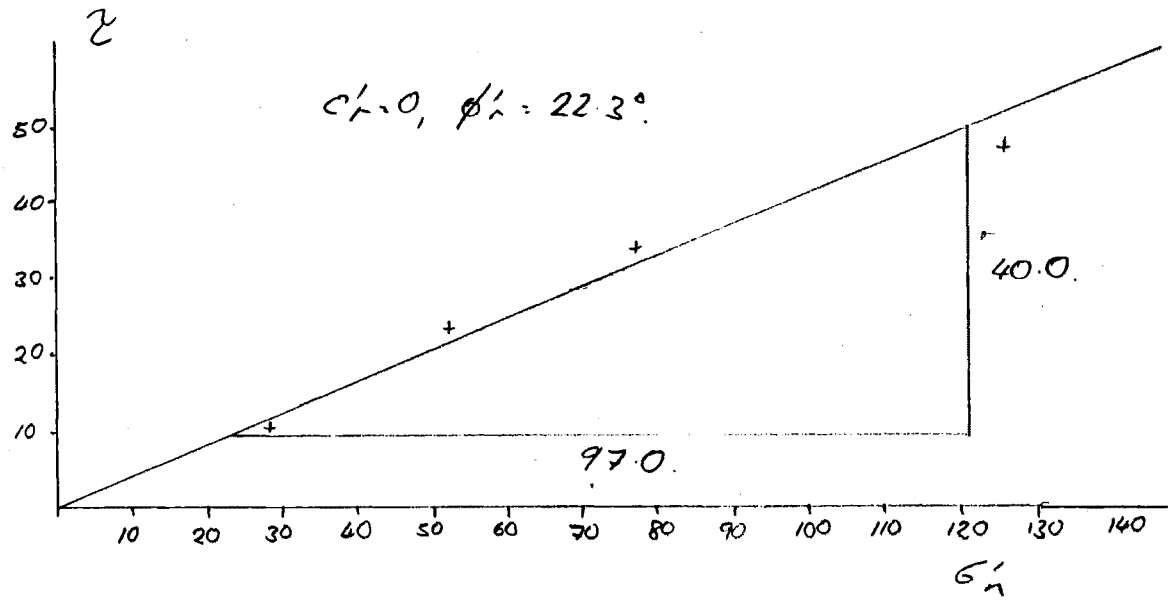

$c'_r = 0$ kPa, $\phi'_r = 22.3°$

DESCRIPTION: Moist, loose/soft greenish brown clayey SAND, with some silt.

CL 5 (lateral shear zone)

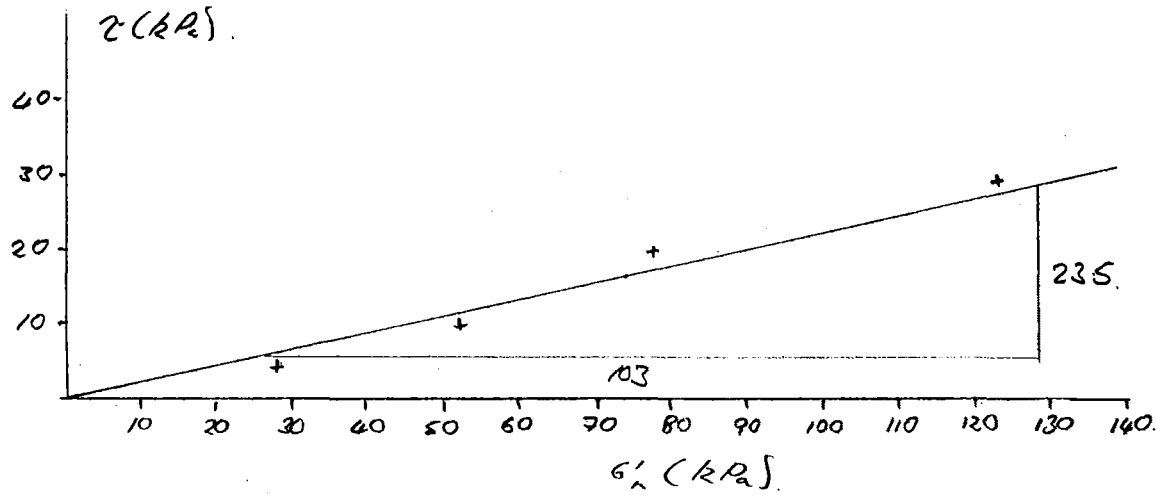

c'_r = 1.0 kPa, ϕ'_r =12.8°

DESCRIPTION: Moist/wet, soft, light brown silty CLAY (CH)

CL 7

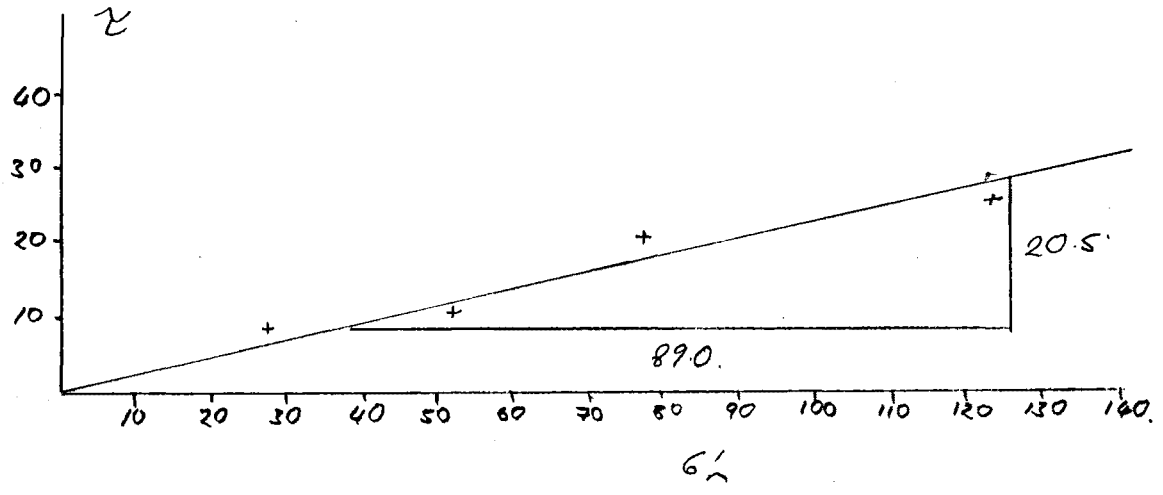

c'_r =1.0 kPa, ϕ'_r = 13.0°

DESCRIPTION: As above

CL 8

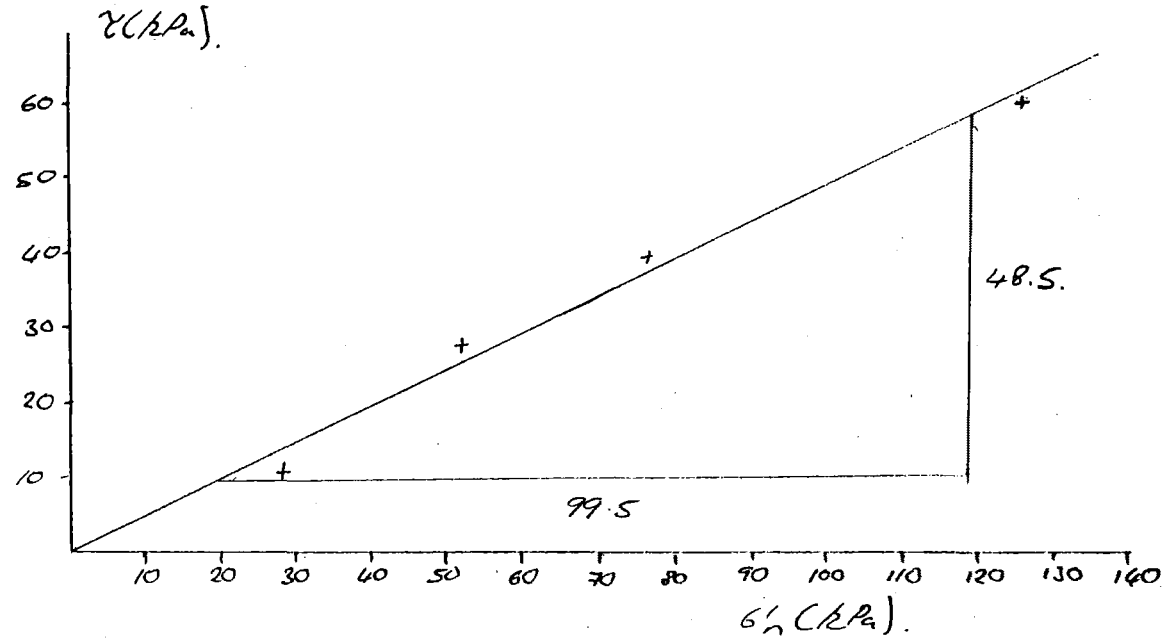

$c'_r = 0$, $\phi'_r = 26.0°$

DESCRIPTION: Moist, loose/soft brownish green silty SAND (SM)

CL 9

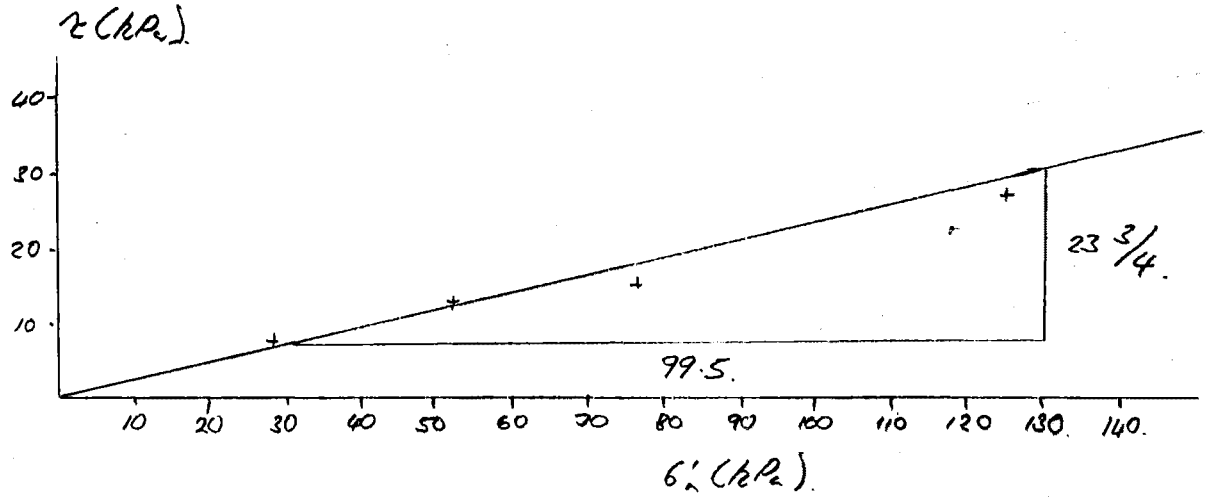

$c'_r = 0$ kPa, $\phi'_r = 13.4°$

DESCRIPTION: Moist, soft, light brown clayey SILT (MH)

EARTHSLIDE A (MT. VULCAN LANDSLIDE COMPLEX)

MVL 1 (lateral shear zone)

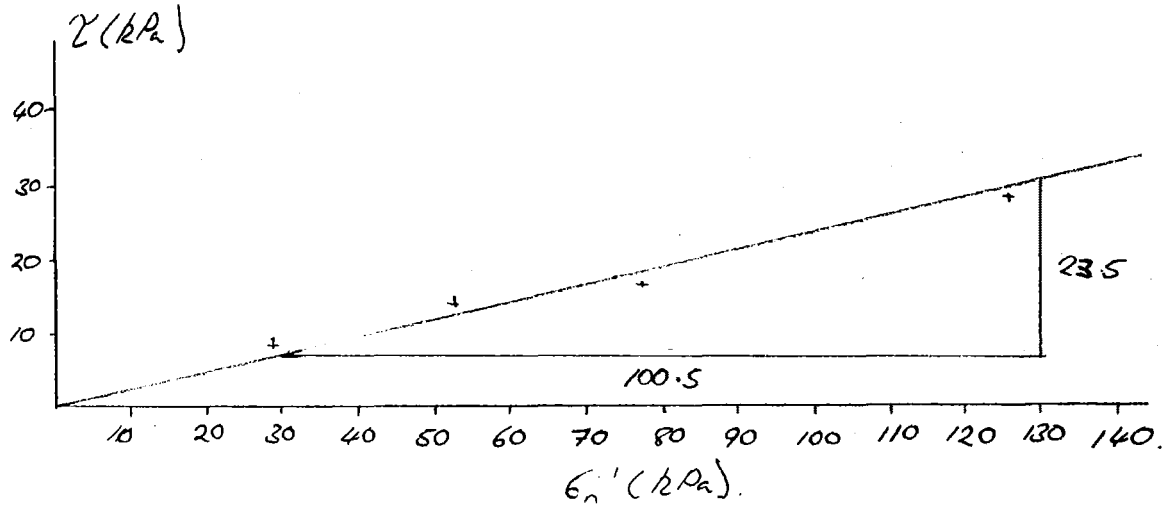

$c'_r = 0$, $\phi'_r = 13.1°$

DESCRIPTION: Wet, soft, light brown sandy silty CLAY

MVL 2 (lateral shear zone)

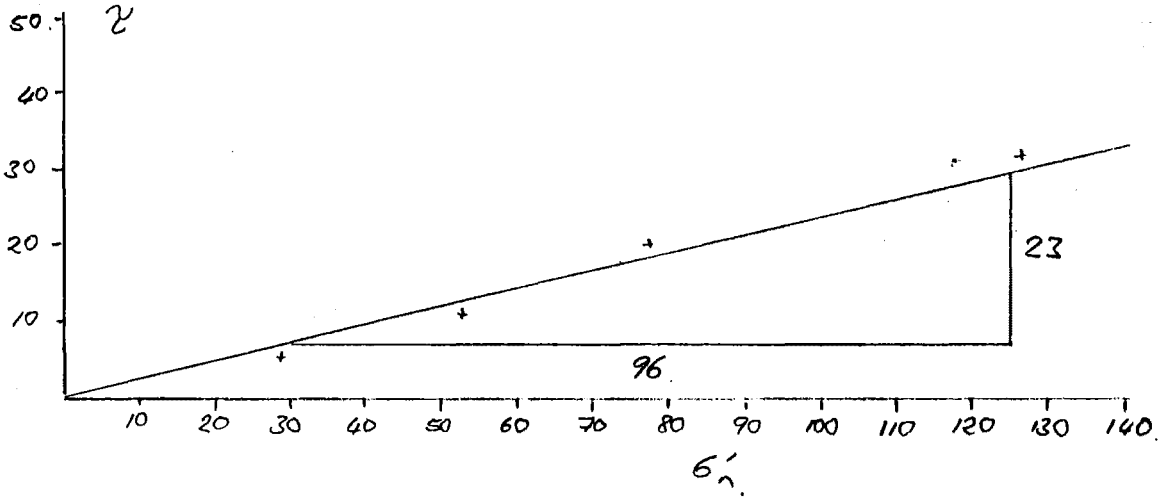

$c'_r = 0.5$ kPa, $\phi'_r = 13.4°$

DESCRIPTION: As above

MVL 3

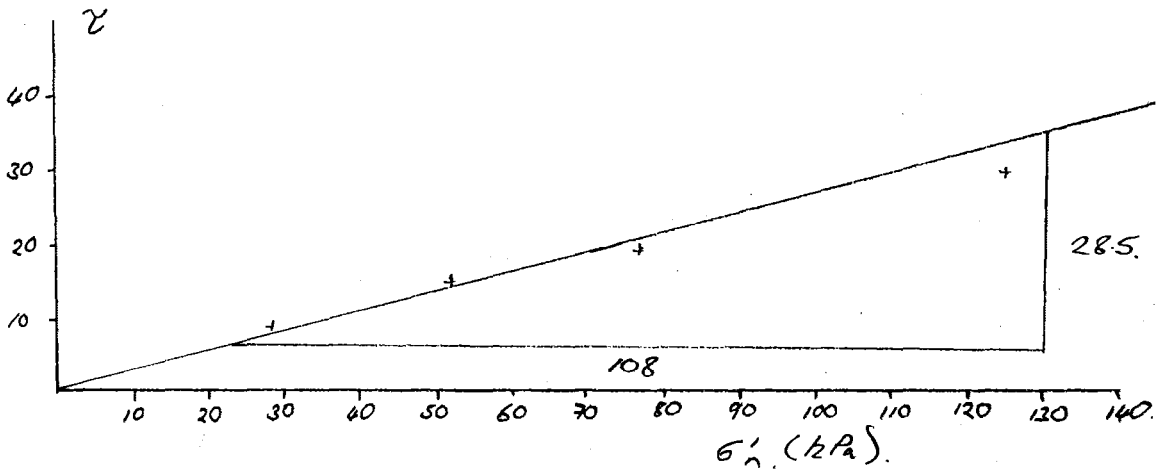

c'_r = 0.5 kPa, ϕ'_r =14.7°

DESCRIPTION: Moist, loose/soft light brown clayey SILT, with some sand (MH).

MVL 4

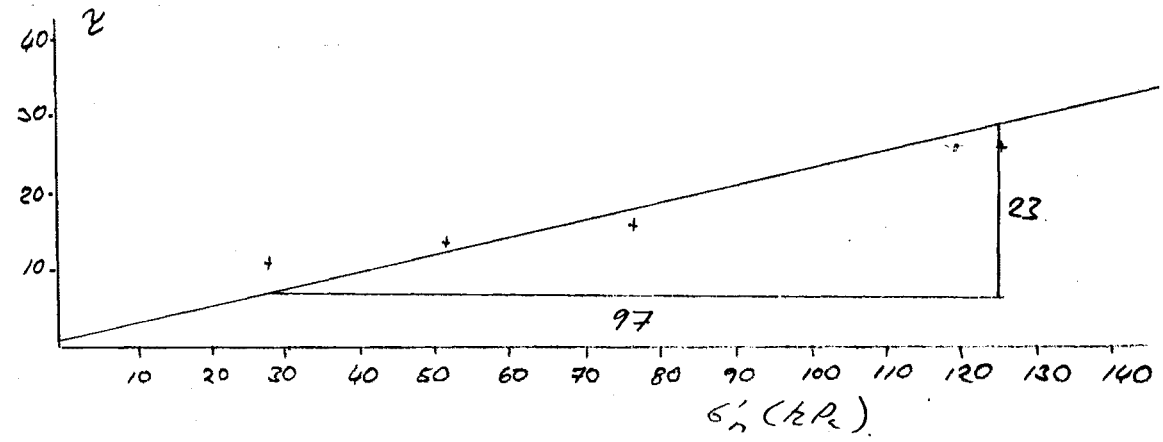

c'_r =0.5 kPa, ϕ'_r = 13.2°

DESCRIPTION: Moist/wet, soft light brown silty CLAY (CH)

MVL 5

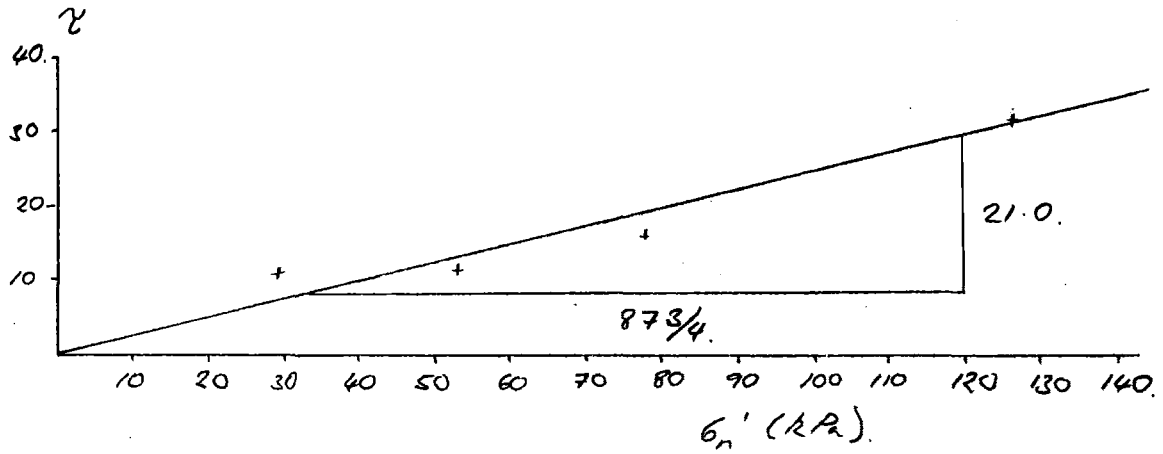

$c'_r = 0$, $\phi'_r = 13.6°$

DESCRIPTION: Moist, soft, light brown silty CLAY, with sone sand (CH)

MVL 6

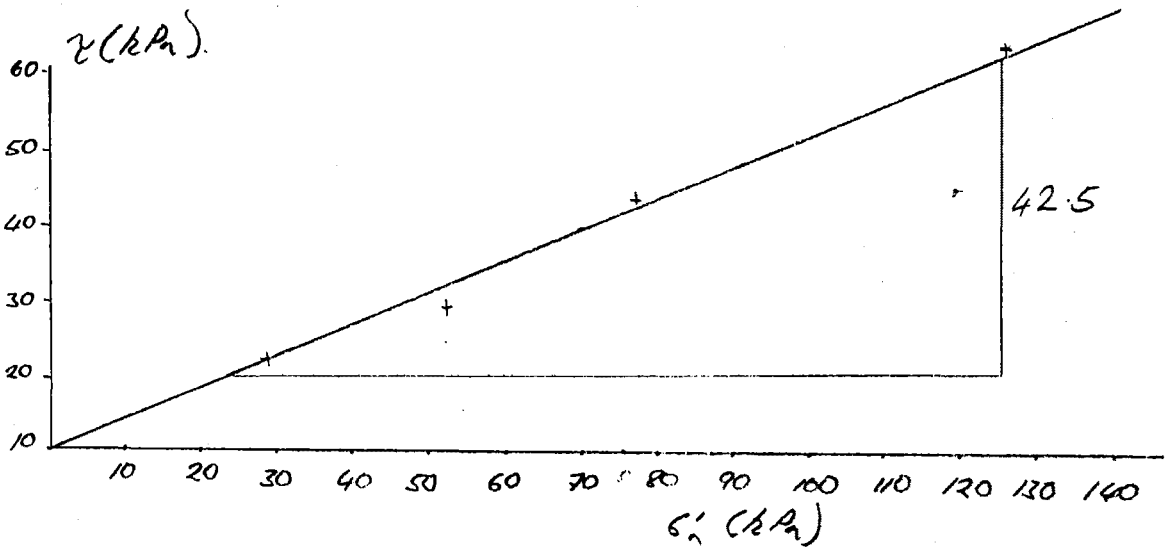

$c'_r = 0$ kPa, $\phi'_r = 22.6°$

DESCRIPTION: Moist, loose/soft, brownish green silty SAND, with some clay

MVL 7

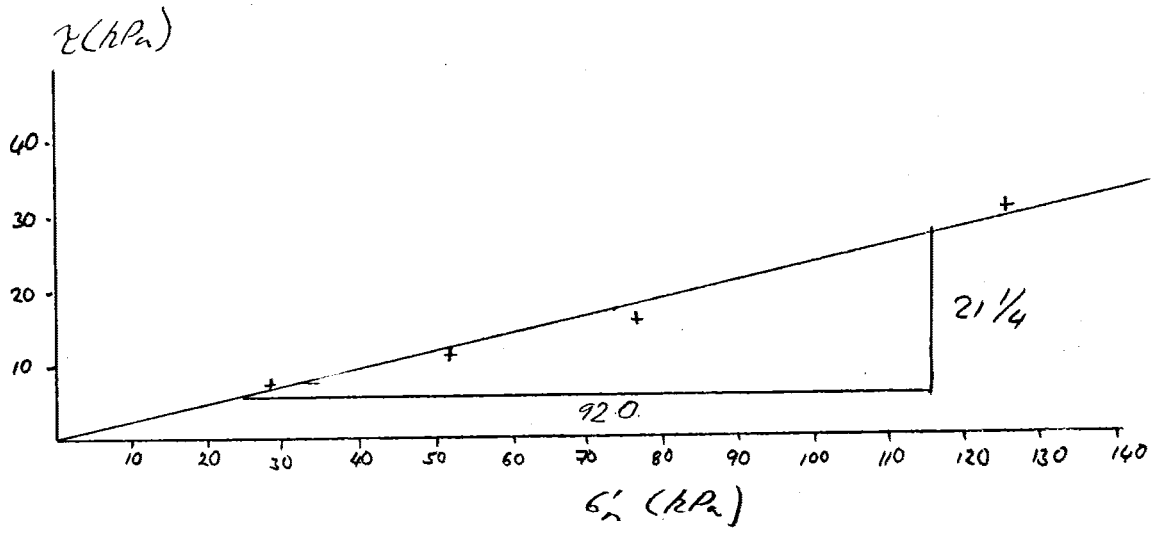

$c'_r = 0$, $\phi'_r = 13.0°$

DESCRIPTION: Moist, soft, light brown silty CLAY(CH)

MVL 8

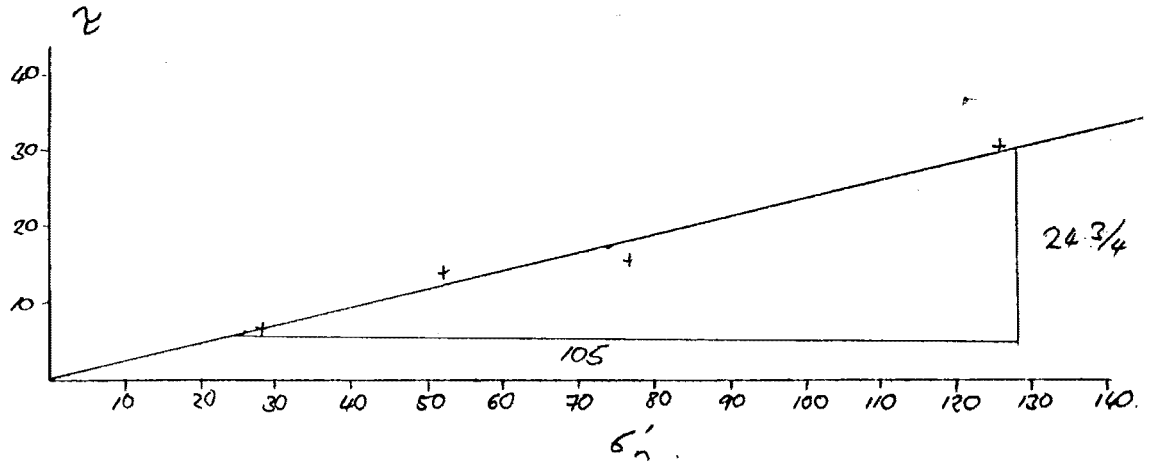

$c'_r = 0$ kPa, $\phi'_r = 13.2°$

DESCRIPTION: As above

D.5. Determination of the Coefficient of Permeability

(Falling head test)

The coefficient of permeability was determined for several samples from Earthslide 3 (Coringa Landslide Complex). The sample was placed in a standard Proctor compaction cell, and compacted in the normal method. The length of the specimen (l) and the cross sectional area of the cell (A) were recorded. A coarse filter was placed at each end of the cell and a stand pipe of known internal area (a) was connected to the top of the cell. The cell was placed in a water bath of constant water level. The standpipe is filled with water to height (h_0), and a note of the time (t_0) made. After some time period t_1 (samples were left for 48 hrs) the water height (h_1) in the standpipe was again measured.

The coefficient of permeability (k) is measured from the expression

$$k = \frac{al}{At_1} \ln \frac{h_0}{h_1}$$

D.5.1 Results

Results of the determination of the coefficient of permeability are given in table D.1.

Sample Name	Moisture Content (%)	Index Properties			Linear Shrinkage (%)	Bulk Density (kg/m^3)	Particle Size			Permeability (k) (mm/s)	Effective shear parameters	
		Liquid Limit (%)	Plastic Limit (%)	Plasticity Index (%)			Sand Fraction (%)	Silt Fraction (%)	Clay Fraction (%)		Residual friction Angle (°)	Residual Cohesion (kPa)
BH1@0.85m(2)	53.4	65.5	31.0	34.5	12.78	1721	45	29	26	$2.54x10^{-6}$		
BH1@1.80m	38.9	76.0	36.8	39.2								
BH2@1.44m	42.5	64.5	34.6	29.9	9.93	1567				$1.96x10^{-6}$		
BH2@3.51m(1)	48.4	76.5	35.9	40.6			10	47	43		12.7	0
BH3@2.90m(1)	49.1	72.5	36.8	35.7			11	44	45		12.8	0.5
BH4@1.42m	35.9	56.4	32.9	23.5		1581	13	53	34			
BH5@3.57m	41.4	67.5	31.0	36.5	13.87	1633						
BH5@4.68m	31.6	57.3	32.6	24.7	9.41							
CL 1	42.2	74.0	38.5	35.5	13.98		18	52	30	$2.00x10^{-6}$	22.9	1.5
CL 2 (l.s.z)	51.2	76.5	36.2	40.3			14	47	39		12.7	0.5
CL 3 (l.s.z)	48.2	84.3	38.2	46.1	15.23	1674	15	64	21		13.5	0
CL 4	33.4	69.7	32.1	37.6						$2.77x10^{-6}$	22.3	0
CL 5 (l.s.z)	55.3	77.3	36.2	41.1	14.94		9	48	43		13.6	1
CL 6(2)	36.5	44.1	29.6	14.5		2004	63	23	14			
CL 7 (l.s.z)	49.8	72.6	33.5	39.1							12.9	1
CL 8	32.4	73.1	31.9	41.2	16.20	1732	56	24	20	$2.76x10^{-6}$	26.0	0
CL 9 (l.s.z)	54.3	70.1	37.6	32.5			15	61	24		12.8	0
Loburn Mudstone (BH3 & 4)	41.7	78.5	33.0	45.5	10.25	1993						

Table D.1. Summary Data of Geotechnical Analyses, Earthslide 3, Coringa Landslide Complex.
(1) basal shear zone material; (2) high Waipara Greensand content; (l.s.z) lateral shear zone material
(copy of table 3.3)

Sample Name	Moisture Content (%)	Index Properties			Linear Shrinkage (%)	Bulk Density (kg/m^3)	Particle Size			Effective shear parameters (ring shear analysis)	
		Liquid Limit (%)	Plastic Limit (%)	Plasticity Index (%)			Sand Fraction (%)	Silt Fraction (%)	Clay Fraction (%)	Residual friction Angle (°)	Residual Cohesion (kPa)
MVL 1 (lsz)	51.6	77.5	38.2	39.3		1704	25	33	42	13.1	0
MVL 2 (lsz)	49.5	68.2	36.5	31.7	14.52		22	46	32	13.6	0.5
MVL 3 (ed)	32.9	51.9	29.3	18.6	9.56	1666	23	51	26	14.7	0.5
MVL 4 (lsz)	48.7	67.5	25.3	42.2	15.55	1654	18	42	40	13.2	0.5
MVL 5 (lsz)	52.3	78.5	36.6	41.9	12.89	1765				13.6	0
MVL 6 (ed)	34.6	72.6	38.5	34.1		1876	48	39	13	22.6	0
MVL 7 (lsz)	39.8	65.2	29.1	36.1		1627	15	38	47	13.0	0
MVL 8 (lsz)	43.5	70.2	32.5	37.7	13.56					13.2	0

Table D.2 Material Properties, Earthslide A, Mt. Vulcan Landslide Complex
(lsz = lateral shear zone material, ed = general earthslide debris)
Copy of table 2.1.

Appendix E. X-ray Diffraction Analysis

E.1 Definitions

1. 'Clay': denotes those grain sizes finer than 2μm.
2. 'Clay Mineral': as defined by Eslinger & Pevear (1988), clay minerals are "the minerals which normally dominate the fine (<2μm) fraction of rocks and soils." These minerals are usually hydrous aluminum phyllosilicates, but Eslinger & Pevear note that exceptions do exist.

E.2 Equipment Used

Clay minerals were identified using a Phillips X-ray diffractometer with CuKα radiation maintained by a 1° divergence slit, a 0.2 mm recieving slit and a 1° antiscatter slit (Morris, 1986). A detector is mounted on an arm which pivots around the axis of the instrument. The sample and detector are mechanically linked so that the rotation of the counter through 2θ° is accompanied by rotation of the specimen through θ°. The crystalline strucutre of clay minerals is such that the most important diffractions occur within the2°-37°2θ scanning distance (Moris, 1986).

E.3 Methodology

Techniques of sample mountings fall into two catergories:

1. Randomly Orientated (RO) Mount: RO mounts were prepared simply by spreading a small amount of a 425 μm seived sample on a glass slide using ethanol. Slides were then left to dry overnight
2. Preferentially Orientated (PO) Mount: PO mounts were prepared by taking a pippette ample of the 2μm and finer fraction from settling columns during particle size analysis (seeAppendix D). These samples, were, like RO mounts, spread on a glass slide and allowed to dry over-night.

RO mounts show all of the diffraction peaks for all clay and non-clay minerals present, wheras PO mounts are sensitive to the clay minerals present.

Samples were initially run through the diffractomer untreated, to give preliminary identification of clat mineral assmblages and non-clay minerals. Mounts were subsequently treated with ethylene glycol and re-ran. This treatment causes distinctive expansions in the C-lattice of swelling clay minerals that is detectable on diffractogram plots. After the glycerol treatment, the mounts were subjectted to heating at 550°C for 1 hour. Heating has the effect of destruction of the crystalline structure of some clays, resulting in amorphous mineral matter.

Results

Earthslide 3, (Coringa Landslide Complex)

MVL 3 was taken as a representative sample of the material comprising the earthslide. RO diffraction and PO diffraction mounts are shown in fig.2.14.

Minerals identified in the random mount are:

1. Non-clay minerals: Calcite; quartz; muscovite (?)
2. Clay minerals: Ca-Mg Smectite (note distinctive expansion upon application of ethylene glycol); Illite.

Clay minerals identified in the PO mount are Ca-Mg Smectite; Illite and Kaolinite.

Earthslide A (Mt. Vulcan Landslide Complex)

MVL 3 was taken as a representative sample of the material comprising the earthslide. RO diffraction and PO diffraction plots are shown in fig. 3.19

Minerals identified in the random mount are:

1. Non-clay minerals: Calcite; quartz;
2. Clay minerals: Ca-Mg Smectite; Illite.

Clay minerals identified in the PO mount are Ca-Mg Smectite; Illite and Kaolinite.

Note that the mixture of Kaolinite and Smectite clay minerals is often termed 'bentonite', however, this term is not recognised as a mineral name (Eslinger & Pevear, 1988).

Appendix F: Borehole Piezometer Installation

F.1 Materials used

20mm ϕ PVC pipe
Geotextile cloth (Bidim U14)
20 mm ϕ caps
Sand

F.2 Construction

The borehole is excavated using standard hand augering equipment. PVC pipe is cut to the desired length and the down-hole end of the pipe is wrapped in geotextile cloth. The tube is inserted into the hole, and sand is poured around the tube. Cuttings from augering are then replaced in the hole, and rammed down to prevent vertical movement of the pipe and surface water seepage. The setup is shown in the figure F1:.

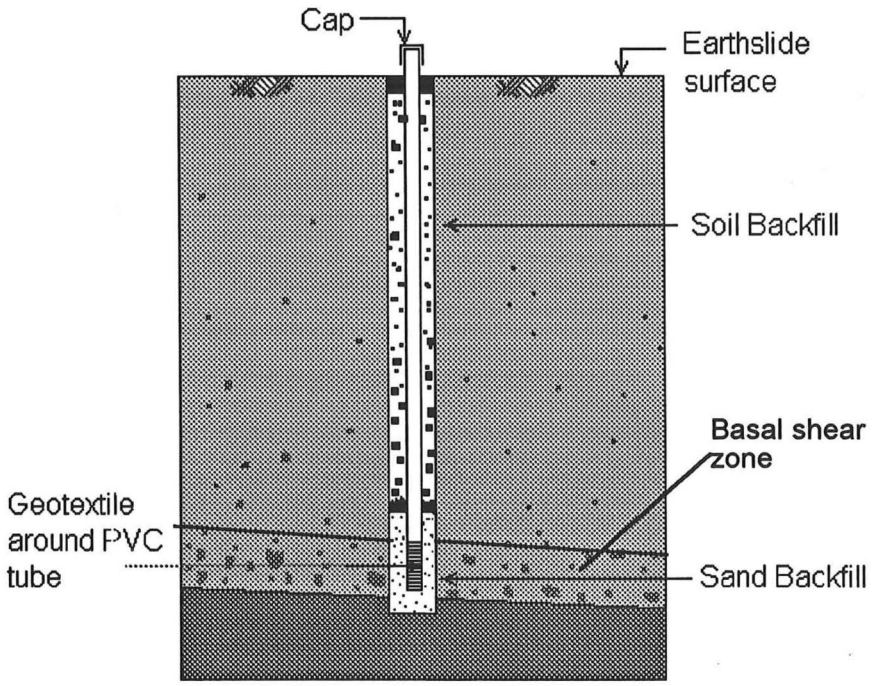

Figure F.1 Casagrande Piezometer setup, Earthslide 3, Coringa Landslide Complex

Measurement of water depth was acheived using a mild steel probe with two well insulated graduated electrical wires fixed to its surface and connected to a multimeter.

Appendix G: E.D.M Surveying and Surface Displacements, Earthslide 3, Coringa Landslide Complex

G.1 Displacement Monitoring

A system of displacement monitoring by means of regular survey was established to determine the nature and amount of surface displacement on earthslide 3. Surveys were conducted using a Wild TI 1000 electronic theodolite and DI 1000 distomat located on IT1 above the western edge of earthslide 3, with the target consisting of a tripod mounted single- or triple-prism.

Barrell (1989) emplaced 12 wooden pegs in 2 lines on the earthslide. For this thesis, this number was increased to 35 points, located in 7 lines. Positions of monitoring points are shown in figures **4** and **5** (map volume).

Barrell's monitoring points consist of wooden pegs driven until about 5 cm above the ground surface. The point of monitoring is located more particularly by a steel nail driven into the top of the peg. Points emplaced for this study consist of 40 cm lengths of 20 mm diameter galvanised iron pipe, driven until flush with the ground surface. The positions of these points are located by means of a wooden marking stake, located immediately adjacent to the iron pipe

G.2. Base Map Compliation

Extensive E.D.M. surveying was used to prepare the 1:1000 base map of Earthslide 3. The theodolite and distomat device were set up on IT1 and spot heights, bearings and distances were taken to various points on the earthslide. Points were electronically collected usiong a data logger, and were subsequqntly downloaded into a PC and reduced using LISCAD, a comprehensive surveying software package.

G.3. Survey Procedure

G.3.1. Stability of Control point IT1

Stability of IT1 was acheived by triangulation with existing DOSLI (Department of Survey and Land Information) survey marks OITD (SO 16896) and OITM (SO 16896) established as part of a rural subdivision survry in 1983. Relative positions of OITD, OITM and IT1 are shown in fig. D.1. Any displacement of IT1 would be noted by a distortion of the triangle formed by OITD, OITM and IT1.

At the start of every survey, a tripod and triple prism were set up on OITM. The E.D.M. device and tripod were setup on IT1, and a zero bearing taken to OITM. It was found

unnecessary to triangulate to OITD on every survey, and no distortion of the control triangle was noted in the 3 triangulations done in the year of monitoring.

G.3.2. Data Collection

Bearing (B), horizontal distance (S) and height difference (d_h) to each monitoring point were recorded. An electronic data logger was used in conjunction with manual recording for the first survey, but subsequent surveys were recorded manually only. A data logger was used extensively in the preparation of the base map and 3 dimensional terrain models of Earthslide 3, where approximately 1200 readings were taken. The first 2 monitoring surveys were taken using a pole-mounted prism. However, it was felt that better accuracy could be gained by using a tripod-mounted prism. This method was used for surveys conducted form July onwards. The base map surveys were conducted using a hand-held prism and staff only.

G.3.3. Sources of Error

Two sources of error exist in general surveying (i) device errors, which principally result from standard inaccuracies in bearing and distance measurement and pressure/temperature induced variations in distance measuremnet (Barrell, 1989); (ii) human error, either in recording or instrument and/or target setup. Standard deviations of ±3" in horizontal and vertical angle measurement and 5mm ±5 ppm in distance measurement are given in the Wild operators manual. For moitoring points on Earthslide 3, a maximum device error of about 10mm is calculated for horizontal and vertical angle measurement, while a maximum error about 7 mm is calculated for distance measurement. Taking into account human error, a maximum deviation for monitoring points on Earthslide 3 of no greater than 20 mm is likely.

G.4. Results

The results of the seven surveys conducted 23 March 1993-23 March 1994 are shown in tables G.1 to G.7.

Figure G2. Relative positions and bearings of base point triangulation.

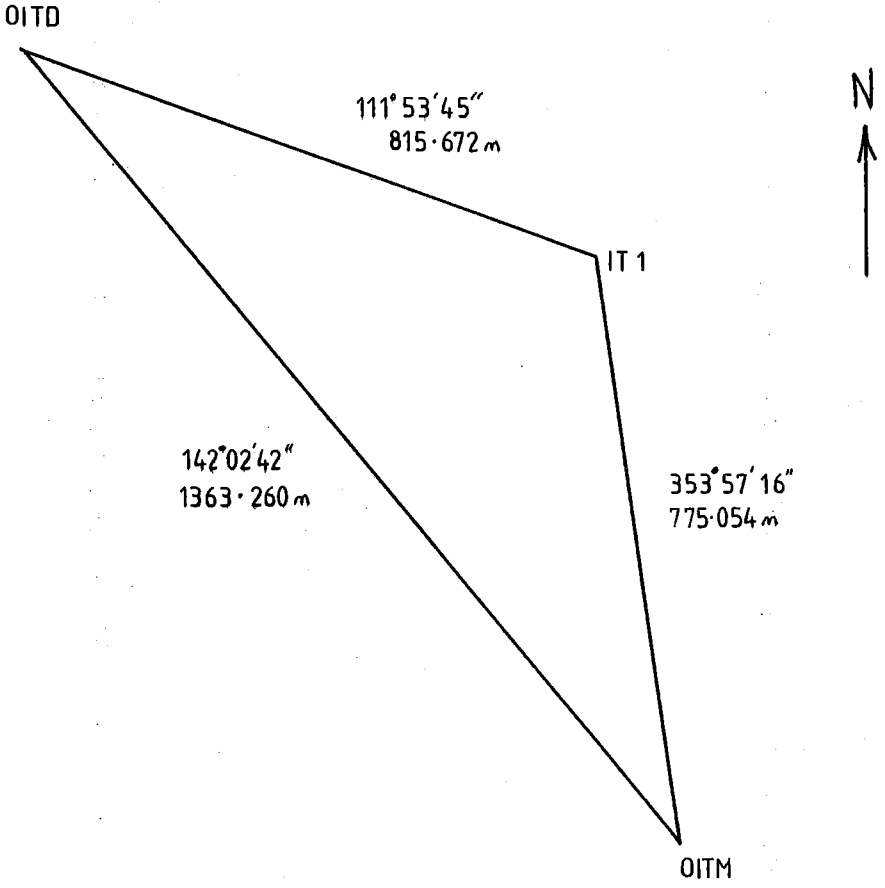

Date of survey		22-Mar-93							
Station	Target	Instrument	Height difference	R.L. (m)	Bearing (raw)	Bearing (true)	Horizontal	TRUE COORDINATES	
	height	height					distance	N	E
IT1				128.700				762082.89	324885.56
A1	2.3	1.692	-58.581	69.511	9.2036	183.1580	384.021	761699.45	324864.40
A2	1.3	1.692	-56.958	72.134	12.1097	186.0641	377.548	761707.45	324845.68
A3	1.3	1.692	-54.258	74.834	18.7114	192.6658	366.981	761724.84	324805.09
A4	1.3	1.692	-54.086	75.006	21.4333	195.3877	358.036	761737.69	324790.56
A5	1.3	1.692	-52.853	76.239	27.5294	201.4838	342.941	761763.78	324759.96
A6	1.3	1.692	-53.931	75.161	32.1697	206.1241	335.535	761781.63	324737.82
B2	1.3	1.692	-50.704	78.388	18.9069	192.8613	302.031	761788.44	324818.33
B3	1.3	1.692	-46.492	82.600	15.2056	189.1600	254.474	761831.66	324845.05
B5	1.3	1.692	-30.038	99.054	332.2614	146.2158	97.17	762002.13	324939.59
B9	1.3	1.692	-6.628	122.464	245.2031	59.1575	218.404	762194.86	325073.08
C1	1.3	1.692	-40.395	88.697	347.7741	161.7285	187.076	761905.25	324944.21
C2	1.3	1.692	-37.838	91.254	352.245	166.1994	162.259	761925.32	324924.27
C3	1.3	1.692	-36.993	92.099	356.2414	170.1958	145.836	761939.18	324910.39
C4	3.15	1.692	-34.585	92.657	7.2528	181.2072	114.146	761968.77	324883.16
C5	1.3	1.692	NOT SURVEYED						
P10	1.3	1.692	-23.590	105.502	300.6983	114.6527	118.577	762033.43	324993.33
P11	1.3	1.692	-24.454	104.638	301.3442	115.2986	113.014	762034.60	324987.74
P12	1.3	1.692	-24.503	104.589	300.1739	114.1283	94.858	762044.11	324972.13
P13	1.3	1.692	-24.507	104.585	301.1864	115.1408	81.143	762048.42	324959.02
P14	1.3	1.692	-23.872	105.220	301.6508	115.6052	68.073	762053.47	324946.95
D1	1.3	1.692	-23.352	105.740	279.3383	93.2927	138.139	762074.96	325023.47
D2	1.3	1.692	-21.548	107.544	273.465	87.4194	111.964	762087.93	324997.41
D3	1.3	1.692	-22.258	106.834	263.3903	77.3447	87.445	762102.05	324970.88
D4	1.3	1.692	-19.091	110.001	254.5525	68.5069	75.015	762110.37	324955.36
P1	1.3	1.692	-19.048	110.044	260.8214	74.7758	105.78	762110.67	324987.63
P2	1.3	1.692	-19.472	109.620	248.6175	62.5719	107.079	762132.21	324980.60
E1	1.3	1.692	-9.851	119.241	253.8944	67.8488	157.403	762142.24	325031.35
E2	1.3	1.692	-11.696	117.396	251.0358	64.9902	155.714	762148.72	325026.67
E3	1.3	1.692	-12.444	116.648	243.8639	57.8183	153.561	762164.68	325015.53
E4	1.3	1.692	-12.314	116.778	239.0283	52.9827	153.437	762175.27	325008.07
P4	1.3	1.692	-9.170	119.922	240.6428	54.5972	189.401	762192.61	325039.94
P5	1.3	1.692	-6.699	122.393	246.7289	60.6833	198.995	762180.33	325059.07
P7	1.3	1.692	-4.356	124.736	249.0003	62.9547	204.839	762176.03	325068.00

Date of survey		11-May							
Station	Staff	Instrument	Height difference	R.L. (m)	Bearing (raw)	Bearing (true)	Horizontal	TRUE	COORDINATES
	height	height					distance	N	E
IT1				128.700				762082.89	324885.56
A1	2.15	1.63	-58.689	69.491	9.2017	183.1561	384.043	761699.43	324864.42
A2	1.3	1.63	-56.905	72.125	12.1131	186.0675	377.573	761707.43	324845.65
A3	1.3	1.63	-54.193	74.837	18.7144	192.6688	367.029	761724.80	324805.07
A4	1.3	1.63	-54.025	75.005	21.435	195.3894	358.03	761737.70	324790.55
A5	1.3	1.63	-52.808	76.222	27.5291	201.4835	342.967	761763.75	324759.95
A6	1.3	1.63	-53.870	75.160	32.1675	206.1219	335.548	761781.62	324737.82
B2	1.3	1.63	-50.641	78.389	18.9086	192.8630	302.068	761788.40	324818.31
B3	1.3	1.63	-46.429	82.601	15.205	189.1594	254.512	761831.62	324845.05
B5	1.3	1.63	-29.977	99.053	332.304	146.2584	97.182	762002.08	324939.54
B9	1.3	1.63	-6.582	122.448	245.1964	59.1508	218.372	762194.87	325073.04
C1	1.3	1.63	-40.332	88.698	347.78	161.7344	187.088	761905.23	324944.20
C2	1.3	1.63	-37.779	91.251	352.2539	166.2083	162.292	761925.28	324924.25
C3	1.3	1.63	-36.933	92.097	356.2506	170.2050	145.864	761939.15	324910.37
C4	1.3	1.63	-36.383	92.647	7.265	181.2194	114.228	761968.69	324883.13
C5	1.3	1.63	-34.624	94.406	11.9719	185.9263	109.114	761974.36	324874.29
P10	1.3	1.63	-23.527	105.503	300.7089	114.6633	118.602	762033.40	324993.34
P11	1.3	1.63	-24.395	104.635	301.3789	115.3333	113.008	762034.54	324987.70
P12	1.3	1.63	-24.441	104.589	300.2158	114.1702	94.835	762044.06	324972.08
P13	1.3	1.63	-24.457	104.573	301.2269	115.1813	81.16	762048.36	324959.01
P14	1.3	1.63	-23.821	105.209	301.6908	115.6452	68.074	762053.43	324946.93
D1	1.3	1.63	-23.286	105.744	279.3456	93.3000	138.114	762074.94	325023.44
D2	1.3	1.63	-21.487	107.543	273.4858	87.4402	111.96	762087.89	324997.41
D3	1.3	1.63	-22.201	106.829	263.4131	77.3675	87.418	762102.01	324970.86
D4	1.3	1.63	-19.028	110.002	254.5536	68.5080	75.018	762110.37	324955.36
P1	1.3	1.63	-18.980	110.050	260.8394	74.7938	105.743	762110.63	324987.60
P2	1.3	1.63	-19.408	109.622	248.6325	62.5869	107.034	762132.17	324980.58
E1	1.3	1.63	-9.771	119.259	253.8933	67.8477	157.379	762142.23	325031.32
E2	1.3	1.63	-11.631	117.399	251.0394	64.9938	155.665	762148.69	325026.63
E3	1.3	1.63	-12.384	116.646	243.8667	57.8211	153.496	762164.64	325015.48
E4	1.3	1.63	-12.233	116.797	239.0264	52.9808	153.436	762175.27	325008.07
P3	1.3	1.63	-7.279	121.751	237.7386	51.6930	197.563	762205.35	325040.59
P4	1.3	1.63	-9.103	119.927	240.6453	54.5997	189.373	762192.59	325039.92
P5	1.3	1.63	-6.626	122.404	246.7281	60.6825	198.977	762180.32	325059.05
P6	1.3	1.63	-4.283	124.747	248.9989	62.9533	204.819	762176.02	325067.98
BH1	1.3	1.63	-9.585	119.445	244.615	58.5694	184.568	762179.14	325043.05

11 May 1993

Date of survey		22-Jul							
Station	Staff	Instrument	Height difference	R.L. (m)	Bearing (raw)	Bearing (true)	Horizontal	TRUE	COORDINATES
	height	height					distance	N	E
IT1				128.700				762082.890	324885.560
A1	1.921	1.610	-58.821	69.568	9.201	183.156	384.097	761699.375	324864.415
A2	1.436	1.610	-56.687	72.187	12.109	186.063	377.659	761707.344	324845.669
A3	1.466	1.610	-53.953	74.891	18.714	192.668	367.122	761724.705	324805.050
A4	1.186	1.610	-54.072	75.052	21.434	195.389	358.136	761737.594	324790.522
A5	1.181	1.610	-52.825	76.304	27.528	201.483	343.063	761763.660	324759.923
A6	1.443	1.610	-53.640	75.227	32.163	206.118	335.560	761781.593	324737.841
B2	1.406	1.610	-50.467	78.437	18.908	192.863	302.163	761788.309	324818.294
B3	1.250	1.610	-46.409	82.651	15.208	189.162	254.616	761831.523	324845.018
B5	1.463	1.610	-29.785	99.062	332.406	146.360	97.319	762001.868	324939.472
B9	1.213	1.610	-6.592	122.505	245.205	59.160	218.199	762194.749	325072.905
C1	1.393	1.610	-40.169	88.748	347.783	161.737	187.121	761905.195	324944.200
C2	1.271	1.610	-37.746	91.293	352.282	166.236	162.444	761925.111	324924.209
C3	1.279	1.610	-36.874	92.157	356.281	170.235	146.000	761939.005	324910.323
C4	1.227	1.610	-36.398	92.685	7.265	181.219	114.384	761968.532	324883.126
C5	1.372	1.610	-34.467	94.471	11.961	185.916	109.131	761974.340	324874.312
P10	1.322	1.610	-23.500	105.488	300.733	114.688	118.571	762033.366	324993.293
P11	1.419	1.610	-24.301	104.590	301.502	115.456	113.009	762034.316	324987.597
P12	1.194	1.610	-24.558	104.558	300.367	114.321	94.829	762043.835	324971.973
P13	1.234	1.610	-24.548	104.528	301.395	115.349	81.126	762048.157	324958.875
P14	1.250	1.610	-23.875	105.185	301.884	115.839	68.070	762053.223	324946.825
D1	1.382	1.610	-23.134	105.794	279.358	93.313	138.106	762074.910	325023.435
D2	1.268	1.610	-21.444	107.598	273.604	87.559	111.896	762087.656	324997.354
D3	1.272	1.610	-22.158	106.880	263.558	77.513	87.310	762101.769	324970.805
D4	1.077	1.610	-19.161	110.072	254.563	68.517	75.018	762110.363	324955.366
P1	1.196	1.610	-19.102	110.012	260.964	74.918	105.623	762110.373	324987.545
P2	1.116	1.610	-19.603	109.591	248.714	62.668	106.854	762131.951	324980.485
E1	1.284	1.610	-9.721	119.305	253.903	67.857	157.351	762142.199	325031.306
E2	1.138	1.610	-11.753	117.419	251.083	65.037	155.407	762148.477	325026.449
E3	1.212	1.610	-12.415	116.683	243.889	57.843	153.187	762164.422	325015.247
E4	1.191	1.610	-12.270	116.849	239.033	52.988	153.436	762175.256	325008.080
P3	1.099	1.610	-7.685	121.526	237.743	51.697	197.564	762205.344	325040.597
P4	1.168	1.610	-9.291	119.851	240.644	54.598	189.110	762192.442	325039.706
P5	1.124	1.610	-6.831	122.355	246.737	60.691	198.745	762180.178	325058.865
P6	0.912	1.610	-4.660	124.738	249.004	62.958	204.787	762175.994	325067.959
BH1	1.256	1.610	-9.655	119.399	244.644	58.598	184.297	762178.915	325042.864
BH2	1.150	1.610	-12.810	116.350	244.411	58.365	160.883	762167.273	325022.537
BH3	1.081	1.610	-15.350	113.879	248.282	62.236	129.744	762143.329	325000.367
BH4	1.001	1.610	-24.289	105.020	302.528	116.483	88.932	762043.233	324965.160
BH5	1.003	1.610	-36.099	93.208	352.251	166.205	128.073	761958.511	324916.098

22 July 1993

Date of survey		6-Oct							
Station	Staff	Instrument	Height difference	R.L. (m)	Bearing (raw)	Bearing (true)	Horizontal	TRUE	COORDINATES
	height	height					distance	N	E
IT1				128.700				762082.890	324885.560
A1	1.423	1.580	-59.297	69.560	9.214	183.168	384.125	761699.352	324864.329
A2	1.179	1.580	-56.888	72.213	12.123	186.077	377.707	761707.306	324845.571
A3	1.388	1.580	-53.992	74.900	18.727	192.681	367.181	761724.666	324804.953
A4	1.327	1.580	-53.876	75.077	21.447	195.401	358.207	761737.547	324790.428
A5	1.320	1.580	-52.666	76.294	27.543	201.497	343.123	761763.637	324759.819
A6	1.371	1.580	-53.651	75.258	32.176	206.130	335.555	761781.631	324737.776
B2	1.360	1.580	-50.456	78.464	18.928	192.882	302.234	761788.263	324818.177
B3	1.347	1.580	-46.269	82.664	15.223	189.177	254.699	761831.451	324844.938
B5	1.355	1.580	-29.879	99.046	332.555	146.509	97.452	762001.617	324939.334
B9	1.520	1.580	-6.254	122.506	245.199	59.153	217.909	762194.621	325072.644
C1	1.368	1.580	-40.150	88.762	347.807	161.761	187.139	761905.153	324944.130
C2	1.331	1.580	-37.670	91.279	352.324	166.278	162.586	761924.944	324924.126
C3	1.230	1.580	-36.904	92.146	356.323	170.277	146.121	761938.868	324910.237
C4	1.187	1.580	-36.422	92.671	7.343	181.297	114.529	761968.390	324882.967
C5	1.479	1.580	-34.323	94.478	11.963	185.917	109.137	761974.335	324874.309
P10	1.337	1.580	-23.442	105.501	300.768	114.722	118.571	762033.301	324993.263
P11	1.205	1.580	-24.507	104.568	301.654	115.608	113.008	762034.046	324987.467
P12	1.260	1.580	-24.482	104.538	300.539	114.493	94.816	762043.580	324971.843
P13	1.314	1.580	-24.472	104.494	301.589	115.543	81.114	762047.914	324958.746
P14	1.410	1.580	-23.732	105.138	302.111	116.065	68.057	762052.986	324946.695
D1	1.275	1.580	-23.193	105.812	279.374	93.328	138.091	762074.873	325023.418
D2	1.472	1.580	-21.194	107.614	273.742	87.696	111.833	762087.385	324997.303
D3	1.425	1.580	-21.971	106.884	263.686	77.640	87.187	762101.552	324970.726
D4	1.460	1.580	-18.742	110.078	254.578	68.532	75.025	762110.347	324955.380
P1	1.370	1.580	-18.904	110.006	261.125	75.079	105.471	762110.047	324987.475
P2	1.380	1.580	-19.346	109.554	248.786	62.740	106.616	762131.723	324980.335
E1	1.345	1.580	-9.588	119.347	253.908	67.862	157.325	762142.175	325031.287
E2	1.195	1.580	-11.605	117.480	251.135	65.089	155.050	762148.198	325026.185
E3	1.295	1.580	-12.345	116.640	243.929	57.883	152.751	762164.100	325014.935
E4	1.475	1.580	-11.960	116.845	239.038	52.992	153.439	762175.248	325008.090
P3	1.550	1.580	-6.969	121.761	237.743	51.697	197.563	762205.342	325040.597
P4	1.370	1.580	-9.121	119.789	240.639	54.593	188.719	762192.229	325039.378
P5	1.440	1.580	-6.540	122.300	246.745	60.699	198.388	762179.979	325058.567
P6	1.295	1.580	-4.230	124.755	249.004	62.958	204.756	762175.980	325067.931
BH1	1.605	1.580	-9.302	119.373	244.653	58.607	183.920	762178.694	325042.557
BH2	1.210	1.580	-11.133	117.937	244.438	58.392	160.461	762166.987	325022.218
BH3	1.260	1.580	-15.198	113.822	248.368	62.322	129.351	762142.973	325000.110
BH4	1.145	1.580	-24.229	104.906	302.758	116.712	88.914	762042.922	324964.985
BH5	1.207	1.580	-35.861	93.212	352.310	166.264	128.215	761958.342	324916.004

9 October 1993

Date of survey		14-Dec							
Station	Staff	Instrument	Height difference	R.L. (m)	Bearing (raw)	Bearing (true)	Horizontal	TRUE	COORDINATES
	height	height					distance	N	E
IT1				128.700				762082.890	324885.560
A1	1.545	1.575	-59.144	69.586	9.213	183.167	384.154	761699.323	324864.334
A2	1.360	1.575	-56.703	72.212	12.123	186.077	377.733	761707.280	324845.569
A3	1.410	1.575	-53.964	74.901	18.722	192.676	367.224	761724.617	324804.975
A4	1.540	1.575	-53.673	75.062	21.444	195.398	358.254	761737.496	324790.433
A5	1.500	1.575	-52.488	76.287	27.536	201.490	343.175	761763.573	324759.839
A6	1.410	1.575	-53.608	75.257	32.168	206.122	335.554	761781.611	324737.819
B2	1.530	1.575	-50.276	78.469	18.925	192.879	302.250	761788.244	324818.189
B3	1.545	1.575	-46.077	82.653	15.214	189.168	254.754	761831.391	324844.968
B5	1.330	1.575	-29.908	99.037	332.625	146.579	97.528	762001.488	324939.277
B9	1.440	1.575	-6.316	122.519	245.189	59.143	217.765	762194.580	325072.501
C1	1.340	1.575	-40.146	88.789	347.803	161.757	187.163	761905.134	324944.150
C2	1.600	1.575	-37.391	91.284	352.336	166.290	162.667	761924.857	324924.112
C3	1.540	1.575	-36.574	92.161	356.336	170.290	146.210	761938.774	324910.219
C4	1.305	1.575	-36.296	92.674	7.364	181.318	114.615	761968.305	324882.923
C5	1.520	1.575	-34.254	94.501	11.963	185.917	109.133	761974.339	324874.309
P10	1.320	1.575	-23.449	105.506	300.782	114.736	118.576	762033.273	324993.256
P11	1.230	1.575	-24.476	104.569	301.738	115.692	113.019	762033.892	324987.405
P12	1.340	1.575	-24.385	104.550	300.630	114.584	94.799	762043.450	324971.765
P13	1.330	1.575	-24.462	104.483	301.688	115.642	81.098	762047.795	324958.671
P14	1.365	1.575	-23.787	105.123	302.239	116.193	68.051	762052.852	324946.623
D1	1.340	1.575	-23.144	105.791	279.386	93.340	138.077	762074.845	325023.402
D2	1.430	1.575	-21.245	107.600	273.823	87.777	111.791	762087.225	324997.267
D3	1.380	1.575	-22.004	106.891	263.768	77.722	87.103	762101.412	324970.671
D4	1.435	1.575	-18.755	110.085	254.578	68.532	75.021	762110.346	324955.376
P1	1.495	1.575	-18.784	109.996	261.213	75.167	105.390	762109.869	324987.438
P2	1.430	1.575	-19.298	109.547	248.852	62.806	106.492	762131.557	324980.281
E1	1.430	1.575	-9.502	119.343	253.913	67.867	157.303	762142.154	325031.272
E2	1.465	1.575	-11.455	117.355	251.165	65.119	154.861	762148.044	325026.048
E3	1.525	1.575	-12.130	116.620	243.940	57.894	152.518	762163.950	325014.753
E4	1.505	1.575	-11.960	116.810	239.038	52.992	153.440	762175.249	325008.090
P3		NOT	SURVEYED						
P4	1.300	1.575	-9.231	119.744	240.629	54.583	188.508	762192.134	325039.186
P5	1.405	1.575	-6.588	122.282	246.744	60.698	198.206	762179.893	325058.407
P6	1.285	1.575	-4.226	124.764	249.001	62.955	204.730	762175.977	325067.903
BH1	1.580	1.575	-9.332	119.363	244.659	58.613	183.716	762178.571	325042.393
BH2	1.290	1.575	-11.064	117.921	244.445	58.399	160.241	762166.855	325022.041
BH3	1.330	1.575	-15.155	113.790	248.423	62.377	129.139	762142.765	324999.980
BH4	1.215	1.575	-24.152	104.908	302.817	116.771	88.893	762042.850	324964.925
BH5	1.180	1.575	-35.858	93.237	352.332	166.286	128.293	761958.254	324915.974

14 December 1993

Date of survey		15-Feb							
Station	Staff	Instrument	Height difference	R.L. (m)	Bearing (raw)	Bearing (true)	Horizontal	TRUE	COORDINATES
	height	height					distance	N	E
IT1				128.700				762082.890	324885.560
A1	1.464	1.552	-59.270	69.518	9.182	183.136	384.242	761699.224	324864.537
A2	1.322	1.552	-56.763	72.167	12.087	186.041	377.841	761707.147	324845.793
A3	1.346	1.552	-54.043	74.863	18.689	192.643	367.352	761724.446	324805.153
A4	1.390	1.552	-53.847	75.015	21.414	195.368	358.388	761737.317	324790.578
A5	1.290	1.552	-52.688	76.274	27.510	201.464	343.310	761763.390	324759.935
A6	1.382	1.552	-53.663	75.207	32.133	206.087	335.563	761781.513	324737.999
B2	1.412	1.552	-50.420	78.420	18.895	192.849	302.405	761788.058	324818.308
B3	1.440	1.552	-46.219	82.593	15.207	189.161	254.904	761831.238	324844.975
B5	1.247	1.552	-30.045	98.960	332.799	146.753	97.752	762001.138	324939.152
B9	1.510	1.552	-6.253	122.489	245.177	59.131	217.020	762194.237	325071.838
C1	1.316	1.552	-40.187	88.749	347.776	161.730	187.219	761905.108	324944.251
C2	1.462	1.552	-37.521	91.269	352.351	166.305	162.907	761924.614	324924.128
C3	1.580	1.552	-36.556	92.116	356.348	170.302	146.428	761938.554	324910.226
C4	1.270	1.552	-36.345	92.637	7.375	181.329	114.852	761968.069	324882.895
C5	1.427	1.552	-34.361	94.464	11.913	185.867	109.150	761974.312	324874.402
P10	1.280	1.552	-23.496	105.476	300.781	114.735	118.577	762033.274	324993.258
P11	1.265	1.552	-24.505	104.482	301.937	115.891	113.045	762033.527	324987.258
P12	1.474	1.552	-24.293	104.485	300.870	114.824	94.788	762043.094	324971.589
P13	1.392	1.552	-24.476	104.384	301.973	115.927	81.080	762047.439	324958.479
P14	1.307	1.552	-23.936	105.009	302.554	116.508	68.022	762052.530	324946.431
D1	1.427	1.552	-23.025	105.800	279.354	93.308	138.049	762074.923	325023.379
D2	1.373	1.552	-21.337	107.542	274.029	87.983	111.704	762086.821	324997.195
D3	1.254	1.552	-22.141	106.857	263.980	77.934	86.880	762101.051	324970.521
D4	1.375	1.552	-18.813	110.064	254.535	68.489	75.023	762110.399	324955.358
P1	1.575	1.552	-18.744	109.933	261.472	75.426	105.114	762109.339	324987.292
P2	1.474	1.552	-19.313	109.465	248.964	62.918	106.053	762131.172	324979.985
E1	1.435	1.552	-9.490	119.327	253.876	67.830	157.271	762142.236	325031.204
E2	1.242	1.552	-11.792	117.218	251.233	65.187	154.121	762147.567	325025.453
E3	1.385	1.552	-12.373	116.494	244.007	57.961	151.606	762163.316	325014.075
E4	1.470	1.552	-11.963	116.819	239.037	52.991	153.436	762175.248	325008.086
P3		NOT	SURVEYED						
P4	1.370	1.552	-9.355	119.527	240.619	54.573	187.674	762191.677	325038.488
P5	1.381	1.552	-6.735	122.136	246.767	60.721	197.396	762179.428	325057.739
P6	1.165	1.552	-4.365	124.722	249.005	62.959	204.692	762175.947	325067.876
BH1	1.555	1.552	-9.414	119.283	244.702	58.656	182.891	762178.024	325041.760
BH2	1.252	1.552	-11.195	117.805	244.500	58.454	159.366	762166.267	325021.376
BH3	1.253	1.552	-15.376	113.623	248.559	62.513	128.337	762142.123	324999.410
BH4	1.310	1.552	-24.076	104.866	303.068	117.022	88.874	762042.511	324964.732
BH5	1.257	1.552	-35.792	93.203	352.368	166.322	128.545	761957.990	324915.956

15 February 1994

Date of survey		22-Mar							
Station	Staff	Instrument	Height difference	R.L. (m)	Bearing (raw)	Bearing (true)	Horizontal	TRUE	COORDINATES
	height	height					distance	N	E
IT1				128.700				762082.890	324885.560
A1	1.639	1.648	-59.301	69.408	9.209	183.163	384.248	761699.228	324864.356
A2	1.405	1.648	-56.901	72.042	12.113	186.067	377.846	761707.161	324845.622
A3	1.438	1.648	-54.244	74.666	18.718	192.672	367.353	761724.486	324804.971
A4	1.461	1.648	-54.036	74.851	21.442	195.396	358.388	761737.364	324790.410
A5	1.414	1.648	-52.869	76.065	27.542	201.496	343.333	761763.439	324759.748
A6	1.428	1.648	-53.716	75.204	32.176	206.130	335.564	761781.623	324737.772
B2	1.559	1.648	-50.480	78.309	18.923	192.877	302.411	761788.085	324818.163
B3	1.507	1.648	-46.344	82.497	15.231	189.185	254.921	761831.238	324844.867
B5	1.344	1.648	-30.039	98.965	332.807	146.761	97.774	762001.112	324939.153
B9	1.398	1.648	-6.464	122.486	245.178	59.132	217.004	762194.225	325071.827
C1	1.413	1.648	-40.192	88.743	347.792	161.746	187.233	761905.079	324944.206
C2	1.444	1.648	-37.670	91.234	352.368	166.322	162.941	761924.570	324924.089
C3	1.457	1.648	-36.782	92.109	356.432	170.387	146.451	761938.496	324910.017
C4	1.449	1.648	-36.295	92.604	7.397	181.351	114.876	761968.046	324882.851
C5	1.484	1.648	-34.430	94.434	11.931	185.885	109.139	761974.326	324874.369
P10	1.374	1.648	-23.490	105.484	300.813	114.767	118.576	762033.214	324993.229
P11	1.355	1.648	-24.506	104.487	301.973	115.927	113.039	762033.466	324987.221
P12	1.314	1.648	-24.545	104.489	300.905	114.859	94.786	762043.043	324971.563
P13	1.386	1.648	-24.582	104.380	302.013	115.967	81.071	762047.392	324958.446
P14	1.354	1.648	-23.991	105.003	302.590	116.544	68.029	762052.488	324946.418
D1	1.364	1.648	-23.179	105.805	279.388	93.342	138.038	762074.842	325023.363
D2	1.356	1.648	-21.422	107.570	274.077	88.031	111.670	762086.726	324997.164
D3	1.467	1.648	-21.993	106.888	264.023	77.977	86.866	762100.984	324970.521
D4	1.500	1.648	-18.742	110.106	254.575	68.529	75.027	762110.352	324955.381
P1	1.402	1.648	-18.983	109.963	261.520	75.474	105.096	762109.249	324987.297
P2	1.338	1.648	-19.497	109.513	249.013	62.967	106.031	762131.081	324980.007
E1	1.387	1.648	-9.590	119.371	253.913	67.867	157.248	762142.133	325031.221
E2	1.417	1.648	-11.673	117.258	251.276	65.230	154.087	762147.448	325025.471
E3	1.458	1.648	-12.339	116.551	244.009	57.963	151.565	762163.289	325014.043
E4	1.470	1.648	-11.994	116.884	239.043	52.997	153.429	762175.231	325008.090
P3		NOT	SURVEYED						
P4	1.308	1.648	-9.505	119.535	240.621	54.575	187.647	762191.656	325038.470
P5	1.316	1.648	-6.892	122.140	246.754	60.708	197.362	762179.450	325057.687
P6	1.197	1.648	-4.407	124.744	249.010	62.964	204.679	762175.926	325067.873
BH1	1.578	1.648	-9.470	119.300	244.707	58.661	182.862	762177.996	325041.744
BH2	1.267	1.648	-11.259	117.822	244.498	58.452	159.330	762166.253	325021.342
BH3	1.254	1.648	-15.415	113.679	248.610	62.564	128.293	762142.001	324999.424
BH4	1.151	1.648	-24.327	104.870	303.108	117.062	88.868	762042.459	324964.698
BH5	1.232	1.648	-35.878	93.238	352.387	166.341	128.874	761957.661	324915.992

23 March 1994

Appendix H: Derivation of Infinite Slope and Infinite Rectangular Landslide Expressions

The stability analysis of a particular slope is commonly performed by employing the use of a limit equilibrium method, where the performance of the slope is considered in terms of its factor of safety (F). Morgenstern & Sangrey (1978) define the factor of safety as (p.156):- "...that factor by which the shear strength parameters may be reduced in order to bring the slope into a state of limiting equilibrium along a given slip surface", but is commonly taken as the ratio of those forces resisting movement to those forces producing movement which act on a given slip surface. When F equals unity, the slope is considered to be in a state of limiting equilibrium. Values of F greater than 1 indicate that the slope is stable, whereas values of F less than 1 indicate that the slope is in a state of failure.

H.1 The Infinite Slope Expression

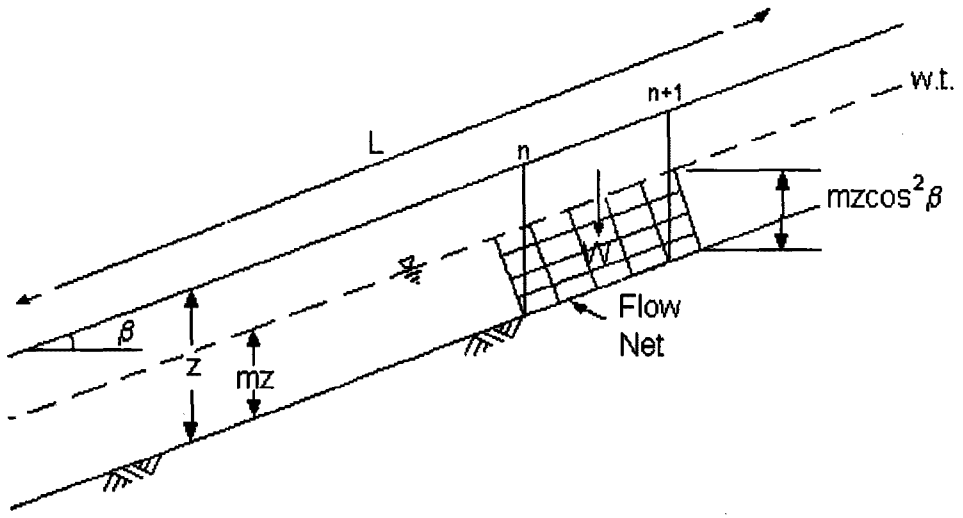

Fig H.1. Conditions of the Infinite Slope expression (w.t. = water table)

The slope is inclined at an angle β to the horizontal and the depth to the failure plane is z. The phreatic surface is assumed to be parallel to the ground at a height of mz ($0<m<1$) above the basal failure plane. Steady seepage is assumed to be taking place in a direction parallel to the slope (Craig, 1992). F_2 = Two dimensional Factor of Safety, defined as:

$$F_2 = \frac{\sum r}{\sum d} = \frac{c + (\sigma - u)\tan\phi}{\tau} \qquad \text{(H1)}$$

where Σr = slope forces resisting movement, which are given by the Mohr-Coulomb equation, Σd = slope forces producing movement, ie, slope *driving* forces; which are the shear stresses acting along the basal failure plane (τ).

The weight of soil in the nth slice (width of the nth slice = l = 1m) is given by W, where

$$W = \rho g z \cos\beta . l \qquad \text{(H2)}$$

W can be resolved into components acting parallel (τ, shear stress) and perpendicular (σ, normal stress) to the slope:-

$$\tau = \frac{W \sin\beta}{l} = \rho g z \cos\beta \sin\beta \qquad \text{(H3)}$$

$$\sigma = \frac{W \cos\beta}{l} = \rho g z \cos^2\beta \qquad \text{(H4)}$$

u (pore water pressure) is given by:-

$$u = \rho_w g z m \cos^2\beta \qquad \text{(H5)}$$

By substituting equations (H3), (H4), and (H5) into (H2), the following is produced:-

$$F_2 = \frac{c + (\rho g z \cos^2\beta - \rho_w g \cos^2\beta)\tan\phi}{\rho g z \cos\beta \sin\beta} \qquad \text{(H5)}$$

By substituting γ for (ρg), equation (H5) can be simplified to:-

$$F_2 = \frac{c' + (\gamma - \gamma_w m) z \cos^2\beta \tan\phi'}{\gamma z \sin\beta \cos\beta} \qquad \text{(H6)}$$

which is the Infinite Slope Expression (Skempton , 1957).

H.2. The Infinite Rectangular Landslide Expression

This expression is an expansion of the infinite slope expression, and was applied (Hutchinson & Del Prete, 1985) to an earthquake reactivated translational mudslide at Calitri, Italy. While based on the simple two-dimensional infinite slope analysis discussed in the preceding pages, the infinite rectangular landslide expression considers the effect of lateral earth pressure, acting at 90° to the direction of movement (fig H2) and hence, the infinite rectangular landslide expression incorporates a three-dimensional factor of safety (F_3).

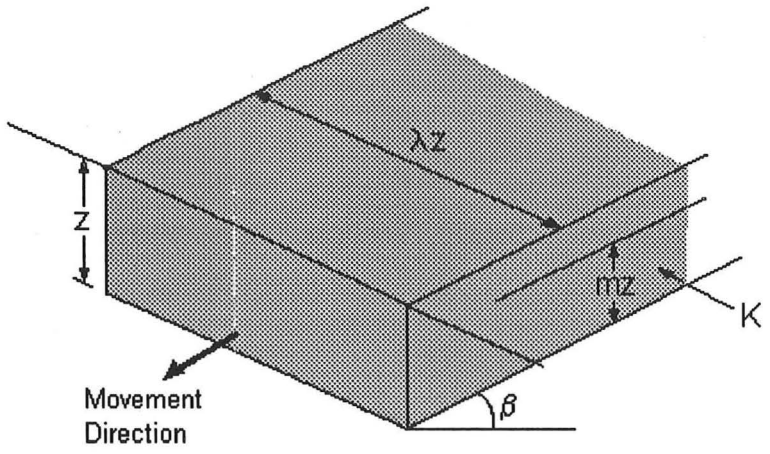

Figure H.2. Elements of the Infinite Rectangular Landslide Expression

F_3 = similarly to F_2, can be defined as:

$$F_3 = \frac{\left(\sum c'\right) + (\sigma_v - u)\tan\phi' + (\sigma_h - u)\cos\beta}{\tau} \qquad \text{(H7)}$$

Note that the additional term, σ_h is included in this expression, and is the horizontal stress acting on the sides of the sliding body due to lateral earth pressure.

From fig. D2, it can be seen that

$$W = \gamma z^2 l\lambda\cos\beta \qquad \text{(H8)}$$

where l = width of single slice. As for section D.1, l =1 m.

Likewise,

$$\sum c' = c'\lambda z l + 2c'\cos\beta.l \qquad \text{(H9)}$$

As for equation (H5) in section G.1, u is given by

$$u = \rho_w gzmz\cos^2\beta.l \qquad \text{(H10)}$$

Likewise, as for D.1., the vertical stress (σ_v) is given by:-

$$\sigma_v = \frac{W\cos\beta}{l} = \gamma z^2\cos^2\beta \qquad \text{(H11)}$$

Horizontal stress (σ_h) is given by

$$\sigma_h = 2l\int_0^z K\rho gy\tan\phi.dy$$

$$\sigma_h = 2lK\rho g\left[\frac{y^2}{2}\right]_0^z\tan\phi \qquad \text{(H12)}$$

Therefore,

$$\sigma_h = lKz^2\gamma\tan\phi \qquad \text{(H13)}$$

where y = distance from surface.

Substituting equations (H8), (H9), (H10), (H11) and (H13) into (H7), the following results:

$$F = \frac{\left(c'\lambda z + 2c'z\cos\beta\right) + \left(\gamma z^2\lambda\cos^2\beta - \gamma_w m z^2\lambda\cos^2\beta\right)\tan\phi' + \left(Kz^2\gamma\tan\phi - K\gamma_w (mz)^2\cos^2\beta.\tan\phi'\right)\cos\beta}{\gamma z^2\lambda\cos\beta\sin\beta}$$

$$F = \frac{1}{\sin\beta}\left(\frac{c'}{\gamma z\cos\beta} + \frac{2c'}{\gamma z\lambda}\right) + \frac{1}{\sin\beta}\left(\cos\beta - \frac{\gamma_w}{\gamma}m\cos\beta\right)\tan\phi' + \frac{1}{\sin\beta}\left(\frac{K\tan\phi}{\lambda\cos\beta} - \frac{K\gamma_w m^2\cos\beta\tan\phi}{\gamma\lambda}\right)\cos\beta$$

(H14)

which can be simplified to:-

$$F = \frac{1}{\sin\beta}\left\{\left(\sec\beta + \frac{2}{\lambda}\right)\frac{c'}{\gamma z} + \left[\cos\beta\left(1 - m\frac{\gamma_w}{\gamma}\right) + \frac{K}{\lambda}\left(1 - m^2\frac{\gamma_w}{\gamma}\cos^2\beta\right)\right]\tan\phi'\right\}$$

(H15)

which is the Infinite Rectangular Landslide Equation (Hutchinson & Del Prete, 1985)

K (coefficient of lateral earth pressure) in the equation above is given by : $K = \frac{\sigma'_h}{\sigma'_v}$. The value of K is not generally known (Prof. J.N. Hutchinson, pers.comm., 1993) but its value depends on the degree of lateral deformation at the boundary of the landslide. If the lateral boundary of the landslide is being de-stressed, ie, if the slide is widening, K approaches K_a, the coefficient of active earth pressure, whereas, if the landslide is narrowing, (ie, the lateral boundary is becoming stressed) K tends to approach K_p, the coefficient of passive earth pressure. In a parallel sided length of a landslide, K tends generally to lie between 2/3 and 1. However, where the landslide is widening, (immediately downslope of the bend on Earthslide 3, Coringa Landslide Complex) K will tend towards the coefficient of active earth pressure, K_a . K_a is given by the expression

$K_a = \frac{1-\sin\phi}{1+\sin\phi}$. (Craig, 1992)

Therefore, for $\phi = 35°$ (the probable maximum value of ϕ), $K_a = 0.271$.